# THE DESIGN AND SYNTHESIS OF PHOSPHONATE-BASED INHIBITORS OF NUCLEOTIDYLYLTRANSFERASES

*by*

Matthew W. Loranger

Submitted in partial fulfilment of the requirements
for the degree of Doctor of Philosophy

at

Dalhousie University
Halifax, Nova Scotia
June 2013

DALHOUSIE UNIVERSITY

DEPARTMENT OF CHEMISTRY

The undersigned hereby certify that they have read and recommend to the Faculty of Graduate Studies for acceptance a thesis entitled "THE DESIGN AND SYNTHESIS OF PHOSPHONATE-BASED INHIBITORS OF NUCLEOTIDYLYLTRANSFERASES" by Matthew W. Loranger in partial fulfilment of the requirements for the degree of Doctor of Philosophy.

Dated: June 24, 2013

External Examiner: _____

Research Supervisor: _____

Examining Committee: _____

_____

_____

Departmental Representative: _____

DALHOUSIE UNIVERSITY

DATE: June 24, 2013

AUTHOR: Matthew W. Loranger

TITLE: The Design and Synthesis of Phosphonate-based Inhibitors of Nucleotidylyltransferases

DEPARTMENT OR SCHOOL: Department of Chemistry

DEGREE: PhD CONVOCATION: October YEAR: 2013



_____

Signature of Author

*For Friends, Family, and Science*

## TABLE OF CONTENTS

## LIST OF FIGURES

## LIST OF TABLES

## LIST OF SCHEMES

# ABSTRACT

Nucleotidylyltransferase inhibitors are designed to target enzymes responsible for one step of cell wall biosynthesis in Gram-positive, Gram-negative and mycobacteria. Glucose 1-phosphate thymidylyltransferase Cps2L/RmlA (EC 2.7.7.24) is an enzyme essential for the growth and proliferation of many bacteria, including *Mycobacterium tuberculosis.* Cps2L/RmlA serves to couple glucose 1-phosphate and deoxythymidine triphosphate to form deoxythymidine diphosphoglucose. dTDP-β-L-rhamnose acts as an inhibitor of RmlA.

Phosphonates are synthetic analogues of natural phosphates that have shown widespread ability to probe biological systems. Several approaches were investigated toward the synthesis of dTDP-β-L-rhamnose analogues, which incorporated phosphonate functionality into their scaffolds. A series of L-rhamnose phosphonate and ketosephosphonate analogues, with varying degrees of fluorination about the 1C position, were synthesized. These compounds were evaluated as potential inhibitors of thymidylyltransferase Cps2L, the first enzyme in the L-rhamnose biosynthetic pathway, and a novel antibiotic target. Enzyme-inhibitor and enzyme-substrate binding experiments were performed using WaterLOGSY NMR spectroscopy for the phosphonate-based compounds and known enzyme sugar nucleotide substrates. $IC_{50}$ values were measured and $K_i$ values were calculated for the compounds determined to be inhibitors. New insights were gained into the binding promiscuity of various enzymes within the L-rhamnose biosynthetic pathway (Cps2L, RmlB-D) and the mechanism of inhibition for the most potent inhibitor, L-rhamnose-1C-phosphonate.

Thiophosphates are analogues of natural phosphates in which the P—O bond has been replaced with a P—S bond. Methods were investigated for the preparation of *O* and *S*-glucosyl thiophosphates. A series new protected glucosyl thiophosphate compounds were synthesized and characterized as precursors to glucose-1-thiophopshate, a probable glucose 1-phosphate substrate analogue for Cps2L.

## LIST OF ABBREVIATIONS USED

| | |
|---|---|
| Å | angstrom |
| AIBN | azoisobutyl nitrile |
| AMBP | adenosine 5′-methylenebisphosphonate |
| app | apparent |
| B | purine and pyrmidine bases |
| Bn | benzyl |
| br | broad |
| BuLi | butyllithium |
| Cps2L | glucose 1-phosphate thymidylyltransferase (*Streptoccus pneumoniae*) |
| CTP | cytidine triphosphate |
| CV | column volume |
| δ | chemical shift |
| d | doublet |
| dd | doublet of doublets |
| DBMP | dibenzyl methylphosphonate |
| DEAE | diethylaminoethyl |
| DEDFMP | diethyl difluoromethylphosphonate |
| DIEA | diisopropylethylamine |
| DNA | deoxyribonucleic acid |
| dTMBP | deoxythymidine 5′-methylenebisphosphonate |
| dTTP | deoxythymidine triphosphate |
| EC | enzyme classification |
| $E_p$ | glucose 1-phosphate thymidylyltransferase (*Salmonella enterica*) |
| EPI | enhanced product ionization |
| ESI | electrospray ionization |
| Gal | galactose |
| Glc | glucose |
| Glc-1-P | glucose 1-phosphate |
| GlcNAc | *N*-acetylglucosamine |

| | |
|---|---|
| GMBP | guanosine 5′-methylenebisphosphonate |
| HPLC | high-pressure liquid chromatography |
| HRMS | high-resolution mass spectrometry |
| $IC_{50}$ | half-maximal inhibitory concentration |
| IPP | inorganic pyrophosphatase |
| $J$ | coupling constant |
| $K_i$ | inhibitor dissociation constant |
| λ | wavelength |
| LDA | lithium diisopropylamine |
| LPA | lysophosphatic acid |
| LRMS | low-resolution mass spectrometry |
| m | multiplet |
| Man | mannose |
| MBP | methylenebisphosphonate |
| MBPDC | methylenebis(phosphonic dichloride) |
| MESG | 7-methyl-6-thioguanine |
| MIC | minimum inhibitory concentration |
| MRSA | methicilin-resistant *Staphylococcus aureus* |
| MSNT | 1-(mesitylene-2-sulfonyl)-3-nitro-1,2,4-triazole |
| NAD | nicotinamide adenine dinucleotide |
| NADPH | nicotinamide adenine dinucleotide phosphate |
| NDP | nucleoside diphosphate |
| NG | neighboring group |
| NMR | nuclear magnetic resonance |
| NOESY | nuclear overhauser enhancement spectroscopy |
| NTP | nucleoside triphosphate |
| PHYLPA | *Physarum* phospholipid |
| PNP | purine nucleoside phosphorylase |
| POM | pivaloyloxymethyl |
| ppm | parts per million |
| pyr | pyridine |

| | |
|---|---|
| q | quartet |
| Rha | rhamnose |
| RmlA | glucose 1-phosphate thymidylyltransferase (*Pseudomonas aeruginosa*) |
| RmlB | dTDP-glucose-4,6-dehydratase |
| RmlC | dTDP-4-hydrorhamnose 3,5 epimerase |
| RmlD | dTDP-4-hydrorhamnose reductase |
| rt | room temperature |
| s | singlet |
| sex | sextet |
| $S_N1$ | substitution nucleophilic unimolecular |
| $S_N2$ | substitution nucleophilic bimolecular |
| t | triplet |
| TBAB | tetrabutylammonium bicarbonate |
| TBAOH | tetrabutylammonium hydroxide |
| TEAA | triethylammonium acetate |
| TEAB | triethylammonium bicarbonate |
| TEP | triethyl phosphate |
| TLC | thin layer chromatography |
| TMP | trimethyl phosphate |
| TMSBr | trimethylsilyl bromide |
| TMSI | trimethylsilyl iodide |
| TP | triphosphate |
| TTP | thymidine triphosphate |
| UDP-GlcNAc | uridine diphosphono-*N*-acetylglucosamine |
| UMBP | uridine 5′-methylenebisphosphonate |
| UTP | uridine triphosphate |
| UV | ultraviolet |
| VRSA | vancomycin-resistant *Staphylococcus aureus* |
| WaterLOGSY | water-ligand observed binding via gradient spectroscopy |

## ACKNOWLEDGEMENTS

First and foremost I would like to acknowledge my supervisor, David Jakeman, for his support, resources and patience with me on this difficult project. Next I would like to thank Dr. Ali Sadeghi-Khomami and Dr. Debabratta Bhattasali for their wealth of knowledge, which has helped me time and time again in trying to develop synthetic routes to my target compounds. Steve Beaton and Thomas Veinott are acknowledged as being integral to my training in conducting enzyme assay and mass spectrometry lab techniques. Special thanks are extended to Stephanie Forget for her contributions to the spectrophotometric enzyme inhibition assays, and to Katie Lines for her synthethic assistance toward the production of glucosyl thiophosphates. Nicole McCormick is also acknowledged for performing all of the protein purifications essential to my enzymatic studies.

Additional thanks are extended to my undergraduate organic chemistry professors, Dr. Ian Pottie, for sparking my interest and desire to pursue a career in organic chemistry, and Dr. Cherif Matta, for being so enthusiastic and encouraging in the role of chemistry professor. I would like to thank Dr. Bruce Grindley for providing me with an extremely useful pool of carbohydrate knowledge to draw from, and Dr. Stephen Bearne for his very thorough course in enzyme kinetics. I would also like to thank Dalhousie University and the College of Pharmacy for housing my research laboratory and NSERC for funding.

In closing I would like to thank all of the members of the Jakeman group for providing an easy going and extremely comfortable work environment, which I enjoyed coming to everyday. Personal thanks are extended to Andrew Robertson, Gaia Aish, and Camilo Farina Martinez. Finally I would like to thank my friends, family and especially my girlfriend Kerry and daughter Keira, for their constant encouragement, support and patience, without which I would not have made it this far.

# CHAPTER 1 INTRODUCTION

Natural products are an important reservoir from which to draw, for the generation of novel compounds, with the potential to act as drugs in modern medicine. Many of these compounds, produced as secondary metabolites from various bacterial species, contain sugar moieties, which are often essential to their bioactivity.[1,2] These sugar moieties are enzymatically transferred to aglycone glycosyl acceptors with glycosyltransferases in many biological pathways. Nucleotidylyltransferases precede glycosyltransferases as key enzymes found within the biosynthetic pathway of various harmful bacteria, including *Streptococcus pneumoniae*, *Pseudomonas aeruginosa* and *Mycobacterium tuberculosis*. These enzymes produce activated sugars in the form of glycosylated nucleoside diphosphates (NDPs). These NDPs are generated from the enzymatic coupling of sugar 1-phosphates with nucleoside triphosphates (NTPs). Once formed, the NDPs may be further modified by intermediate enzymes before serving as substrates for glycosyltransferases.[3]

Sugar 1-phosphate nucleotidylyltransferases, also known as sugar nucleotide pyrophosphorylases (EC 2.7.7._), are vital to most biological glycosylation systems and are often used for the synthesis of sugar nucleotides.[4] α-D-glucose 1-phosphate thymidylyltransferase (Cps2L/RmlA) (EC 2.7.7.24) couples α-D-glucose 1-phosphate (Glc-1-P, **1**) and deoxythymidine triphosphate (dTTP, **2**), with the release of inorganic pyrophosphate ($PP_i$), to form deoxythymidine diphosphate-α-D-glucose (dTDP-Glc, **3**). This process occurs during the cell wall biosynthesis of many infectious pathogens (Scheme 1).[5] In general, thymidylyltransferases show high amino acid sequence identity (>60%). Cps2L from *S. pneumoniae* shares 89% identity with RmlA from *S. mutans* and 68% identity with RmlA from *P. aerugenosa*. See Appendix A for comparisons of Cps2L with select α-D-glucose 1-phosphate thymidylyltransferases.

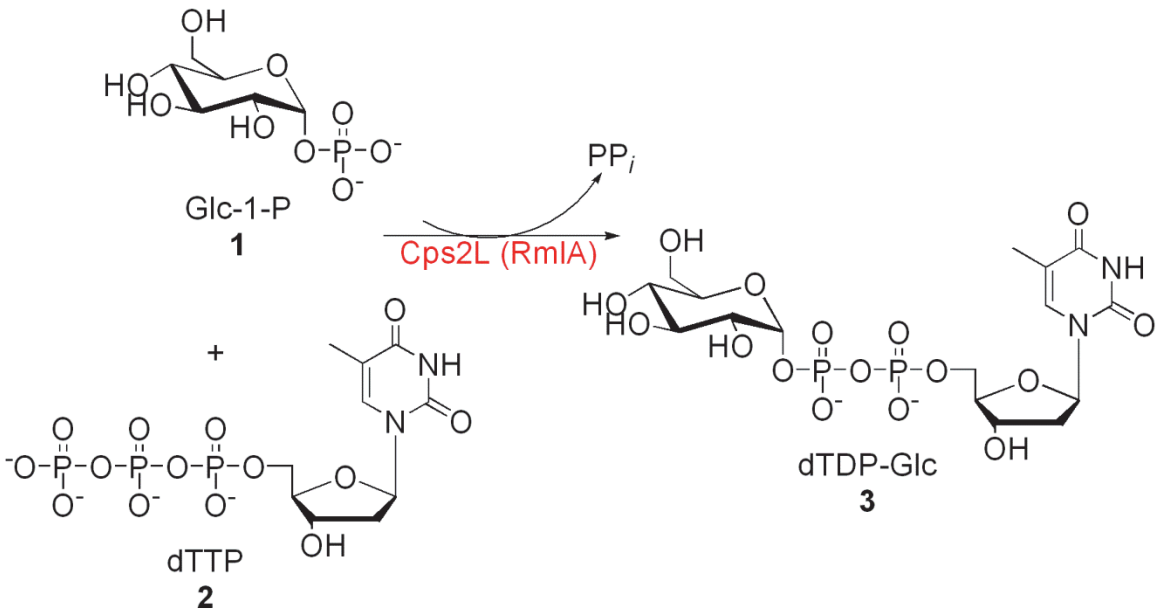


**Scheme 1** Cps2L/RmlA catalyzed reaction

## 1.1 Cps2L/RmlA Substrate Specificity

α-D-glucose 1-phosphate thymidylyltransferases (Cps2L/RmlA) have been shown to be promiscuous with respect to both their NTP and sugar-1-P substrates. With respect to NTP specificity, Cps2L/RmlA shows a particular preference for dTTP, but will also accept UTP as a substrate.[3,6,7,8,9,10,11] Cps2L/RmlA has shown even wider promiscuity with respect to sugar 1-phosphate substrates. Over 30 distinct sugar 1-phosphates have demonstrated substrate activity for the wild-type α-D-glucose 1-phosphate thymidylyltransferase and various mutants.[3,6,7,8,9,11,12] The ability of the thymidylyltransferase to accept such a broad range of substrates has allowed for the production of a variety of dTDP and UDP α-D-hexopyranosyl analogues.[6,7] The crystal structure of the *rml*A-encoded nucleotidylyltransferase, α-D-glucose 1-phosphate thymidylyltransferase ($E_p$) from *Salmonella enterica*, bound to UDP-α-D-glucose, was one of the first crystal structures of a thymidylyltransferase. This structure has provided clues to the catalytic mechanisms of all thymidylyltransferases.[3] Cps2L (*S. pneumoniae*) was the thymidylyltransferase used in all enzymatic experiments reported herein. Cps2L and $E_p$ share 67% identity (Appendix A). The protein sequence of $E_p$ is shown in Figure

1. The residues essential to substrate and cofactor binding are highlighted (see section 1.2).

| | | |
|---|---|---|
| **1** | mktrkgiila ggsgtrlypv tmavsqqllp iydkpmiyyp lstlmlagir diliistpqd | **60** |
| **61** | tprfqqllgd gsqwglnlqy kvqpspdgla qafiigeefi ghddcalvlg dnifyghdlp | **120** |
| **121** | klmeaavnke sgatvfayhv ndperygvve fdqkgtavsl eekplqpksn yavtglyfyd | **180** |
| **181** | nsvvemaknl kpsargelei tdinriymeq grlsvammgr gyawldtgth qslieasnfi | **240** |
| **241** | atieerqglk vscpeeiafr knfinaqqvi elagplsknd ygkyllkmvk gl | **292** |

**Figure 1** Protein Sequence of thymidylyltransferase $E_p$ (*S. enterica*)

## 1.2 Cps2L/RmlA Substrate Active Site Binding and the Role of $Mg^{2+}$

α-D-glucose 1-phosphate thymidylyltransferases, including Cps2L, RmlA and $E_p$, accept both dTTP and UTP as nucleotide substrates, however, cytidine triphosphate (CTP) does not generally act as a substrate for these enzymes. The reason for this is the capacity of the natural nucleotide substrates to hydrogen bond with specific amino acids within the active site of the enzyme. The N3 and O4 atoms of dTTP and UTP have been shown to exhibit hydrogen bonding to Gln 83. O4 and O2 are additionally bound to the N atoms of Gly 88 and Gly 11 respectively. The pentose ring contains a 3′-OH unit, which forms a final hydrogen bond with Gln 27.[3] The C4 amino group of CTP generates unfavorable interactions with Gln 83 and Gly 88, which hinders its capacity to act as a substrate. A variety of van der Waals interactions also come into play between dTTP and various leucine residues within the active site, which facilitate the formation of a hydrophobic cavity for the nucleoside (Figure 2a). Purine bases are too large to bind within the nucleoside pocket. The methyl substituent of dTTP is small enough to prevent any steric constraint for the binding of the pyrimidine moiety. The phosphate groups of the dTTP nucleotide are bound via a cascade of interactions with the main chain nitrogen units of Ser 13, Gly 14 and Thr 15.

The glucose-binding pocket of $E_p$ reveals that the glucose O2, O3 and O4 units form hydrogen bonds to amino acid residues directly, whereas the O6 connection to the enzyme is by way of a water linker molecule. O2 and O3 are both bound to Gln 162. O3

and O4 are both bound to N on the main chain N of Gly 147 and the Val 173 main chain O binds O4. Thr 201 may also play a role in hydrogen binding given that it is in close proximity to O2 and O3. A bridge of four water molecules additionally serves to link the glucose component of Glc-1-P to the enzyme. Trp 224 and Tyr 146 residues, which are close to the substrate in the binding pocket, are believed to be stabilized via van der Waals interactions between the bottom of the pyranose ring and the Leu 109, Leu 89 and Ile 200 residues.

It has been demonstrated that the divalent cation $Mg^{2+}$ plays a vital role in stabilizing $PP_i$ as a leaving group in the thymidylyltransferase catalyzed formation of dTDP-Glc.[13] $Mg^{2+}$ is in close proximity to the β-phosphate oxygen atom and coordinates directly to Gln 26 via the side chain, and the O of Gly 11 via the main chain. The N of Ser 13, along with two water molecules, also facilitates $Mg^{2+}$ binding. The amino acid residues are slightly disordered in the presence of $Mg^{2+}$ within the enzyme-UDP-Glc structure and, as a result, it is suspected that $Mg^{2+}$ also plays a role in structural organization of the active site with respect to orientation of the nucleotide substrate (Figure 2c).

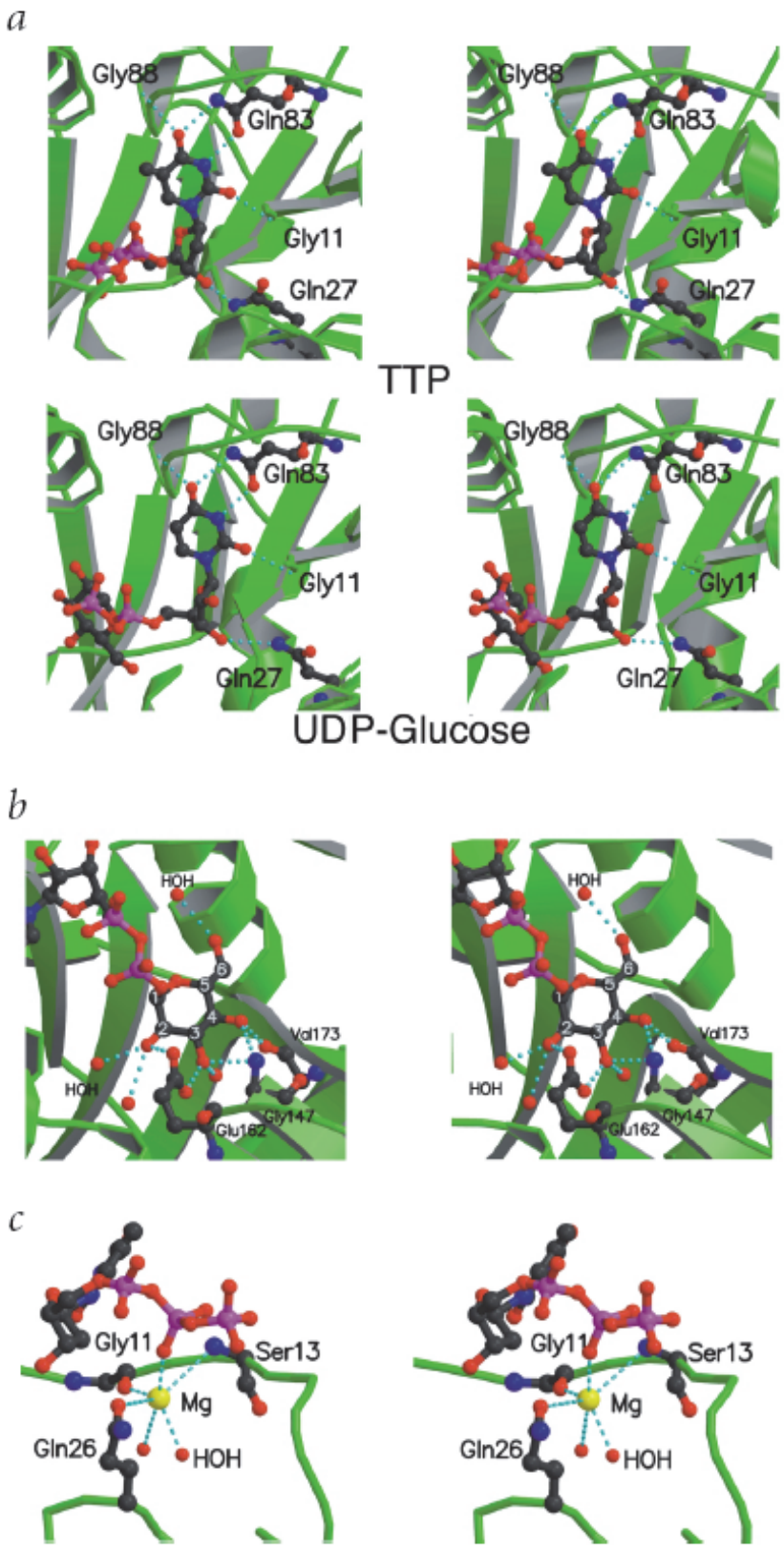


**Figure 2** Crystal structures of thymidylyltransferase $E_p$ (*S. enterica*)[3]

## 1.3 Cps2L/RmlA Inhibition

Prokaryotic nucleotidylyltransferases are often prone to allosteric inhibition by biosynthetic pathway compounds, which differ from their natural substrates or products.[14] A hydrophobic pocket located at the monomeric junction of Cps2L/RmlA is likely to serve as an allosteric binding site for inhibitors. Allosteric inhibitors can be advantageous to active site inhibitors in that they frequently exhibit higher selectivity. This is due to lower homology, relative to active site residues, across an array of similar functioning enzymes. The binding of inhibitors to the thymidylyltransferase allosteric site effectively leads to changes in the conformation of the monomeric active site and reduces the effectiveness of natural substrate binding. The product of RmlD is dTDP-β-L-rhamnose (dTDP-Rha, **6**), which serves as the substrate for the glycosyltransferase in the biosynthetic pathway of many harmful bacteria. dTDP-β-L-rhamnose was shown to act as an allosteric inhibitor for RmlA.[15,16] Figure 3 shows RmlA bound to dTDP-β-L-rhamnose. There are no direct amino acid interactions with the P—O—P bisphosphonate functionality of dTDP-β-L-rhamnose when it is allosterically bound to RmlA.[16] The allosteric site is the presumed point of regulatory control for the L-rhamnose biosynthetic pathway. In addition to dTDP-β-L-rhamnose, dTDP-α-D-glucose, dTDP and dTMP are all capable of binding to the allosteric site.[16] This suggests that the thymidine moiety is an important component for allosteric binding to RmlA.

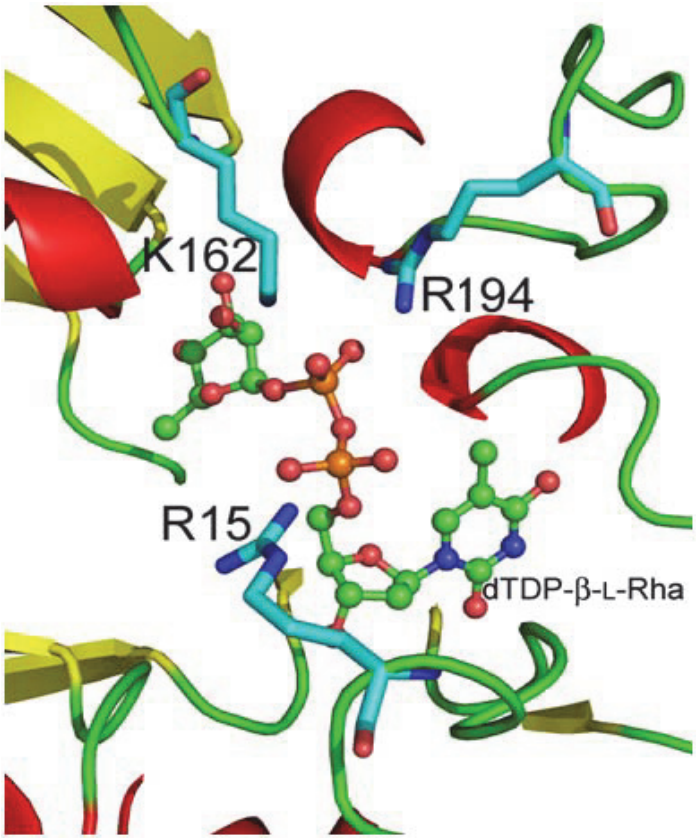


**Figure 3** Allosteric site binding of dTDP-β-L-rhamnose to RmlA (*P. aeruginosa*)

A series of thymidine based small molecule inhibitors were developed by Alphey, Naismith and coworkers[16] and found to exhibit nanomolar inhibition against *P. aeruginosa*. Figure 4 shows the general structure for the inhibitors, as well as the structure of the most potent inhibitor. The inhibitors work by mimicking the thymidine portion of dTTP and were found, via crystal structure analysis, to bind only to the allosteric site. Despite binding to a secondary site, the inhibitors were determined to be competitive in nature. They function by locking the conformational state of RmlA and preventing adequate Glc-1-P binding. To date, these are the most potent small molecule RmlA inhibitors reported. Even though thymidine is ubiquitous in various eukaryotic systems, human nucleotidylyltransferases do not possess the allosteric regulatory site that is so prevalent in prokaryotic thymidylyltransferase containing organisms. Additionally, as imperfect thymidine mimics, they are not expected to be effective against other thymidine binding enzymes.

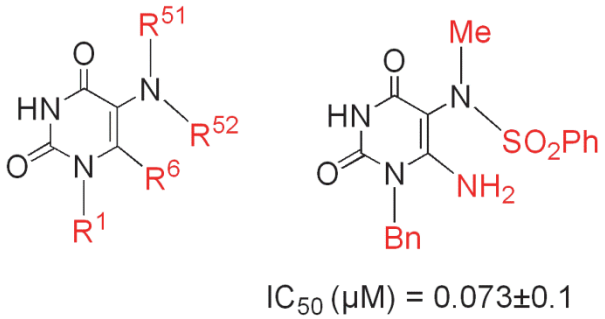


**Figure 4** Potent thymidine analogue inhibitors of RmlA (*P. aeruginosa*)[16]

## 1.4 Cps2L/RmlA Mechanism and the Role of RmlB-D

Carbohydrates play essential roles in substrate recognition and cell signaling.[17] They have higher functionalization density than most amino acids in the sense that most carbon atoms within carbohydrates are bound to one or more heteroatoms, with oxygen being the most common.[18] Naturally occurring sugars found in mammalian eukaryote species, like glucose and fructose, are usually D-configured. By contrast, bacteria often incorporate L-configured sugars, like L-rhamnose, into their cell walls. The bacterial cell wall and its sugar constituents are particularly unique, making them, or their associated biosynthetic enzymes, viable targets for antibiotics.

Vancomycin-resistant *Staphylococcus aureus* (VRSA), methicilin-resistant *Staphylococcus aureus* (MRSA), and *M. tuberculosis* are some of the current most prevalent pathogens in hospital acquired infections.[19] These bacteria have shown increasing clinical resistance to commonly used antibiotics like β-lactams, tetracyclines and fluoroquinolones. The mechanisms of resistance for pathogens, like *M. tuberculosis*, usually entail alterations to drug target proteins involved in cell wall synthesis..[20,21,22,23] Cell wall assembly is a commonly pursued target for various bacterial enzyme inhibitors in that the cell wall is essential for bacterial survival and virulence. The L-rhamnose sugar serves as a linking unit between arabinogalactan and peptidoglycan[17] and is a necessary constituent of the bacterial cell wall in many bacterial species.[16]

The biosynthetic pathway of L-rhamnose has been actively investigated for several decades.[24] Since dTDP-β-L-rhamnose has been shown to inhibit RmlA, the intermediate enzymes (RmlB-D) can potentially be exploited for the generation of novel

RmlA and Cps2L inhibitors. This makes understanding the function and mechanism of RmlB-D to be of great importance in the design and synthesis of inhibitors for thymidylyltransferases like Cps2L and RmlA. The synthesis of dTDP-Glc, the primary source of L-rhamnose for the cell wall, was outlined in Scheme 1. The thymidylyltransferase is the first enzyme in the pathway. Its role in substrate binding has already been discussed. The mechanism of action of Cps2L/RmlA is addressed below. RmlB-D are the subsequent intermediate enzymes, which lead to the final dTDP-β-L-rhamnose sugar donor product. The transfer of L-rhamnose from dTDP-β-L-rhamnose to an acceptor by a rhamnosyltransferase provides the driving force for the Rml catalyzed reactions.[18] The mechanism of action of RmlB dehydratase is discussed below, followed by a discussion of a proposed mechanism for the action of RmlC epimerase. The RmlD reductase will not be discussed in detail.

Cps2L/RmlA catalyzes the formation of dTDP-Glc in an ordered Bi-Bi mechanism. By this mechanism, the dTTP substrate binds first, followed by Glc-1-P. An $S_N2$ attack of the phosphate group of Glc-1-P on the α-P of dTTP then facilitates the formation of a pentavalent transition state. $PP_i$ is first released followed by the dTDP-Glc product.[25] The mechanism of action of Cps2L/RmlA is outlined in Scheme 2.

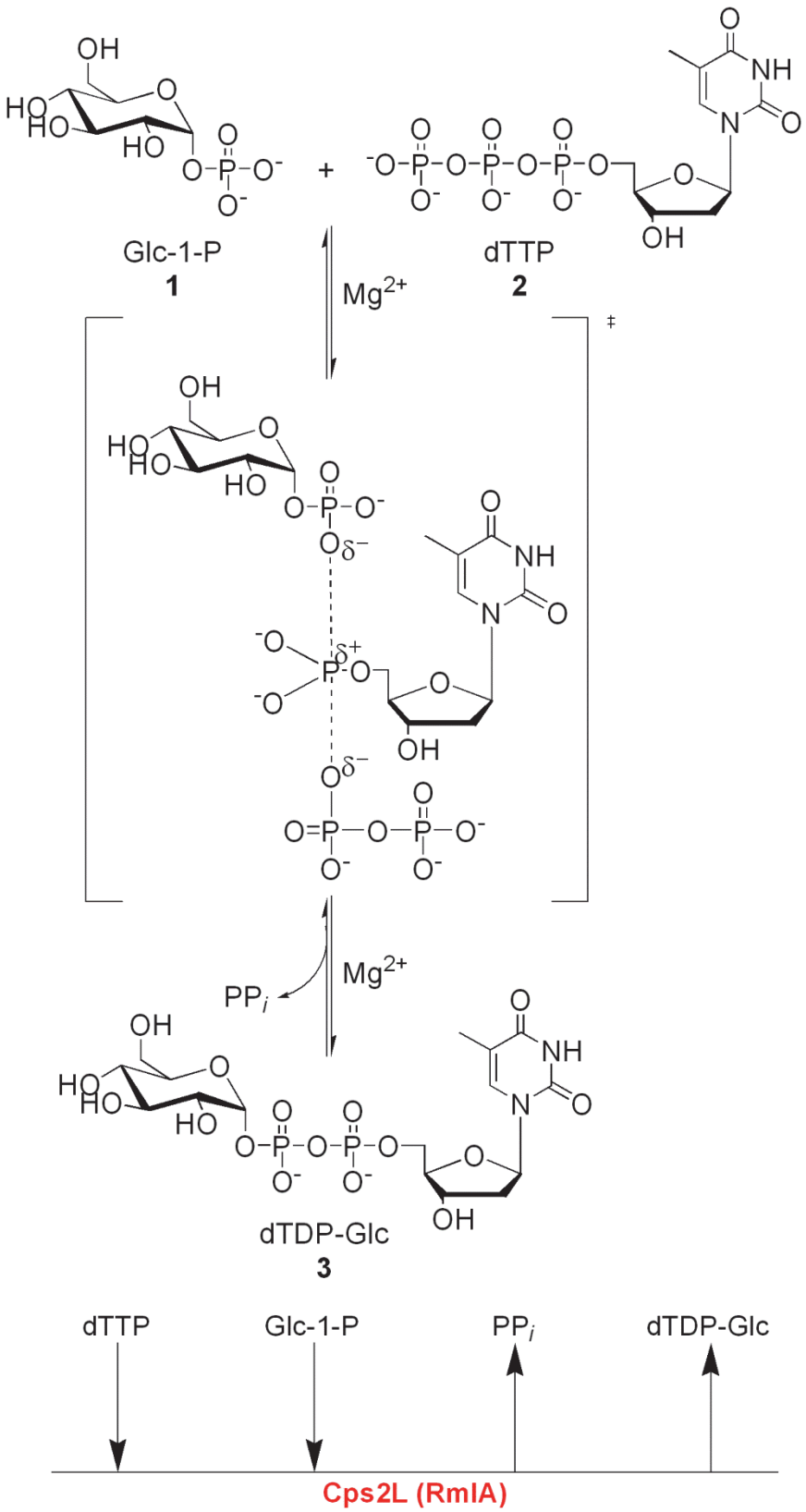


**Scheme 2** Cps2L/RmlA mechanism

RmlB (EC 4.2.1.46) is responsible for the oxidation of the C4″ hydroxyl unit and C6″ dehydration. RmlC (EC 5.1.3.13) catalyzes an uncommon double-epimerization at both C3″ and C5″. RmlD (EC 1.1.1.113) lastly serves to carry out a reduction at C4″ to produce dTDP-β-L-rhamnose (Scheme 3).[18]

The mechanism of action for RmlB involves three steps in the order of an oxidation, dehydration and reduction (Scheme 4).[26] A group of Tyr, Lys and Ser/Thr residues serve to remove the C4″ proton to start the process, which is assisted by $NAD^+$.[27] The Glu 135 residue acts as a general base for the abstraction of a proton at C5″. The next step is an Asp 135 assisted dehydration. The subsequent reduction of the C5″/C6″ double bond by NADH and a Glu residue generates dTDP-4-keto-6-deoxy-D-glucose (**4**).

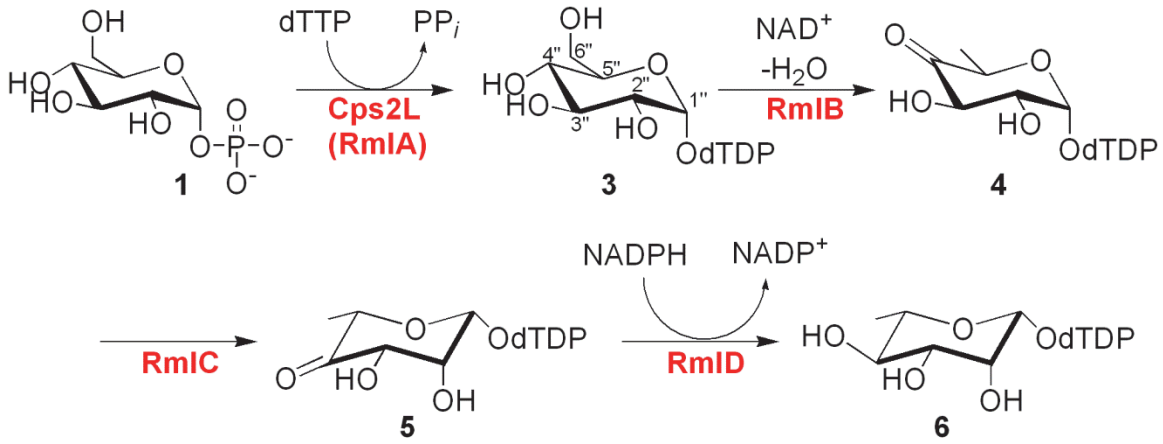


**Scheme 3** The biosynthetic pathway of L-rhamnose

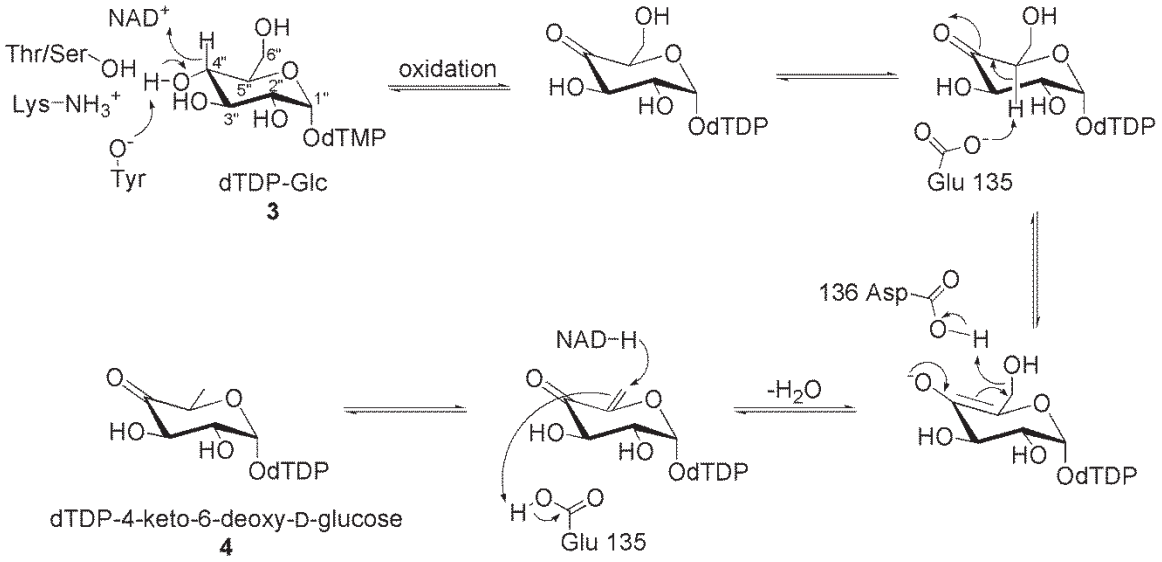


**Scheme 4** RmlB mechanism

RmlC substrate binding is facilitated by Trp 146, which stacks against the thymine moiety. The mechanism of action of RmlC has not been fully elucidated. It is speculated to begin with either a C3″ or C5″ proton abstraction from a His 76 residue to generate an enolate. The Lys 82 residue is believed to play a role in reducing the p$K_a$ of these protons by stabilizing the charge on the C4″ oxygen. A Tyr residue contributes the proton for the first epimerization. The second epimerization is believed to proceed, again, with the aid of a His base and a Tyr acid residue.[18]

The RmlD reductase possesses a similar fold to the RmlB dehydratase. NADPH is serves as a cofactor for the enzyme, with the nicotinamide ring forming an internal hydrogen bond with the amide and α-phosphate of NADPH. The hexose ring of dTDP-β-L-rhamnose is suspected to sit between the NADPH carboxamide and a supporting Tyr 106 residue. One significant difference between RmlB and RmlD is that RmlD requires stoichiometric quantities of reactants, whereas RmlB does not.

It has been shown that disruption of any of the *rml* genes, which encode for the Rml enzymes, will effectively result in inhibition of cell wall polysaccharide biosynthesis.[28] The bacteria were found to survive in certain circumstances when they were in a sucrose-rich environment, however their ability to sustain infection was eliminated.[29] Manipulation of the pathway for *P. aeruginosa* was shown to have a particularly lethal effect on the bacteria, making it an important avenue to explore for antibiotics.[29]

# CHAPTER 2 PHOSPHONATES AND THIOPHOSPHATES AS ANALOGUES OF NATURAL PHOSPHATES

Since the 1960s, there have been a variety of methods focusing on the preparation and investigation of phosphonates and their ability to act as analogues of natural phosphates.[30] Phosphonates possess a phosphorous-carbon (P—C) bond that is stable to hydrolysis mediated by typical phosphate-cleaving enzymes. The phosphorus-oxygen (P—O) ester linkages present in the phosphonates are still vulnerable to hydrolysis, providing the potential for phosphonate groups to be transferred between substrates during enzymatic reactions. If the P—O group of the phosphate is not directly involved in the site of action of the enzyme, a phosphonate analogue may provide a longer-lived substrate than the natural phosphate, thus enhancing metabolic activity. Contrarily, if the P—O group is directly involved in the reactivity of the enzyme (by means of binding and/or activity) than the P—C unit of a phosphonate group may potentially bring about an inhibitory effect by preventing the natural phosphate from interacting with the enzyme.

Most studies on phosphonates investigate the modification or inhibition of natural phosphate transfer processes by introducing a phosphonate analogue in the place, or presence of, the natural phosphate. Many phosphonates, particularly those possessing halogenated substituents on the methylene unit, have biomedical applications.[30,31] Blackburn first proposed the introduction of halogens into the methylene functionality in an effort to better mimic the properties of the natural phosphate.[32] Fosfomycin, a phosphonate containing natural product isolated from soil bacteria in 1969, has broad-spectrum antibacterial activity.[33] Dichloromethylene diphosphonic acid (chlodronic acid) has been shown to inhibit RNA polymerase activity in influenza,[34] and both the related mono and difluoromethylene diphosphonates have been implicated as bone lysis inhibitors[35] and antiviral agents.[36,37] Several monofluoro phosphonates have also been probed as enzyme inhibitors in biochemical processes.[38,39]

## 2.1 Phosphonate Acidity and Geometry

The acidic properties of phosphonic acids, as compared to their analogous phosphoric acids, differ distinctly at the second p$K_a$ value. A series of p$K_a$ experiments determined the p$K_a$2 for a group of primary alkyl phosphonates to be within the range of 7.7-8.2.[40] These values are higher than the corresponding alkyl phosphate equivalent compounds, which possessed p$K_a$2 values around 6.4-7.0.[40] Both mono and difluorophosphonates, possessing CHF and $CF_2$ units respectively, have been shown to better mimic the electronic properties of a phosphate oxygen than the $CH_2$ unit of the phosphonate. The inductive effect of the fluorine atoms(s) brings about a reduction in the p$K_a$2 of the phosphonates, which effectively brings it closer to the physiological value of a natural phosphate. Monofluoro phosphonate p$K_a$2 values are in the range of 5.5-6.5,[41] and difluoro phosphonates have reported p$K_a$2 values in the range of 5.0-5.4.[40,41] A decrease of approximately 0.5-1 p$K_a$ unit per fluorine atom can be expected when comparing the acidity of the fluorinated phosphonates to a standard alkyl phosphonate.[42,43,44] The number of fluorine atoms (0-2) and resultant p$K_a$2 value are believed to play a qualitative role in the ability for phosphonate analogues to act as enzyme substrates or inhibitors.

Phosphonates exist in their salt forms under physiological conditions (pH ~7.4). As a result, few of the many phosphonates with therapeutic properties have been developed into effective drugs, due to low bioavailability.[45] One approach, implemented by medicinal chemists, has been to produce prodrug phosphonates by masking them as neutral esters. The most commonly used prodrug phosphonates are the acyloxyalkyl esters (e.g. pivaloyloxymethyl (POM) esters).[46] The decrease in polarity of the phosphonate esters, relative to their salt forms, allows them to more easily permeate cells or tissues. The esters are cleaved intracellularly to generate the active phosphonates. These compounds may then go on to bring about their biological effect directly, or be converted to potentially more active therapeutics (e.g. sugar nucleotide analogues) via intracellular mechanisms.[45]

There are notable geometric differences between inorganic pyrophosphate ($PP_i$) and its phosphonate equivalent, methylene bisphosphonate (MBP). Significant angular differences (greater than 10%) were apparent around the central methylene unit of MBP

when compared to the central oxygen of $PP_i$.[47] An analysis of the 5-atom internuclear distance for the conformation of each species (OPOPO and OPCPO) revealed a 16% increase in length for MBP relative to $PP_i$.[47,48,49,50,51,52] The deviation in angle and distance could potentially impair or inhibit the MBP analogues from enzymatic binding to pyrophosphate sites if the P—O—P region is significantly involved in substrate binding or orientation.

## 2.2 Nucleoside Bisphosphonates

Methylene bisphosphonic acid (**7**) is one of several $PP_i$ analogues that have been commonly employed in organic synthesis (Figure 5).[30] It is easily prepared by acid catalyzed hydrolysis of a tetraalkyl ester equivalent. Bisphosphonate analogues containing a substituent bearing a lone pair between the phosphorous groups (i.e. **8-9**, **11-13**) have been demonstrated to mimic the binding capability of the P—O—P unit of the bisphosphate better than the P—C—P unit of MBP, in some cases.[53,54] It is expected that these compounds can enhance enzyme-complex binding via stabilizing interactions with amino acid residues, or by way of a divalent cation coordination.

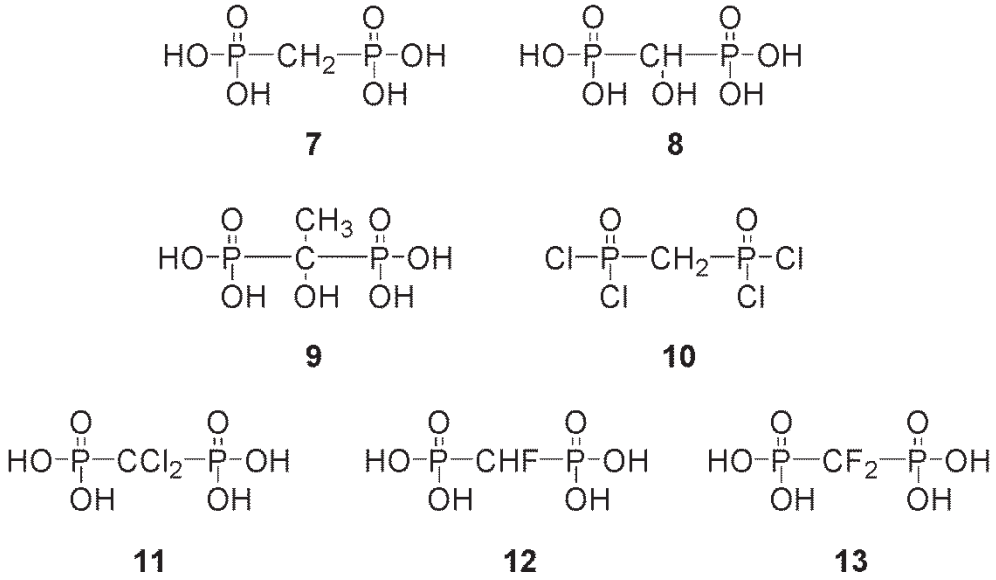


**Figure 5** Some examples of commonly used $PP_i$ analogues in organic synthesis

Ribonucleoside 5′-oligophosphates (e.g. ATP) are active participants in many biochemical processes, which prompts the need for the production of ribonucleoside 5′-oligophosphate analogues. The pyrophosphate chain is an ideal target for modification of these compounds. Several methods are commonly employed in the synthesis of ribonucleoside 5′-methylene bisphosphonates. The first of these methods involves a reaction with an appropriately protected nucleoside nucleophile and an efficiently activated MBP electrophile.[55,56,57] The second method utilizes a nucleophilic MBP reacted with a 5′-sulfonyl nucleoside electrophile.[58,59,60] A third, and more recent method, was developed by Shipitsyn and colleagues, which produces the MBP-nucleoside product and does not involve any prior electrophilic activation of the MBP or the nucleoside.[61] This method utilizes methylenebis(phosphonic dichloride) (MBPDC) (**10**), which effectively condenses with a protected nucleoside in the presence of tributylamine and triethylphosphate (TEP). MBPDC has been commonly used to prepare many symmetric and asymmetric di and tetraalkyl MBP derivatives,[62] however its use in the production of monoalkylated MBP derivatives is rare. Unfortunately, the above mentioned three methods only generate the desired compounds in poor to modest yields.

Kalek, Darzynkiewicz and coworkers were able to expand on previous methods,[61,63] to produce MBP-nucleoside compounds with an approach that was both efficient and high yielding.[64] By using trimethylphosphate (TMP) as the solvent, they were able to develop a route to a series of ribonucleoside 5′-methylene bisphosphonates using unprotected adenosine, guanosine, uridine and cytidine (A, G, U ,C) bases with HPLC conversions ranging from 65-89% (Scheme 5). To date this appears to be the most effective method for producing these compounds.

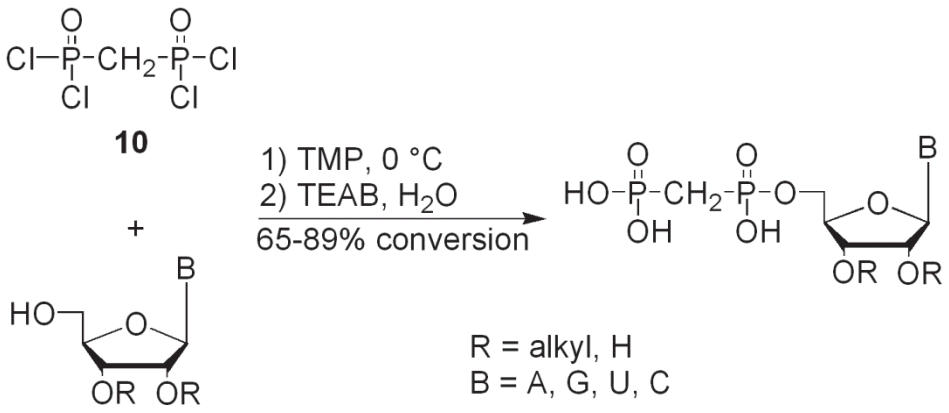


**Scheme 5** Kalek method for synthesizing MBP-nucleosides[64]

## 2.3 Carbohydrate Containing Phosphonates and Bisphosphonates

There is a lack of biochemical investigation into the role of phosphonate analogues of sugar containing phosphates. Several approaches to synthesizing carbohydrate phosphonate analogues of natural sugar phosphates have been reported.[65,66,67] The first examples for the preparation of α-D-glucose-1-MBP were reported by Krahl and Cori, and Posternak in 1949.[68,69] There are very few literature reports on the synthesis of sugar-MBP derivatives and even less so on the synthesis of sugar-phosphonate-nucleoside compounds. Cipolla *et. al.* recently reported an effective synthesis of the 1C phosphonate analogue of UDP-*N*-acetylglucosamine (UDP-GlcNAc) and its evaluation as an *O*-linked GlcNAc transferase inhibitor.[70] This compound makes use of replacing the anomeric phosphate ester linkage of UDP-GlcNAc with a methylene unit. Examples of methods for producing sugar-MBP-nucleoside products, with the methylene unit at the central pyrophosphate position, are even rarer.

Vaghefi and coworkers provide the only known method for the synthesis of a glucose-MBP-nucleoside in their efforts to generate potential inhibitors for glycosyltransferase enzymes.[71] They were able to fuse the MBP derivative (**15**) with β-D-glucopyranose pentaacetate (**14**) at 170°C, under vacuum. The reaction produced 2,3,4,6-tetra-*O*-acetyl-α-D-glucopyranosyl 1-[[(diphenoxyphosphinyl)methyl]phosphonate] (**16**) in 52% yield, as the α diastereomer. Platinum catalyzed hydrogenation served to remove the phenyl protecting groups on the MBP unit, and alkylation with 2′,3′-di-*O*-

acetyladenosine (**17**) was carried out using 1-(mesitylene-2-sulfonyl)-3-nitro-1,2,4-triazole (MSNT) as a bisphosphonate activation reagent. The acetyl protecting groups were then removed under basic conditions to give rise to the final sugar-MBP-nucleoside compound, adenosine 5′-[[(α-D-glucopyranosyl]hydroxyphosphinyl)methyl]phosphonate] (**18**), in less than 15% overall yield (Scheme 6). Uridine 5′-[[(α-D-galactopyranosyl]hydroxyphosphinyl)methyl]phosphonate] (UMBP-α-D-gal) and guanosine 5′-[[(α-D-mannopyranosyl]hydroxyphosphinyl)methyl]phosphonate] (GMBP-α-D-man) were also synthesized in an analogous manner. The three compounds were tested for their inhibitory effect on galactosyltransferase (EC 2.4.1.38). Only the UMBP-α-D-gal was shown to act as a competitive inhibitor, with a $K_i$ of 97 μM. This appears to be one of the only examples of glycosyltransferase inhibition involving these sugar-MBP-nucleoside compounds. The capacity for these sugar-MBP-nucleosides to act as nucleotidylyltransferase inhibitors has never been investigated.

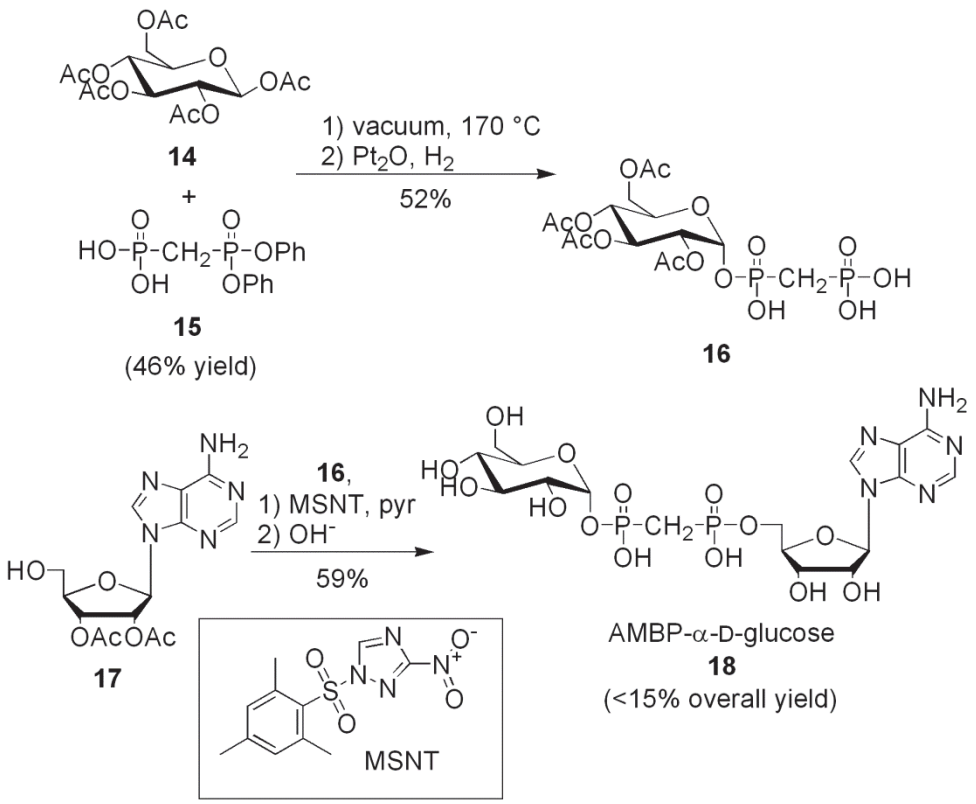


**Scheme 6** Synthesis of AMBP-α-D-Glc[71]

## 2.4 Glycosylated Thiophosphates

Thiophosphates are analogues of natural phosphates in which the P—O bond has been replaced with a phosphorous-sulfur P—S bond. The sulfur atom in the thiophosphate scaffold has the capability to mimic both the binding and nucleophilic properties of an oxygen atom in the scaffold of the natural phosphate.[72,73] Glycosyl thiophosphates are important to evaluate as analogues of glycosyl phosphates, which are of paramount importance in biological systems as key metabolic intermediates and cell wall constituents.[74,75] Many classes of enzymes use phosphate or pyrophosphate as substrates or recognition elements. The mechanism of enzymatic phosphoryl transfer remains a contentious issue, with metal fluoride complexes providing a new class of transition-state analogues as mechanistic probes.[76] In recent years, the use of phosphate using enzymes (phosphorylases) toward the production of oligosaccharides has increased.

Oligosaccharides are often products of phosphorylases, which can be difficult to synthesize in stereospecific forms, as many synthetic methodologies produce compounds in diastereotopic mixtures, with varying α/β selectivity. The strict regio- and stereoselectivity of phosphorylases validates the use of these enzymes as appealing alternatives to the chemical synthesis of oligosaccharides.[77] Phosphonothioates derivatives of the form $RPS(OR')_2$ (R = alkyl, R′ = alkyl, H) have sparked interest as plausible inhibitors of enzymes in metabolic reactions involving natural phosphates. Xu, Prestwich and coworkers reported the synthesis and evaluation of several phosphonothioate analogues as inhibitors of lysophosphatic acid (LPA) receptors, which are involved in the proliferation and differentiation of metastatic cancer cells.[78] Glycosyl thiophosphates are potential candidates for probing the substrate and inhibition mechanisms of phosphorus using enzymes. To date, the only example of an enzymatically generated free sugar glycosyl thiophosphate was reported by Cai, Wang and coworkers in 2011.[79] Using NahK (EC 2.7.1.162), an *N*-acetylhexosamine 1-kinase, they were able to produce GlcNAc-1-thiophosphate on a milligram scale from GlcNAc and commercially available γ(S)ATP. The GlcNAc-1-P uridyltransferase GlmU (EC 2.3.1.157) was then utilized to produce UDP(βS)-GlcNAc in 43% yield (Scheme 7). While these are some of the few examples of exploring the enzymatic and therapeutic

applications of thio substitutions on natural phosphates or phosphonates, more will undoubtedly arise in the near future.

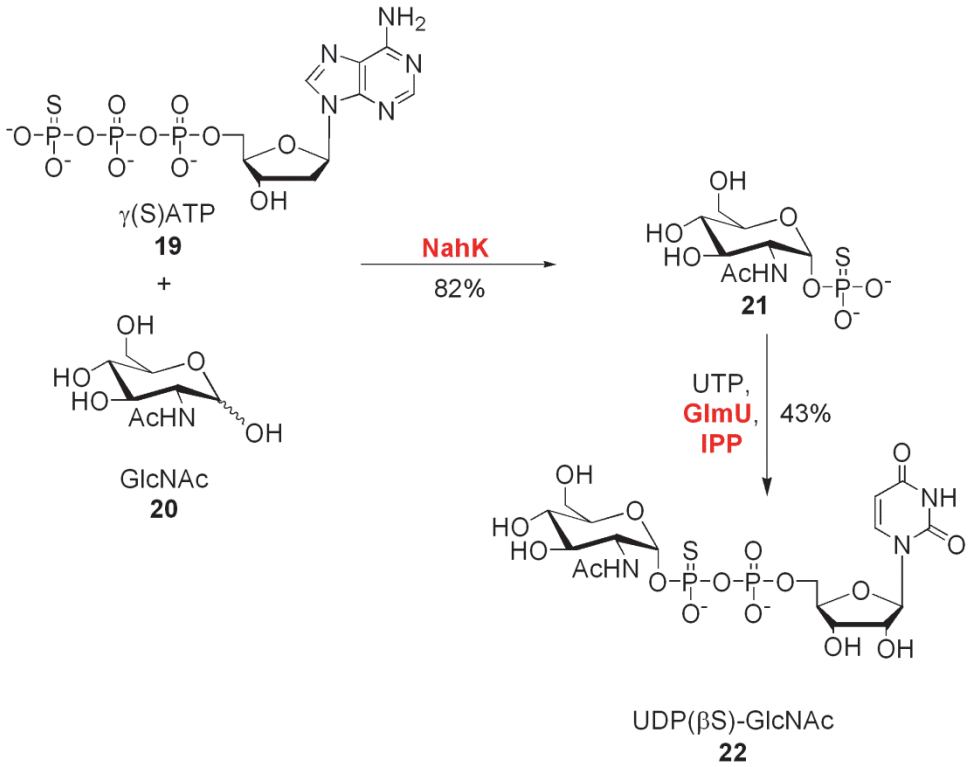


**Scheme 7** Enzymatic synthesis of GlcNAc-1TP and UDP(βS)-GlcNAc[79]

Through chemical synthesis, glycosyl thiophosphates have been produced in both *O* and *S*-glycosylated forms. *O*-glycosyl thiophosphates have been previously synthesized as glycosyl donors for the stereoselective production of glycosides. Zhang, Hui and coworkers report the synthesis of acetyl and benzyl-protected glycosyl dimethylthiophosphates in 51% and 86% yields respectively.[80] They were able to generate several diastereotopic mixtures of fully protected glycosyl thiophosphates with varying α/β selectivity depending on the nature of the glycosyl protecting groups. *S*-glycosyl thiophosphates have been prepared, originally for studies on the stereochemistry of phosphorous in enzyme coupled reactions.[81] More recently, Piekutowska and Pakulski generated a series of benzoyl-protected mannose, galactose and glucose *S*-glycosyl thiophosphates by reacting anomeric thiocyanates with *O*-alkyl or *O*-trimethylsilyl phosphites.[82] The global deprotection of these glycosyl thiophosphates has not been reported. Both α and β glucose 1-phosphate have been implicated as intermediates in

bacterial cell wall assembly, making their thiophosphate analogues attractive synthetic targets. β-D-glucose 1-phosphate is a substrate for β-phosphoglucomutase and is suspected to be a precursor for cell wall material in *Lactococcus lactis*.[83,84] α-D-glucose 1-phosphate is a substrate for various nucleotidylyltransferases in a number of the biosynthetic pathways of harmful pathogens.[16,85] Cps2L is a prime candidate for evaluating glycosyl thiophosphates as substrate mimics of glycosyl phosphates. No synthetic route currently exists to access fully deprotected *O*-glycosyl and *S*-glycosyl sugar 1-thiophosphates. Based on their similar isoelectronic and isosteric properties to sugar 1-phosphates, there is a strong potential for these compounds to act as substrates for various enzyme systems.

## 2.5 Thesis Objectives

The aims of the project were as follows:

- To design, synthesize and evaluate phosphonate-based inhibitors of Cps2L.
- To gain insights into the binding promiscuity of the L-rhamnose biosynthetic pathway enzymes (Cps2L, RmlB-D) with respect to sugar nucleotides.
- To explore synthetic methodologies for the generation phosphonate containing analogues of sugar nucleotides.
- To explore synthetic routes toward the production of α-D-glucose 1-thiophosphate, a probable substrate for Cps2L and potential precursor toward novel glycosyltransferase substrates or inhibitors.

### 2.5.1 The Design and Synthesis of Glycosylated Phosphonate and Thiophosphate Compounds

The synthesis of nucleotidylyltransferase inhibitors was inspired by the structure of dTDP-β-L-rhamnose, which was shown to act as an allosteric inhibitor for RmlA.[15] Two strategies for the generation of the sugar nucleotide analogues were explored and evaluated. The first focused on using commercially available L-rhamnose to synthesize β-

L-rhamnose-1C-phosphonate analogues. It was postulated that these phosphonate analogues could be evaluated as Cps2L inhibitors directly, or coupled with nucleoside monophosphates to produce the sugar nucleotide analogues (Scheme 8).

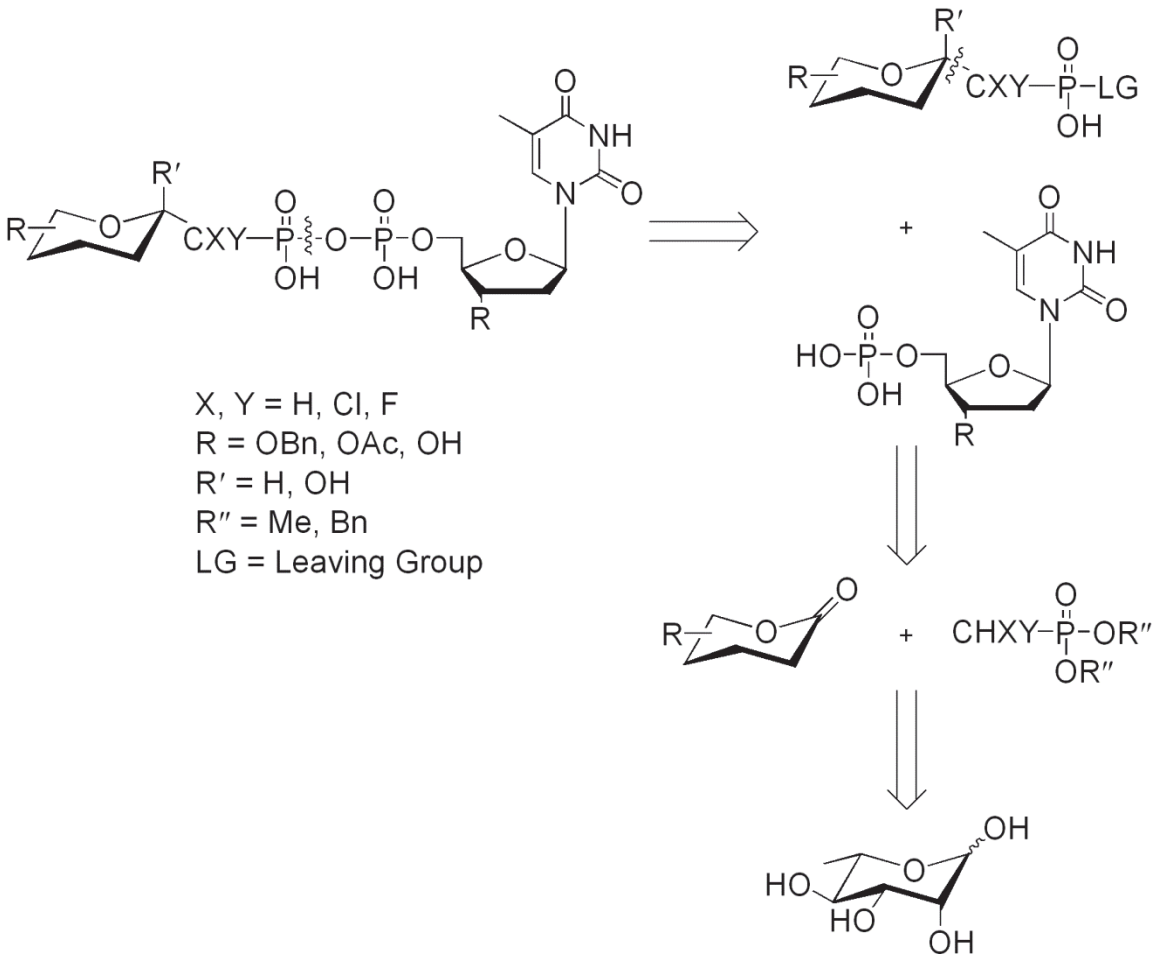


**Scheme 8** Retrosynthetic strategy 1

The second approach that was explored used synthetic methodology based on the assembly of phosphonate linkages to produce deoxythymidine 5′-[[(α-D-glucopyranosyl]hydroxyphosphinyl)methyl]phosphonate] (dTMBP-α-D-Glc) analogues. These compounds could act as phosphonate mimics of dTDP-α-D-glucose, the natural substrate for RmlB. Generation of the dTMBP-α-D-Glc analogues was attempted using the retrosynthetic strategy outlined in Scheme 9. The strategy entailed appending the glucose and thymidine moieties to each of the terminal ends of the preassembled bisphosphonate centre scaffold.

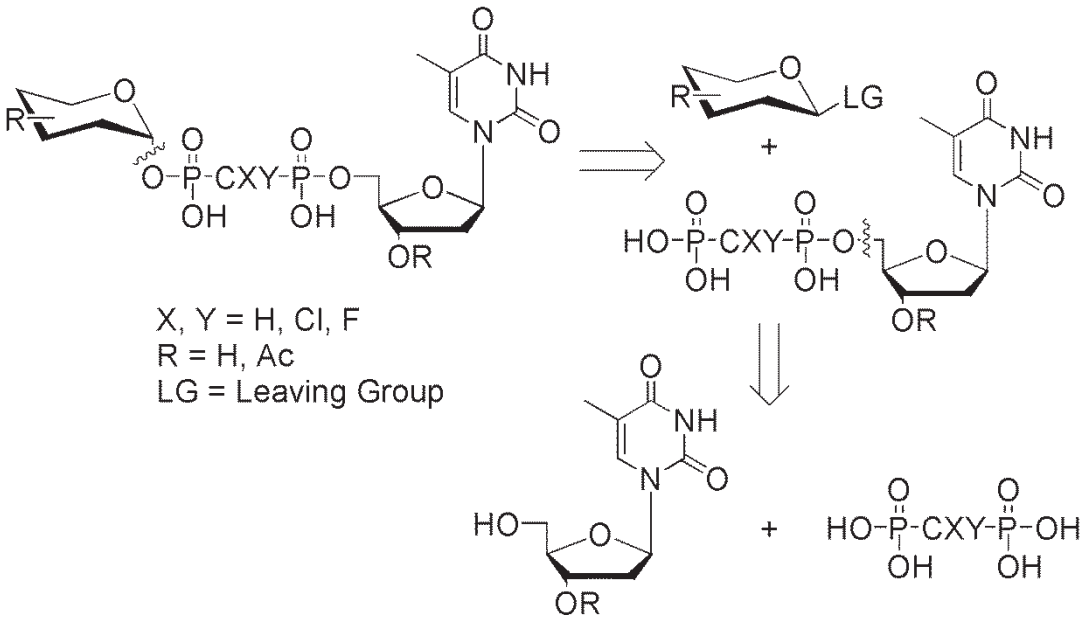


**Scheme 9** Retrosynthetic strategy 2

While the β-L-rhamnose-1C-phosphonate nucleoside monophosphate analogues could be chemically synthesized, the dTMBP-β-L-rhamnose analogues would need to be formed using the L-rhamnose biosynthetic pathway (Scheme 10). This is because the 1,2-*cis* β-L-rhamnose linkages are synthetically challenging targets due to both the anomeric effect and neighboring group participation phenomenon driving toward the preferential formation of α-L-rhamnosides. The use of 4,6-*O*-benzylidene protecting groups have been effective in the production of 1,2-*cis* glycosides bearing a C2 axial substituent (e.g. β-D-mannosides),[86] however, the absence of the 6-OH group in the L-rhamnose scaffold renders this method ineffective for the synthesis of β-L-rhamnosides.

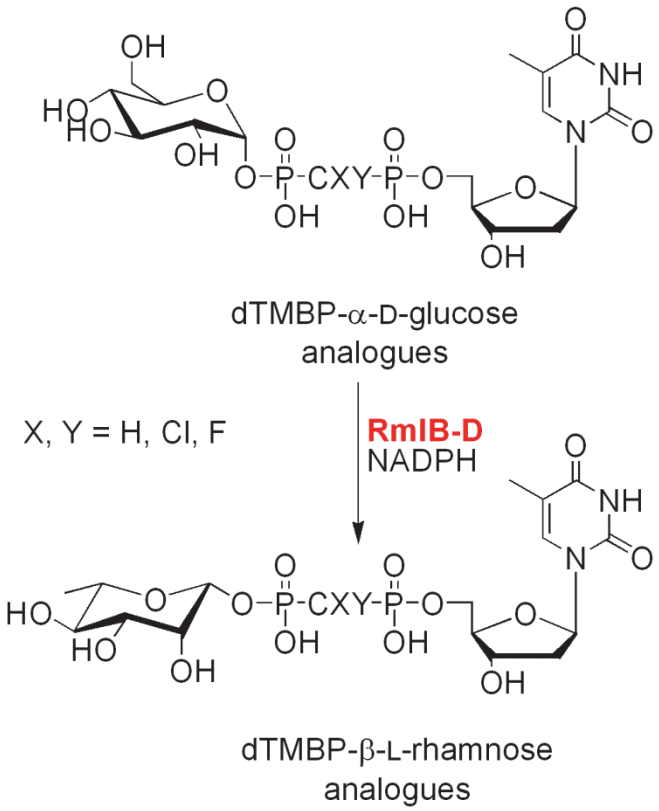


**Scheme 10** Enzymatic strategy to produce nucleotidylyltransferase inhibitors

The synthesis of substrates for nucleotidylyltransferases could be investigated by using thiophosphate analogues of α-D-glucose 1-phosphate. The analogues could be substituted for the natural α-D-glucose 1-phosphate substrate of Cps2L, in an effort to generate novel sugar nucleotide products, which incorporate the thiophosphate functionality into their structures (Scheme 11).

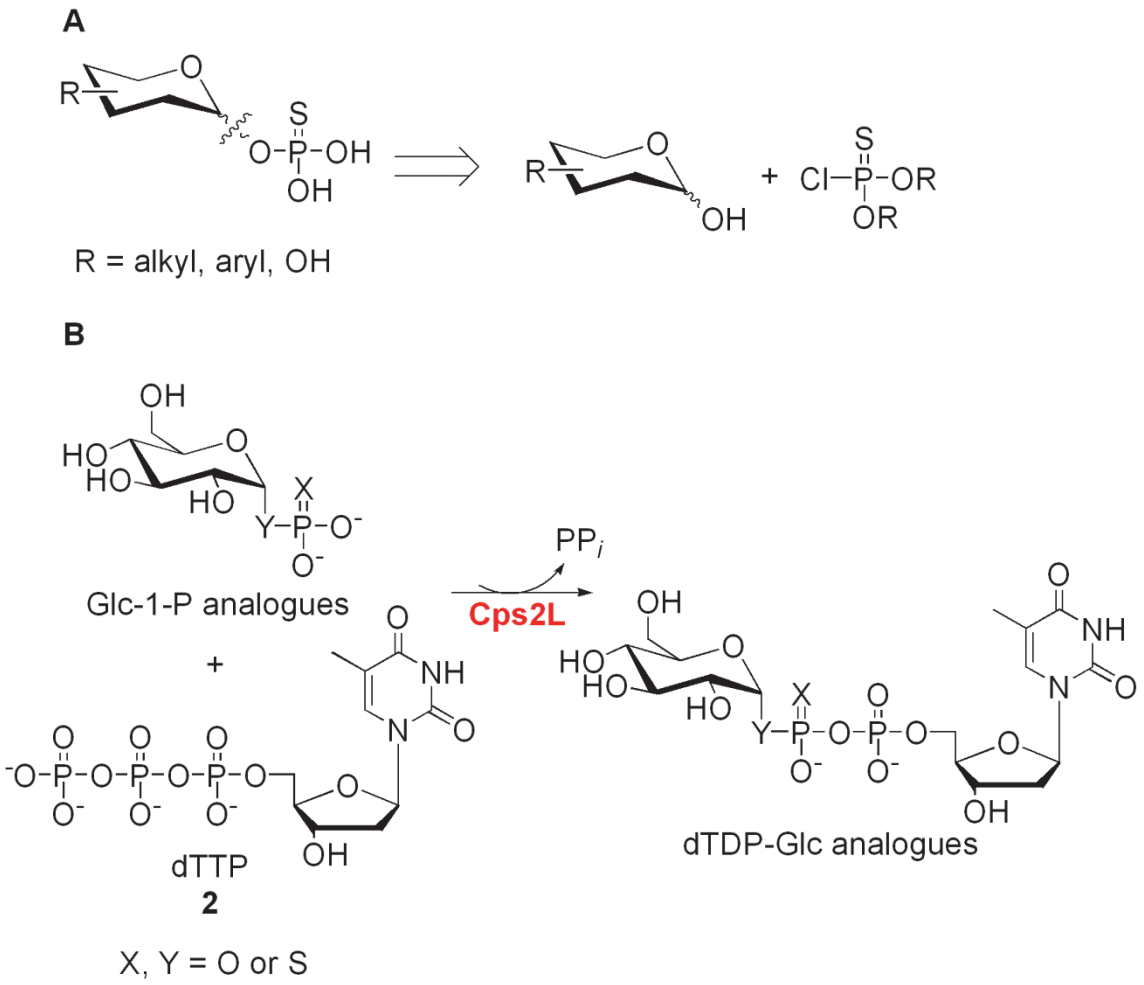


**Scheme 11** Retrosynthetic (A) and enzymatic (B) strategies for the production of glucosyl thiophosphates and thiophosphate containing sugar nucleotides

# CHAPTER 3 RESULTS AND DISCUSSION PART 1

## 3.1 L-Rhamnose-1C-phosphonate Analogues

### 3.1.1 The Synthesis of R1CP Analogues

The synthesis of L-rhamnose-1C-phosphonate (R1CP) analogues was accomplished starting from commercially available L-rhamnose (**23**), using a modified procedure from Norris and Toyokuni.[87] L-rhamnose was first methylated at the anomeric position using approximately two equivalents of acetyl chloride in methanol overnight. Quenching of the excess acid was then accomplished using a slight excess of triethylamine. The crude product, which consisted of an anomeric mixture of the α and β methylglycosides, was concentrated directly and the remaining hydroxyl residues were benzylated using sodium hydride (60% dispersion in mineral oil or dry 95%) and benzyl bromide in dry DMF. The benzyl protected methyl glycoside (**24**) was isolated in a 58% yield over two steps. Direct demethylation of the anomeric methyl linkage was achieved using a mixed glacial acetic acid/2 M HCl system added to a solution of **24** in THF and refluxing for approximately three hours. 2,3,4,-Tri-O-benzyl-α/β-D-rhamnopyranose (**25**) was isolated in an 89% yield and directly transformed into the corresponding lactone by stirring in a 2:1 mixture of DMSO:$Ac_2O$ overnight.[88] Workup with ether and water, followed by freeze drying, was sufficient to obtain the desired tri-O-benzyl-1,5-rhamnolactone (**26**) as a white solid in quantitative yield when less than 1 g of **25** and approximately 5 mL DMSO or less were used. For quantities and volumes exceeding 1 g of **25** and 5 mL of DMSO, normal phase silica purification was preferred to obtain the desired product (**26**) in 75% yield (Scheme 12). All characterization data for compounds **24**, **25** and **26** were consistent with what was reported by Norris and Toyokuni.[87] Lactone **26** served as the model electrophile for all subsequent nucleophilic reactions toward the L-rhamnose-1C-phosphonate analogues. The mechanism of lactone formation using DMSO/$Ac_2O$ is presented in Scheme 13.

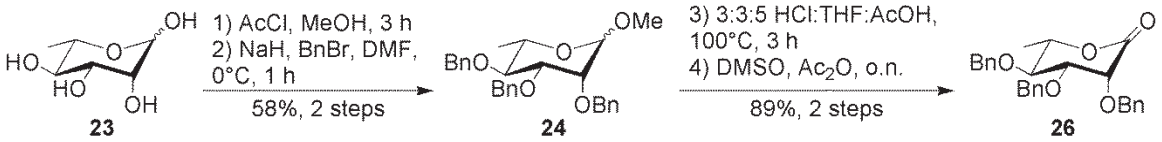


**Scheme 12** Synthesis of tri-*O*-benzyl-1,5-rhamnolactone **26**

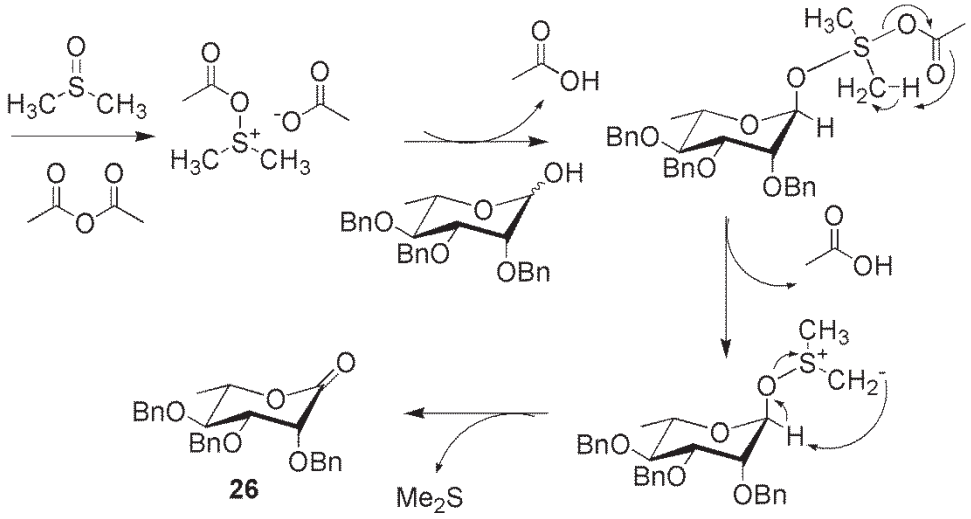


**Scheme 13** Mechanism of DMSO/$Ac_2O$ oxidation of anomerically deprotected sugars

Lactone **26** was transformed into the dimethyl or dibenzyl ketosephosphonate species **28a** (88% yield) and **28b** (76% yield) using lithiated salts of dimethyl methylphosphonate (**27a**) and dibenzyl methylphosphonate (**27b**),[89] respectively, in THF at -78°C (Scheme 14). Both compounds were isolated as the dominantly axial hydroxyl isomers, as determined by $^{31}P$ and $^{1}H$ NMR spectroscopy. Olefins **30a** and **30b** were produced from the *in situ* formation and subsequent elimination of the oxalyl esters (**29a** and **29b**), which formed when ketosephosphonates **28a** and **28b** were treated with methyl oxalyl chloride in a 7:2 $CH_2Cl_2$**:**pyridine solvent mixture. Complete deoxygenation of the oxalyl esters was not achieved, as the reaction conditions generally produced an approximate 2:1 ratio of the desired olefin products to intermediate oxalyl esters. Previously, the use of freshly distilled pyridine or further refluxing in toluene had facilitated complete deoxygenation of related gluco-ketosephosphonate oxalyl esters.[41] Such measures were found to be ineffective for the L-rhamnose analogues. The intermediate esters were always visible, using TLC analysis, as the less polar species. Olefins **30a** and **30b** were single *Z* stereoisomers, as determined by $^{31}P$, $^{1}H$ NMR, and 1D

NOESY NMR spectroscopy (Figure 6). Irradiation of the olefin proton H1 of compound **30a** produced a n*O*e effect at the equatorial H3 proton suggesting, a *Z* orientation about the double bond. If H1 had been in an *E* orientation, a n*O*e effect with the axial H6 and or L-rhamnose methyl $CH_3$ moiety would have been expected. Such effects were not observed. Determination of stereochemistry about the double bond of rhamnosyl olefin phosphonate **30a** has not been reported in its previous synthesis.[87]

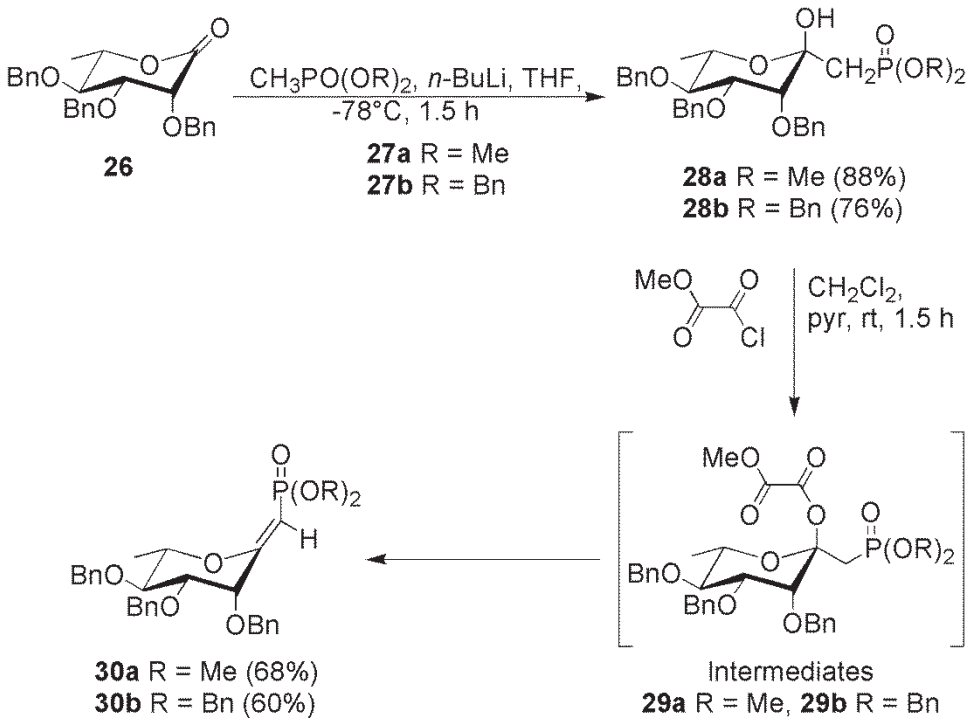


**Scheme 14** Synthesis of olefins **30a** and **30b** from tri-*O*-benzyl-1,5-rhamnolactone **26**

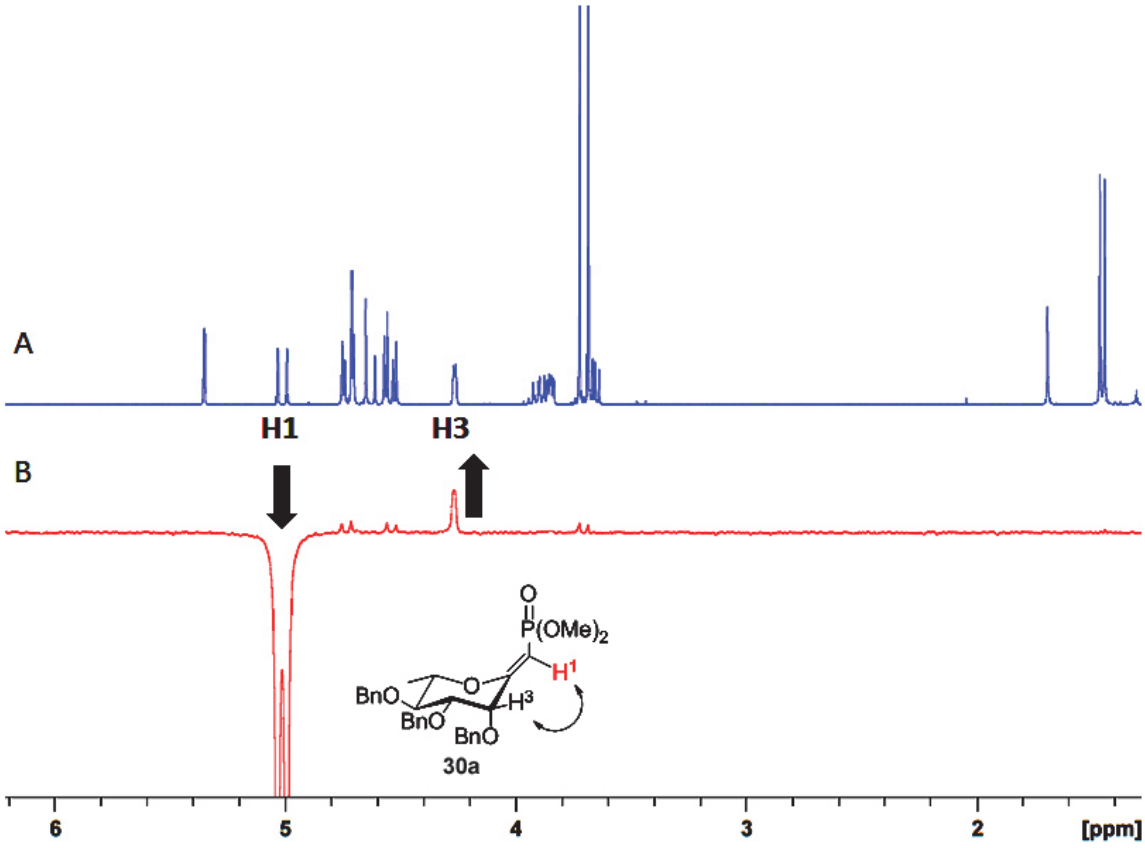


**Figure 6** $^{1}$H NMR and 1D NOESY NMR spectra (300 MHz, $CDCl_3$) for **30a**. (A) $^{1}$H NMR spectroscopy for **30a**. (B) 1D NOESY for **30a** H1. Down arrow indicates site of irradiation. Up arrow indicates a positive n*O*e.

The L-rhamnose olefins (**30a** and **30b**) were found to be significantly more prone to C=C hydration than analogous glucose compounds.[41] If left exposed to atmosphere or in $CDCl_3$ overnight, partial reversion to ketosephosphonates **28a** and **28b** was observed using TLC analysis and $^{31}$P NMR spectroscopy. As a result, NMR characterization of **30a** and **30b** was carried out in neutral $CD_2Cl_2$ and subsequent reactions or deprotections using **30a** and **30b** were performed within 24 hours of isolation. Treatment of **30a** or **30b** with Selectfluor®[90] (**31**), an electrophilic fluorinating reagent, followed by addition of water across the double bond, afforded a diastereotopic mixture of monofluorinated ketosephosphonates (Scheme 15). The major products **32a** and **32b** were isolated in 54% and 22% yields, respectively. It was suspected that the additional steric bulk of the benzyl protecting groups of **32b** reduced the fluorination efficiency, accounting for the reduced yield of **32b** relative to methyl protected **32a**.

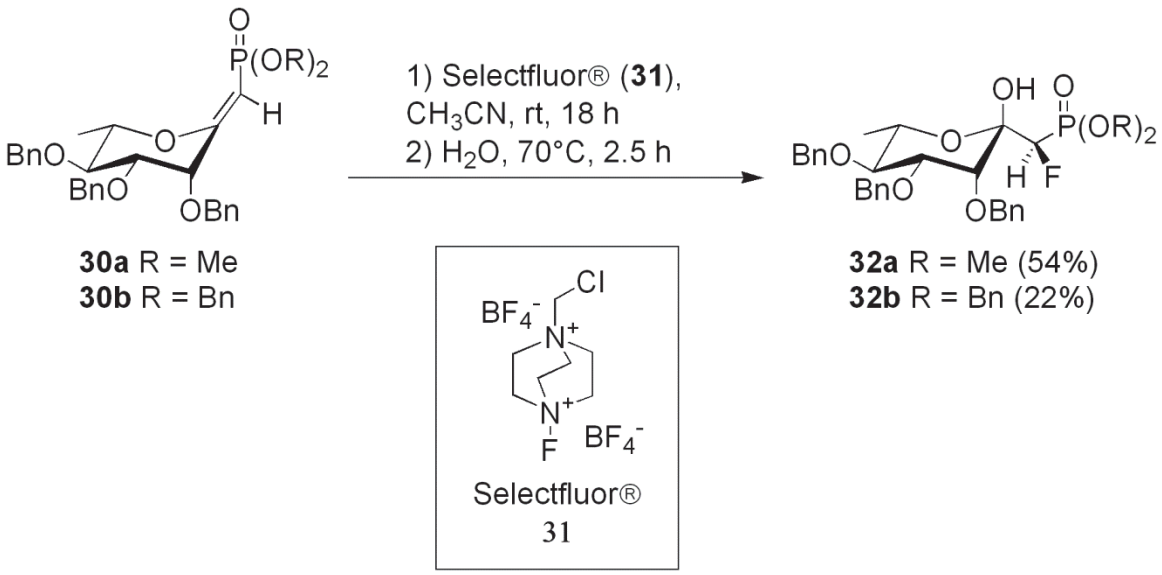


**Scheme 15** Synthesis of monofluoro ketosephosphonates **32a** and **32b**

In previous studies, direct determination of phosphonate stereochemistry for the analogous glucose analogue of **32b** was possible using X-ray diffraction analysis.[41] In this instance, however, both the methyl (**32a**) and benzyl (**32b**) phosphonate protected L-rhamnose analogues were clear viscous liquids, rendering X-ray crystallographic techniques ineffective for stereochemical determination about the C1 position. 1D NOESY NMR experiments of compounds **28a** and **32a** were hence used to deduce the stereochemistry for compound **32a** as *R*. By irradiating the hydroxy proton of **32a**, methylene proton H1a produced a n*O*e effect (Figure 7). Irradiation of the second methylene proton H1b showed only a n*O*e effect with H1a and not the hydroxyl proton (Figure 7). It was thus reasoned that because only one of the methylene protons of **28a** showed a n*O*e effect with the hydroxyl proton, that free rotation about the C1–C2 bond for the ketosephosphonates was not occurring. The subsequent 1D NOESY of **32a**, in which the hydroxyl proton was irradiated, showed that the H1a n*O*e effect had been lost, suggesting that the fluorine was occupying the H1a position at C1 (Figure 7). For **32b** the C1 stereochemistry was assumed the same as **32a**, as benzyl protecting groups on the phosphonate moiety would be unlikely to invert the position of fluorination. Such findings were consistent with X-ray crystal structures of the analogous glucose compounds, which also showed the *R* stereoisomer to be the major product.[41]

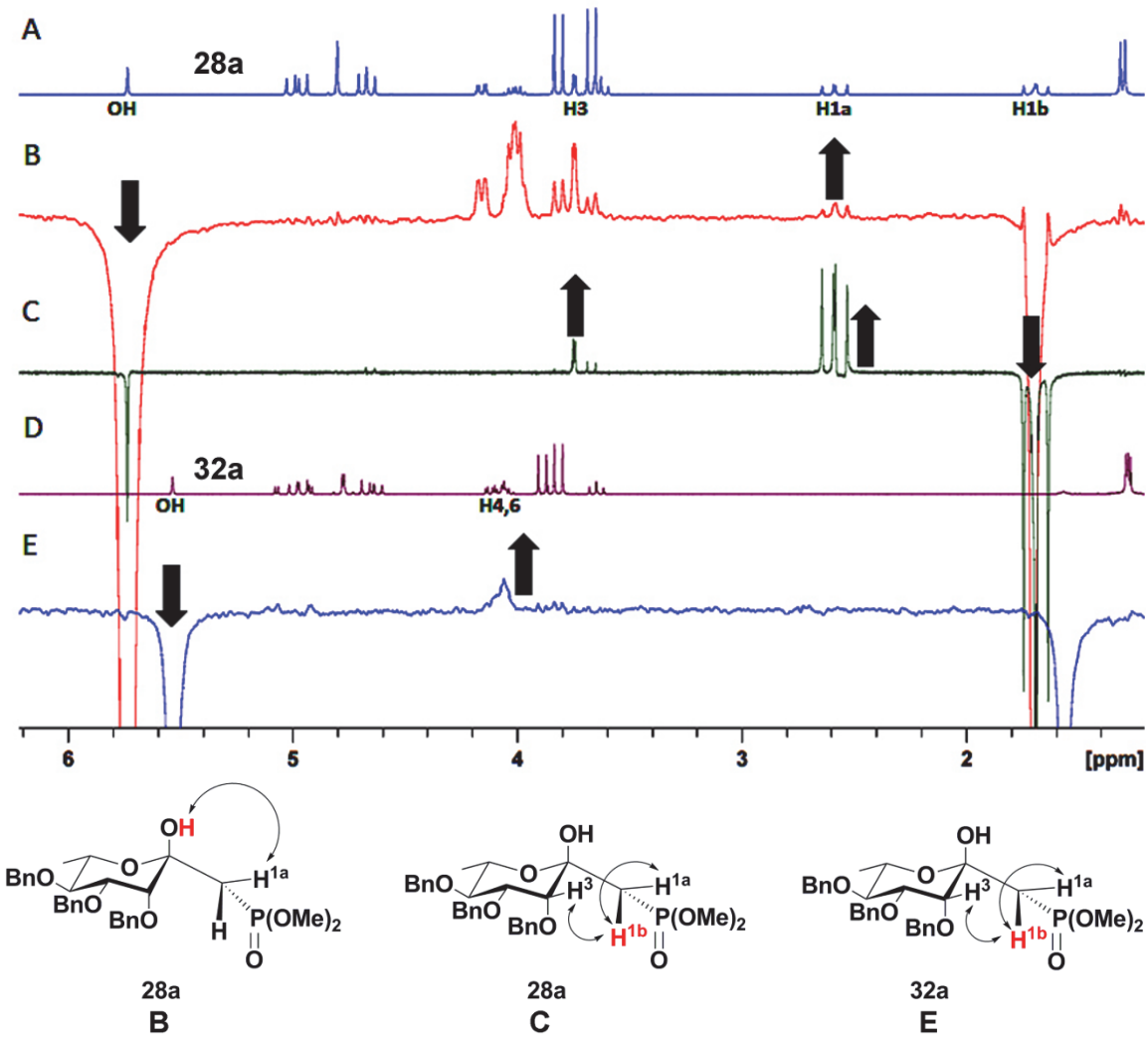


**Figure 7** $^{1}$H NMR and 1D NOESY spectra (300 MHz, $CDCl_3$) for **28a** and **32a**. (A) $^{1}$H NMR spectrum for **28a**. (B) 1D NOESY for **28a** OH. (C) 1D NOESY for **28a** H1b. (D) $^{1}$H NMR spectrum for **32a**. (E) 1D NOESY for **32a** OH. Down arrow indicates site of irradiation. Up arrow indicates a positive n*O*e. Structure letters (B, C, E) correspond with spectrum letters. Structure bond lengths exaggerated for clarity. Spectra B and E show a residual water artifact (1.5-1.7 ppm) which should not be confused with H2b.

Difluoroketosephosphonate **34** was produced from the treatment of lactone **26** with diethyl difluoromethylphosphonate (DEDFMP) (**33**) using LDA at -78°C in 74% yield (Scheme 16). Compound **34** was converted to the corresponding oxalyl ester **35** using identical reaction conditions used to produce olefins **30a** and **30b**. The presence of the fluorine atoms at the C1 position renders the possibility of *in situ* elimination of the ester moiety unlikely, given that there are no methylene protons available for abstraction. The oxalyl ester hydrolysis product **34** was detected by $^{31}$P and $^{19}$F NMR spectroscopy in

a minor amount (<3%) relative to the major product **35** after purification, indicating sensitivity of these esters to hydrolysis. Subsequent radical deoxygenation using azoisobutyl nitrile (AIBN) (**76**) and tributyl tin hydride (**77**) in toluene, at 105°C, afforded the difluorophosphonate **36** in an excellent yield of 85%. A minor side product (<5%) detected by $^{19}F$ NMR spectroscopy, and suspected to be the axial analogue of **36**, produced from *in situ* mutarotation of **35**, under the reflux conditions required for radical deoxygenation. The mechanism of AIBN/$Bu_3SnH$ radical deoxygenation is shown in Scheme 17.

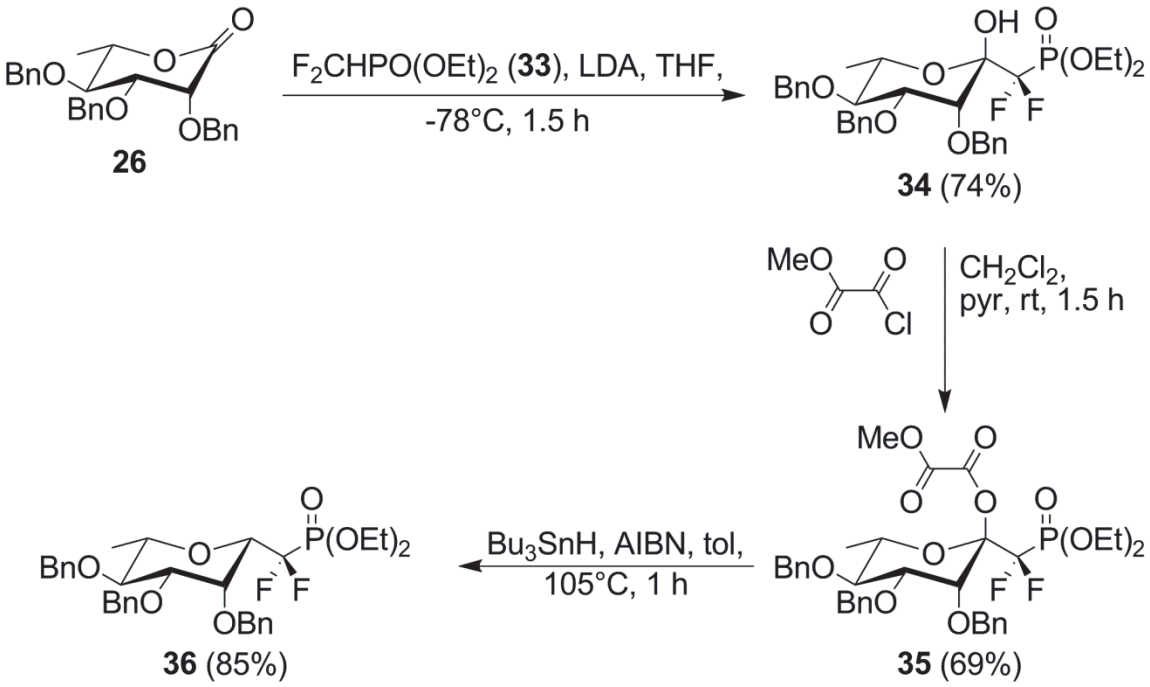


**Scheme 16** Synthesis of difluorophosphonate analogues **34** and **36**

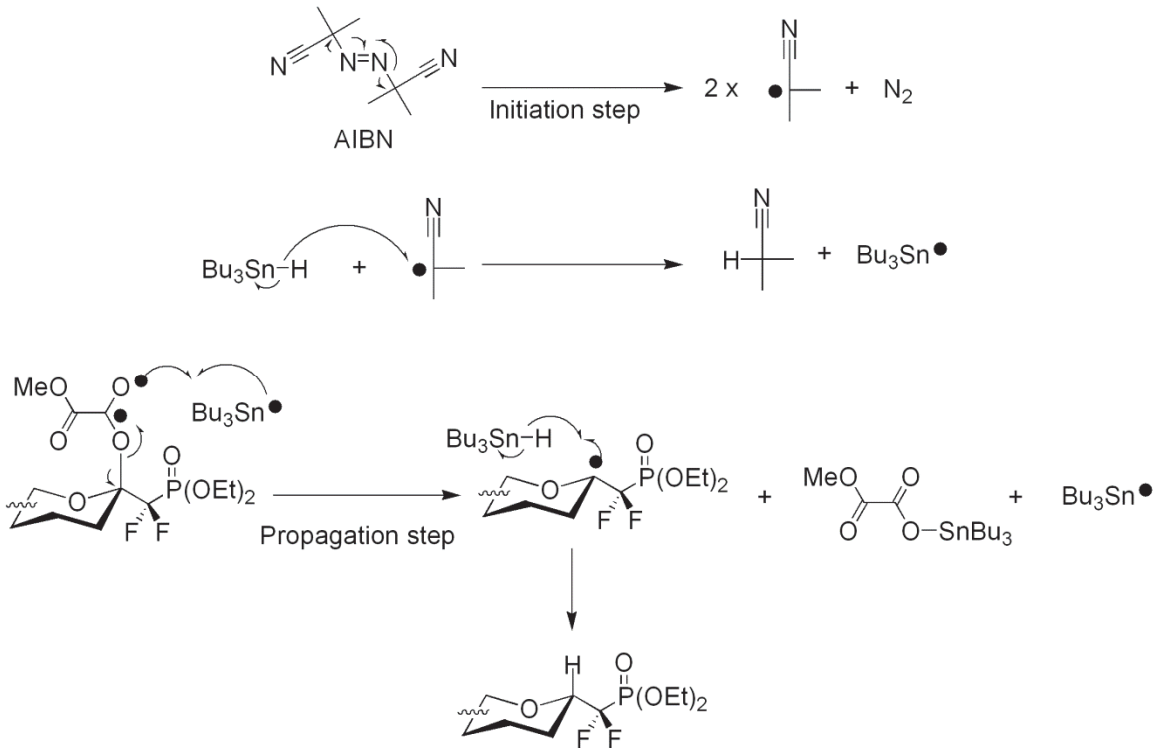


**Scheme 17** AIBN/$Bu_3SnH$ radical deoxygenation mechanism of oxalyl esters

The synthesis of the monofluorinated phosphonate analogue of **36** was attempted from **32a** using the oxalyl ester methodology employed for generation of the difluoro oxalyl ester analogue **35** (Scheme 18). While complete formation of the oxalyl ester **37** was detected using TLC, standard aqueous workup or direct removal of the pyridine via concentration of the crude reaction mixture resulted in complete breakdown of the desired product into an inseparable mixture of the hydrolysis product **32a** and olefin product **38**. An alternative method of ketosephosphonate deoxygenation[41] starting from the monofluoro ketosephosphonates **32a** and using $Et_3SiH$ and TMSOTf was explored but resulted in complete breakdown of the starting material, as determined by TLC analysis. Attempts to perform hydrogenation on the mixture of olefin products and ketosephosphonates resulted in the production of the desired compound **39** (~40%) as well as significant amounts of the de-fluorinated material **40** (~20%) and the monofluoro ketosephosphonate **41** (~40%) (Scheme 18) as determined by $^{31}P$ NMR spectroscopy. Conceivably, demethylation of the resultant mixture of phosphonates (**39**–**41**), and subsequent inhibition studies on the mixture could be performed, and qualitatively

compared to compounds **42**, **43** and **44**. Due to the complexity of the mixture of phosphonates, such additional studies were not pursued.

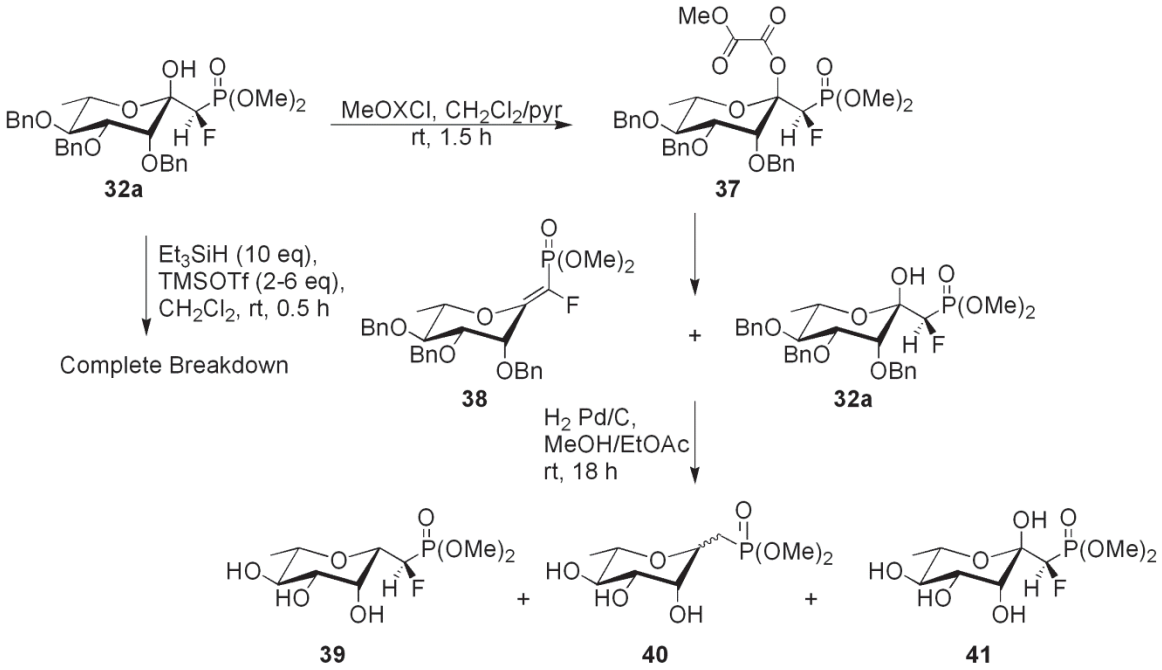


**Scheme 18** Attempted synthesis of monofluoro phosphonate analogue **39**

The global deprotection of the methylene and monofluorinated methyl protected analogues **28a**, **30a** and **32a** was achieved using hydrogenolysis followed by acid hydrolysis (Scheme 19). The compounds were stirred overnight in the presence of 20 mol% $H_2$-Pd/C, in 1:1 MeOH:EtOAc to effect removal of the benzyl protecting groups and carry out hydrogenation of the double bond of **30a**. The compounds were next treated with 6 M HCl (aq) at reflux temperatures for 3 h to cleave the phosphonate methyl esters, and subsequently titrated to pH 8 with 0.2 M $NH_4OH$ (aq) to produce the corresponding ammonium salts for enzymatic analysis. In the case of the benzyl-protected analogues **28b**, **30b** and **32b**, hydrogenolysis was performed directly followed by titration to generate the final compounds **42**, **43** and **44**. All hydrogenation and aqueous acidic deprotection reactions produced the desired compounds in essentially quantitative yields (>95%).

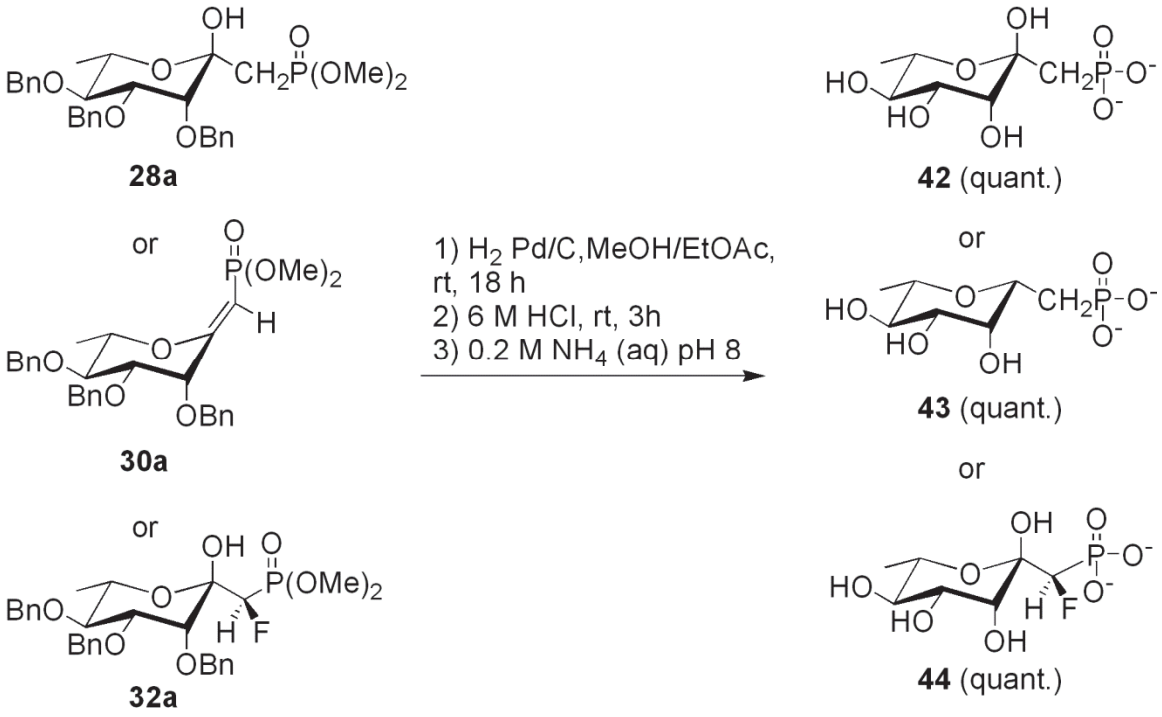


**Scheme 19** Global deprotection of compounds **28a**, **30a** and **32a**

In the case of the difluoro analogues **34** and **36**, both benzyl and ethyl protecting groups were removed using TMSI in $CH_2Cl_2$ followed by aqueous workup and titration to afford **45** and **46** in high yields (~95%) as their ammonium salts (Scheme 20). The presence of the two fluorine atoms at C1 for the difluoro ketosephosphonate **34** seemed to be essential for stabilizing the anomeric phosphonate linkage under the harsh TMSI deprotection conditions, given that attempted global deprotection of the non-fluoro ketosephosphonate **28a** resulted in complete breakdown of the material. The increasing acidity of **42**<**44**<**45** was anticipated to correlate to a greater preference for the cyclic (α-pyranose) form of the ketose. However, the ratios between the α, β and open chain species were for **42** (18:2.5:1), for **44** (100% *a*) and for **45** (11:3:1) as determined by $^{31}P$ and $^{19}F$ NMR spectroscopy (Figure 8). This remains contrary to previous studies on analogous D-gluco-ketosephosphonates, in which the difluoro analogue was found to exist solely in the α-pyranose form.[41] Other examples of sugar ketoses bearing one[91] or two[92] fluorine atoms at the carbon neighboring the anomeric position also report the α-pyranose as the dominant form. In the case of the L-rhamno-ketosephosphonates, the monofluoro analogue (**44**) was found to be the only exclusive α-pyranose. In the case of

the difluoro ketosephosphonate **45**, $^{19}F$ NMR spectroscopy was used to determine the relative ratios of the various tautomers, due to signal overlap in the $^{31}P$ NMR spectrum. Individual fluorine atoms were observed as doublet of doublet signals for the diastereotopic fluorines in both the α and β forms of **45** and, only in the case of the open chain form, were both fluorine signals observed as a sole 2F doublet. This is presumably due to the loss of chirality at the C2 position, which would result if the pyranose were to shift to the open chain form. NMR binding studies and enzyme inhibition studies for compounds (**43**-**46**) can be found in sections 3.1.2, and 3.1.3 respectively. The synthesis of sugar nucleotide analogues of L-rhamnose phosphonate analogues is discussed in section 3.2.1.

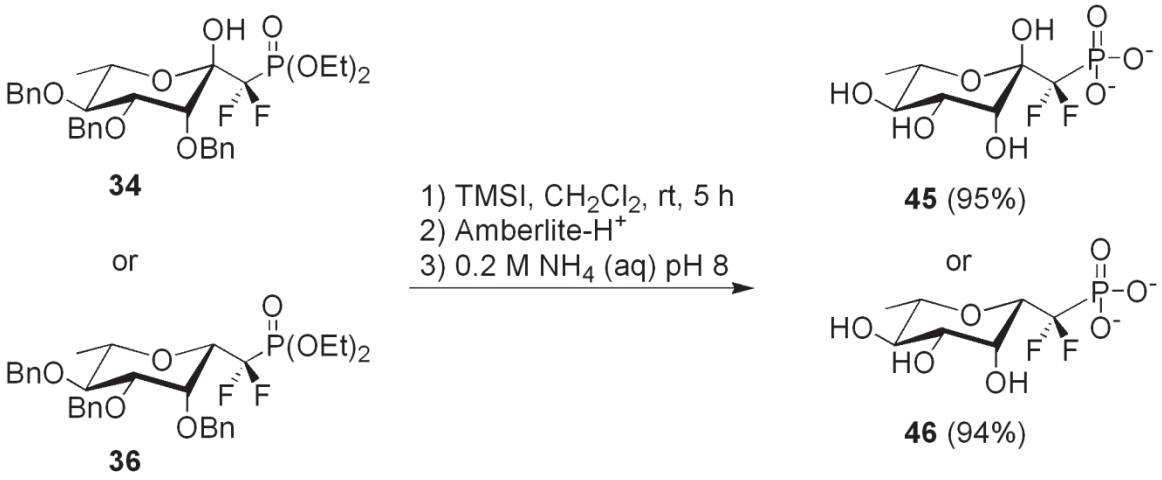


**Scheme 20** Global deprotection of compounds **34** and **36**

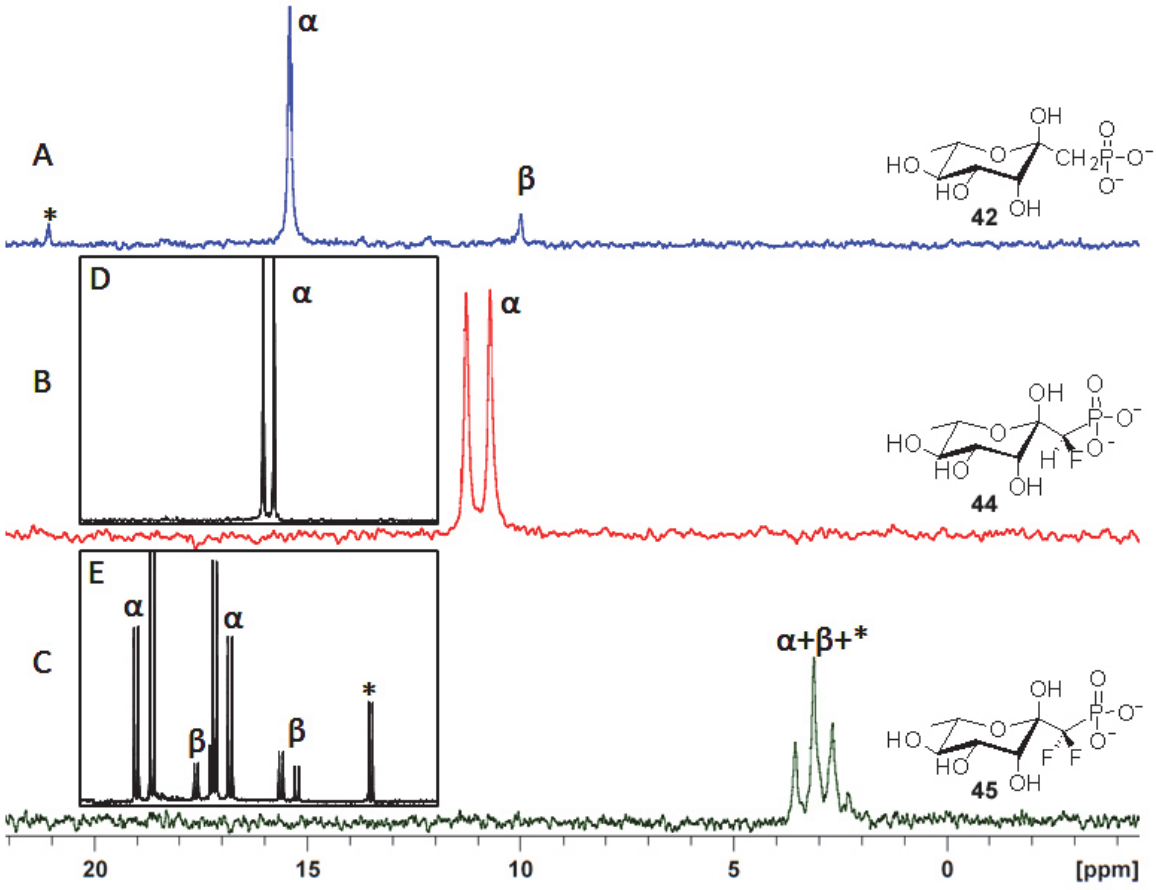


**Figure 8** $^{31}P$ and $^{19}F$ (insert) NMR (300 MHz, $D_2O$, pH 7.5) spectra for **42**, **44** and **45** showing ratios of α:β:open chain (*) of ketosephosphonates. (A) **42** 19:2.5:1, (B) **44** (100% α), verified by D ($^{19}F$ insert), (C) **45** 11:3:1 as determined by E ($^{19}F$ insert) due to $^{31}P$ NMR signal overlap.

### 3.1.2 WaterLOGSY NMR Binding Studies

Enzyme inhibitor binding experiments were performed (a) to investigate the binding of phosphonate analogues to enzymes (Cps2L, RmlB-D) and to gain insight into the possible mechanism of inhibition for these compounds, (b) to investigate the capacity for sugar-nucleotides dTDP-α-D-glucose (**3**) and dTDP-β-L-rhamnose (**6**) (isolated using previously established literature protocols)[93] to bind to multiple enzymes (Cps2L, RmlB-D) within the bacterial biosynthetic pathway, and (c) to substantiate the ordered Bi-Bi mechanism of **3** and the allosteric binding model of **6** to Cps2L. Water-ligand observed binding via gradient spectroscopy (WaterLOGSY) NMR was the method used to carry

out these objectives. WaterLOGSY NMR is a 1D n*O*e experiment in which the irradiation of bulk water effectively facilitates magnetization transfer from active-site bound water molecules to bound ligands via the enzyme-ligand complex.[94] Binding compounds will maintain a perturbed magnetic state when released back into solution from the enzyme-ligand complex and produce an opposite sign n*O*e relative to non-binding compounds. It is noted that a strong WaterLOGSY binding event ($K_d$ sub nM) could result in a spectrum that appears to be from a non-binder.[94] However, since these phosphonates were expected to be in the nM to mM range, this situation was not anticipated. In addition, a week or non-specific binding event could result in the "vanishing" of peaks due to signal cancellation resulting from the effects from bound and unbound states.[95] Figure 9 illustrates the magnetization mechanism underlying WaterLOGSY NMR spectroscopy.[94]

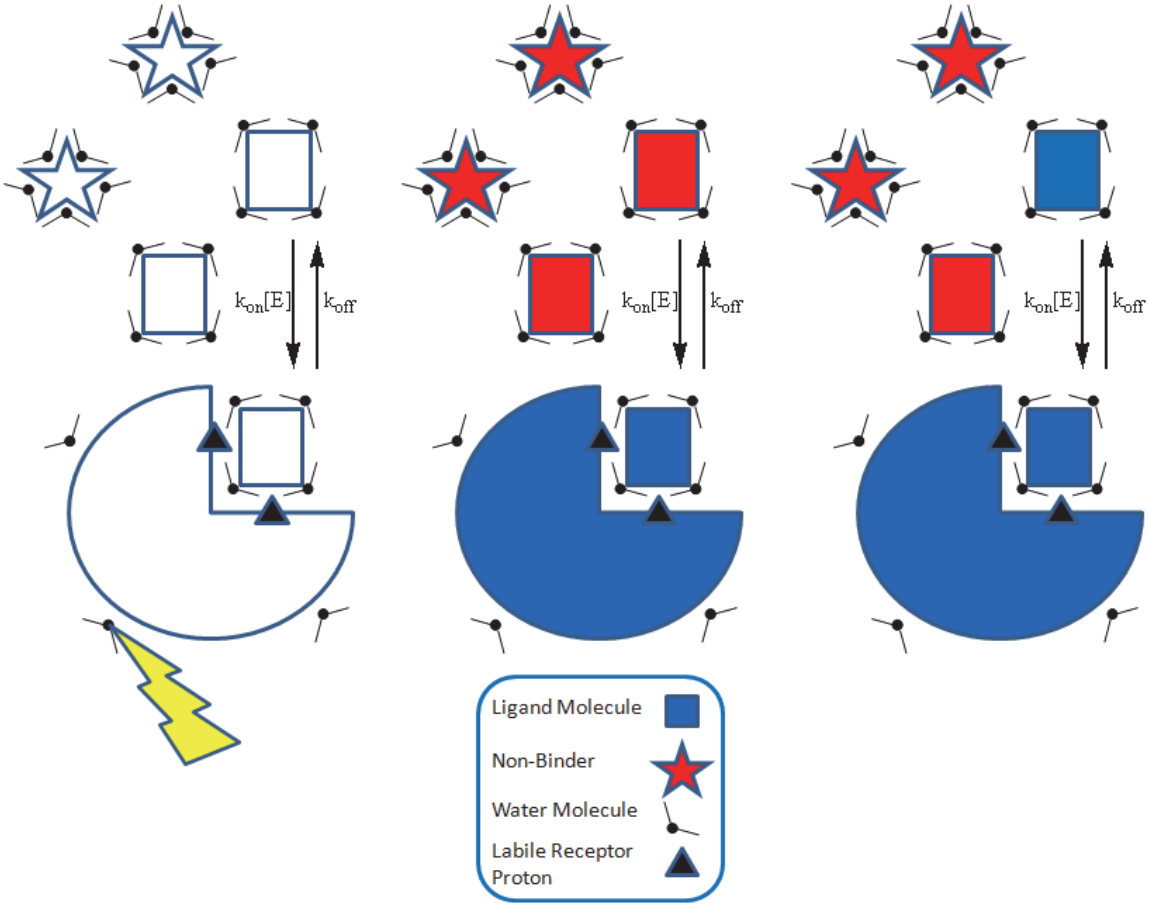


**Figure 9** Magnetization transfer mechanism underlying WaterLOGSY NMR.[94]

Due to significant signal overlap within the carbohydrate region (3-4 ppm), binding events were most easily determined by the isolated L-rhamnose and/or thymidine methyl signals between 1–2 ppm. The WaterLOGSY experiments of inhibitors **42** and **43** both showed binding to Cps2L (Figure 10). Binding was observed most clearly by the distinct methyl peak at (~1.1 ppm) and methylene protons (1.5-2.5 ppm) phasing in the opposite direction to the benzoic acid signals (7.0–8.0 ppm). Compound **43** also bound epimerase RmlC, but did not appear to bind to RmlB or D (Figure 11). Competitive binding experiments were performed to determine whether compound **43** would bind in the presence of the natural substrates Glc-1-P (**1**) or dTTP (**2**). As expected, Glc-1-P (**1**) did not bind to Cps2L given that the ordered Bi-Bi mechanism (Scheme 2) first requires the binding of dTTP (**2**) to induce a conformational change necessary to facilitate the binding of **1** (Figure 12). However, analogue **43** was found to bind in the presence of substrate **1**, yet not in the presence of substrate **2**. This suggests that **43** may, in fact, be binding to the same site as substrate **1**, and that the conformational change induced by **2** hinders the ability of **43** to bind to the Cps2L.

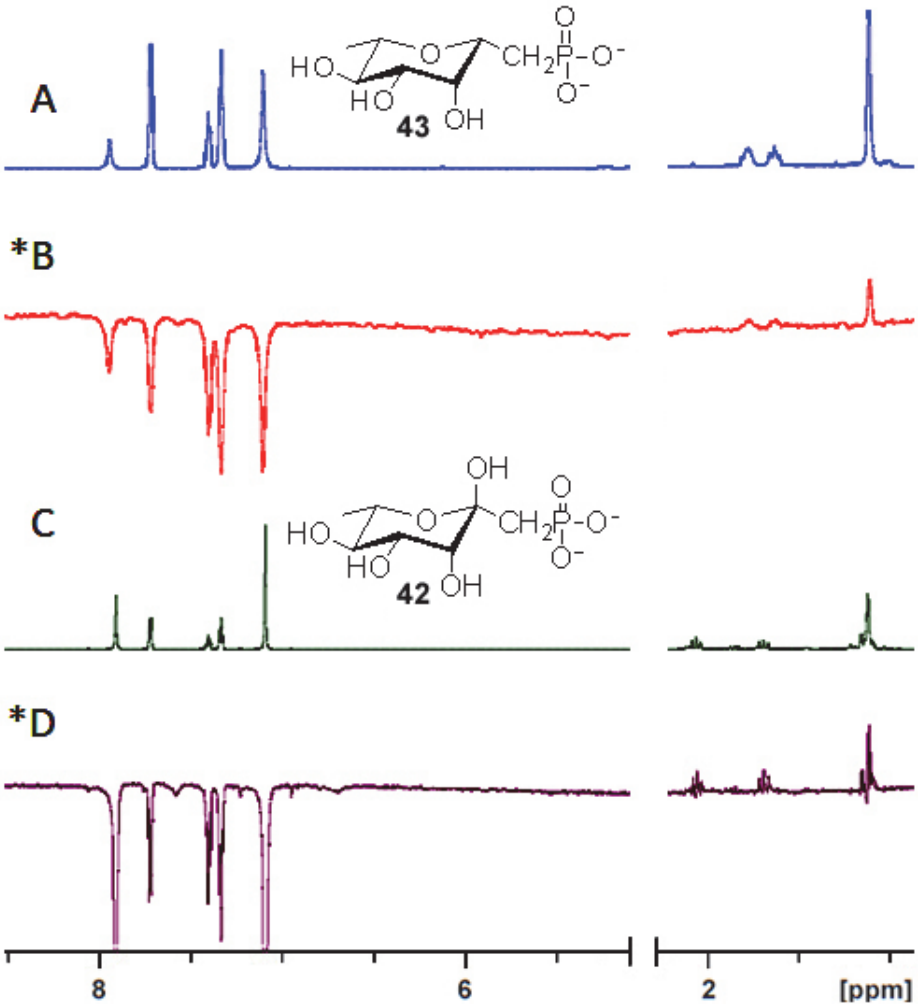


**Figure 10** WaterLOGSY NMR spectra (700 MHz, 10/90 $D_2O/H_2O$) showing binding of **42** and **43** to Cps2L. (*) Indicates spectrum showing binding (peaks above line). Sample compositions (see Methods) (A) $^1$H NMR spectrum of **43** and benzoic acid. (B) **43** with Cps2L. (C) $^1$H NMR of **42** and benzoic acid. (D) **42** with Cps2L. [a]Residual imidazole binding the $His_6$-Tag on Cps2L. [b]Benzoic acid control non-binder.

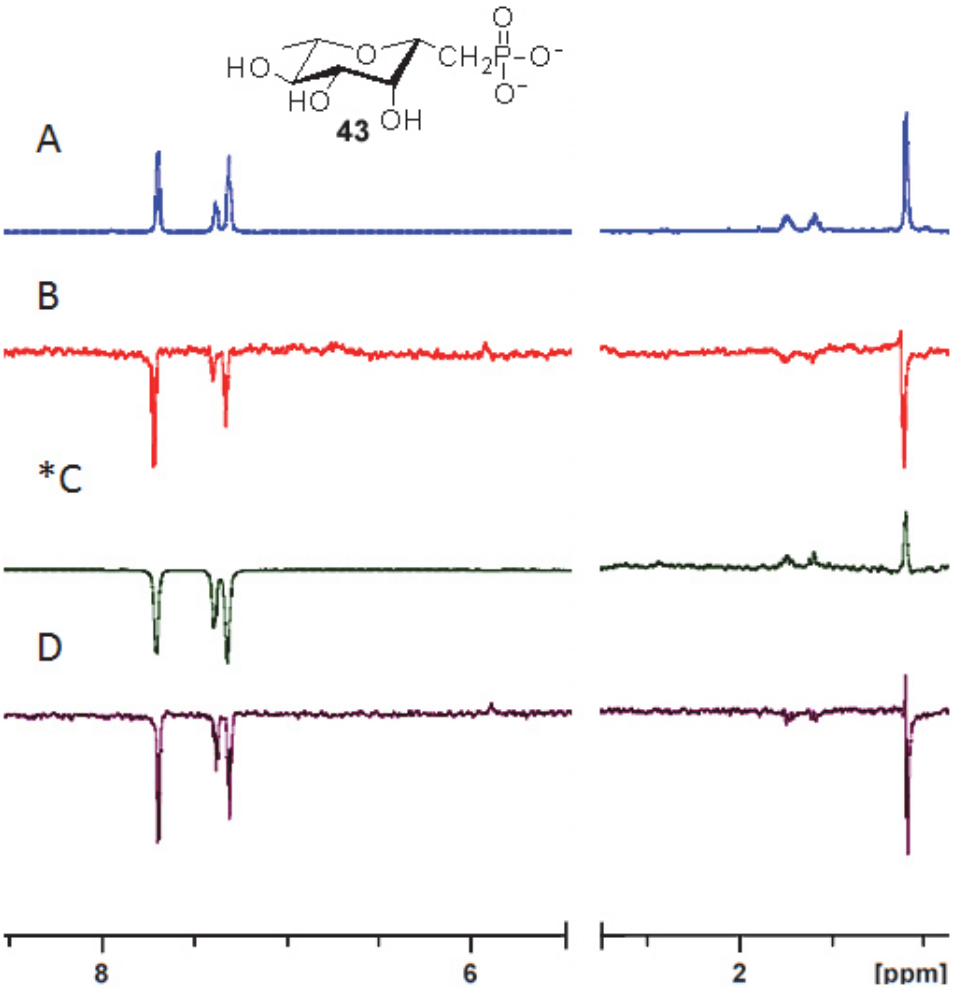


**Figure 11** WaterLOGSY NMR spectra (700 MHz, 10/90 $D_2O/H_2O$) for **43**. (*) Indicates spectrum showing binding. Sample compositions (see Methods). (A) $^1H$ NMR spectrum of **43** and benzoic acid. (B) **43** with RmlB. (C) **43** with RmlC. (C) **43** with RmlD.

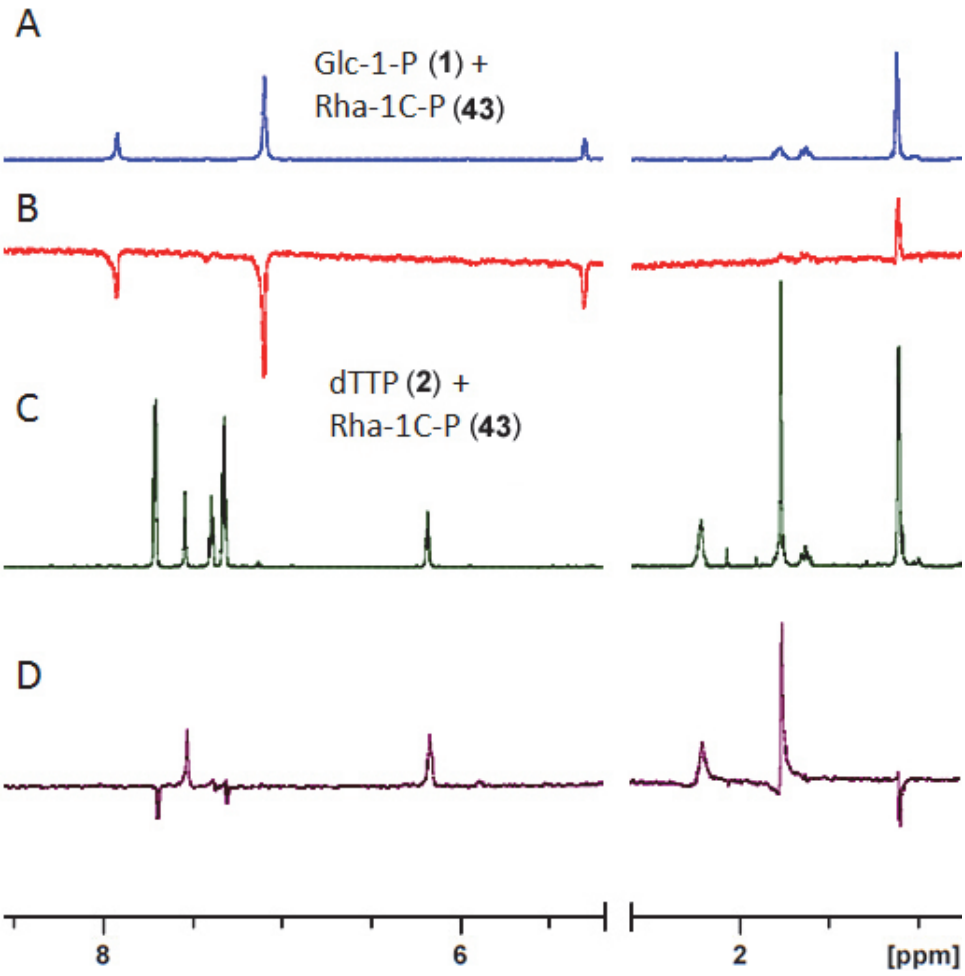


**Figure 12** WaterLOGSY NMR spectra (700 MHz, 10/90 $D_2O/H_2O$) of **43** and substrates **1** or **2** with Cps2L. Sample compositions (see Methods). (A) $^1$H NMR of **1** and **43**. (B) **43** binding to Cps2L, **1** non-binding. (C) $^1$H NMR spectrum of **2**, **43** and benzoic acid with Cps2L. (D) **2** binding to Cps2L, **43** non-binding.

The WaterLOGSY of Cps2L showed bound dTDP-Glc (**3**) (Figure 13A) (refer to Scheme 3 for the roles of Cps2L and RmlB-D relative to compounds **1**-**6**). In the time it took to prepare the sample, RmlB turned **3** over to **4**, despite no exogenous $NAD^+$, as demonstrated by the new peak at ~1 ppm for the methyl substituent (Figure 13B). Binding of **3** to RmlC was clearly observed (Figure 13C) whereas, based on the cancellation of signals, weak binding to RmlD was observed (Figure 13D). The WaterLOGSY spectra of dTDP-Rha (**6**) with Cps2L and RmlB-D are shown in Figure 14. dTDP-Rha (**6**) bound Cps2L as anticipated by crystallography and kinetic studies for homologous enzymes.[96] Unequivocal binding was also observed for **6** to RmlC. For

RmlB and RmlD reduction in intensity of the signals for **6** was observed, relative to the benzoic acid control, and the signals for **6** were also difficult to phase and remained dispersive. As indicated above, this is likely due to a weak binding interaction with these enzymes.

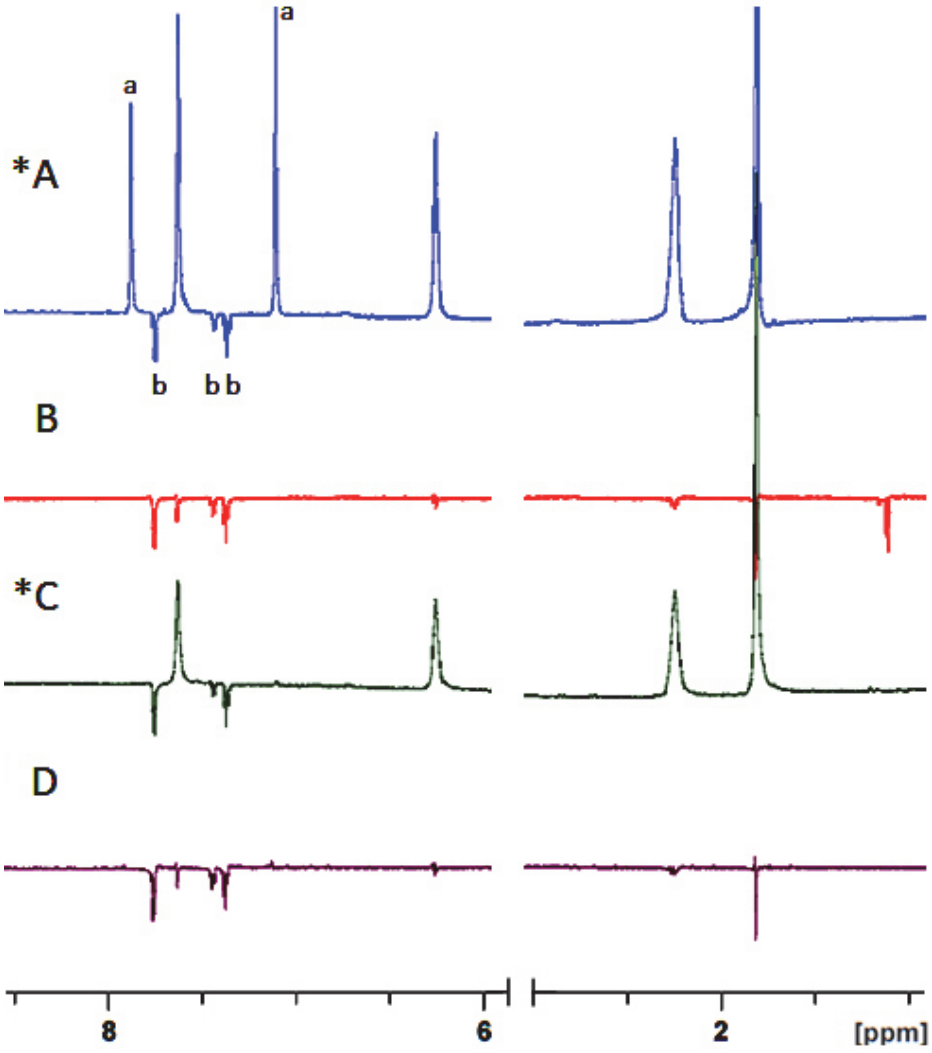


**Figure 13** WaterLOGSY NMR spectra (700 MHz, 10/90 $D_2O/H_2O$) showing dTDP-Glc (**3**) binding or non-binding. (*) Indicates spectrum showing binding. (A) **3** with Cps2L. (B) **3** with RmlB. Sample compositions (see Methods). (C) **3** with RmlC. (D) **3** with RmlD. [a]Residual imidazole binding the $His_6$-Tag on Cps2L. [b]Benzoic acid control non-binder.

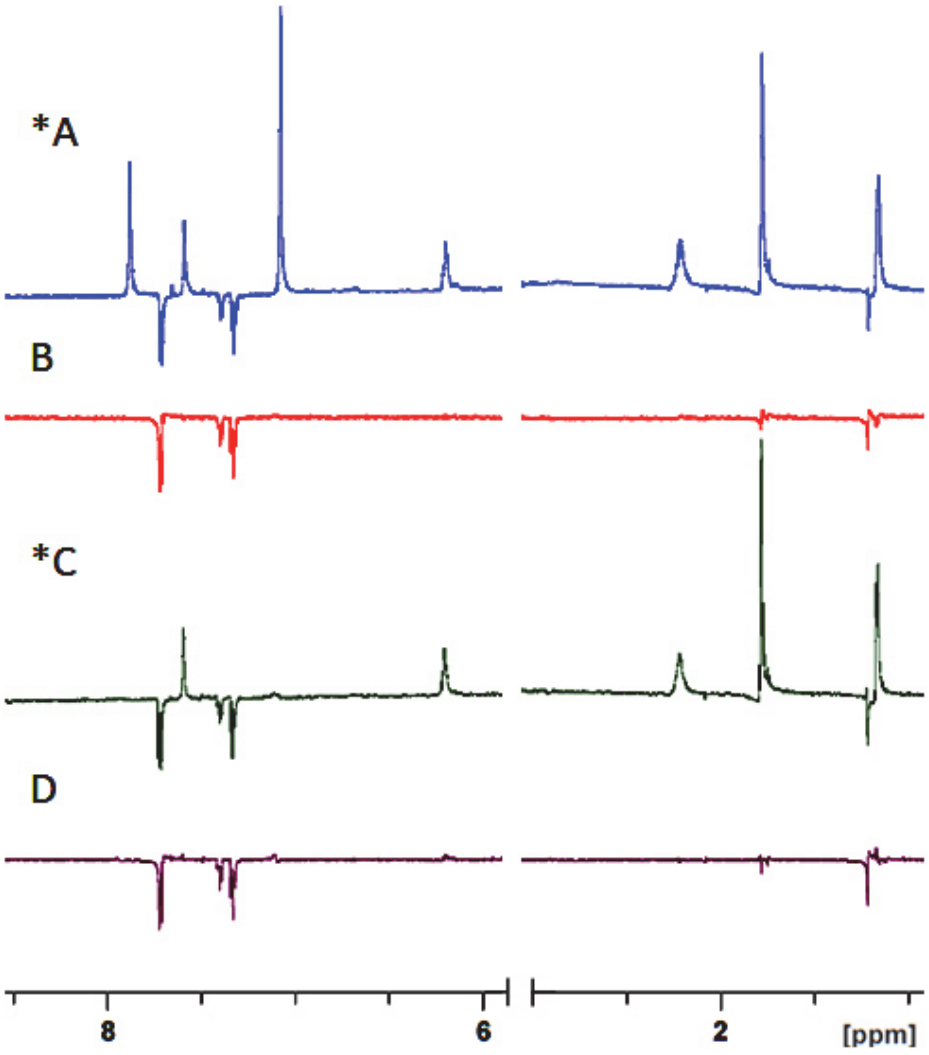


**Figure 14** WaterLOGSY NMR spectra (700 MHz, 10/90 $D_2O/H_2O$) showing dTDP-Rha (**6**) binding or non-binding. (*) Indicates spectrum showing binding. (A) **6** with Cps2L. (B) **6** with RmlB. (C) **6** with RmlC. (D) **6** with RmlD.

### 3.1.3 Enzyme Studies

Prior to inhibition studies, compounds **42** and **43** were first evaluated as Glc-1-P (**1**) analogue substrates for thymidylyltransferase Cps2L, given that the enzyme had previously demonstrated a broad substrate specificity,[11,93,97] including poor conversion observed for β-L-fucosyl phosphate.[93] Negligible turnover (<1%) to sugar nucleotide products were observed by HPLC over 24 hours using 2–10 EU of Cps2L with a 8:1 ratio of compounds **42** or **43** relative to dTTP substrate **2**, suggesting that the L-rhamnose phosphonate analogues did not act as substrates for Cps2L. Compounds **42**, **43**, **44**, **45**

and **46** were each evaluated as inhibitors of Cps2L at various concentrations between 0-100 mM against 10 mM concentrations of substrates **1** and **2**. The percentage conversion was calculated as the concentration of product formed (**3**) relative to the remaining starting material (**2**) for each concentration of inhibitor tested, relative to a control reaction in which no inhibitor was present (refer to Scheme 1 for the Cps2L catalyzed reaction). $IC_{50}$ curves were generated for compounds **42**, **43** and **44** (Figure 15). While compounds **45** and **46** did exhibit minor inhibition (<10%) at concentrations approaching 100 mM, $IC_{50}$ curves could not be generated within the concentration range sampled (0-100 mM). The Cheng-Prusoff[98] equation shows the relationship between the $IC_{50}$ and $K_i$ value of a given competitive inhibitor as $K_i = ((IC_{50}/(1 + [S]/K_m))$. The $IC_{50}$ and $K_i$ values (as calculated using the Cheng-Prusoff equation) are presented in Table 1.

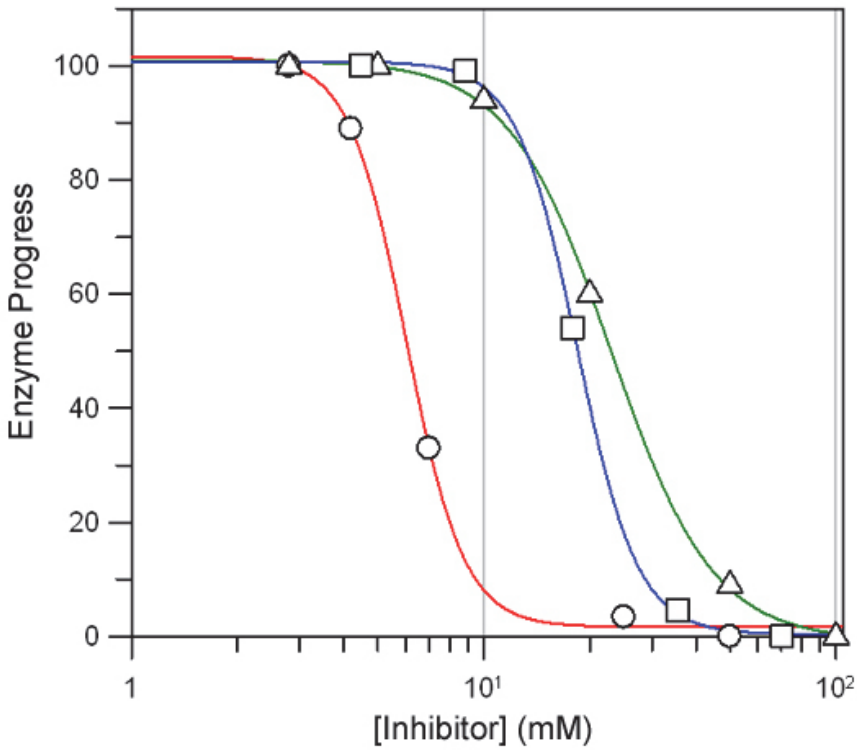


**Figure 15** $IC_{50}$ curves for Inhibitors **42**(△), **43**(○) and **44**(□)

**Table 1** Inhibition of Cps2L by L-rhamnose phosphonates

| Entry | Compound | $IC_{50}$ (mM) | $K_i$* (μM)[a] | $K_i$** (μM)[a] | p$K_a$2[b] |
|---|---|---|---|---|---|
| 1 | **42** | 23.9 | 295 | 358 | 6.5 |
| 2 | **43** | 5.7 | 70 | 85 | 7.0 |
| 3 | **44** | 18.3 | 225 | 274 | 5.7 |
| 4 | **45** | >100[c] | — | — | 5.0 |
| 5 | **46** | >100[c] | — | — | 5.0 |
| 6 | **47** | >25[c] | — | — | — |

*With respect to Glc-1-P, **With respect to dTTP. [a]Calculated using the Cheng-Prusoff equation, assuming competitive inhibition. [b]Estimated from previous p$K_a$2 studies of analogous fluoro and non-fluoro gluco-phosphonate and ketosephosphonate analogues.[41] [c]$IC_{50}$ value beyond limit of inhibitor concentrations tested.

It was found the L-rhamnose-1C-P analogue **43** exhibited the most potent inhibition ($IC_{50}$ = 5.7 mM) (entry 2) relative to ketosephosphonate **42** ($IC_{50}$ = 23.9 mM) (entry 1) and monofluoro ketosephosphonate **44** ($IC_{50}$ = 18.3 mM) (entry 3). This is likely due to the lack of the C2 axial hydroxyl moiety in the phosphonate scaffold, which may reduce inhibitor-enzyme binding efficiency for the ketosephosphonates. The presence and quantity of fluorine atoms (0-2) seems to have a significant impact on the potency of inhibition. The incorporation of fluorine into phosphonate analogues of natural phosphates has been shown to reduce the p$K_a$2 of phosphonates by ~0.5-1 units per fluorine atom.[41] The assays were conducted at pH 7.5 to ensure complete ionization of phosphonate functionality. Monofluoro analogue **44** produced noticeably improved inhibition (entry 3) relative to its non-fluorinated analogue **42** (entry 1). Based on previous studies[41] of fluorinated ketosephosphonates, the p$K_a$2 values for these compounds are estimated to be ~5.7 and ~6.5 for **44** and **42**, respectively. The ability of ketosephosphonate **42** to undergo mutarotation, as determined by $^{31}$P and $^{1}$H NMR spectroscopy, relative to the exclusively α-pyranose analogue **44**, is also a probable factor in explaining the reduced inhibition observed for **42**. The fact that difluoro analogues **45** and **46** (p$K_a$2 ~ 5.0) showed only minor inhibitory activity (<10%) (entry 4 and 5) relative to the other analogues (**42**, **43** and **44**) further suggests that the presence of an additional fluorine atom, and further p$K_a$2 reduction, is detrimental to inhibition.

Thymidylyltransferases Cps2L (*S. pneumoniae*) and RmlA (*P. aerugenosa*) share 68% identity (see Sequence Alignment in Appendix A). Commercially available thymidine analogue **47** (Figure 16) was shown to be a potent inhibitor of RmlA (*P. aeruginosa*).[16] Alphey, Naismith and coworkers report an $IC_{50}$ value of 0.32 μM for allosteric competitive inhibitor **47**.[16] This compound was chosen as a benchmark for synthesized compounds **42**-**44**.

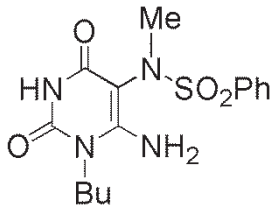


**47**

**Figure 16** Structure of RmlA (*P. aeruginosa*) inhibitor (**47**)

A $K_i$ value of ~0.2 μM was predicted, using the Cheng-Prusoff equation, for both Glc-1-P and dTTP relative to RmlA, for compound **47** (using $K_m$ and $IC_{50}$ values reported by Alphey *et. al.*).[16] With RmlA and Cps2L sharing 68% identity, it was expected that comparable inhibition might be observed for Cps2L. Using the predicted $K_i$ for RmlA, an $IC_{50}$ value between 10-20 μM was predicted for the HPLC based Cps2L inhibition assay. A solution of **47** (50 mM in 1:1 DMSO:Tris-HCl, pH 7.5) was prepared and used in the inhibition assays. Concentrations between 0-25 mM of **47** were tested, in an attempt to determine an $IC_{50}$ value for **47** against Cps2L. All control samples were run in the absence of **47**, with equal volume proportions of DMSO, to ensure any inhibition observed could not be attributed to solvent effects. For compound **47**, no inhibition was observed up to 20 mM. At 25 mM, minor inhibition (<10%) was observed (entry 6). Due to the reduced solubility of **47** in Tris-HCl (pH 7.5) and reduced efficiency of Cps2L in the presence of increasing concentrations of DMSO, concentrations beyond 25 mM of **47** were not investigated. While compound **47** may be a poor inhibitor for Cps2L, its $IC_{50}$ is significantly higher than that of phosphonate and ketosephosphonate analogues **42**, **43** and **44**. It was surprising that compound **47** failed to significantly inhibit Cps2L, based on the high homology between Cps2L and RmlA. Compound **47** binds to the allosteric site in RmlA by interacting with seven key residues. These are Gly115, Phe118, His119, Lys249, Ala251, Cys252 and Glu255. In Cps2L, only three of these residues are

conserved (Gly115, Ala251 and Glu255), which could result in reduced binding and, consequently, poorer inhibition of Cps2L relative to RmlA in the presence of compound **47** (see Sequence Alignment in Appendix A for highlighted conserved residues).

The most potent phosphonate inhibitor (**43**) was subjected to a coupled spectrophotometric inhibition assay to determine the mode of inhibition with respect to substrates **1** and **2**. The Cps2L reaction was coupled with inorganic pyrophosphatase (IPP) to produce phosphate, which was used as a substrate for human purine nucleoside phosphorylase (PNP) along with 7-methyl-6-thioguanosine (MESG) (**48**) ($\lambda_{max}$ = 330 nm) to produce 7-methyl-6-thioguanine (**49**) ($\lambda_{max}$ = 355 nm) and β-D-ribose-1-phosphate (**50**). A coupled assay was necessary because Cps2L substrate **2** and product **3** have the same $\lambda_{max}$ value (254 nm). The coupled assay is shown in Scheme 21. The kinetic parameters for Cps2L are displayed in Table 2. The $K_m$ value for **1** matched closely with previously reported studies using HPLC based assays (entry 1).[11] The $K_m$ value for **2** with Cps2L has not been reported previously. Inhibitor **43** was found to be competitive with respect to variable **1** ($K_i$ = 536 μM) and uncompetitive with respect to variable **2** ($K_i$ = 497 μM) using the coupled assay method. The Michaelis-Menten and Lineweaver-Burk plots can be found in Appendix B. Both values were significantly higher than predicted from the Cheng-Prusoff equation and $IC_{50}$ values determined by the HPLC method, using only Cps2L.

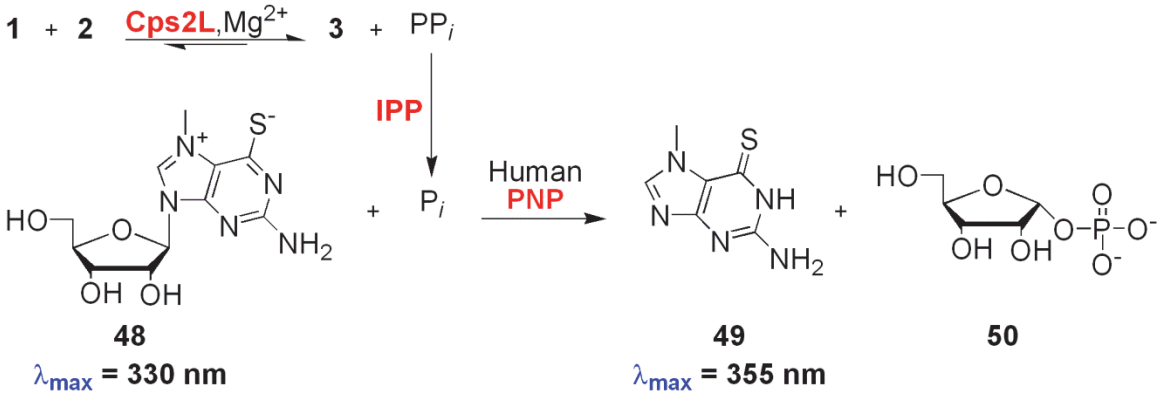


**Scheme 21** Cps2L, IPP and Human PNP coupled assay

**Table 2** Apparent kinetics and inhibition parameters for Cps2L in the presence of **43**

| Entry | Compound | $K_{m,app}$ (μM) | $K_i$ (μM) | $k_{cat}$ ($s^{-1}$) | $k_{cat}/K_m$ ($s^{-1}\mu M^{-1}$) |
|---|---|---|---|---|---|
| 1 | **1** | [a]125* | — | [a]60 | [a]0.475 |
| | | [b]139* | | | |
| 2 | **2** | [a]152** | — | [a]54 | [a]0.352 |
| 3 | **43** | — | [c]536* | — | — |
| | | | [d]497** | | |

*With respect to variable Glc-1-P, **With respect to variable dTTP. [a]Calculated from coupled spectrophotometric assay. [b]Previously reported.[11] [c]Competitive inhibition. [d]Uncompetitive inhibition.

Based on the coupled inhibition assay results, it is expected that inhibitor **43** binds to the same site as **1** both prior to (competitive model) and after (uncompetitive model) the conformational change induced by the binding of **2**. While binding in the presence of **2** was not observed by WaterLOGSY NMR spectroscopy, it could be rationalized by Cps2L having higher affinity for **2** ($K_{m,app}$ = 152 μM, entry 2) relative to **43** ($K_i$ = 497 μM, entry 3). Past[15] and recent[16] studies of nucleotidylyltransferase inhibition have all focused on the study of allosteric inhibitor compounds, with a common trend being that each of the allosteric binders contained a thymidine derived moiety necessary for binding. The scaffold of inhibitor **43** is more similar to substrate **1**, with no thymine analogue component. To our knowledge, it is the first reported sugar-phosphonate active site binding competitive inhibitor of Cps2L. The synthesis of the sugar nucleotide analogues of **42**, **43** and **44** would produce analogues of dTDP-Rha (**6**). These analogues would be predicted to be more potent inhibitors than their phosphonate analogues and, with the introduction of the thymidine component into their scaffolds, would potentially function as allosteric competitive inhibitors. The synthesis of these sugar nucleotide analogues is discussed in section 3.2

## 3.2 The Synthesis of NMP-R1CP Sugar Nucleotide Analogues

The synthesis of NMP-R1CP analogues was accomplished using a sulfonyl imidazolium salt, developed by Mohamady, Taylor and coworkers in 2012, for the rapid and efficient synthesis of nucleoside polyphosphates.[99] It was chosen for its ease of preparation and ability to turnover nucleoside polyphosphates (including sugar nucleotides) in high yields (67-99%).[99] The synthesis of 1-methyl-3-benzenesulfoniumimidazolium triflate (**52**) is shown in Scheme 22.

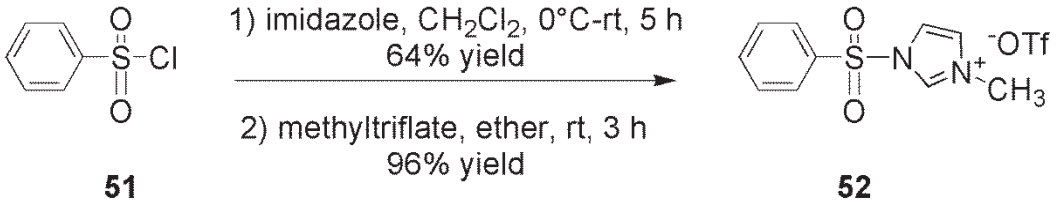


**Scheme 22** Synthesis of 1-methyl-3-benzenesulfoniumimidazolium triflate (**52**)[99]

Sulfonyl imidazolium triflates (i.e. **52**) are effective in activating phosphate groups toward nucleophilic coupling with other phosphates. The sulfonyl imidazolium triflate reacts rapidly with the phosphate to form a mixed anhydride intermediate, which can then become activated to form a highly reactive imidazolium salt. Both the mixed anhydride and imidazolium salt can potentially act as electrophiles toward nucleophilic coupling reactions with phosphates (Scheme 23), hower the imidazolium salt is believed to be the dominant activated form.[99]

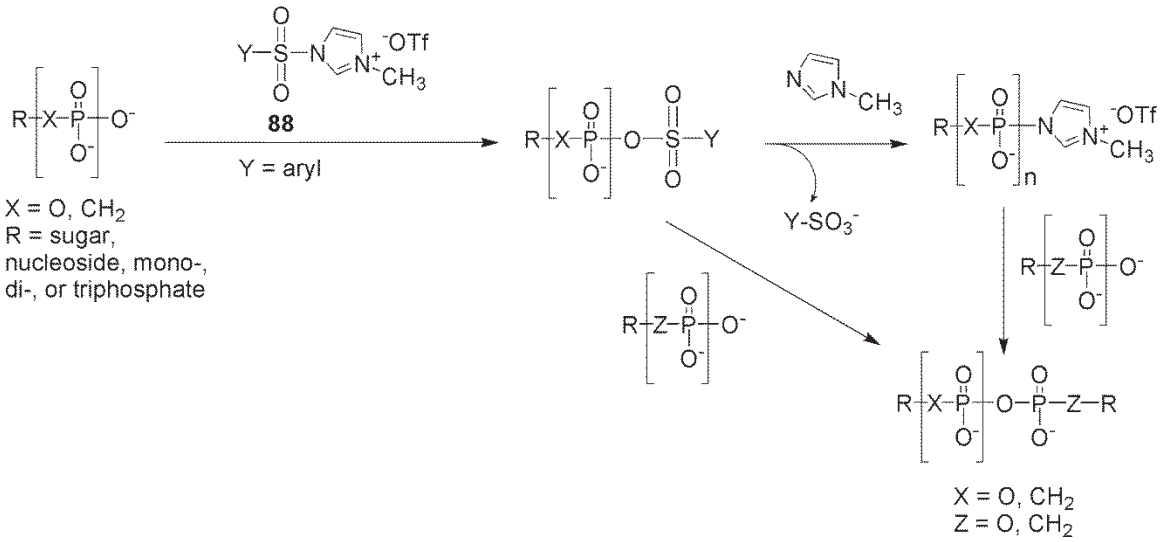


**Scheme 23** General procedure for the preparation of nucleotide or sugar nucleotide polyphosphate analogues[99]

Compound **52** was found to be stable and effective for up to three months, provided it was stored at -20°C. On occasion activity was lost, presumably due to moisture exposure. A qualitative test was developed to determine the activation potential of the reagent, prior to use. An NMP (1 mg of dTMP or UMP) was dissolved as its ditetrabutylammonium salt in MeCN (1 mL) with DIEA (20 μL) in an epindorph tube. Compound **52** (2 eq) was added to the tube followed by shaking. If **52** was active, the solution would turn from pale clear colorless to yellow within 30 seconds of addition, indicating the formation of the activated imidazolium salt. If **52** had been spoiled, the solution would remain clear and colorless. Successful phosphate activation could be verified by $^{31}$P NMR spectroscopy, with the appearance of the sulfonyl imidazolium salt signal at ~ -9 to -12 ppm. This activation test was performed ~1 hour prior to all coupling reactions to ensure activity of compound **52**. Figure 17 shows the color changed observed for UMP prior to, and after addition of **52**.

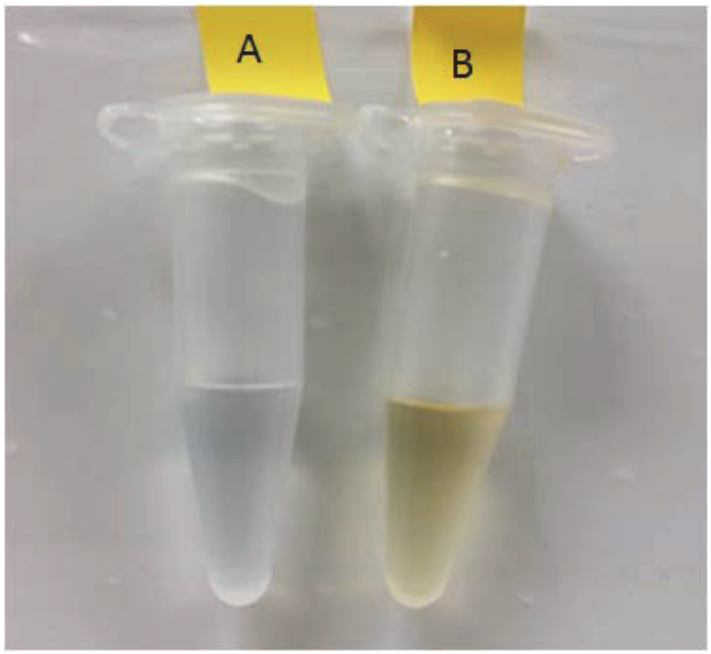


**Figure 17** Qualitative test for activation of phosphates by compound **52**. (A) UMP in MeCN prior to addition of **52**. (B) imidazolium salt of UMP formed after addition of **52**.

Cps2L has shown broad substrate tolerance to UTP.[11] Thus, UMP (**53**) and dTMP (**54**) were chosen as NMPs to be reacted with R1CP (**43**) for the formation of NMP-R1CP sugar nucleotide analogues. While phosphates had been demonstrated to be readily activated by sulfonyl imidazolium triflates, (Scheme 23, X = O), it was uncertain if phosphonates (Scheme 23, X = $CH_2$) could be activated in the same way. Both the phosphonate (**43**) and phosphate (UMP or dTMP) were evaluated as the nucleophile and the electrophile in the chemical coupling reactions shown in Scheme 24.

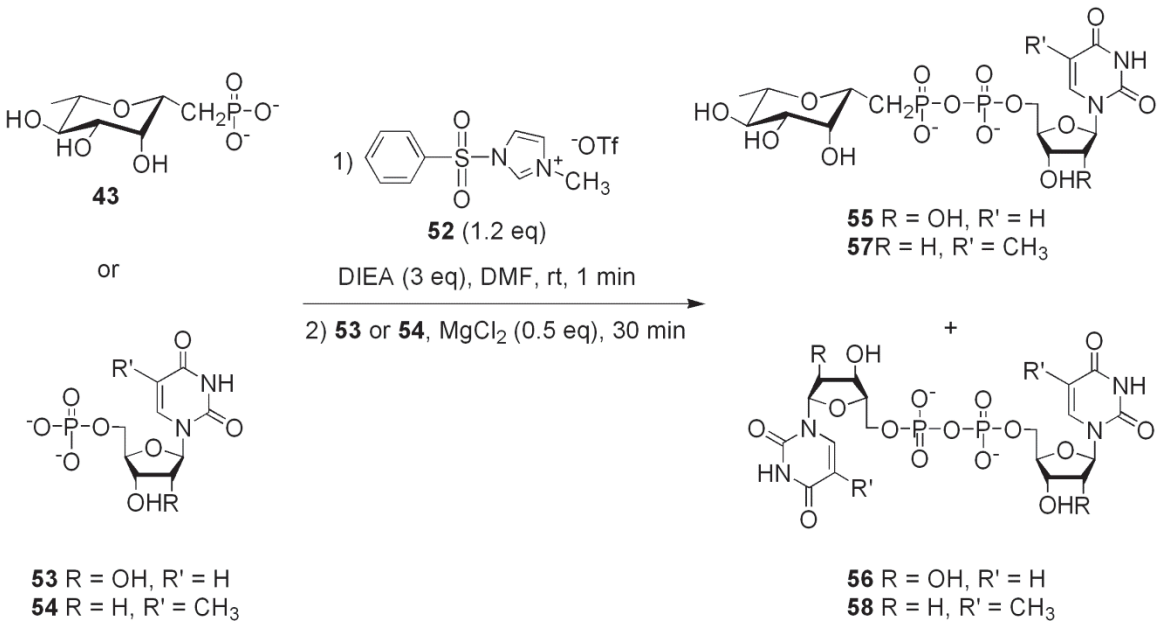


**Scheme 24** General procedure for the preparation of R1CP-NMP sugar nucleotide analogues

All phosphonates and phosphates used in the coupling were prepared as their ditetrabutylammonium salts by lyophilization with two equivalents of tetrabutylammonium hydroxide 30-hydrate. Reactions were conducted on a 0.2 mmol scale in DMF (2 mL) (**43**, **53** or **54**), and monitored by LRMS. The reactions were quenched with triethylammonium acetate (TEAA) (8 mL, 30 mM, pH ~7) upon completion (~30 minutes) and extracted with $CH_2Cl_2$ ( 2 x 10 mL). The aqueous layers were freeze dried and purified by C18 reversed phase column chromatography with a 30 mM TEAA/MeOH buffer system. It was found that when UMP (**53**) was used as the activated electrophile, significant amount of the unwanted self-condensation side product (**56**) were detected relative to the desired product (**55**) (Table 3, entry 1).

**Table 3** Results for the synthesis of R1CP-NMP analogues

| Entry | Nucleophile | Electrophile | Product | Ratio of Product to Side Product |
|---|---|---|---|---|
| 1 | **43** | **53** | **55** | 2:1 |
| 2 | **53** | **43** | **55** | 1:0 |
| 3 | **54** | **43** | **57** | 1:0 |

The ratios for **55**:**56** were determined to be 2:1 by $^{31}$P NMR spectroscopy (Figure 18). The phosphonate phosphorous atom of **55** appears as a distinct doublet at (~13 ppm). The accompanying phosphate doublet appears buried under the broad singlet phosphorous signal of both of the side-product (**56**) phosphorous signals (~ -11.5 ppm). The side-product and desired product were not separated, via reversed phase chromatography, due to their highly similar polarities. Figure 19A shows the HPLC trace of compounds **55** and **56**, after purification. When R1CP-UMP (**55**) was observed by HPLC, in the Tris-HCl buffer (50 mM, pH 7.5) required for enzymatic studies, it was found to rapidly breakdown at the central pyrophosphate (CPOPO) linkage, while the side product (**56**) remained relatively stable (Figure 19B). When the reaction was carried out using the phosphonate (**43**) as the activated electrophile and the NMP (**53** or **54**) as the nucleophile, the unwanted NMP self-condensation product was not detected by $^{31}$P NMR spectroscopy or LRMS (Table 3 entry 2-3). Under pH 7.5, however, R1CP-dTMP (**57**) proved to be just as labile as R1CP-UMP (**55**), as determined by $^{31}$P NMR spectroscopy analysis. Figure 19C shows the breakdown of **57** by HPLC to starting material dTMP (**54**), and thymidine (pH 5.5). The lability of the CPOPO sugar nucleotide analogues may also explain why the self-condensation products do not form when the phosphonate (**43**) was used as the activated species. The more robust OPOPO linkage of the side products (**56** or **58**) would be predictably more stable than the analogous CPOPC linkage that would result if the phosphonate imidazolium salts had self-condensed.

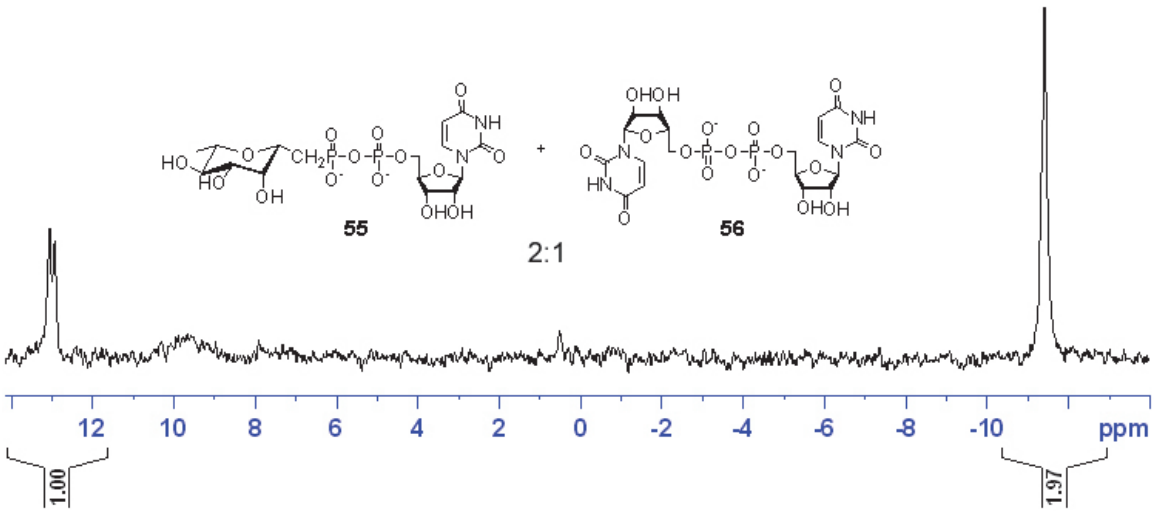


**Figure 18** $^{31}$P NMR (300 MHz, $H_2O$) spectrum of **55** and **56**

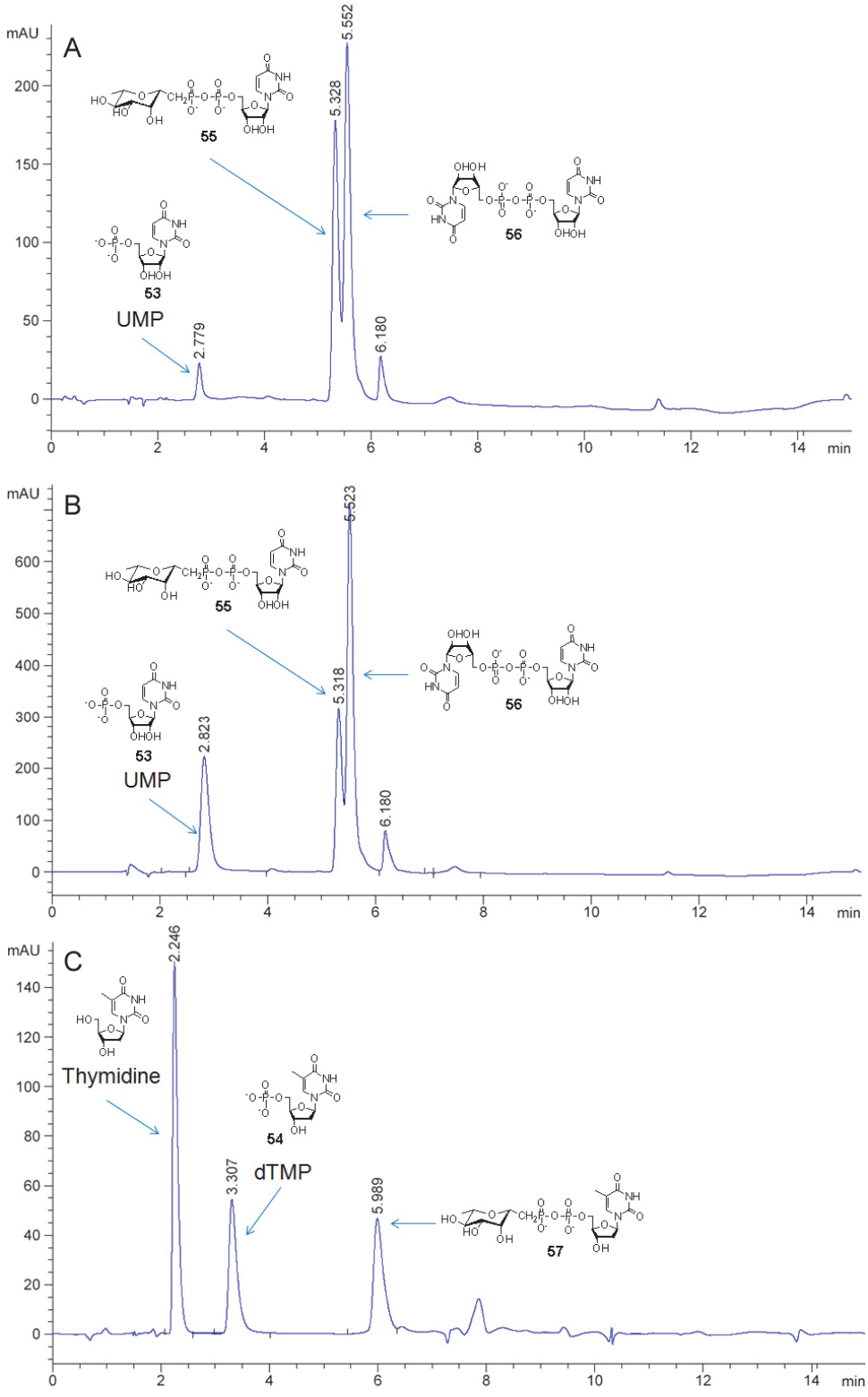


**Figure 19** HPLC trace of R1CP-NMPs after purification. (A) **55** and **56** (pH 6.5). (B) **55** and **56** (pH 7.5). (C) **57** (pH 5.5).

It was reasoned the monofluoro analogue, compound **44**, possessing a predicted p$K_a$2 (~5.7) value closer to a natural sugar phosphate, might produce a more stable sugar nucleotide analogue than compound **43**. Compound **44** was activated with **52** in the same manner as **43** (Scheme 24). While activation of the monofluoro ketosephosphonate was observed by the resultant color change of the solution (clear to yellow) upon addition of **52**, no sugar nucleotide analogues were detected by mass spectrometry, $^{31}$P, or $^{19}$F NMR spectroscopy.

It appeared that, while reinforcing the anomeric linkage of R1CP-NMPs with a methylene unit, the central CPOPO bond was effectively made more labile. The R1CP-NMPs were found to be vulnerable to hydrolysis under weakly basic (pH 7.5) physiological conditions. Consequently, these compounds would not be ideal for enzymatic inhibition studies with Cps2L. To address the problem of stability, it was reasoned that replacing the central oxygen of CPOPO bond of the R1CP-NMPs with a second methylene unit (CPCPO) might produce more hydrolytically stable sugar nucleotide analogues. The synthesis of R1CPCP analogues is discussed in section 3.4. The synthesis of CPCPO analogues, as precursors to R1CPCP analogues, is discussed in Section 3.3.

## 3.3 The Synthesis of CPCPO Analogues

The versatility of using sulfonyl imidazolium salts was demonstrated in Section 3.1.4, when both phosphates and phosphonates were successfully reacted with sulfonyl imidazolium triflate **52** to generate activated phosphates or phosphonates. The ability for these compounds to react with nucleophilic phosphates was well established,[99] however their reactivity toward other anions had not yet been explored in depth. As demonstrated in Section 3.1.1, the lithium salts of phosphonates were shown to be highly effective nucleophiles when coupling with sugar lactones to produce sugar ketosephosphonates. It was reasoned that the lithium salts of phosphonates might couple with the activated imidazolium salts of phosphonates to produce phosphonates with a CPCPO scaffold. These compounds have not before been reported in the literature. The goal was to react R1CP (**43**) with dimethyl or dibenzyl methylphosphonate (**54** or **32a**) to generate an

R1CPCP analogue which, after deprotection, could be evaluated as an inhibitor directly with Cps2L and compared to **43**, or subsequently be converted to a full sugar nucleotide analogue via reaction with an activated nucleoside (thymidine or uridine). Given that **43** required seven synthetic steps to produce, a model substrate in the form of **59** was prepared to test the coupling conditions. Compound **59** was prepared by refluxing **54** in tertbutylamine overnight as shown in Scheme 25.[100]

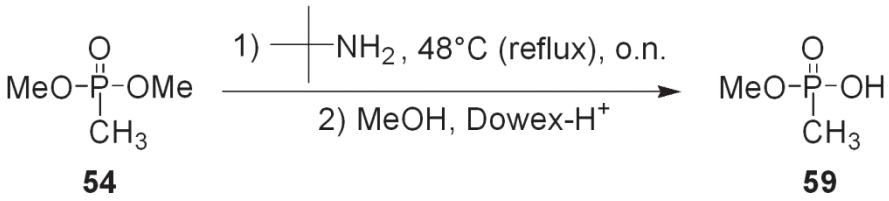


**54** **59**

**Scheme 25** Synthesis of monomethyl methylphosphonate (**59**)

To effect full conversion from **54** to **59**, approximately 10 mL of tertbutylamine solvent was required for 0.1 mL (116 mg) of **54**. The reaction was monitored by removing 700 μL aliquots and observing them by $^{31}$P NMR spectroscopy for the disappearance of **54**. The material was concentrated and redissolved in methanol (10 mL), in the presence Dowew-$H^+$ (~1 g), to remove the tertbutylammonium group. After stirring for 5 minutes, the material was filtered and **59** was recovered as a clear liquid, in its free acid form. Compound **59** was found to be relatively volatile (b.p. <100°C), as most of the material was lost during the concentration step required to remove the tertbutylamine solvent. On a 500 mg scale, usually 50 mg was recovered, which was sufficient to evaluate as a test substrate to be activated and coupled with **54**. If necessary, isolation in higher yield may be possible using fractional distillation.

Nucleophilic coupling reactions with *n*-BuLi and select phosphonates were generally carried out at -78°C in THF to reduce the ability of the *n*-BuLi to react with the solvent. THF has been shown to be susceptible to deprotonation by *n*-BuLi at temperatures in excess of -20°C.[101] THF was chosen initially to test the coupling reaction between **59** and **54** to produce a CPCPO scaffold, due to its widespread use in couplings involving lithium phosphonates. Unfortunately, it was found that sulfonyl imidazolium triflate **52** was insoluble in THF, and no formation of the activated imidazolium salt of **59** was observed by $^{31}$P NMR spectroscopy. DMF (used previously for successful activation

of both phosphates and phosphonates) and MeCN were both evaluated as potential solvents for the initial activation of **59** by **52**. The single methyl-protecting group of phosphonate **59** facilitated solubility in both DMF and MeCN, so conversion of **59** to its tetrabutylammonium salt was not necessary. It was unclear, however, how the presence of a single protecting group at the phosphonate position would affect activation of **59** by **52** (Scheme 26). A $^{31}$P NMR spectrum was recorded to see if the imidazolium salt (**60**) could be detected. Figure 20 shows the rapid successful formation of **60** in both DMF and MeCN. Reaction with **52** produced a chiral mixture of imidazolium salts, which was observed by $^{31}$P NMR spectroscopy.

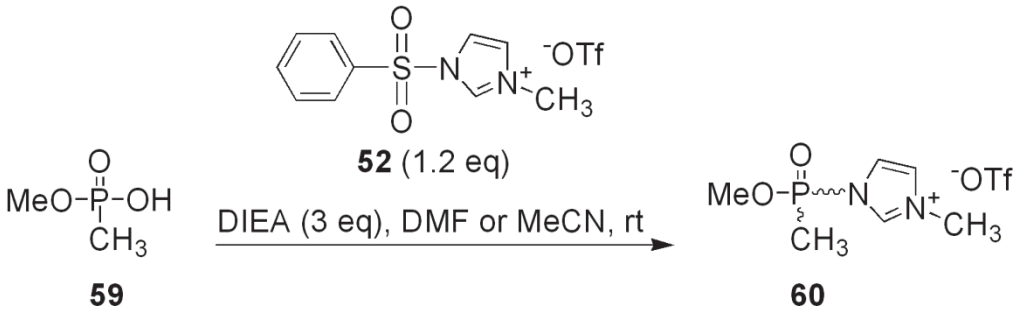


**Scheme 26** Activation of monomethyl methylphosphonate (**59**)

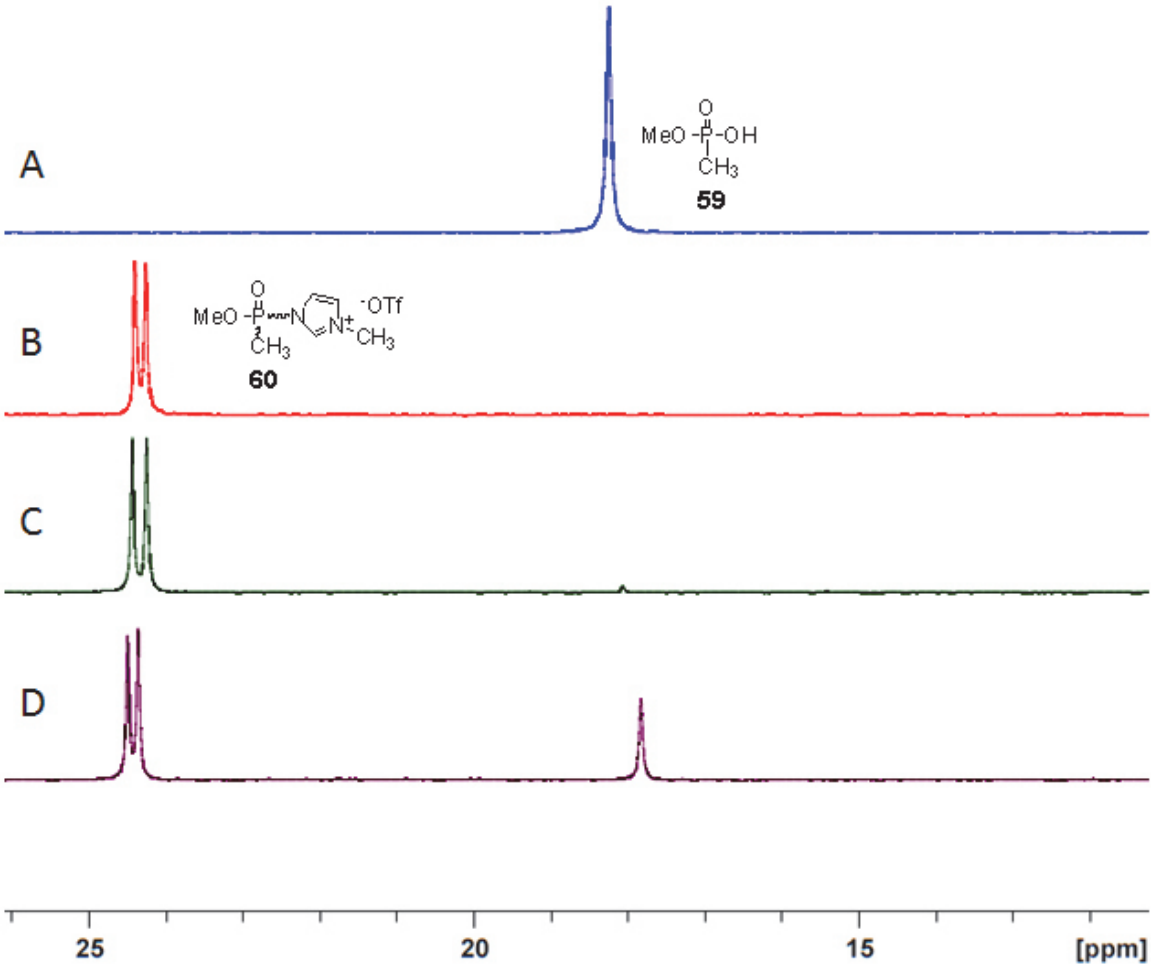


**Figure 20** $^{31}$P NMR spectra (300 MHz) showing formation of imidazolium salt (**60**). (A) $^{31}$P NMR spectra of **59** (DMF). (B) $^{31}$P NMR spectra of **59** (DMF) 2 minutes after addition of **52.** (C) $^{31}$P NMR spectra of **59** (MeCN) 2 minutes after addition of **52.** (D) $^{31}$P NMR spectra of **59** (DMF) 24 hours after addition of **52.**

The ability for **59** to form the activated imidazolium salt (**60**), in both DMF and MeCN, after immediate addition of **52**, was an encouraging result for the potential coupling of monomethylated phosphonates with the lithium salts of phosphonates. Activated phosphonate **60** showed only 25% breakdown to starting material **59**, in DMF, 24 hours after the initial addition of **52** (Figure 20D), which suggested the imidazolium salts should be sufficiently stable for coupling with lithium phosphonates. While MeCN and DMF proved equally valid for activation, it was unclear if there would be a difference in their coupling efficiency for the production of the CPCPO compounds. Both were evaluated separately in a mixed solvent system with THF. THF was maintained as

the solvent of choice for the formation of the lithium phosphonates via reaction of DMMP (**54**) or DBMP (**32a**) with *n*-BuLi at -78°C. Due to the capacity of both DMF (m.p. -60°C) and MeCN (m.p. -44°C) to flash freeze at -78°C, the coupling reactions were conducted at ~ -40°C when DMF was used, and ~ -30°C when MeCN was used as the activation solvent. Scheme 27 shows the coupling reaction for the production of CPCPO compounds **61** and **62**.

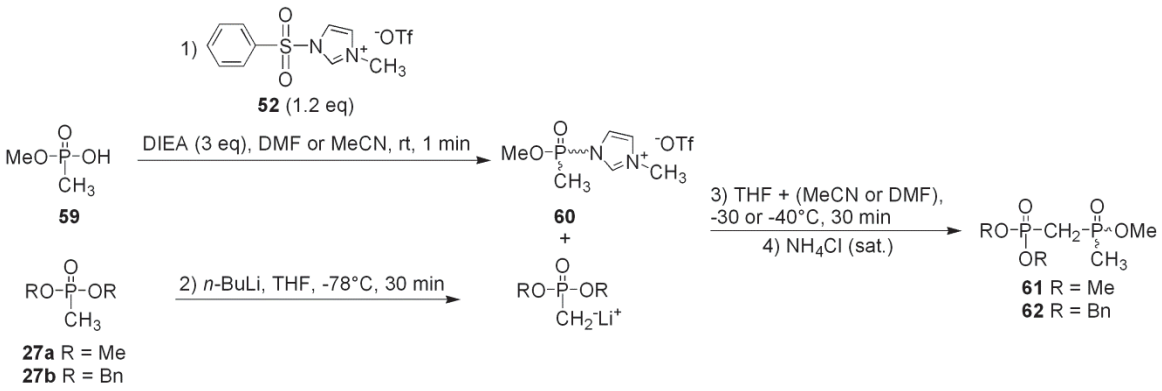


**Scheme 27** Synthesis of CPCPO compounds **61** and **62**

The products were detected by LRMS/MS and $^{31}$P NMR spectroscopy. Figure 21 shows the LRMS/MS spectra of **61** and **62**. Conversions were generally 33-38% for **61** and **62** relative to the starting material **59** after 30 minutes, as determined by $^{31}$P NMR spectroscopy. Additional reaction times (up to 3 hours) did not improve conversions. There were no significant advantages in using one solvent (DMF or MeCN) or nucleophile (**27a** or **27b**) over the other. Reactions were conducted on a 25 mg scale of **59** in 2 mL total volume of 1:1 THF:(DMF or MeCN). To achieve ~ -40°C (for coupling reactions using DMF) a dry ice slurry was made with MeCN. For coupling reactions using MeCN a temperature range of -20 to -40°C was necessary, as the phosphonate anion could potentially deprotonate the THF if the temperature rose above -20°C, and the MeCN (m.p. -44°C) reaction solvent could potentially freeze if the temperature dropped below -40°C. To achieve these conditions, a dry ice slurry was made with an approximate 1:1 mixture of MeCN:$CCl_4$. The slurry was ideal for maintaining temperature conditions between -25 and -35°C. Reactions were quenched with 5 mL $NH_4Cl$ (sat.) and extracted with $CH_2Cl_2$ (2 x 5 mL). The globally protected CPCPO compounds were always

recovered in the organic layer after extraction. As compounds **61** and **62** were test substrates to see if compounds with CPCPO scaffold could be synthesized, their isolation and purification was not pursued. Given the success of the newly developed reaction conditions, the next step was to see if R1CP analogues could be used in place of **59** to produce compounds with and R1CPCP scaffold.

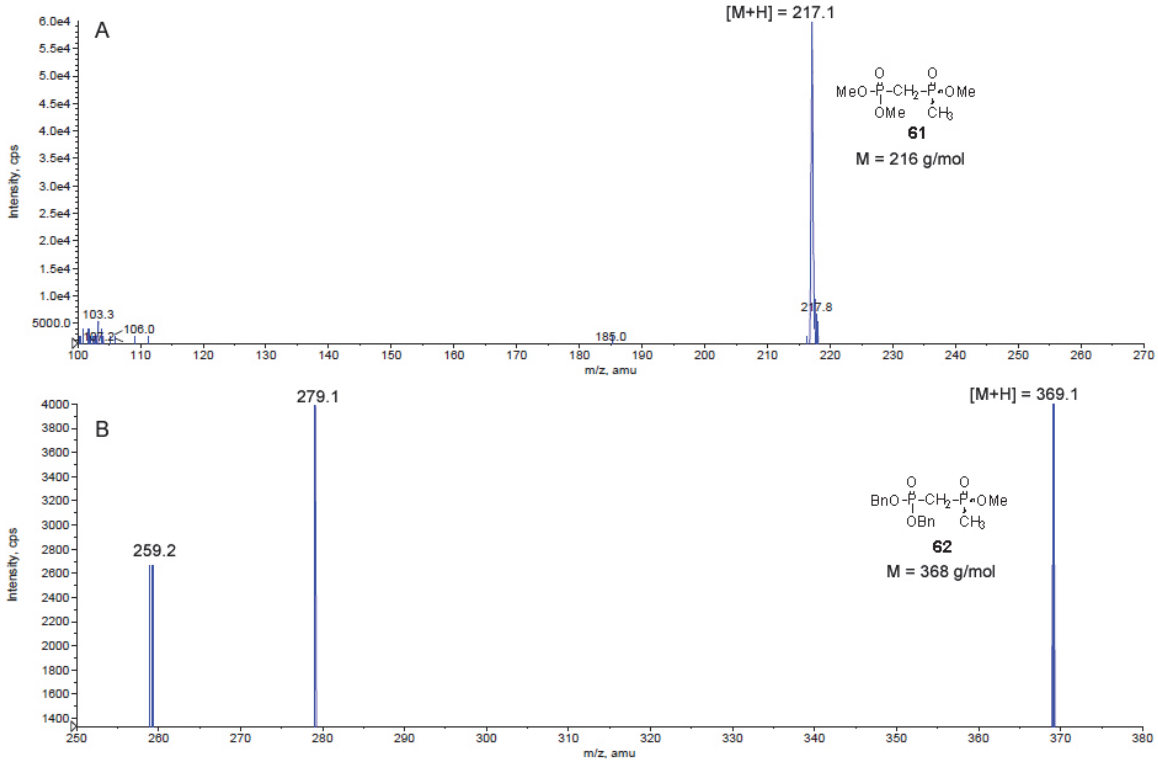


**Figure 21** LRMS/MS for compounds **61** and **62**. (A) EPI(+) for [M+H] = 217 shows compound **61**. (B) EPI(+) for [M+H] = 369 shows compound **62.**

## 3.4 The Synthesis of R1CPCP Analogues

A series of R1CP analogues were investigated for activation by **52** and coupling with alkyl or aryl protected phosphonates (**27a**, **27b** or **33**) (Scheme 28). The reactions were carried out on a 0.05 mmol scale of the electrophile with five equivalents of the nucleophile in 2 mL total reaction solvent (1:1 MeCN:THF). MeCN (b.p. = 82°C) was chosen as the activation solvent over DMF (b.p. = 152°C), for easy removal *in vacuo*. The phosphonates were activated from their tetrabutylammonium salt forms, except in cases where solubility in MeCN was not an issue (**43′** and **44′**), in which case the free

acids were used. To ensure complete ionization of the phosphonates, five equivalents of DIEA were used for all reactions. To maximize coupling efficiency and ensure full consumption of the electrophile, five equivalents of the base (*n*-BuLi or LDA) and phosphonate nucleophile were used, as is common for *n*-BuLi or LDA coupling reactions in THF. The use of three or less equivalents of phosphonate and base resulted in reduced or negligible conversions. Table 4 summarizes the results.

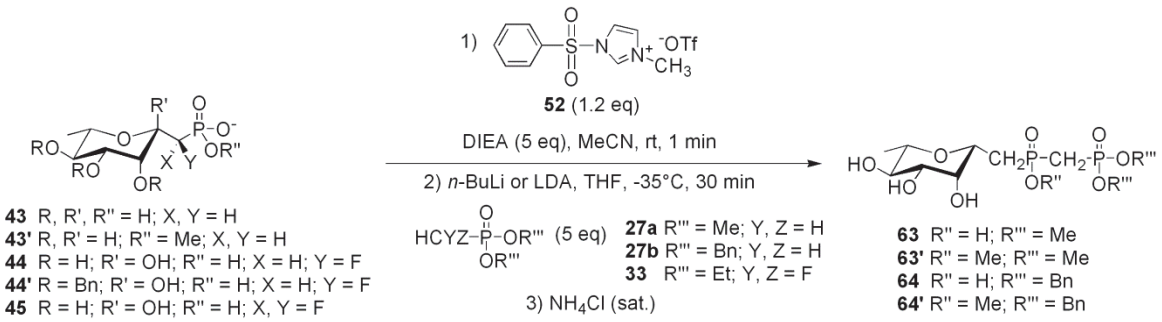


**Scheme 28** Synthesis of R1CPCP analogues

**Table 4** Results for the synthesis of R1CPCP analogues

| Entry | Electrophile | Nucleophile | Base | Product | Conversion |
|---|---|---|---|---|---|
| 1 | **43** | **27a** | *n*-BuLi | **63** | ~70% |
| 2 | **43** | **27a** | LDA | **63** | ~70% |
| 3 | **43** | **27b** | *n*-BuLi | **64** | ~70% |
| 4 | **43** | **33** | LDA | — | 0% |
| 5 | **43′** | **27a** | *n*-BuLi | **63′** | ~35% |
| 6 | **43′** | **27b** | *n*-BuLi | **64′** | ~35% |
| 7 | **44** | **27a** | *n*-BuLi | — | 0% |
| 8 | **44′** | **27a** | *n*-BuLi | — | 0% |
| 9 | **45** | **27a** | *n*-BuLi | — | 0% |

It was found that the base (*n*-BuLi or LDA) and nucleophile protecting groups (methyl, **54**, or benzyl, **27b**) did not affect the conversion to the R1CPCP product (entry 1-3). The use of diethyl difluoromethylphosphonate (**33**) resulted in no product formation (entry 4). This could be explained by the reduced nucelophilicity of the lithiated salt of **33** relative to the non-fluorinated phosphonates (**27a** and **27b**). The expected R1CP$\underline{CF_2}$P

product would also be predictably less stable than an R1CP$\underline{CH_2}$P analogue, and may breakdown under the harsh basic reaction conditions. When the monomethylated phosphonate (**43′**) was used as the electrophile (entry 5-6), conversions (~35%) were comparable to the analogous coupling reactions with **59**, discussed in section 3.1.4, and half that of the conversions when the globally deprotected phosphonate (**43**) was used (~70%). This could be explained by the increased hindrance that the methyl group would add to **43′**, relative to the fully demethylated compound (**43**). Additionally, the imidazolium salt of **43′** would exist in two diastereotopic forms, one of which may be more accessible than the other, toward coupling with the lithium salt of phosphonate **27a** or **27b**. When the monofluoro ketosephosphonate (**44**) was evaluated as an electrophile, no product formation was detected by $^{31}$P NMR spectroscopy or LRMS (entry 7). The benzyl protected analogue (**44′**) was prepared by treating the methyl protected form (**32a**) with two equivalents of TMSBr, followed by direct concentration *in vacuo* (Scheme 29). The complete loss of the methyl protecting groups was verified by LRMS. The presence of benzyl protecting groups on the L-rhamnose moiety of the monofluoro phosphonate (**44′**) did not result in any product formation (entry 8). Similar results were obtained for the difluoro compound (**45**) (entry 9). It appeared that the presence of any fluorine atoms (1-2) at the C1 position was detrimental to product formation. This could be explained the potential reduced stability of the imidazolium salts of **44**, **44′** and **45**, relative to the non-fluorinated analogue, **43**. The ability of ketosephosphonate functionality to interchange between the α, β, and open-chain forms may also be a factor in preventing the coupling reaction from occurring. Under no circumstances, when fluorine was present in the electrophile (entry 4) or nucleophile (entry 7-9) scaffold, was any product detected by NMR spectroscopy ($^{31}$P and $^{19}$F) or LRMS.

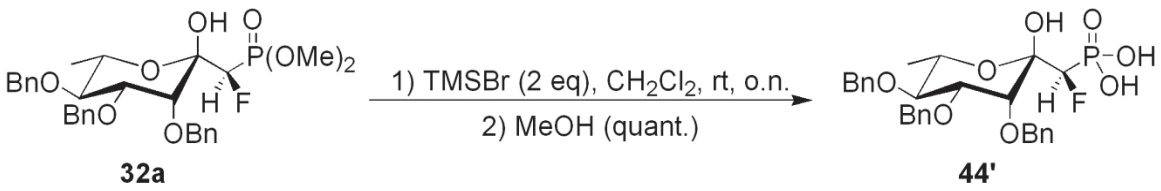

**32a** **44'**

**Scheme 29** Demethylation of **32a** with TMSBr

The reactions were worked up by quenching with 5 mL of ice cold $NH_4Cl$ (sat., pH 7), and extracting with $CH_2Cl_2$ (2 x 5 mL). Product **63**, bearing two methyl-protecting groups at the terminal phosphonate and one free P—$O^-$ at the anomeric phosphonate position, was recovered in the aqueous layer. Products **63′**, **64** and **64′** were all recovered in the organic layer, after workup. The product masses were verified by LRMS and LRMS/MS in both positive and negative modes. The product masses for **63**, **63′**, **64** and **64′** were always observed ~10 fold less than the separate major products, which were identified as the compounds that would form from anomeric cleavage of the R1CPCP scaffold. The fact that the presence (**63′** and **64′**) or absence (**63** and **64**) of a methyl substituent on the R1CPCP scaffolds was reflected in the structures of the major products indicates that **61**, **62**, **65**, and **66** were formed from the breakdown of the R1CPCP compounds. The free L-rhamnose sugar (**23**) was assumed to be the additional product formed upon quenching the oxacarbenium intermediate with aqueous $NH_4Cl$ (Scheme 30).

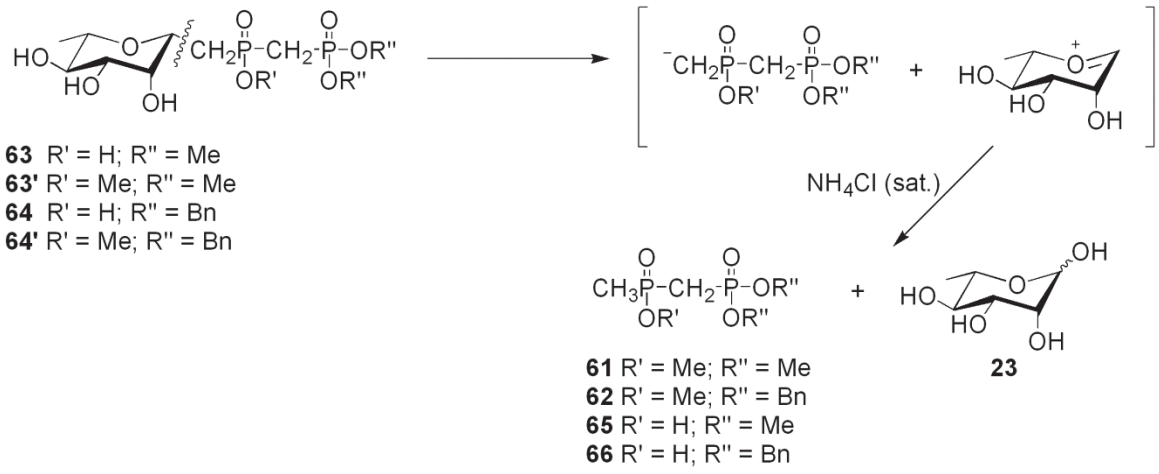


**Scheme 30** Anomeric cleavage of R1CPCP analogues

Figure 22 shows the LRMS/MS positive mode scans for the reaction of **43** with **27b** (entry 3). Figure 23 shows the $^{31}P$ NMR spectrum for the crude reaction of **43** with **27b**. The conversions (Table 4) of ~70% (entry 1-3) and ~35% (entry 5-6) were estimated as the ratio of products formed (including desired product and breakdown product) relative to the remaining phosphonate starting material (**27a** or **27b**). The desired product was always detected as the minor product relative to the major breakdown product in

~1:3 ratio. The CPC $^{31}$P NMR shift of the CPCPO scaffold was observed in the 45-60 ppm range, with the CPO shift appearing in the 20-30 ppm range, for all desired products (**63**, **63′**, **64**, **64′**) and their breakdown products (**61**, **62**, **65**, **66**). The $^{2}J_{P,P}$ constant could be used to distinguish between desired and breakdown compounds. If the L-rhamnose scaffold was intact, a larger coupling constant ($^{2}J_{P,\,P}$ ~14 Hz) was observed. If it had been lost, a smaller coupling constant ($^{2}J_{P,\,P}$ ~6 Hz) was observed. Additional breakdown of the desired product was not observed after workup with $NH_4Cl$ (sat., pH 7), suggesting that it was the harsh reaction conditions required for coupling that ultimately facilitated anomeric cleavage of the products. All of the breakdown products were found to be very polar. Isolation of benzyl protected breakdown products (**62** and **66**) was attempted using normal phase silica column chromatography and a 5-15% MeOH in EtOAc elutant system. The compounds were found to be pure by $^{31}$P NMR spectroscopy, however various impurities were still present by $^{1}$H NMR spectroscopy. Figure 24 shows the $^{31}$P NMR spectrum of compound **66**.

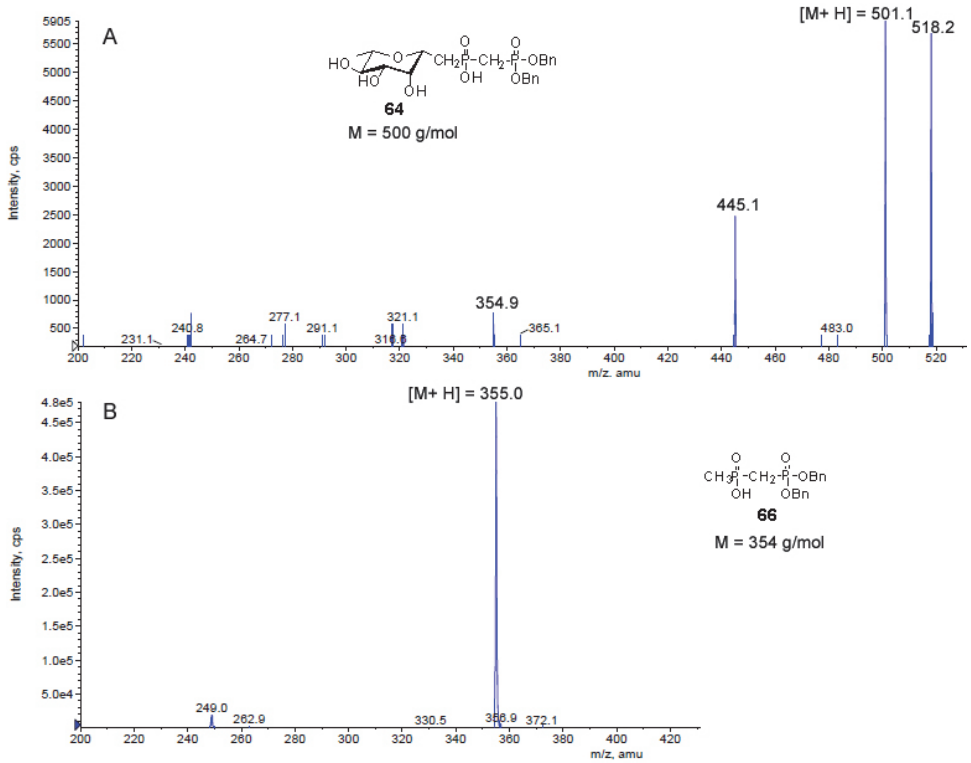


**Figure 22** LRMS/MS for compounds **64** and **66**. (A) EPI(+) for [M+$NH_4$] = 518 shows compound **64**. (B) EPI(+) for [M+$NH_4$] = 372 shows compound **66.**

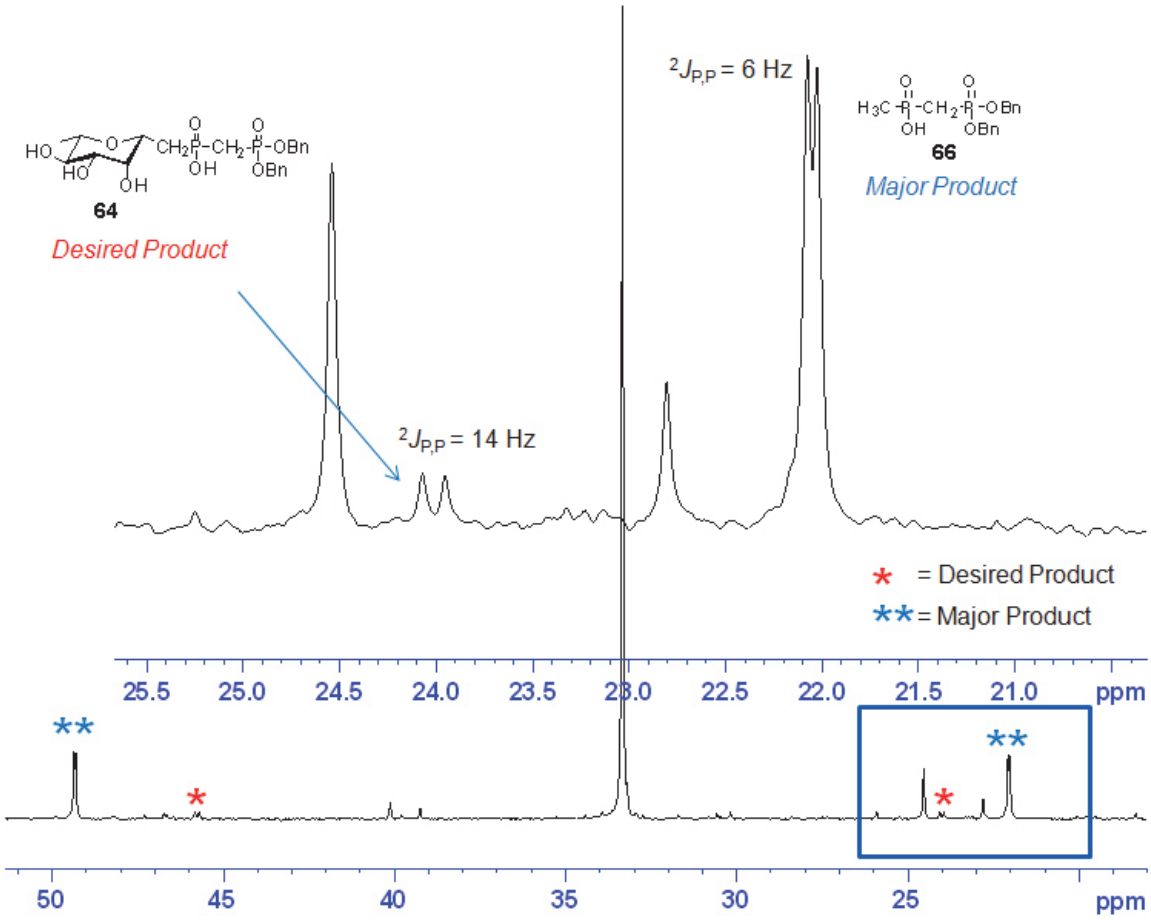


**Figure 23** $^{31}$P NMR spectra (300 MHz, MeOH) showing formation and R1CPCP analogue **64** and breakdown product **66**.

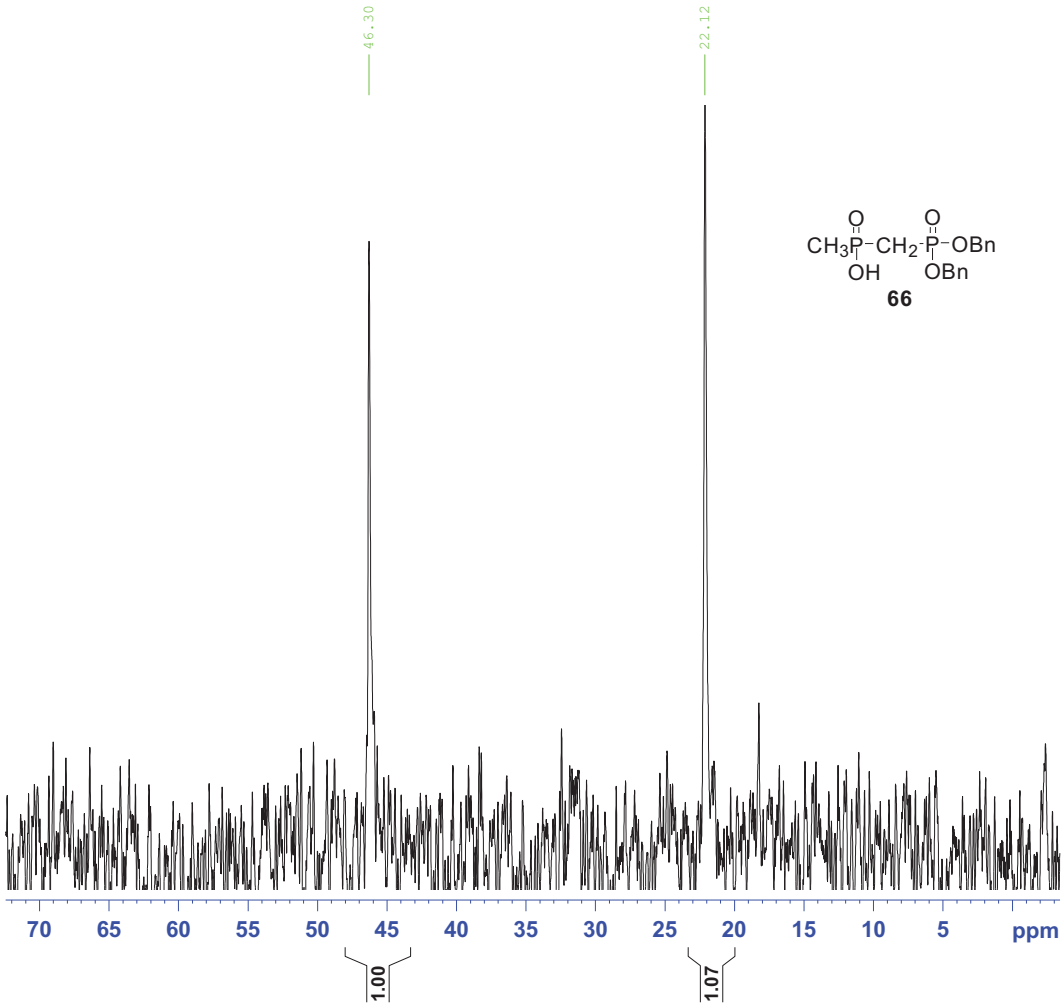


**Figure 24** $^{31}$P NMR spectra (300 MHz, $CD_3CN$) of compound **66** after purification.

In conclusion, the synthesis of R1CPCP analogues was successful when R1CP analogues **43** and **43′** were used as the nucleophile and coupled with DMMP (**54**) or DBMP (**27b**)**.** A complex reaction system of mixed solvents (MeCN and THF), a specific temperature range (-25 to -40°C), and harsh base (*n*-BuLi or LDA) were required to facilitate coupling. The target products were prone to anomeric cleavage under the harsh coupling conditions. The breakdown products, possessing the CPCPO scaffold, were found to be quite stable and represent the first examples of CPCPO phosphonate analogues reported. The stability of these compounds can potentially be exploited to produce a series of CPCPO analogues, which may yet be used to access stable R1CPCP analogues, under more mild conditions. These conditions are discussed in Chapter 5.

# CHAPTER 4 RESULTS AND DISCUSSION PART 2

## 4.1 Methylene Bisphosphonate Glycosylated Conjugates

### 4.1.1 The Synthesis of deoxythymidine 5′-Methylenebisphosphonate (**68**)

Kalek and coworkers[64] reported the synthesis of a variety of analogues of methylenebis phosphonate-based nucleosides using varying equivalents of methylenebis(phosphonic dichloride) (**10**). Thymidine was not one of the nucleosides used in their synthesis, however, the most analogous pyrimidine nucleoside, uridine, was found to be the least reactive of the nucleosides. Uridine produced only moderate conversions and required up to six equivalents of **10** for reactivity in contrast to guanosine, which required only one equivalent. Initial attempts at coupling thymidine to **10** were entirely unsuccessful even with six equivalents of **10** under identical conditions. By switching from thymidine to 3′-*O*-acetylthymidine (**67**), quantitative conversions were achieved when four equivalents of MBPDC were used. The reason for the enhanced reactivity of the 3′-*O*-acetylthymidine relative to thymidine is not exactly clear. In work reported by Stepinski *et. al.*, MBPDC was used in the synthesis of a variety of symmetric esters, which used DIEA as a base and 1H-tetrazole as a catalyst.[62] By incorporating these reagents into the conditions described by Kalek and coworkers,[64] a new method was developed, which reduces both the reaction time (2.5 h from 24 h) and required MBPDC equivalents (2 from 4) (Scheme 31).

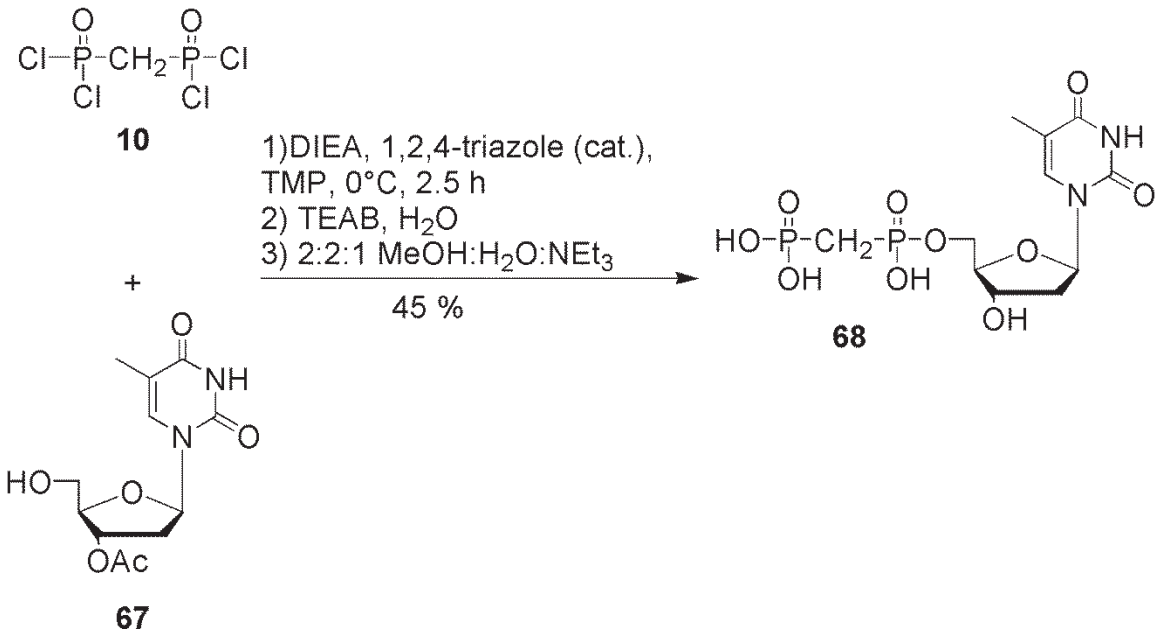


**Scheme 31** Method 1: Synthesis of deoxythymidine 5′-methylenebisphosphonate (**68**)

Anion exchange purification of the material was carried out using a TEAB buffer (1 M, pH 8). The material had to be titrated to pH 7 using the TEAB buffer and heavily diluted for adequate binding. If the material was too concentrated, insufficient binding would occur, resulting in the material being lost in the flow-through during the loading process. A simple TLC plate test for the absence of UV activity of the flow through was sufficient to confirm binding. A dilution factor of 200 mL solution per 1 mmol of MBPDC (conductivity = 0.39 mS) was used was sufficient to ensure adequate binding to a 5 g DEAE-Sephadex A25 ($HCO_3^-$ form), 12 mL column. Purification of the material was initially very difficult due to the similar polarities of the product and MBP, which often coeluted together at ~20-25% 1 M TEAB. Meticulous analysis of the fractions by $^{31}P$ NMR was necessary to determine when coelution occurred (Figure 25). It was found that an isocratic gradient at 20% 1 M TEAB and reduced flow rates (5 mL/min) were effective for increasing separation.

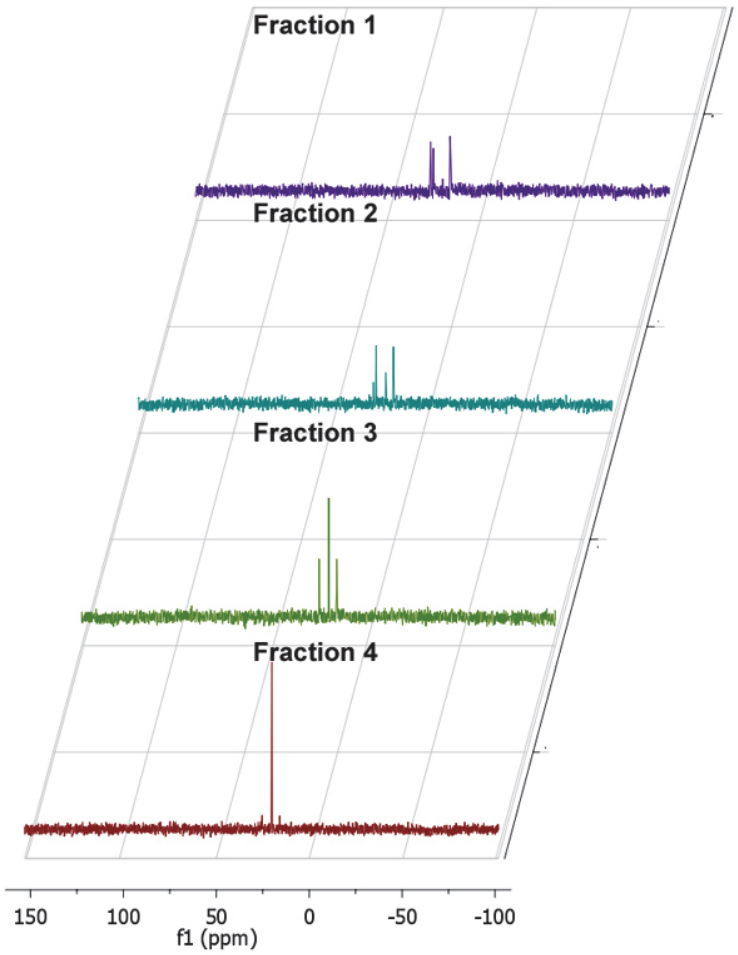


**Figure 25** $^{31}$P NMR (250 MHz) spectra of fractions after dTMBP purification. Fraction 1 (isolated dTMP). Fraction 2-3 (coelution). Fraction 4 (isolated MBP).

Due to the basic conditions of the purification (pH ~8) the material was often isolated as a mixture of protected (acetylated) and deprotected compounds. For simplification, full deprotection was carried out using a solution of 2:2:1 MeOH:$H_2O$:$NEt_3$. An additional bi-product, monomethyl methylenebisphosphonate, was later discovered to be present and inseparable from the desired product via anion exchange chromatography. The material initially eluded detection because it did not show up by HPLC analysis, was mistaken for trace amounts of TMP by $^1$H NMR, and possessed an overlapping $^{31}$P NMR spectrum with the desired product (**68**). Monomethyl MBP was eventually detected by mass spectrometry and found to be present in ratios as high as 1:1 with **68**. It appeared that the TMP solvent was acting, to some degree, as a

methylating agent with the MBPDC (**10**) starting material. It should be noted that no di, tri, or tetramethyl MBP was detected by mass spectrometry.

The methyl-MBP could potentially be deprotected using reagents such as TMSI or TMSBr, which would convert the material into MBP and allow for anion exchange separation from the target compound (**68**). The addition of an extra deprotection step and subsequent purification rendered Method 1 less practical. Consequently, a new method was designed (Method 2, Scheme 32) which did not include the TMP methylating solvent. Using Method 2, **10** and **67** could be coupled using pyridine to generate **68** in 10 min. A comparison of Method 1 and Method 2 is given in Table 5.

**Table 5** Comparison of Method 1 and Method 2

| **Entry** | **Comparison:** | **Method 1** | **Method 2** |
|---|---|---|---|
| 1 | Solvent/base/cat: | TMP, DIEA, 1,2,4-triazole | Pyridine |
| 2 | Reaction time: | 2.5 h | 10 min |
| 3 | Required MBPDC eq: | 2 | 3 |
| 4 | HPLC conversion: | 100% | 67% |
| 5 | Bi-products: | Inseparable | Separable |
| 6 | Isolated yield: | 45% | 48% |

The production of the dinucleoside-MBP was determined to be present in a ~1: 5 ratio with (**68**) by HPLC. Since two equivalents of **67** are required to synthesize the dinucleoside analogue, the conversion to **68** was calculated, by HPLC, to be approximately 67%. The dinucleotide analogue was separated from **68** using the same anion exchange purification from Method 1. The disadvantage of Method 2 is that it requires an extra equivalent of MBPDC and produces lower conversions of **68** than Method 1. The advantages of Method 2 are that it is significantly faster than Method 1 and the product can be isolated in a marginally greater yield with only one purification step. Overall Method 2 was selected as the preferential method for the synthesis of **68**.

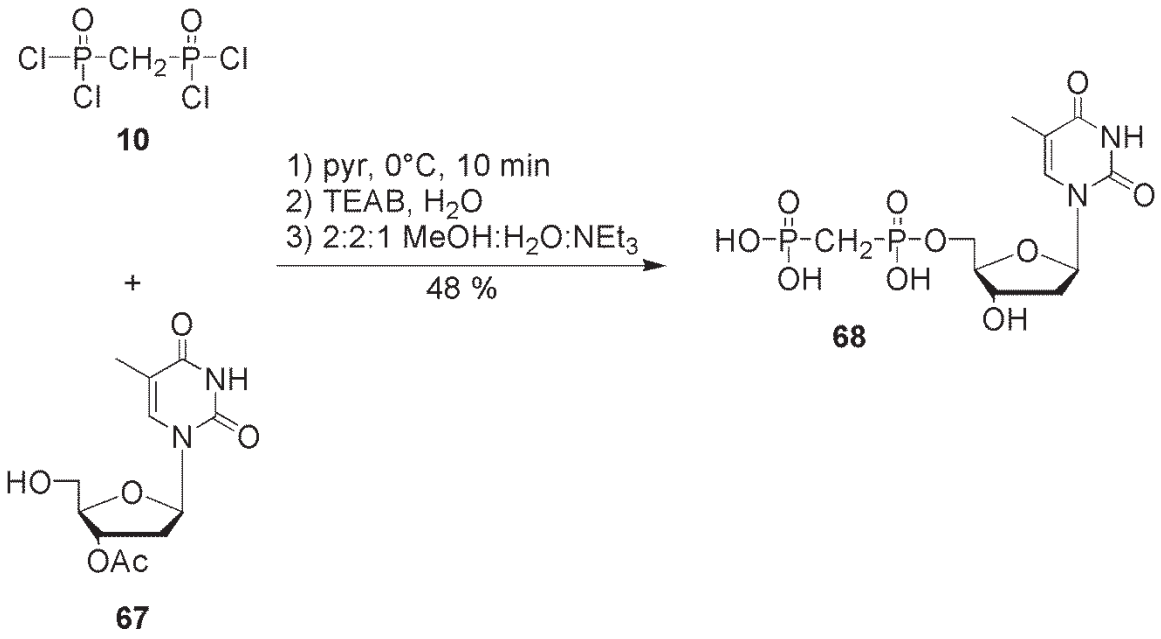


**Scheme 32** Method 2: Synthesis of deoxythymidine 5′-methylenebisphosphonate (**68**)

## 4.1.2 The Synthesis of β-D-Glucopyranosyl 1-methylenebisphosphonate (**71**)

Timmons and Jakeman[102] reported the successful synthesis of sugar nucleotides, such as UDP-α-D-mannose, via the coupling of the tetrabutylammonium salts of NDPs with acetyl-protected glycosyl bromides. The synthesis of β-D-glucopyranosyl 1-methylenebisphosphonate was investigated using this approach to test the ability of the MBP to couple with glycosyl bromides in an analogous manner as the NDPs. The first step was the synthesis of the 2,3,4,6-tetra-*O*-acetyl-α-D-glucopyranosyl bromide (**70**), which formed as the α-bromide product due to the higher stability of substituents in the axial orientation at the anomeric position (Scheme 33). It was suspected that any of the β-bromide formed would equilibrate to the more stable α-product.

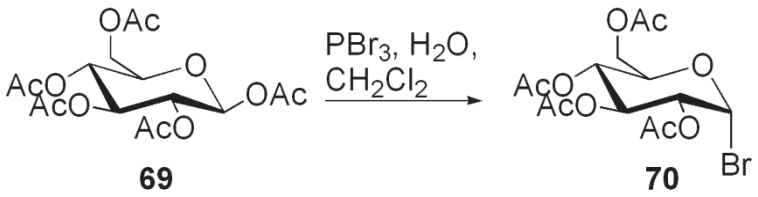


**Scheme 33** Synthesis of 2,3,4,6-tetra-*O*-acetyl-α-D-glucopyranosyl bromide (**70**)

The next step was the conversion of MBP (**7**) to the ditetrabutylammonium salt (**7′**) via titration to pH 6 using tetrabutylammonium hydroxide (TBAOH). It was found that pH 6 was adequate to achieve exactly two equivalents of tetrabutylammonium per one equivalent of MBP, as confirmed by $^{1}$H NMR. The coupling of **7′** and **70** was achieved using the same conditions described by Timmons and Jakeman (Scheme 34).[102]

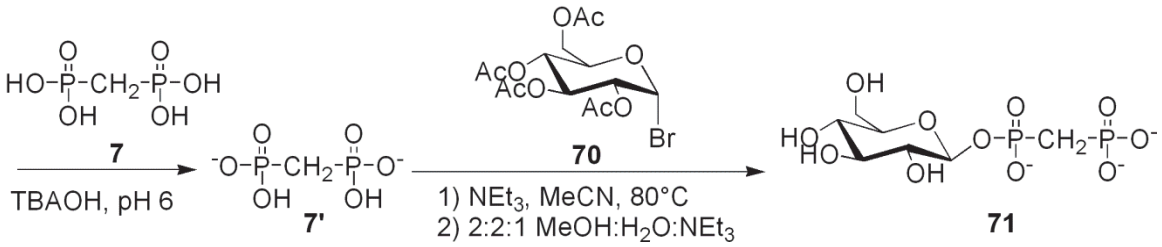


**Scheme 34** Synthesis of β-D-glucopyranosyl 1-methylenebisphosphonate (**71**)

The reaction proceeded via an $S_N1$ mechanism to give exclusively the β product, with conversions comparable to those described for the synthesis of sugar nucleotides (~30%).[102] The β selectivity of the reaction is attributed to the contributions of the C2 neighboring participating acetyl group on the glucose as well as the nitrile effect, which dictates that nitrile groups can coordinate to the axial position of the anomeric center.[103] These effects drive the formation of β products (Scheme 35). Anomeric stereoselectivity was determined from the anomeric H1-H2 coupling constant, using $^{1}$H NMR spectroscopy.

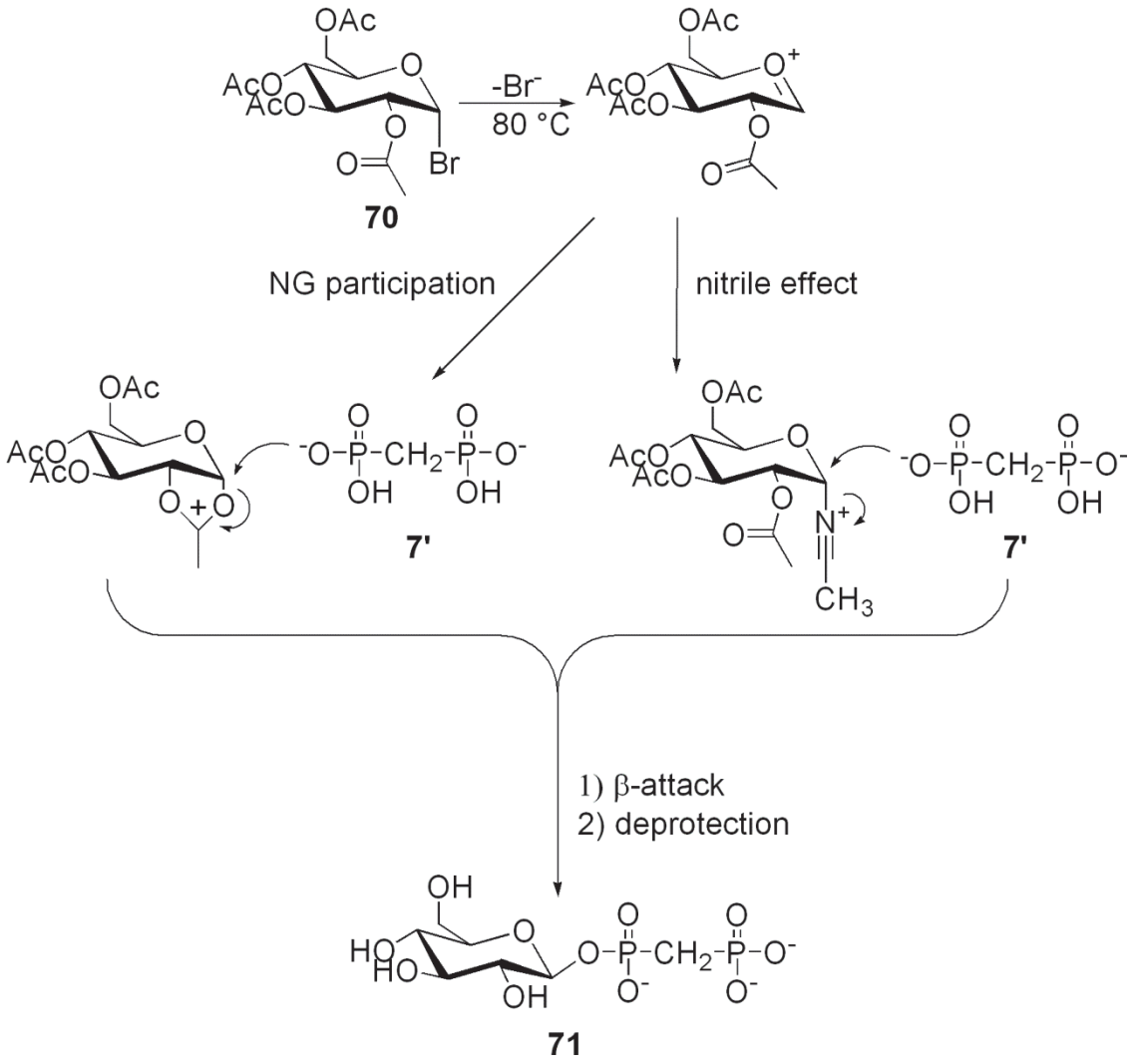


**Scheme 35** Mechanism of action of neighboring group participation and the nitrile effect in the production of β-glucosides

The product was isolated as a mixture of the ditetrabutylammonium salts of MBP-glucose and remaining MBP starting material (~70%) using C18 ion-pair reversed phase chromatography with 10 mM tributylammoniumbicarbonate (TBABC) as the buffer. Unlike the purification of the sugar nucleotide products, in which alkaline phosphatase was added to degrade unreacted nucleoside 5′-diphosphate starting material, the methylene linker of the MBP prevents degradation. As a result, the product and unreacted MBP starting material (~70%) coelute together, due to their similar polarities. Additional purification techniques were not attempted as the purpose of this reaction was not to isolate material to carry on to subsequent reactions, given that the product was the β

diastereomer, but rather to explore the glycosyl coupling conditions to see if they were compatible with MBP analogues.

### 4.1.3 The Synthesis of 2,3,4,6-Tetra-*O*-acetyl-α-D-glucosyl 1-methylenebisphosphonate (**16**)

Given the stereochemical outcome of the glycosyl bromide coupling reaction with MBP, the synthesis of α-D-glucosyl 1-methylenebisphosphonate was investigated. The first step in the synthesis was finding a suitable protected glycosyl donor that might give preferential α selectivity. 2,3,4,6-tetra-*O*-acetyl-β-D-glucopyranosyl chloride (**72**) was selected and synthesized in accordance with the method reported by Ibatullin and Selivanov.[104] 2,3,4,6-Tetra-*O*-acetyl-β-D-glucopyranosyl chloride (**72**) was coupled to **7′** using the same method as described for the synthesis of β-D-glucosyl 1-methylenebisphosphonate (**71**) (Scheme 36).

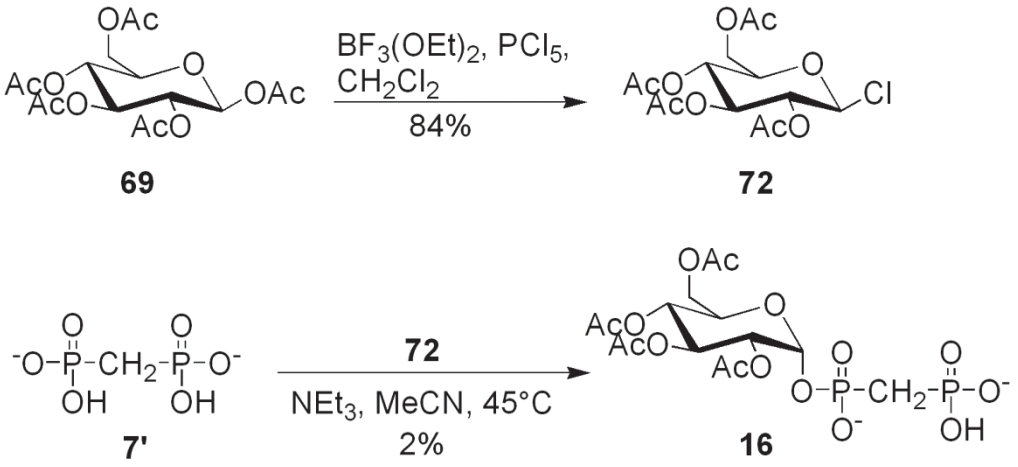


**Scheme 36** Synthesis of 2,3,4,6-tetra-*O*-acetyl-α-D-glucosyl 1-methylenebisphosphonate (**16**)

It was discovered that carrying out the reaction at 45°C, as opposed to 80°C, was sufficient to achieve α selectivity for the product, as determined by $^{1}$H NMR spectroscopy. As the temperature of reaction was increased from 45-80°C the proportion of β product increased to approximately 25%. This suggests that at 45°C the reaction proceeds through an $S_N2$ mechanism, in which the equatorial chloride is displaced via

axial attack from the MBP nucleophile to give the α product. As the temperature is increased beyond 45°C it is suspected that the chloride leaving group becomes more labile to facilitate the formation of the oxacarbenium intermediate, stabilized via neighboring group participation and the nitrile effect,[103] as previously described. The competition between the $S_N2$ and $S_N1$ mechanism of nucleophilic attack produced an anomeric mixture of α and β products.

Due to the difficulties encountered in separating MBP starting material from glycosylated product in the synthesis of β-D-glucosyl 1-methylenebisphosphonate (**71**), an attempt was made to isolate the product in its acetyl-protected form. Using the same purification method, as previously described, the ditetrabutylammonium salt of 2,3,4,6-tetra-*O*-acetyl-α-D-glucosyl 1-methylenebisphosphonate (**16**) was successfully separated from MBP, although the product was obtained in very low yields (<2%) relative to the method reported by Vaghefi and coworkers (52%).[71] The coupling conditions were next evaluated with of 3′-*O*-acetylthymidine 5′-methylenebisphosphonate (**73**) to see if a similar result would be observed (discussed in 4.1.4).

### 4.1.4 The Synthesis of 3′-*O*-Acetylthymidine 5′-[[(2′′,3′′,4′′,6′′-tetra-*O*-acetyl-α-D-glucopyranosyl]hydroxyphosphinyl)methyl]phosphonate] (**74**)

The triethylammonium salt of 3′-*O*-acetylthymidine 5′-methylenebisphosphonate (**73**) was converted to the ditetrabutylammonium salt and reacted with the acetyl-protected glycosyl chloride (**72**) to see if glycosylation would occur. Two equivalents of **72** and were used per equivalent of 3′-*O*-acetylthymidine 5′-methylenebisphosphonate (**73**). The reaction was monitored by HPLC with the starting material eluting at ~6.3 min. After approximately 40 min, a new peak was visible at ~5.8 min, showing ~45% conversion (Figure 26). The reaction was allowed to proceed overnight at 45°C, however no significant improvement in conversion was observed by HPLC analysis. The new peak possessed a retention time very similar to that of the deprotected starting material (~5.8 min) however, the presence of the desired product, 3′-*O*-acetylthymidine 5′-[[(2″,3″,4″,6″-tetra-*O*-acetyl-α-D-

glucopyranosyl]hydroxyphosphinyl)methyl]phosphonate] (**74**) was confirmed by LRMS/MS (Figure 27). Purification and isolation of the material was attempted using C18 reversed phase chromatography with a TBABC (pH 7)/methanol elution system. Ultimately, as was the case with 2,3,4,6-tetra-*O*-acetyl-α-D-glucosyl 1-methylenebisphosphonate (**16**), the conversion to the desired product was very low (<2%) and compound **74** was isolated in a mixture with the dominant recovered products being 3′-*O*-acetylthymidine 5′-methylenebisphosphonate (**73**) and deoxythymidine 5′-methylenebisphosphonate (**68**). It follows that the method reported by Vaghefi and coworkers[71] still remains the preferred procedure for the synthesis of glycosyl-MBP-nucleoside conjugates.

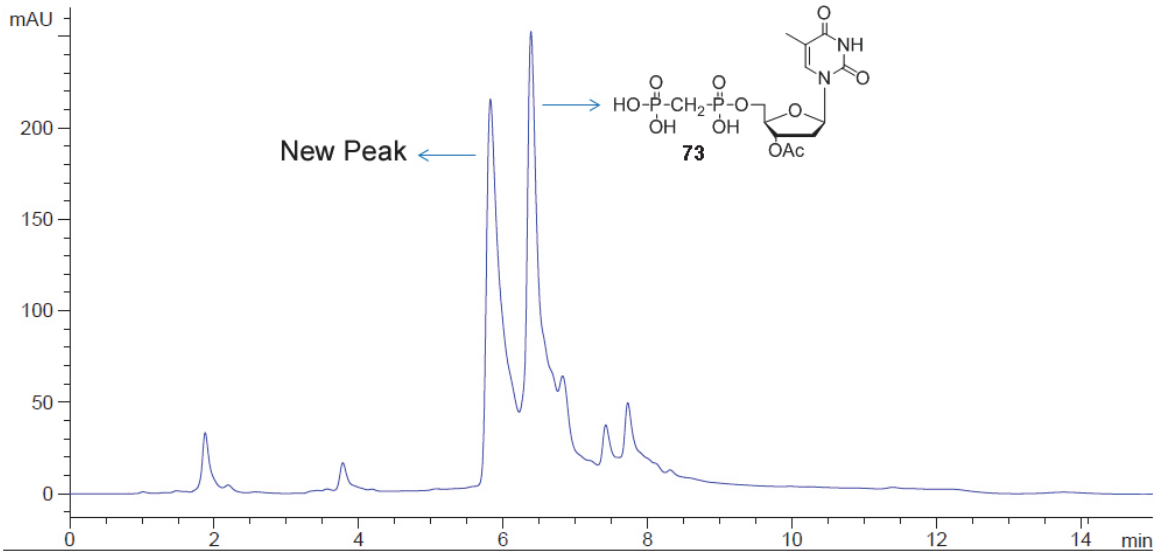


**Figure 26** HPLC trace of 3′-*O*-acetylthymidine 5′-[[(2″,3″,4″,6″-tetra-*O*-acetyl-α-D-glucopyranosyl]hydroxyphosphinyl)methyl]phosphonate] (**74**) reaction (40 min at 45°C)

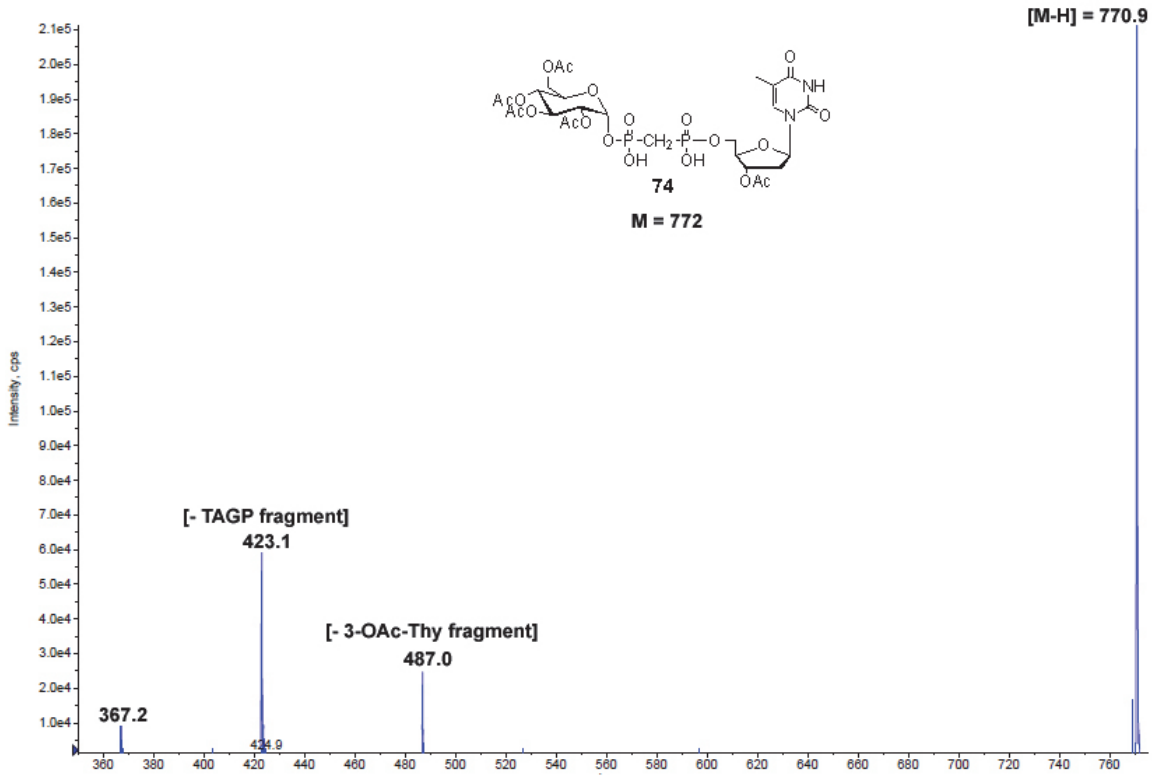


**Figure 27** LRMS/MS spectrum of 3′-*O*-acetylthymidine 5′-[[(2″,3″,4″,6″-tetra-*O*-acetyl-α-D-glucopyranosyl]hydroxyphosphinyl)methyl]phosphonate] (**74**)

## 4.2 The Synthesis of Glucosyl Thiophosphates

The formation of glucosylated thiophosphates was accomplished using acetyl (**75**) or benzyl (**76**) protected glucopyranose as the starting sugar together with diethylchlorothiophosphate (**77a**) using the conditions described by Zhang, Deng and Hui[80] or diphenylchlorothiophosphate (**77b**) using the conditions described by Huestis, Jakeman and coworkers,[105] for the purpose of preparing glycosyl phosphates (Scheme 37). Table 6 summarizes the various reaction conditions and isolated yields for α/β-D-glucopyranosyl thiophosphate synthesis.

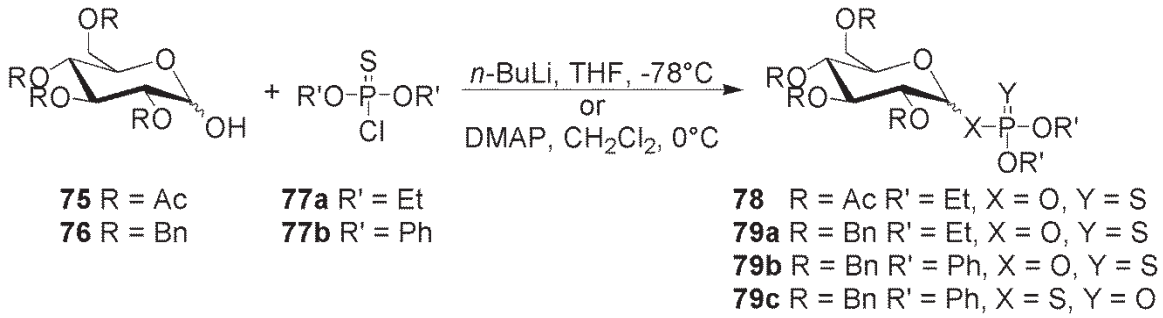


**Scheme 37** Synthesis of protected α/β-D-glucopyranosylthiophosphates (**78-79**)

**Table 6** Reaction conditions for α/β-D-glucopyranosyl thiophosphates synthesis

| Entry | Reactants | Conditions | T (°C) | Product(s) | α/β | Yield[c] |
|---|---|---|---|---|---|---|
| **1** | **75 + 77a** | THF/*n*-BuLi | -78 | **78** | 1:3 | 57% |
| **2** | **76 + 77a** | THF/*n*-BuLi | -78 | **79a** | 2:1 | 67% |
| **3** | **76 + 77a** | $CH_2Cl_2$/DMAP | 0 | — | — | 0% |
| **4** | **76 + 77b** | $CH_2Cl_2$/DMAP | 0 | **79b/79c** | 1[a], 4:1[b] | 24% |
| **5** | **76 + 77b** | THF/*n*-BuLi | -78 | **79b/79c** | 6:1[a], 4:1[b] | 16% |

[a]Initial ratio for *O*-linked product **79b**. [b]Final ratio for *S*-linked product **79c**. [c]Yields are reported as overall isolated yields for all anomers and isomers.

The reaction solvent and base were investigated in an attempt to enhance yield and selectivity. When diethylchlorothiophosphate (**77a**) was used as the glycosyl acceptor (entry 1-3), both *n*-butyllithium (*n*-BuLi) and lithium diisopropylamide (LDA) were comparably effective bases in tetrahydrofuran (THF), however 4-dimethylaminopyridine (DMAP) in dichloromethane ($CH_2Cl_2$) was ineffective in promoting glycosyl coupling. The yields for **78** and **79a** (entry 1-2) were comparable will analogous methyl protected glycosyl thiophosphates reported by Zhang, Deng and Hui (51-86%).[80] For ease of preparation, *n*-BuLi was chosen as the base of choice for the production of **78** and **79a**. When diphenylchlorothiophosphate (**77b**) was used as the electrophile (entry 4-5), either *n*-BuLi/THF or DMAP/$CH_2Cl_2$ conditions proved to be sufficient for the production of **79b**. The complete structures of **79b** and **79c** can be found in Scheme 38. The reactions conditions used affected both the diastereotopic ratio of α/β products as well as the overall yield. When *n*-BuLi/THF conditions were used the resultant α/β ratio of **79b** was found to be ~6:1 with a 16% overall yield (entry 5). When

DMAP/$CH_2Cl_2$ conditions were used, only the α isomer was obtained, with a 24% overall yield (entry 4). The yields of **79b/79c** (entry 4) were significantly less than analogous glycosyl phosphates synthesized using DMAP/$CH_2Cl_2$ conditions reported previously (55-82%).[105] While reduced coupling efficiency can be partially attributed to the steric bulk of the phenyl protecting groups of **77b** relative to the ethyl protected **77a**, the driving factor in the reduced yields is believed to be the excellent leaving group capacity of the diphenylthiphosphate moiety. This is expected to contribute to hydrolysis during purification. The DMAP/$CH_2Cl_2$ method was preferred in the synthesis of **79b** due to its stereospecificity and improved yield relative to the *n*-BuLi/THF coupling method.

The diastereotopic ratios of the starting sugars **75** (β only) and **76** (α/β ~3:1) were not retained in the production of any of the glucosyl thiophosphates (**78-79**). Varying temperature conditions from -78°C to -40°C did not affect the diastereotopic ratio of products for compounds **78** and **79a**. Using the benzyl-protected sugar (**76**) moderate improvement in overall yield was observed relative to the acetyl-protected sugar (**75**), which can be attributed to the acetyl groups of **75** deactivating the anomeric hydroxyl group's ability to act as a nucleophile in the coupling reaction with the chlorothiophosphate. Reactions involving diethylchlorothiophosphate (**77a**) produced an α/β ratio of 1:3 (entry 1) with respect to coupling with the acetyl-protected sugar (**75**), and an α/β ratio of 2:1 (entry 2) with respect to coupling with the benzyl-protected sugar (**76**). In the absence of neighboring group participating, the anomeric effect drives the ratio of axial α products for the benzyl-protected sugar and accounts for the formation of the dominant α product in **79a**. The C2 acetate group of **75** effectively increases the proportion of the equatorial (β) hydroxyl group in the free sugar by way of blocking the axial site via neighboring group participation, which consequently drives the reaction to the preferential β form in **78**. Complete α selectivity was achieved with the coupling of **77b** and benzyl-protected sugar **76** using the DMAP/$CH_2Cl_2$ conditions (entry 4), although the yields were significantly reduced relative to the *n*-BuLi/THF coupling conditions with **77b** (entry 2). The enhanced selectivity can be attributed to the phenyl protecting groups on **77b**, which make the thiophosphate moiety more electron rich, driving it to the α position via the anomeric effect.

The *S*-linked isomer **79c** was isolated in an 8% yield, following purification, relative to the *O*-linked **79b** (16%), using the preferred DMAP/$CH_2Cl_2$ coupling conditions (combined yield = 24%) (entry 4). For the purification of **79b** and **79c**, triethylamine neutralization of the silica using a 95:5 hexane:triethylamine slurry was required. In the absence of triethylamine, the material was found to break down completely during purification and only the hydrolysis products were recovered. The *O*-linked species was found to break down, in the presence of $CDCl_3$, to the free benzyl sugar and phenyl thiophosphoric acid within 24 hours, as was observed using TLC analysis. The compounds were found to be more stable in $CD_2Cl_2$. In $CD_2Cl_2$ an interesting isomerization (Scheme 38) with sugar thiophosphate **79b** was observed, in which the exclusively α **79b** compound gradually interconverted to the *S*-linked species **79c** with a resulting α/β ratio of 4:1, within 48 hours after isolation. This transformation was observed by the large up-field shift in the $^{31}P$ NMR spectrum when the phosphorous-sulfur bond shifts from a double bond, as in the case of the *O*-linked species, to a single bond as in the case of the *S*-linked species. The $^{31}P$ NMR spectra overlay of the various forms of the benzyl glucosyl thiophosphates (**79a-c**) is shown in Figure 28. Compound **79c** was confirmed to be the *S*-linked isomer by $^{1}H$ NMR spectroscopy, which showed the H-P coupling of the α *O*-linked species ($^{3}J_{1,\,P}$ = 9.5 Hz, 6.20 ppm) had changed and shifted slightly down-field ($^{3}J_{1,\,P}$ = 11.1 Hz, 6.30 ppm). An overlay of the H1 splitting patterns for compounds (**79a-c**) is shown in Figure 29. The *S*-glycosyl thiophosphate appeared to be the more stable isomeric form and was not as vulnerable to glycosidic cleavage in $CDCl_3$, relative to its *O*-glycosyl counterpart.

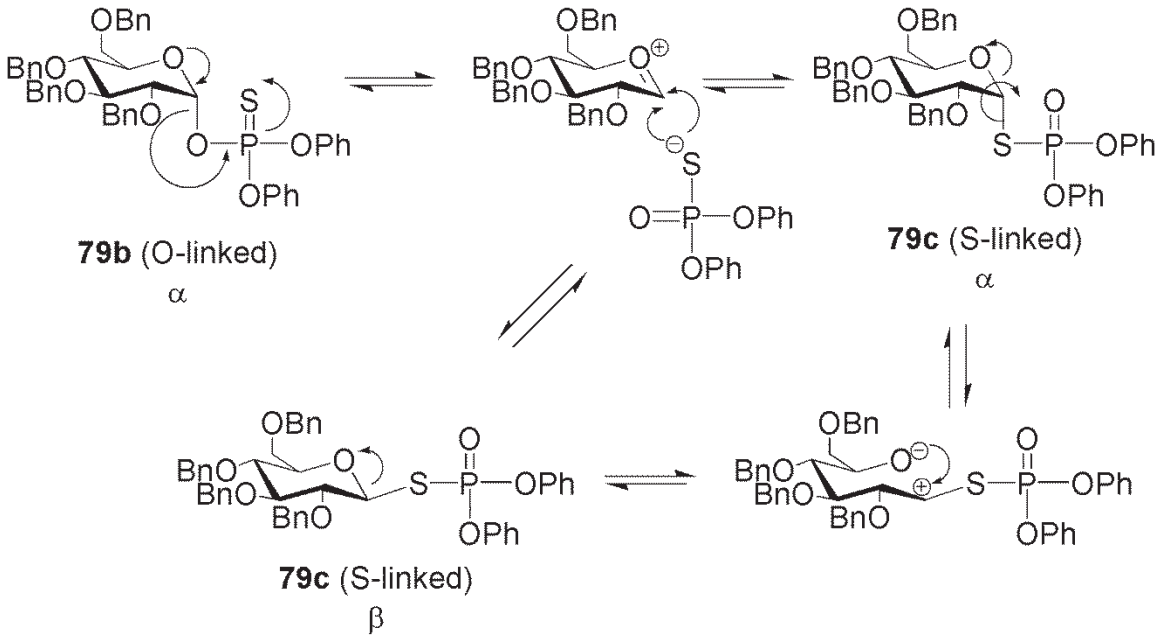


**Scheme 38** Proposed isomerization mechanism of glucopyranosylthiophosphate (**79b**)

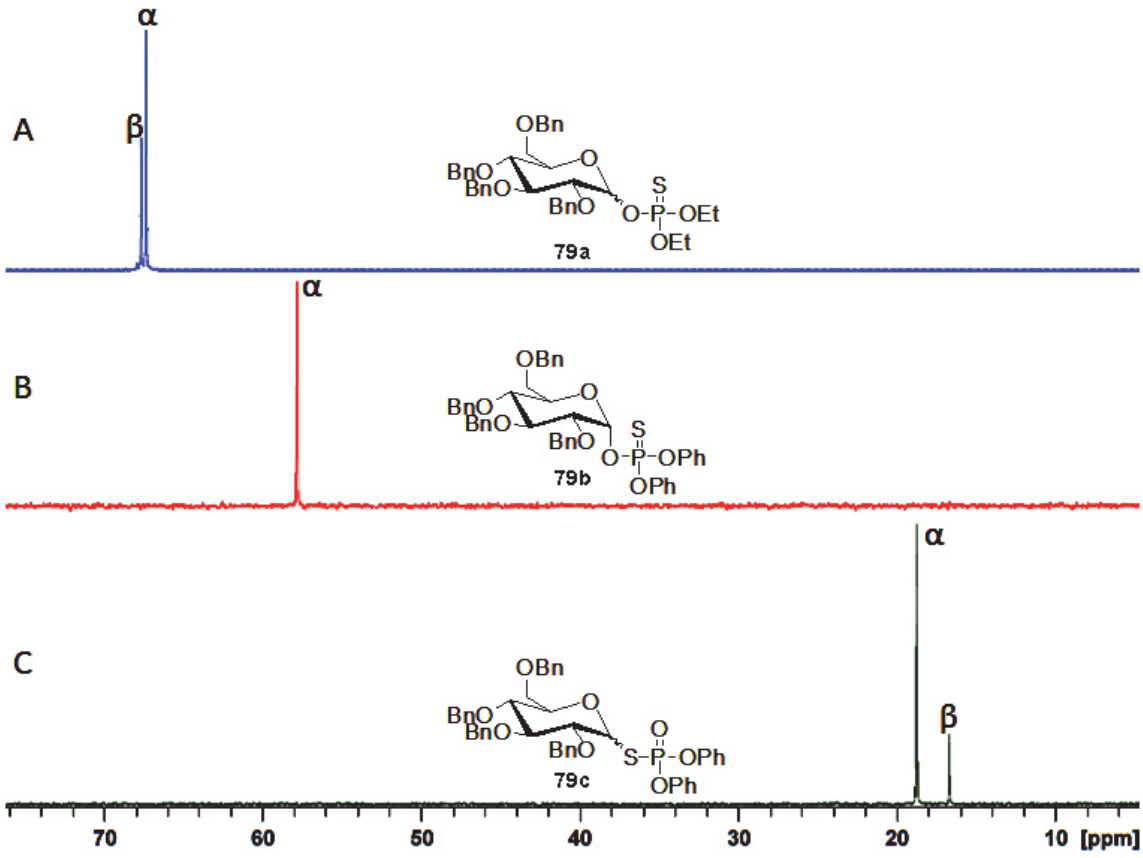


**Figure 28** $^{31}$P NMR spectra for glucosyl thiophosphates **79a** (A) in $CDCl_3$, **79b** (B) and **79c** (C) in $CD_2Cl_2$.

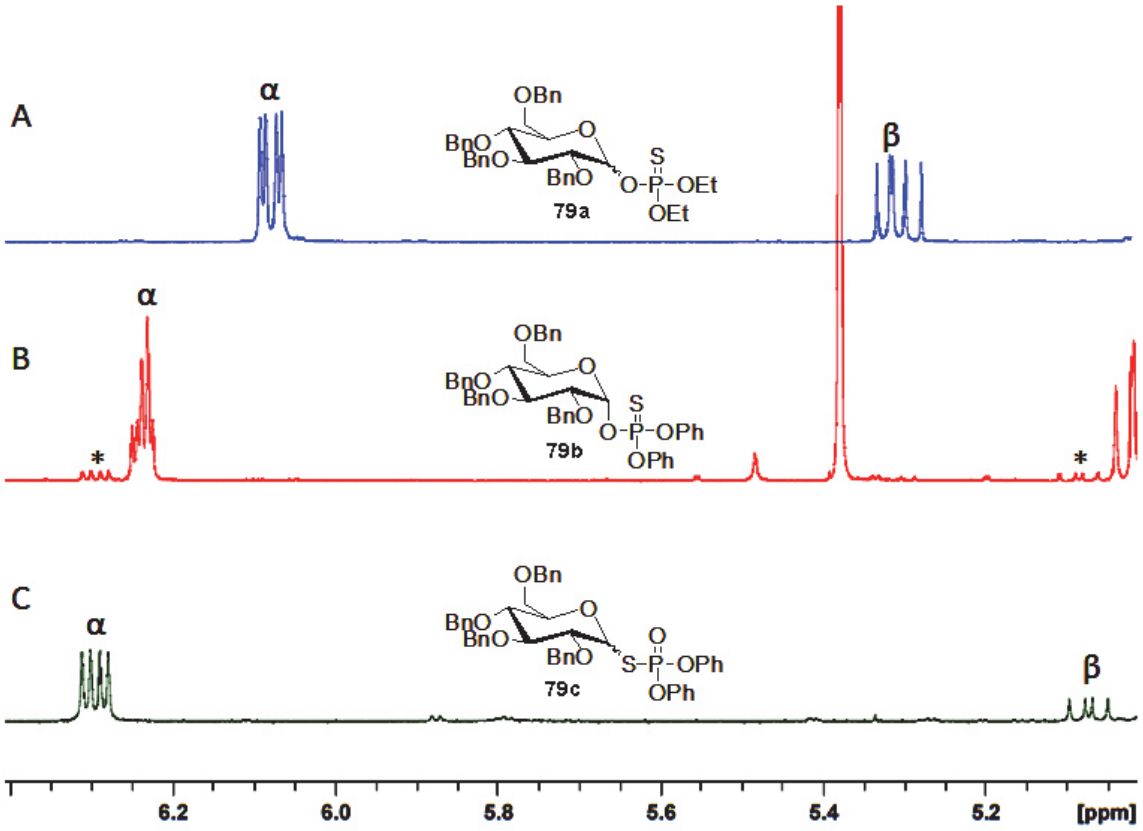


**Figure 29** $^{1}$H NMR spectra for glycosyl thiophosphates **79a** (A) in $CDCl_3$, **79b** (B) and **79c** (C) in $CD_2Cl_2$ displaying α and β splitting patterns. The (*) indicates the start of isomerization from **79b** to **79c** ~6 hours after isolation.

The significantly higher yields of the diethylthiophosphates relative to the diphenyl thiophosphate prompted an attempt at separating the α and β diastereomers of **79a**. Many possible separation conditions were explored using various elutants (EtOAc/hexane, water/MeOH), as well as normal phase silica, silver impregnated silica, reversed phase C18 silica, alumina and basic alumina media conditions. Under all circumstances, the product was either recovered as a diastereotopic mixture of anomers or hydrolyzed during the separation.

Despite unsuccessful separation attempts, the α/β mixtures of glycosyl thiophosphates may not be of crucial concern. Given the stereospecificity of nucleotidylyltransferases and glycosyl transferases, they can potentially select, and hence drive the equilibrium toward the preferred form (α or β) of the glycosyl thiophosphate. After attempted separation of the anomers, deprotection of the glycosyl thiophosphates was explored. The attempted deprotection conditions are summarized in Table 7. Basic

LiOH[106] conditions (entry 1) were found to be unsuccessful and the acidic conditions of TMSI,[107] (entry 2) TMSBr[108] (entry 3) and $BCl_3$[109] (entry 4) were all too harsh, resulting in anomeric cleavage of the product. Hydrogenolysis of the products was next explored for removal of the benzyl protecting groups on the sugar moiety and/or the phenyl protecting groups on the thiophosphate moiety. While compounds containing sulfur have been well known to poison hydrogenation catalysts,[110,111] the incorporation of ammonium formate into the reaction media has been shown to circumvent this problem in certain circumstances involving sulfate hydrogenolysis.[112] None of these hydrogenolysis conditions enabled deprotection of the glucosyl thiophosphates (entry 5-7).

**Table 7** Attempted deprotection conditions for α/β-D-glucopyranosyl diethylthiophosphates

| Entry | Compound | Deprotection Conditions | Result |
|---|---|---|---|
| **1** | **79a** | LiOH(sat), dioxane/water, 50°C | No reaction |
| **2** | **79a** | TMSI, $CH_2Cl_2$, 0°C | Anomeric cleavage |
| **3** | **79a** | TMSBr, $CH_2Cl_2$, 0°C | Anomeric cleavage |
| **4** | **79b, 79c** | $BCl_3$, $CH_2Cl_2$, -78°C | Anomeric cleavage |
| **5** | **79b, 79c** | $H_2$ Pd/C, MeOH/EtOAc | No reaction |
| **6** | **79b, 79c** | $H_2$ $PtO_2$, MeOH/EtOAc | No reaction |
| **7** | **79b, 79c** | $H_2$ Pd/C or $PtO_2$, $NH_4CO_2$ (1-15 eq), MeOH/EtOAc | No reaction |

Several methods for the synthesis of glucosyl-thiophosphates were explored. Four new globally protected glucosylated thiophosphates were synthesized and characterized. The coupling method and protecting groups had a significant impact on both the stereoselectivity and yield of the reactions. The diastereoselectivity was not affected by varying the temperature conditions. Separation of α/β diastereomers was not achieved. The first example of isomerization from an *O*-linked glucosyl thiophosphate to an *S*-linked species was reported. Deprotection of the various glucosyl thiophosphates was unsuccessful, despite various techniques, due to glycosidic bond fragility or hydrogenolysis catalyst poisoning by sulfur. The difficulties encountered during the attempted deprotection of the glycosylated thiophoposphates highlight the need for alternative deprotection strategies or modified thiophosphorylating reagents.

# CHAPTER 5 CONCLUSION

## 5.1 SUMMARY & CONCLUSIONS

In conclusion, a series of L-rhamnose-1C-phosphonate and ketosephosphonate analogues were synthesized and evaluated as inhibitors of Cps2L. WaterLOGSY NMR studies demonstrated the potential of synthetic substrate analogues to bind to multiple enzymes within a single biosynthetic pathway. WaterLOGSY studies of dTDP-Glc and dTDP-Rha also highlight the capacity for sugar nucleotides to bind to (and potentially inhibit) multiple enzymes within a single bacterial biosynthetic pathway. The R1CP analogues were assumed to competitive and bind to the Glc-1-P substrate site of Cps2L based on spectrophotometric inhibition assays and WaterLOGSY NMR studies. The presence of one fluorine atom at the C1 postion was found to increase inhibition by approximately 25%, whereas the presence of two fluorine atoms was detrimental to inhibition for the ketosephosphonate compounds. L-rhamnose-1C-P was found to be the most potent inhibitor of the series of R1CP analogues.

The synthesis of phosphonate containing sugar nucleotide analogues was explored using two approaches. The first entailed joining glycosyl phosphonates with NMPs to form a CPOP scaffold. The second entailed appending nucleoside and glycosyl moieties to a preassembled MBP scaffold. The final sugar nucleotides analogues were found to be unstable under the physiological pH essential to enzymatic studies with Cps2L. The first examples of CPCPO and R1CP phosphonate analogues were reported. A new method for the synthesis of MBP-nucleoside conjugates was developed.

A series of globally protected glycosylated thiophosphates were synthesized. The first example of isomerization from an *O*-linked glucosyl thiophosphate to an *S*-linked species was reported. These compounds represent new novel precursors toward the synthesis of glucose-1-thiophosphate, a probable substrate for Cps2L.

## 5.2 FUTURE WORK

### 5.2.1 A New Route to R1CPCP Analogues

As demonstrated in Chapter 3, compounds with a CPCPO scaffold could be synthesized directly from the imidazolium salt of monomethyl methylphosphonate (**59**), or produced *in situ* from the breakdown of R1CPCP analogues. While these compounds were quite stable, their high polarities made them difficult to isolate and purify by normal phase silica chromatography. In an effort to produce less polar CPCPO compounds, the monobenzyl methylphosphonate (**80**) could be synthesized and activated toward coupling with nucleophilic phosphonates DBMP (**27b**) and DEDFMP (**33**) as shown in Scheme 39.

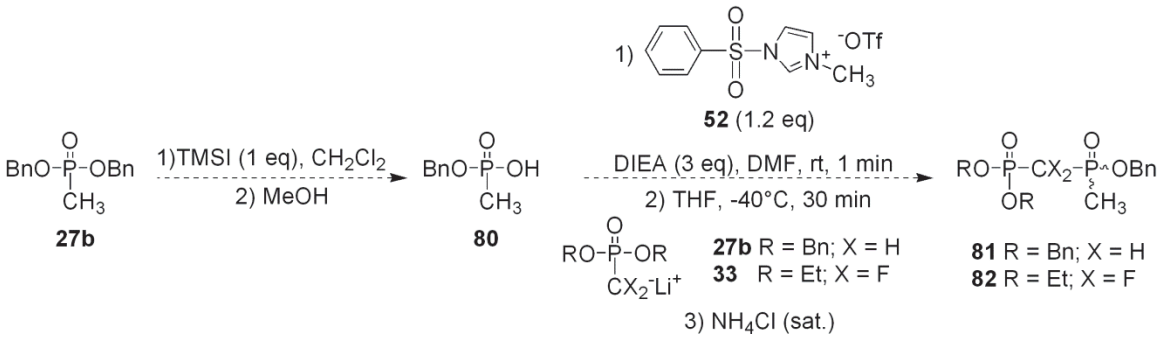


**Scheme 39** Proposed synthetic route to new CPCPO compounds **81** and **82**

The CPCPO compounds (**81** and **82**) each possesses a terminal methylene group, which can be deprontonated and used as a nucleophile toward coupling with the rhamnolactone **26**. This could be accomplished following the analogous reaction conditions required to produce ketosephosphonates **28b** and **34**, as discussed in Chapter 3. Scheme 40 outlines a potential route towards isolating stable R1CPCP analogues, and subsequent R1CPCP sugar nucleotide analogues.

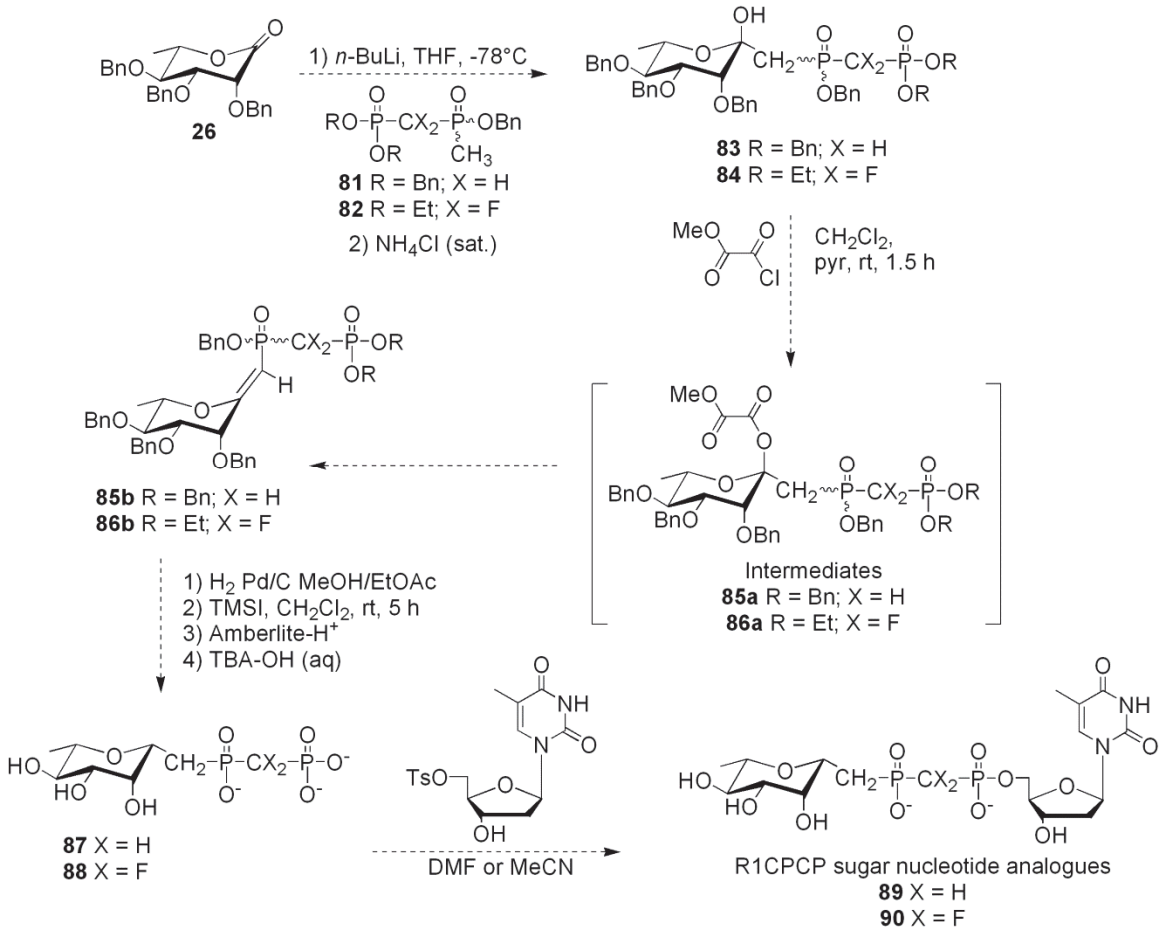


**Scheme 40** Proposed synthetic route to new R1CPCP sugar nucleotide analogues

If successfully generated, phosphonate nucleophile **81** and its difluoro analogue (**82**) will be investigated as nucleophiles. Compound **81** will be first be evaluated, as it is synthetically more probable to isolate over **82**, given the problems encountered with using fluorinated phosphonates in the coupling reactions with activated R1CP (**43**). The major anticipated problem with using **81** as the nucleophile is that it has two methylene sites accessible for deprotonation. The target terminal $CH_3$ would be the site of the less acidic proton relative to the proton on the central $CH_2$ group. To address this, two equivalents of *n*-BuLi could be used per equivalent of **81** to encourage the deprotonation of both sites. The terminal $CH_2^-$ anion should prevail as the dominant nucleophile, as it would be significantly less hindered than the central $CH_2^-$ anion. The substitution of two protons with two fluorine atoms in the central methylene scaffold of **82** would mean that the terminal $CH_3$ group would be the only site of deprotonation for that compound. As a result, only one equivalent of *n*-BuLi would be required.

The R1CPCP ketosephosphonate analogues (**83** and **84**) would be predictably more stable, under the new reaction conditions, than the previously synthesized R1CPCP analogues, for several reasons. They would be formed at a lower temperature (-78 instead of -35°C), in a mono solvent system (THF), without presence of the highly reactive sulfonyl imidazolium activator (**52**). If compounds **83** and/or **84** can be produced, then they could potentially be transformed to olefins **85b** and **86b** via the formation and *in situ* elimination of their oxalyl esters (**85a** and **86a**). It is assumed this would proceed in an analogous manner to the formation of olefins **30a** and **30b** (Scheme 14). If the oxalyl esters are isolated, they may be deoxygenated using $Bu_3SnH$ and AIBN, as demonstrated for the synthesis of **36** (Scheme 16). Direct hydrogenation and deprotection could produce the R1CP analogues **87** and **88**. These compounds could be evaluated as Cps2L inhibitors directly and compared to R1CP (**43**). They may also be transformed into R1CPCP sugar nucleotide analogues **89** and **90** via coupling with tosyl activated dTMP. The final R1CPCP sugar nucleotide analogues would predictably be potent inhibitors of Cps2L and potentially other α-D-glucose 1-phophate thymidylyltransferases.

### 5.2.2 Prodrug R1CP Analogues

The R1CP analogues which showed inhibitory activity against Cps2L (**42**, **43** and **44**) may be converted to phosphonate prodrugs using the procedure developed by Hwang and Cole.[113] The bis(POM) esters can be generated from the methyl protected forms of the R1CP analogues reacted in chloromethyl pivalate (POM-Cl), as outlined in Scheme 41.

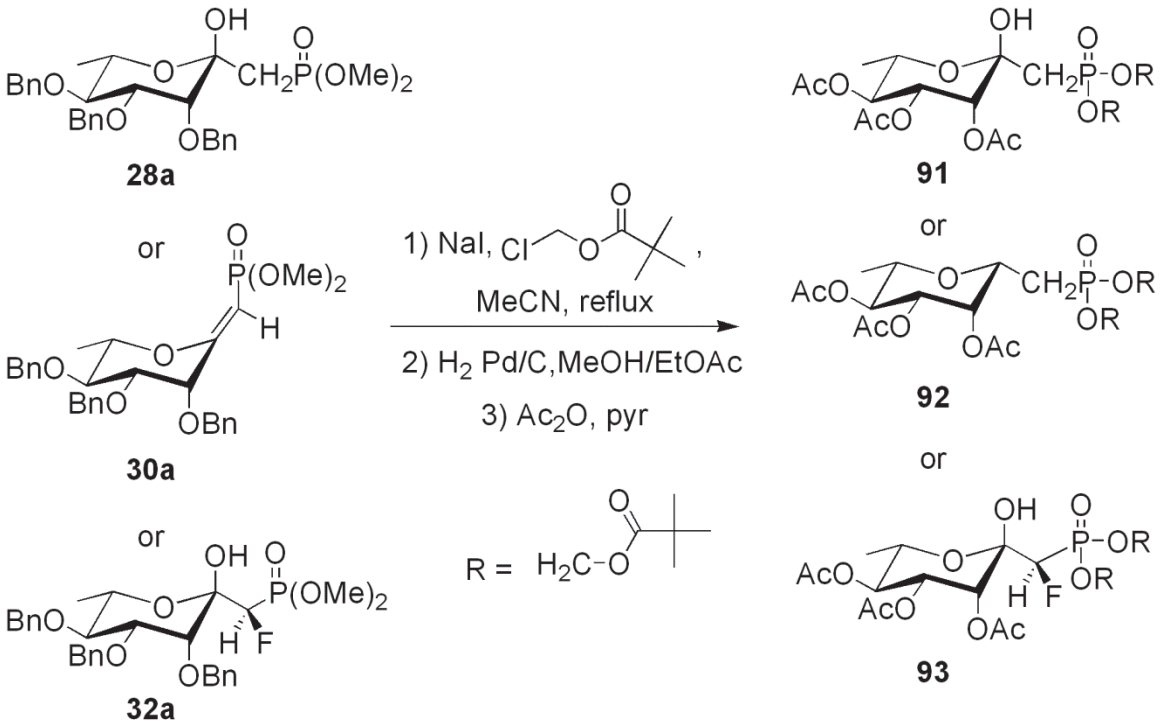


**Scheme 41** Synthesis of R1CP esters analogues

The C1-C2 double bond and/or C3-5 benzyl protecting groups can be removed using hydrogenolysis and subsequently acetylated to produce prodrug compounds (**91-93**). The acetyl L-rhamnose and POM protected phosphonate scaffolds would have significantly reduced polarities relative to the analogous deprotected phosphonates (**42**, **43** and **44**). Consequently, they should be able to permeate bacterial cells and minimum inhibitory concentration (MIC) values may be measured for compounds **91-93** against various bacterial species.

# EXPERIMENTAL

## General Methods

All chemicals and solvents were purchased from Sigma-Aldrich and used without further purification. All solvents were reagent grade unless otherwise specified. Thin-layer chromatography was performed on glass-backed TLC plates pre-coated with silica gel (SilicycleTM, 250 μm) and compounds were monitored using UV absorbance (254 nm) or by dipping in a KMnO4 visualization solution (3 g $KMnO_4$ 20 g $K_2CO_3$, 5 mL 5% (w/v) NaOH (aq), 300 mL $H_2O$). Automated normal phase and reversed phase silica gel chromatography was performed using a Biotage SP1™ flash chromatography system. The compounds were precipitated with Isolute HM-N in $CH_2Cl_2$ before being loaded onto the columns. Anion exchange purification of select compounds was carried out using the Biotage instrument, in which case the compounds were column loaded in a highly diluted elution buffer adjusted to pH 7-8. Molecular sieves (3 Å) were activated by storing in an oven (>180°C) for 12 h, and heated with a heat gun under vacuum for approximately one minute prior to use. Evaporations were performed using a Büchi rotary evaporator, followed by drying on an Edward rotary vacuum pump. A Hero PowerDry LL1500 freeze dryer was used for lyophilization of samples. Nuclear magnetic resonance experiments were performed using Bruker AC-250, AV-300 and AV-500 MHz spectrometers in the Nuclear Magnetic Resonace Research Resource ($NMR^3$) Centre. All final characterization data for $^1H$, $^{13}C$ and $^{31}P$ spectra was collected on an AV-500 MHz spectrometer. All $^{19}F$ spectra were recorded on an AV-300 MHz spectrometer. Chemical shifts are reported in parts per million (ppm) relative to a tetramethylsilane (TMS) internal standard at 0.00 ppm for $^1H$ (500 MHz) and $^{13}C\{^1H\}$ (126 MHz) spectra. $^{31}P\{^1H\}$ (202 MHz) and $^{19}F\{^1H\}$ (282 MHz) spectra were referenced relative to external 85% (w/v) aq $H_3PO_4$ and $CFCl_3$ samples respectively, at 0.00 ppm. Low-resolution mass spectra were obtained using an Applied Biosystems hybrid triple quadrupole linear ion trap (*Qtrap 2000*) mass spectrometer equipped with an electrospray ionization (ESI) source. All High-resolution mass spectra were provided by Xiao Feng in the Department of Chemistry at Dalhousie University.

## WaterLOGSY NMR experiments:

WaterLOGSY NMR samples were composed of binding substrates Glc-1-P (5 mM) and/or dTTP (5 mM) with $MgCl_2$ (5 mM) cofactor, or sugar nucleotides (5 mM) with $MgCl_2$ (5 mM) and enzymes Cps2L, RmlB, RmlC, or RmlD (0.05 mM). Benzoic acid (5 mM) was used as a control non-binder for select experiments. For sample containing phosphonate analogues, 5 mM concentrations were used. All samples were prepared in Tris-HCl (100 mM, pH 7.5) buffer with 10% $D_2O$ to a total volume of 50 µL. All Water LOGSY experiments were run on an AV 700 MHz spectrometer. Benzoic acid was used as a control non-binder in all experiments, with the exception of the competitive model of Glc-1-P (**1**) and Rha-1C-P (**43**) (Figure 12). In spectra containing Cps2L, residual signals of imidazole left over from purification (~7.1 and 7.8 ppm) could not be removed and should not be confused with thymidine or benzoic acid aromatic proton signals.

## HPLC enzyme assay and inhibition conditions:

RmlB-D (*Aneurinibacillus thermoaerophilis*) plasmids were provided by Dr. Joseph Lam, Department of Molecular and Cellular Biology, University of Guelph, Canada. Cps2L and RmlB-D were over-expressed and purified as previously described.[93,114] The concentration of Cps2L was measured spectrophotometrically at 280 nm using a calculated extinction coefficient of 29.8 $mM^{-1}cm^{-1}$. All stock solutions were prepared in Tris-HCl buffer (100 mM, pH 7.5). Inhibition assays were conducted using phosphonate analogues (0-100 mM), or compound **47** (0-25 mM) with Glc-1-P (10 mM), dTTP (10 mM), $MgCl_2$ (20 mM) and Cps2L (1 EU) in a final volume of 50 µL of Tris-HCl buffer. Samples were incubated for 17 minutes at 37°C at which point 25 µL aliquots were quenched in an equal volume of HPLC grade MeOH. Conversions were approximately 30% after 17 minutes. In the absence of inhibitors, the physiological reaction went to completion using 10 mM substrates **1** and **2** with two equivalents of $Mg^{2+}$ cofactor and 8 EU of Cps2L within 30 minutes at 37°C, as determined by HPLC. In the case of compound **47**, a concentrated stock solution (50 mM in 1:1 DMSO:Tris-HCl, pH 7.5)

was used. $IC_{50}$ curves and values were generated, based on HPLC conversion, using Grafit 5 Erithacus Software. $K_i$ values were approximated relative to Glc-1-P and dTTP substrates using the Cheng-Prusoff equation, which assumes a competitive mode of inhibition. Due to the time intensive processes of performing HPLC based inhibition assays, experiments were not carried out in duplicate.

## Spectrophotometric enzyme coupled kinetic and inhibition assay conditions:

Human PNP plasmid was provided by Dr. Vern L. Schramm, Department of Biochemistry, Albert Einstein College of Medicine, USA. It was over-expressed and purified using the same procedure as described for Cps2L and RmlB-D, with the following modifications; overnight induction at 37°C was initiated with 0.1% (w/v) lactose.[115] The concentration of Human PNP was measured spectrophotometrically at 280 nm using an extinction coefficient of 29.8 $mM^{-1}cm^{-1}$. Inorganic pyrophosphatase (IPP) from *Escherichia coli* was purchased from Sigma Aldrich. Stock solutions of IPP (0.1 EU/μL) were prepared in Millipore water and stored at -30°C. Thawed aliquots were kept in the fridge and used for up to one month after thawing. MESG was purchased from Berry and Associates. MESG stock solutions were prepared in Millipore water no more than two weeks prior to use, and aliquots were stored at -30°C. MESG solutions were used as soon as possible after thawing. All other stock solutions were prepared in Tris-HCl buffer (50 mM, pH 7.5). Enzyme kinetic assays were performed for each both dTTP and Glc-1-P substrates. Reactions containing Glc-1-P or dTTP (1 mM), dTTP or Glc-1-P (0-300 μM), Human PNP (8 μM), IPP (0.05 EU), $MgCl_2$ (5.6 mM), and MESG (400 μM) in Tris-HCl (50 mM, pH 7.5) were initiated by the addition of Cps2L (4.9 nM). Assays were made to a final reaction volume was 80 μL and performed in a 384 well plate. Initial velocities were monitored continuously by UV spectrometry at $\lambda$ = 360 nm using Softmax pro 4.8. Inhibition assays were performed using the same reaction conditions with variable concentrations (250-1000 μM) of Rha-1C-P. Initial velocities were converted from mAu/min to μM/min using a $P_i$ (0-100 μM) standard curve. Michaelis-Menten and inhibition equations were fit using Grafit 5 Erithacus Software.

## Steps in the Synthesis of Protected R1CP Analogues

### Dimethyl (tri-*O*-benzyl-1-deoxy-L-rhamno-heptulopyranosyl)phosphonate (**28a**)

The procedure for the synthesis of dimethyl (tri-*O*-benzyl-1-deoxy-L-rhamno-heptulopyranosyl)phosphonate (**28a**) was adopted from Norris and Toyokuni.[87] Dimethyl methylphosphonate (**27a**) (0.93 mL, 8.31 mmol) was dissolved in anhydrous THF (5 mL) under nitrogen and cooled to -78°C using a dry ice/acetone slurry. *n*-Butyllithium (0.35 mL, 8.31 mmol) was added and the solution was stirred for 30 minutes before 2,3,4,-tri-*O*-benzyl-L-rhamno-l,5-lactone (**26**) (1.197 g, 2.8 mmol) was added dropwise in a solution of THF (5 mL). After 75 minutes, TLC showed complete consumption of (**26**). The reaction was quenched with 10% $NH_4Cl$ (10 mL) and the THF layer was extracted. The aqueous layer was then extracted with $CH_2Cl_2$ (3 x 10 mL). The organic extracts were combined, dried ($Na_2SO_4$) and concentrated. The material was purified using column chromatography (40/60 EtOAc/hexane) to afford the product (**28a**) as a clear liquid (1.378 g, 88% yield), $R_F$ = 0.25 (40/60 EtOAc/hexane). $\delta_H$ ($CDCl_3$) 7.20-7.50 (m, 15H, 3 x $C_6H_5$), 5.74 (s, 1H, H2), 4.50-5.10 (m, 6H, 3 x $CH_2Ph$), 4.12 (dd, 1H, H4 $^3J_{4,5}$ = 9.4 Hz, $^3J_{4,3}$ = 2.7 Hz), 4.03 (m, 1H, H6), 3.83 (d, 3H, $OCH_3$, $^3J_{H,P}$ = 11.1 Hz), 3.76 (d, 1H, H3 $^3J_{3,4}$ = 2.7 Hz), 3.69 (d, 3H, $OCH_3$, $^3J_{H,P}$ = 11.1 Hz) 3.64 (t, 1H, H5, $^3J_{5,4}$ = $^3J_{5,6}$ = 9.4 Hz) 2.60 (dd, 1H, H1a, $^2J_{H,P}$ = 17.9 Hz, $^2J_{H,H}$ = 16.0 Hz), 1.69 (dd, 1H, H1b, $^2J_{H,P}$ = 17.9 Hz, $^2J_{H,H}$ = 16.0 Hz) 1.32 (d, 3H, H7, $^3J_{7,6}$ = 6.4 Hz), $\delta_C$ 138.3-138.8 (3 x C, $C_6H_5$), 127.5-129.0 (15 x CH, $C_6H_5$), 97.1 (d, C, C2, $^2J_{C,P}$ = 7.6 Hz), 81.5 (CH, C4), 80.3 (CH, C5), 78.2 (d, CH, C3, $^3J_{C,P}$ = 12.5 Hz), 75.4, ($CH_2$, $CH_2Ph$), 74.8 ($CH_2$, $CH_2Ph$), 73.2 ($CH_2$, $CH_2Ph$), 69.0 (CH, C6), 53.9 (d, $CH_3$, $OCH_3$, $^2J_{C,P}$ = 5.8 Hz), 51.8 (d, $CH_3$, $OCH_3$, $^2J_{C,P}$ = 5.8 Hz), 33.2 (d, $CH_2$, C1, $^1J_{C,P}$ = 135.12 Hz) 18.0 ($CH_3$, C7), $\delta_P$ 32.22 (s, 1P), HRMS ($ESI^-$): found $[M-1]^-$ 555.2164. $C_{30}H_{36}O_8P_1$ requires $[M-1]^-$ 555.2153.

## Dibenzyl (tri-*O*-benzyl-1-deoxy-L-rhamno-heptulopyranosyl)phosphonate (**28b**)

The procedure for the synthesis of dibenzyl (tri-*O*-benzyl-1-deoxy-L-rhamno-heptulopyranosyl)phosphonate (**28b**) was adopted from Norris and Toyokuni's synthesis of **28a**.[87] Dibenzyl methylphosphonate (**27b**) (0.374 g, 1.35 mmol) was dissolved in anhydrous THF (5 mL) under nitrogen and cooled to -78°C using a dry ice/acetone slurry. *n*-Butyllithium (0.5 mL, 1.25 mmol) was added and the solution was stirred for 30 minutes before 2,3,4,-tri-*O*-benzyl-L-rhamno-l,5-lactone (**26**) (0.220 g, 0.5 mmol) was added dropwise in a solution of THF (1 mL). After 75 minutes, TLC showed complete consumption of (7). The reaction was quenched with 10% $NH_4Cl$ (10 mL) and the THF layer was extracted. The aqueous layer was then extracted with $CH_2Cl_2$ (3 x 10 mL). The organic extracts were combined, dried ($Na_2SO_4$) and concentrated. The material was purified using column chromatography (25/75 EtOAc/hexane) to afford the product as a clear viscous liquid (**28b**) (0.270 g, 76% yield), $R_F$ = 0.22 (20/80 EtOAc/hexane). $\delta_H$ 7.25-7.45 (m, 25H, 5 x $C_6H_5$), 5.80 (s, 1H, H2), 4.60-5.24 (m, 10H, 5 x $CH_2Ph$), 4.23 (dd, 1H, H4, $^3J_{4,5}$ = 9.3 Hz, $^3J_{4,3}$ = 2.6 Hz), 4.10 (m, 1H, H6), 3.76 (d, 1H, H3 $^3J_{3,4}$ = 2.6 Hz), 3.67 (t, 1H, H5, $^3J_{5,4}$ = $^3J_{5,6}$ = 9.5 Hz), 2.70 (dd, 1H, H1a, $^2J_{H,P}$ = 18.8 Hz, $^2J_{H,H}$ = 15.4 Hz), 1.78 (dd, 1H, H1b, $^2J_{H,P}$ = 18.8 Hz, $^2J_{H,H}$ = 15.7 Hz), 1.37 (d, 3H, H7, $^3J_{7,6}$ = 6.3 Hz), $\delta_C$ 135.8-138.8 (5 x C, $C_6H_5$), 127.5-129.2 (25 x CH, $C_6H_5$), 97.3 (d, C, C2, $^2J_{C,P}$ = 7.72 Hz), 81.4 (CH, C4), 80.4 (CH, C5), 78.5 (d, CH, C3, $^3J_{C,P}$ = 12.77 Hz), 75.4 ($CH_2$, $CH_2Ph$), 74.9 ($CH_2$, $CH_2Ph$), 73.1 ($CH_2$, $CH_2Ph$), 69.0 (CH, C6), 68.5 (d, $CH_2$, $POCH_2Ph$, $^2J_{C,P}$ = 5.5 Hz), 66.9 (d, $CH_2$, $POCH_2Ph$, $^2J_{C,P}$ = 5.5 Hz), 34.3 (d, $CH_2$, C1, $^1J_{C,P}$ = 136.40 Hz), 18.0 ($CH_3$, C7), $\delta_P$ 30.49 (s, 1P), HRMS ($ESI^-$): found $[M-1]^-$ 707.2762. $C_{42}H_{44}O_8P_1$ requires $[M-1]^-$ 707.2779.

## Dimethyl (2,6-anhydro-tri-*O*-benzyl-1-deoxy-L-rhamno-hept-1-enopyranosyl)phosphonate (**30a**)

The procedure for the synthesis of dimethyl (2,6-anhydro-tri-*O*-benzyl-1-deoxy-L-rhamno-hept-1-enopyranosyl)phosphonate (**30a**) was adopted from Norris and

Toyokuni.[87] Dimethyl (tri-*O*-benzyl-1-deoxy-L-rhamno-heptulopyranosyl)phosphonate (**28a**) (0.660 g, 1.18 mmol) was dissolved in a mixture of 7: 2 $CH_2Cl_2$: pyridine (9 mL) and methyl oxalyl chloride (1.13 mL, 10.58 mmol) was added dropwise with stirring under nitrogen. After 90 minutes, TLC showed complete consumption of **28a**, so the reaction was quenched with EtOH (1 mL) and allowed to stir for 10 minutes before $CH_2Cl_2$ (13 mL) and $NaHCO_3$ (5 mL, sat.) were added. The reaction was stirred for an additional 5 minutes after which it was poured into $NaHCO_3$ (10 mL) and extracted with $CH_2Cl_2$ (3x15 mL) before being dried ($Na_2SO_4$) and concentrated. The material was purified using column chromatography (70/30-100/0 EtOAc/hexane) to afford the product (**30a**) as a clear viscous liquid (0.433 g, 68% yield), $R_F$ = 0.46 (80/20 EtOAc/hexane). $\delta_H$ ($CD_2Cl_2$) 7.20-7.50 (m, 15H, 3 x $C_6H_5$), 5.02 (d, 1H, H1, $^2J_{H,\,P}$ = 12.4 Hz ), 4.40-4.80 (m, 6H, 3 x $CH_2Ph$), 4.19 (d, 1H, H3 $^3J_{3,\,4}$ = 2.8 Hz), 3.89 (m, 1H, H6), 3.80 (dd, 1H, H4, $^3J_{4,\,5}$ = 5.6 Hz, $^3J_{4,\,3}$ = 2.8 Hz), 3.75 (dd, 6H, 2 x $OCH_3$, $^3J_{H,\,P}$ = 11.4 Hz, $^5J_{H,\,H}$ = 1.1 Hz), 3.70 (dd, 1H, H5, $^3J_{5,\,6}$ = 8.7 Hz, $^3J_{5,\,4}$ = 5.6 Hz), 1.46 (d, 3H, H7, $^3J_{7,\,6}$ = 6.2 Hz), $\delta_C$ 165.75 (C, C2), 137.3-138.0 (3 x C, $C_6H_5$), 127.5-129.0 (15 x CH, $C_6H_5$), 92.8 (d, CH, C1, $^1J_{C,\,P}$ = 191.4 Hz ), 80.5 (CH, C5), 78.1 (CH, C4), 75.9 (CH, C6), 75.2 (d, CH, C3, $^3J_{C,\,P}$ = 14.9 Hz) 73.8 ($CH_2$, $CH_2Ph$), 72.4 ($CH_2$, $CH_2Ph$), 71.5 ($CH_2$, $CH_2Ph$), 52.7 (d, $CH_3$, $OCH_3$, $^2J_{C,\,P}$ = 5.5 Hz), 52.3 (d, $CH_3$, $OCH_3$, $^2J_{C,\,P}$ = 5.5 Hz), 19.1 ($CH_3$, C7), $\delta_P$ 20.17 (s, 1P), HRMS ($ESI^+$): found $[M+Na]^+$ 561.2009. $C_{30}H_{35}Na_1O_7P_1$ requires $[M+Na]^+$ 561.2013.

## Dibenzyl (2,6-anhydro-tri-*O*-benzyl-1-deoxy-L-rhamno-hept-1-enopyranosyl)phosphonate (**30b**)

The procedure for the synthesis of dibenzyl (2,6-anhydro-tri-*O*-benzyl-1-deoxy-L-rhamno-hept-1-enopyranosyl)phosphonate (**30b**) was adopted from Norris and Toyokuni's synthesis of **30a**.[87] Dibenzyl (tri-*O*-benzyl-1-deoxy-L-rhamno-heptulopyranosyl)phosphonate (**28b**) (0.318 g, 0.45 mmol) was dissolved in a mixture of 7:2 $CH_2Cl_2$:pyridine (7 mL) and methyl oxalyl chloride (0.4 mL, 4.18 mmol) was added dropwise with stirring under nitrogen. After 90 minutes, TLC analysis showed complete consumption of the starting material so the reaction was quenched with EtOH (0.5 mL)

and allowed to stir for 10 minutes before $CH_2Cl_2$ (13 mL) and $NaHCO_3$ (5 mL, sat.) were added. The reaction was stirred for an additional 5 minutes after which it was poured into $NaHCO_3$ (10 mL) and extracted with $CH_2Cl_2$ (3x15 mL) before being dried ($Na_2SO_4$) and concentrated. The material was purified using column chromatography (35/65 EtOAc/hexane) to afford the product as a clear viscous liquid (**30b**) (0.188 g, 60% yield), $R_F$ = 0.44 (50/50 EtOAc/hexane). $\delta_H$ ($CD_2Cl_2$) 7.00-7.20 (m, 25H, 5 x $C_6H_5$), 4.86 (d, 1H, H1, $^2J_{H,\,P}$ = 12.7 Hz ), 4.20-4.80 (m, 10H, 5 x $CH_2Ph$), 4.01 (d, 1H, H3 $^3J_{3,\,4}$ = 1.8 Hz), 3.58 (m, 2H, H4, H6), 3.37 (dd, 1H, H5, $^3J_{5,\,6}$ = 8.5 Hz, $^3J_{5,\,4}$ = 4.6 Hz), 1.11 (d, 3H, H7, $^3J_{7,\,6}$ = 6.4 Hz), $\delta_C$ 165.6 (C, C2), 137.5-138.7 (5 x C, $C_6H_5$), 128.0-129.2 (25 x CH, $C_6H_5$), 92.2 (d, CH, C1, $^1J_{C,\,P}$ = 190.9 Hz), 81.2 (CH, C5), 78.2 (CH, C4), 78.0 (d, CH, C3, $^3J_{C,\,P}$ = 14.5 Hz), 75.8 (CH, C6), 73.7 ($CH_2$, $CH_2Ph$), 72.8 ($CH_2$, $CH_2Ph$), 72.3 ($CH_2$, $CH_2Ph$), 67.6 (d, $CH_2$, $POCH_2Ph$, $^2J_{C,\,P}$ = 5.0 Hz), 67.3 (d, $CH_2$, $POCH_2Ph$, $^2J_{C,\,P}$ = 5.0 Hz), 19.2 ($CH_3$, C7), $\delta_P$ 17.78 (s, 1P), HRMS ($ESI^+$): found $[M+Na]^+$ 713.2606. $C_{42}H_{43}Na_1O_7P_1$ requires $[M+Na]^+$ 713.2639.

## Dimethyl (tri-*O*-benzyl-1-deoxy-L-rhamno-heptulopyranosyl)-1-*R*-monofluorophosphonate (**32a**)

Dimethyl (2,6-anhydro-tri-*O*-benzyl-1-deoxy-L-rhamno-hept-1-enopyranosyl)phosphonate (**30a**) (0.250 g, 0.464 mmol) was dissolved in acetonitrile (5 mL) and selectfluor® (**31**) (0.350 g, 0.99 mmol) was added all at once with stirring overnight at room temperature under nitrogen. Water (2 mL) was then added and the solution was heated at 70°C for 2.5 hours before being poured into water (10 mL) and extracted with $CH_2Cl_2$ (2 x 10 mL). The organic layer dried ($Na_2SO_4$), concentrated and purified using column chromatography (25/75 EtOAc/hexane) to afford the single stereoisomer (**32a**) (0.141 g, 54% yield), $R_F$ = 0.24 (30/70 EtOAc/hexane). By n*O*e analysis, the CHFP stereocentre was determined to be *R* configuration. $\delta_H$ ($CDCl_3$) 7.20-7.50 (m, 15H, 3 x $C_6H_5$), 5.57 (s, 1H, H2), 4.50-5.10 (m, 7H, 3 x $CH_2Ph$, H1), 4.15 (dd, 1H, H4 $^3J_{4,\,5}$ = 9.1 Hz, $^3J_{4,\,3}$ = 2.7 Hz), 4.09 (m, 2H, H3, H6), 3.91 (d, 3H, $OCH_3$, $^3J_{H,\,P}$ = 11.1 Hz), 3.84 (d, 3H, $OCH_3$, $^3J_{H,\,P}$ = 11.1 Hz), 3.68 (t, 1H, H5, $^3J_{5,\,4}$ = $^3J_{5,\,6}$ = 9.1 Hz), 1.31 (d, 3H, H7, $^3J_{7,\,6}$ = 6.2 Hz), $\delta_C$ 138.4-138.8 (3 x C, $C_6H_5$), 127.5-129.0 (15 x CH,

$C_6H_5$), 97.9 (d, C, C2, $^2J_{C,\,F}$ = 24.7 Hz), 85.8 (m, CH, C1), 81.2 (CH, C4), 80.1 (CH, C5), 75.4 (dd, CH, C3, $^3J_{C,\,F}$ = 19.5 Hz, $^3J_{C,\,P}$ = 13.7 Hz), 72.8 ($CH_2$, $CH_2Ph$), 69.4 (CH, C6), 54.4 (d, $CH_3$, $OCH_3$, $^2J_{C,\,P}$ = 5.9 Hz), 54.1 (d, $CH_3$, $OCH_3$, $^2J_{C,\,P}$ = 5.9 Hz), 17.9 ($CH_3$, C7), $\delta_P$ 20.60 (d, 1P, $^2J_{P,\,F}$ = 74.8 Hz), $\delta_F$ -216.8 (d, 1F, $^2J_{F,\,P}$ = 75.1 Hz), HRMS (ESI$^-$): found $[M\text{-}1]^-$ 573.2045. $C_{30}H_{35}F_1O_8P_1$ requires $[M\text{-}1]^-$ 573.2059.

## Dibenzyl (tri-*O*-benzyl-1-deoxy-L-rhamno-heptulopyranosyl)-1-*R*-monofluorophosphonate (**32b**)

Dibenzyl (2,6-anhydro-tri-*O*-benzyl-1-deoxy-L-rhamno-hept-1-enopyranosyl)phosphonate (**30b**) (0.142 g, 0.206 mmol) was dissolved acetonitrile (3 mL) and selectfluor® (**75**) (0.157 g, 0.44 mmol) was added all at once with stirring overnight at room temperature under nitrogen. Water (1 mL) was then added and the solution was heated at 70°C for 2.5 hours before being poured into water (10 mL) and extracted with $CH_2Cl_2$ (2 x 10 mL). The organic layer dried ($Na_2SO_4$), concentrated and purified using column chromatography (16/84 EtOAc/hexane) to afford the (**32b**) as a clear viscous liquid (0.033 g, 22% yield), $R_F$ = 0.45 (20/80 EtOAc/hexane). The CHFP stereocentre was assumed to be *R*, as was the case with **32a**. $\delta_H$ ($CDCl_3$) 7.29-7.45 (m, 25H, 3 x $C_6H_5$), 5.66 (s, 1H, H2), 4.63-5.25 (m, 11H, 5 x $CH_2Ph$, H1), 4.17 (dd, 1H, H4 $^3J_{4,\,5}$ = 9.6 Hz, $^3J_{4,\,3}$ = 2.7 Hz), 4.08-4.15 (m, 2H, H3, H6), 3.69 (t, 1H, H5, $^3J_{5,\,4}$ = $^3J_{5,\,6}$ = 9.6 Hz), 1.30 (d, 3H, H7, $^3J_{7,\,6}$ = 6.3 Hz), $\delta_C$ 135.0-139.0 (5 x C, $C_6H_5$), 127.6-129.1 (25 x CH, $C_6H_5$), 98.1 (d, C, C2, $^2J_{C,\,F}$ = 25.2 Hz), 85.1 (m, CH, C1), 81.3 (CH, C4), 80.2 (CH, C5), 75.4 (dd, CH, C3, $^3J_{C,\,F}$ = 25.8 Hz, $^3J_{C,\,P}$ = 12.8 Hz), 72.8 ($CH_2$, $CH_2Ph$), 69.4 (CH, C6), 69.2 (d, $CH_2$, $POCH_2Ph$, $^2J_{C,\,P}$ = 6.4 Hz), 69.0 (d, $CH_2$, $POCH_2Ph$, $^2J_{C,\,P}$ = 6.4 Hz), 18.0 ($CH_3$, C7), $\delta_P$ 18.92 (d, 1P, $^2J_{P,\,F}$ = 76.5 Hz), $\delta_F$ -215.70 (d, 1F, $^2J_{F,\,P}$ = 76.2 Hz), HRMS (ESI$^-$): found $[M\text{-}1]^-$ 725.2668. $C_{42}H_{43}F_1O_8P_1$ requires $[M\text{-}1]^-$ 725.2685.

## Diethyl (tri-*O*-benzyl-1-deoxy-L-rhamno-heptulopyranosyl)-1-difluorophosphonate (**34**)

The procedure for the synthesis of diethyl (tri-*O*-benzyl-1-deoxy-L-rhamno-heptulopyranosyl)-1-difluorophosphonate (**34**) was modified from Norris and Toyokuni's original synthesis of **28a**.[87] Diisopropylamine (0.49 mL, 2.9 mmol) was dissolved in anhydrous THF (3 mL) and cooled to -78°C using a dry ice/acetone slurry. *n*-Butyllithium (1.2 mL, 2.9 mmol) was added and the solution was stirred for 5 minutes before being transferred to an ice bath and allowed to warm to 0°C over the course of 30 minutes. Diethyl difluoromethylphosphonate (**33**) (0.5 mL, 3.2 mmol) was cooled to -78°C in THF (2 mL) and added dropwise to the solution of LDA at -78°C. After stirring for 15 minutes 2,3,4,-tri-*O*-benzyl-L-rhamno-l,5-lactone (**26**) (0.40 g, 0.93 mmol) in THF (3 mL) was added dropwise to the solution. TLC analysis showed complete consumption of the lactone after 30 minutes. The reaction was quenched with 10% $NH_4Cl$ (15 mL) followed by addition of diethyl ether. The aqueous layer was removed and extracted with diethyl ether (3 x 15 mL). The organic extracts were combined, dried ($Na_2SO_4$) and concentrated. The material was purified using column chromatography (24/76 EtOAc/hexane) to afford the product as a clear viscous liquid (**34**) (0.423 g, 74% yield), $R_F$ = 0.37 (25/75 EtOAc/hexane). $\delta_H$ ($CDCl_3$) 7.20-7.60 (m, 15H, 3 x $C_6H_5$), 5.91 (s, 1H, H2), 4.70-5.05 (m, 6H, 3 x $CH_2Ph$), 4.33-4.45 (m, 4H, 2 x $OC\underline{H}_2CH_3$), 4.27 (d, 1H, H3, $^3J_{3,4}$ = 2.8 Hz), 4.16 (dd, 1H, H4 $^3J_{4,5}$ = 9.6 Hz, $^3J_{4,3}$ = 2.8 Hz), 4.10 (m, 1H, H6), 3.79 (t, 1H, H5, $^3J_{5,4}$ = $^3J_{5,6}$ = 9.6 Hz), 1.47 (td, 3H, $OCH_2C\underline{H}_3$, $^3J_{H,H}$ = 7.0 Hz, $^4J_{H,P}$ = 0.6 Hz), 1.43 (td, 6H, 2 x $OCH_2C\underline{H}_3$, $^3J_{H,H}$ = 7.0 Hz, $^4J_{H,P}$ = 0.6 Hz), 1.39 (d, 3H, H7, $^3J_{7,6}$ = 6.3 Hz), $\delta_C$ 138.5-138.7 (3 x C, $C_6H_5$), 127.4-128.8 (15 x CH, $C_6H_5$), 96.4 (m, C, C2), 89.8 (m, $CF_2$, C1), 81.1 (CH, C4), 79.7 (CH, C5), 75.6 (d, CH, C3, $^3J_{C,P}$ = 5.5 Hz), 75.4 ($CH_2$, $CH_2Ph$), 74.9 ($CH_2$, $CH_2Ph$), 72.5 ($CH_2$, $CH_2Ph$), 69.4 (CH, C6), 65.6 (d, $CH_2$, $O\underline{C}H_2$, $^2J_{C,P}$ = 6.2 Hz), 17.7 ($CH_3$, C7), 16.5 (d, $CH_2\underline{C}H_3$, $^3J_{C,P}$ = 6.1 Hz), $\delta_P$ 8.17 (t, 1P, $^2J_{P,F}$ = 96.9 Hz), $\delta_F$ -117.36– -119.00 (dd, 1F, $^2J_{F,F}$ = 307.0 Hz, $^2J_{F,P}$ = 96.9 Hz), -119.12– -120.70 (dd, 1F, $^2J_{F,F}$ = 307.0 Hz, $^2J_{F,P}$ = 96.9 Hz), HRMS ($ESI^-$): found $[M-1]^-$ 619.2296. $C_{32}H_{38}F_2O_8P_1$ requires $[M-1]^-$ 619.2278.

## Diethyl (tri-*O*-benzyl-2-deoxy-methyloxalyl-L-rhamno-heptulopyranosyl)-1-difluorophosphonate (**35**)

The procedure for the synthesis of diethyl (tri-*O*-benzyl-2-deoxy-methyloxalyl-L-rhamno-heptulopyranosyl)-1-difluorophosphonate (**35**) was adopted from Norris and Toyokuni's synthesis of **30a**.[87] Diethyl (tri-*O*-benzyl-1-deoxy-L-rhamno-heptulopyranosyl)-1-difluorophosphonate (**34**) (0.149 g, 0.24 mmol) was dissolved in a mixture of 7:2 $CH_2Cl_2$:pyridine (5 mL) and methyl oxalyl chloride (0.2 mL, 2.1 mmol) was added dropwise with stirring under nitrogen. After 90 minutes, TLC analysis showed complete consumption of **34**, so the reaction was quenched with EtOH (0.5 mL) and allowed to stir for 10 minutes before $CH_2Cl_2$ (13 mL) and $NaHCO_3$ (5 mL, sat.) were added. The mixture was stirred for an additional 5 minutes after which it was poured into $NaHCO_3$ (10 mL) and extracted with $CH_2Cl_2$ (3x15 mL) before being dried ($Na_2SO_4$) and concentrated. The material was purified using column chromatography (30/70 EtOAc/hexane) to afford the product as a clear viscous liquid (**35**) (0.101 g, 69% yield), $R_F$ = 0.64 (50/50 EtOAc/hexane). $\delta_H$ ($CDCl_3$) 7.28-7.48 (m, 15H, 3 x $C_6H_5$), 5.37 (br s, 1H, H3), 4.62-5.00 (m, 6H, 3 x $CH_2Ph$), 4.21-4.43 (m, 4H, 2 x $OC\underline{H}_2CH_3$), 4.07 (m, 1H, H6), 3.94 (s, 3H, $OCH_3$), 3.86 (t, 1H, H5, $^3J_{5,4} = {}^3J_{5,6} = 9.4$ Hz), 3.72 (dd, 1H, H4 $^3J_{4,5} = 9.4$ Hz, $^3J_{4,3} = 2.4$ Hz), 1.43 (d, 3H, H7, $^3J_{7,6} = 6.2$ Hz), 1.47 (m, 6H, 2 x $OCH_2C\underline{H}_3$), $\delta_C$ 157.1 (CO, $\underline{C}(O)C(O)OCH_3$), 154.5 (CO, $C(O)\underline{C}(O)OCH_3$), 137.6-138.6 (3 x C, $C_6H_5$), 127.5-128.8 (15 x CH, $C_6H_5$), 106.3 (m, $CF_2$, C1) 80.0 (CH, C4), 78.9 (CH, C5), 75.8 ($CH_2$, $CH_2Ph$), 75.3 ($CH_2$, $CH_2Ph$), 73.0 (CH, C3), 72.3 ($CH_2$, $CH_2Ph$), 72.1 (CH, H6), 65.5 (d, $CH_2$, $O\underline{C}H_2$, $^2J_{C,P} = 6.3$ Hz), 65.2 (d, $CH_2$, $O\underline{C}H_2$, $^2J_{C,P} = 6.3$ Hz) 54.0 ($CH_3$, $OCH_3$), 17.9 ($CH_3$, C7), 16.5 (m, $CH_2\underline{C}H_3$), $\delta_P$ 3.82 (dd, 1P, $^2J_{P,F} = 104.9$ Hz, $^2J_{P,F} = 91.3$ Hz), $\delta_F$ -109.6– -111.22 (dd, 1F, $^2J_{F,F} = 320.6$ Hz, $^2J_{F,P} = 91.3$ Hz), -113.60– -115.25 (dd, 1F, $^2J_{F,F} = 320.6$ Hz, $^2J_{F,P} = 104.9$ Hz), HRMS ($ESI^+$): found $[M+Na]^+$ 729.2258. $C_{35}H_{41}F_2Na_1O_{11}P_1$ requires $[M+Na]^+$ 729.2247.

### Diethyl (tri-*O*-benzyl-L-rhamno-heptulopyranosyl)-1-difluorophosphonate (**36**)

Diethyl (tri-*O*-benzyl-2-deoxy-methyloxalyl-L-rhamno-heptulopyranosyl)-1-difluorophosphonate (**35**) (0.100 g, 0.140 mmol) was dissolved in toluene (7 mL) and transferred to a three-neck round bottom flask that had been degassed for 10 minutes. Tributyltin hydride ($Bu_3SnH$) (87 μL, 0.33 mmol) was added followed by dropwise addition of azobisisobutylnitrile (AIBN) (20 mol%, 0.14 mL, 0.028 mmol) over 1 minute. The reaction was heated to 105°C and stirred for 1 hour. The reaction was then cooled to room temperature and diluted with EtOAc (7 mL) followed by concentration. The material was purified using column chromatography (3:8 EtOAc/hexane) to afford the product as a clear viscous liquid (**36**) (0.076 g, 85% yield), $R_F$ = 0.32 (40/60 EtOAc/hexane). $\delta_H$ ($CDCl_3$) 7.25-7.50 (m, 15H, 3 x $C_6H_5$), 4.60-5.00 (m, 6H, 3 x $CH_2Ph$), 4.20-4.40 (m, 5H, H3, 2 x $OC\underline{H_2}CH_3$), 3.91 (m, 1H, H2), 3.75 (t, 1H, H5, $^3J_{5,4}$ = $^3J_{5,6}$ = 9.4 Hz), 3.54 (dd, 1H, H4 $^3J_{4,5}$ = 9.5 Hz, $^3J_{4,3}$ = 2.7 Hz), 3.50 (m, 1H, H6), 1.30-1.45 (m, 9H, H7, 2 x $OCH_2C\underline{H_3}$), $\delta_C$ 138.2-138.6 (3 x C, $C_6H_5$), 127.6-128.8 (15 x CH, $C_6H_5$), 84.0 (CH, C4), 80.0 (CH, C5), 77.2 (CH, C6), 75.7 (CH, $CH_2$, C2, $CH_2Ph$), 74.6 ($CH_2$, $CH_2Ph$), 72.7 (CH, C3, $^3J_{C,P}$ = 5.9 Hz), 72.4 ($CH_2$, $CH_2Ph$), 64.9 (t, $CH_2$, $O\underline{C}H_2$, $^2J_{C,P}$ = 7.4 Hz), 17.7 ($CH_3$, C7), 16.6 (d, $CH_2\underline{C}H_3$, $^3J_{C,P}$ = 4.9 Hz), $\delta_P$ 6.20 (t, 1P, $^2J_{P,F}$ = 108.0 Hz), $\delta_F$ -115.27– -117.01 (dd, 1F, $^2J_{F,F}$ = 314.7 Hz, $^2J_{F,P}$ = 102.3 Hz), -123.62– -125.34 (dd, 1F, $^2J_{F,F}$ = 314.7 Hz, $^2J_{F,P}$ = 102.3 Hz), HRMS ($ESI^+$): found $[M+Na]^+$ 627.2320. $C_{32}H_{39}F_2Na_1O_7P_1$ requires $[M+Na]^+$ 627.2294.

## Deprotection of R1CP Analogues

### Representative Procedure for the Deprotection of Methyl-protected Analogues:

A solution of methyl protected compound **28a**, **30a** or **32a** (50 mg), 10% palladium on carbon (20 mg, 0.02 mmol), ethyl acetate (3 mL) and methanol (3 mL) was degassed under vacuum and saturated with hydrogen gas (1 atm balloon). The reaction was stirred

overnight before the catalyst was filtered and the solution was concentrated. The material was directly dissolved in HCl (5 mL, 6 M) and refluxed for 3 h before being concentrated with methanol (3 x 5 mL) and titrated to pH 8 with aqueous $NH_4OH$ (0.2 M). Upon lyophilization compounds **42**, **43** and **44** were obtained in quantitative yields as their diammonium salts.

## Representative Procedure for the Deprotection of Benzyl-protected Analogues:

A solution of methyl protected compound **28b**, **30b** or **32b** (50 mg), 10% palladium on carbon (20 mg, 0.02 mmol), ethyl acetate (3 mL) and methanol (3 mL) was degassed under vacuum and saturated with hydrogen gas (1 atm balloon). The reaction was stirred overnight before the catalyst was filtered and the solution was concentrated to a colorless oil. The material was dissolved in water (2 mL) and titrated to pH 8 with aqueous $NH_4OH$ (0.2 M). Upon lyophilization compounds **42**, **43** and **44** were obtained in quantitative yields as their diammonium salts.

## Representative Procedure for the Deprotection of Ethyl-protected Analogues:

A solution of ethyl protected compound **34** or **35** (50 mg) was dissolved in dichloromethane (2 mL) and cooled to 0°C in an ice bath before TMSI (55 eq) was added dropwise with stirring. The ice bath was removed and the reaction was allowed to stir at room temperature for 5 h before being quenched with methanol (4 mL) and concentrated. The crude mixture was dissolved in water (10 mL) and extracted with diethyl ether (8 x 10 mL). The aqueous layer was concentrated with methanol (3 x1 0 mL) before being taken up in water (2 mL) and passed though an Amberlite-$H^+$ cation exchange column. Acid fractions were pooled, concentrated and titrated to pH 8 with aqueous $NH_4OH$ (0.2 M). Upon lyophilization, compounds **45** and **46** were obtained in high yields (94-95%) as their diammonium salts.

Ammonium-(7-anhydro-1-deoxy-β-L-rhamno-heptulopyranosyl)phosphonate (L-rhamnose-1C-ketosephosphonate) (**42**)

$\delta_H$ ($D_2O$) 3.86 (m, 1H, H4), 3.60-3.83 (m, 2H, H3, H6), 3.24 (m, 1H, H5), 1.70-2.00 (m, 2H, H1), 1.15 (d, 3H, H7, $^3J_{7,6}$ = 6.2 Hz), $\delta_C$ 93.9 (s, C, C2), 68.2-72.9 (4 x s, 4 x CH, C3-6), 48.8 (s, $CH_2$, C1) 16.8 (s, $CH_3$, C7), $\delta_P$ 15.41 (s, 1P), HRMS ($ESI^-$): found $[M-1]^-$ 257.0417 $C_7H_{14}O_8P_1$ requires $[M-1]^-$ 257.0432.

Ammonium-(2,7-anhydro-1-deoxy-β-L-rhamno-heptulopyranosyl)phosphonate (L-rhamnose-1C-phosphonate) (**43**)

$\delta_H$ ($D_2O$) 3.80 (br d, 1H, H3, $^3J_{3,4}$ = 3.3 Hz), 3.74 (m, 1H, H2), 3.50 (dd, 1H, H4, $^3J_{4,5}$ = 9.1 Hz, $^3J_{4,3}$ = 3.3 Hz), 3.30-3.15 (m, 2H, H5, H6), 1.95 (ddd, 2H, H1a, H1b, $^2J_{H,P}$ = 18.2 Hz, $^3J_{1,2}$ = 6.7 Hz, $^2J_{H,H}$ = 1.42 Hz), 1.15 (d, 3H, H7, $^3J_{7,6}$ = 6.0 Hz), $\delta_C$ 76.1-72.2 (3 x CH, C4-6), 73.7 (d, CH, C2, $^2J_{C,P}$ = 11.1 Hz), 71.1 (d, CH, C3, $^3J_{C,P}$ = 9.3 Hz), 28.7-29.8 (d, $CH_2$, C1, $^1J_{C,P}$ = 135.8 Hz), 17.0 (s, $CH_3$, C7) $\delta_P$ 24.81 (s, 1P), HRMS ($ESI^-$): found $[M-1]^-$ 241.0478 $C_7H_{14}O_7P_1$ requires $[M-1]^-$ 241.0483.

Ammonium-(7-anhydro-1-deoxy-*R*-monofluoro-β-L-rhamno-heptulopyranosyl)phosphonate (L-rhamnose-1CF-ketosephosphonate) (**44**)

$\delta_H$ ($D_2O$) 4.43 (dd, 1H, H1, $^2J_{H,F}$ = 45.4 Hz, $^2J_{H,P}$ = 4.2 Hz), 3.86 (m, 1H, H4), 3.70-3.78 (m, 2H, H3, H6), 3.27 (t, 1H, H5, $^3J_{5,4}$ = $^3J_{5,6}$ = 9.8 Hz), 1.16 (d, 3H, H7, $^3J_{7,6}$ = 6.1 Hz), $\delta_C$ 97.7 (d, C, C2, $^2J_{C,F}$ = 24.5 Hz) 86.3-87.6 (m, CH, C1), 72.6 (s, CH, C5), 70.6 (s, CH, C3), 70.1 (s, CH, C4), 68.3 (s, CH, C6), 16.9 ($CH_3$, C7), $\delta_P$ 11.00 (d, 1P, $^2J_{P,F}$ = 67.9 Hz), $\delta_F$ –213.80 (d, 1F, $^2J_{F,P}$ = 68.7 Hz), HRMS ($ESI^-$): found $[M-1]^-$ 275.0338 $C_7H_{13}F_1O_8P_1$ requires $[M-1]^-$ 275.0338.

### Ammonium-(2,7-anhydro-1-deoxy-difluoro-β-L-rhamno-heptulopyranosyl)phosphonate (L-rhamnose-1CF2-ketosephosphonate) (**45**)

$\delta_H$ ($D_2O$) 4.09 (d, 1H, H3, $^3J_{3,4}$ = 3.6 Hz), 3.79 (dd, 1H, H4, $^3J_{4,5}$ = 10.2 Hz, $^3J_{4,3}$ = 3.6 Hz), 3.75 (m, 1H, H6) 3.31 (t, 1H, H5, $^3J_{5,4} = {}^3J_{5,6}$ = 9.7 Hz), 1.20 (d, 3H, H7, $^3J_{7,6}$ = 6.3 Hz), $\delta_C$ 72.0 (s, CH, C5), 70.3 (s, CH, C3), 68.9-70.2 (2 x s, 2 x CH, C4, C6), 16.8 (s, $CH_3$, C7), $\delta_P$ 3.92 (t, 1P, $^2J_{P,F}$ = 77.2 Hz), $\delta_F$ -116.84– -118.43 (dd, 1F, $^2J_{F,F}$ = 295.4 Hz, $^2J_{F,P}$ = 77.2 Hz), -122.08- -123.62 (dd, 1F, $^2J_{F,F}$ = 295.4 Hz, $^2J_{F,P}$ = 77.2 Hz), HRMS ($ESI^-$): found $[M-1]^-$ 293.0240 $C_7H_{12}F_2O_8P_1$ requires $[M-1]^-$ 293.0243.

### Ammonium-(2,7-anhydro-1-deoxy-difluoro-β-L-rhamnoheptulopyranosyl)phosphonate (L-rhamnose-1CF2-phosphonate) (**46**)

$\delta_H$ ($D_2O$) 4.41 (br d, 1H, H3, $^3J_{1,2}$ = 2.4 Hz), 3.80 (m, 1H, H2), 3.54 (dd, 1H, H4, $^3J_{4,5}$ = 9.3 Hz, $^3J_{4,3}$ = 3.4 Hz), 3.33 (m, 2H, H5, 6), 1.23 (d, 3H, H7, $^3J_{7,6}$ = 5.7 Hz), $\delta_C$ 78.0 (s, CH, C2), 76.7 (s, CH, C6), 73.1 (s, CH, C4), 72.2 (s, CH, C5), 68.2 (s, CH, C3), 16.7 (s, $CH_3$, C7), $\delta_P$ 3.08 (t, 1P, $^2J_{P,F}$ = 89.2 Hz), $\delta_F$ -110.09– -111.60 (dd, 1F, $^2J_{F,F}$ = 297.1 Hz, $^2J_{F,P}$ = 80.5 Hz), -119.76– -121.22 (dd, 1F, $^2J_{F,F}$ = 296.0 Hz, $^2J_{F,P}$ = 78.3 Hz), HRMS ($ESI^-$): found $[M-1]^-$ 277.0289 $C_7H_{12}F_2O_7P_1$ requires $[M-1]^-$ 277.0294.

## Steps in the Synthesis of CPCPO Analogues 61 and 62

### Monomethyl methyl phosphonate (**59**)

Dimethyl methylphosphonate (**27a**) (0.10 mL, 0.89 mmol) was dissolved in tertbutylamine (10 mL) and refluxed over night at 48°C. The tertbutylammonium salt was found to partially precipitate out of solution. The material was concentrated *in vacuo* and redissolved in methanol (5 mL) and dowex-$H^+$ (1 g) was added followed by stirring for 10 minutes. The dowex-$H^+$ was filtered off and the solution was concentrated *in vacuo* to

recover monomethyl methyl phosphonate (**59**) as a free acid (0.01 g, 10%) $\delta_P$ (DMF) 18.68 (s, 1P).

### Representative Procedure for the Synthesis of CPCPO Analogues **61** and **62**

Dimethyl or dibenzyl methyl phosphonate (**27a** or **27b**) (0.3 mmol) was dissolved in anhydrous THF (1 mL) under nitrogen and cooled to -78°C using a dry ice/acetone slurry. *n*-Butyllithium (0.1 mL, 0.25 mmol) was added and the solution was stirred for 20 minutes before the dry ice/acetone bath was removed and replaced with a dry ice/(MeCN/$CCl_4$) bath (-30°C) or dry ice/(MeCN) bath (-40°C). As the solution warmed, monomethyl methyl phosphonate (**59**) (5.5 mg, 0.05 mmol) was dissolved in MeCN or DMF (1 mL) under nitrogen and DIEA (5 eq) was added followed by stirring for 10 minutes. The sulfonyl imidazolium salt (**52**)[99] (1.2 eq) was then added as a solid to the solution of **59**. After stirring for 2-5 minutes, the solution containing the activated imidazolium salt (**60**) was added dropwise to the THF solution, and the reaction was allowed to stir at -30°C or -40°C for 30 minutes before being quenched with 10% $NH_4Cl$ (5 mL) and extracted with $CH_2Cl_2$ (5 mL). Compounds **61** and **62** were detected in the organic layer by LRMS ($ESI^+$): found $[M+H]^+$ 217.1 (**61**) or $[M+H]^+$ 369.1 (**62**).

## Steps in the Synthesis of deoxythymidine 5′-[[(α-D-glucopyranosyl]hydroxyphosphinyl)methyl]phosphonate] (34)

### 6.5.1 Methylene diphosphonic acid (**7**)

Tetraisopropyl methylenediphosphonate (**38**) (1.08g, 3.10 mmol) in HCl (20 mL, 6 M) was refluxed for 17 h after which time $^{31}P$ NMR spectroscopy indicated complete hydrolysis of **38** (19.4 ppm) into **7** (16.7 ppm). The mixture was concentrated *in vacuo* (0.54 g, 100 % yield). $\delta_P$ ($D_2O$) 16.7 (s, 2P, $PCH_2P$).

## Ditetrabutylammonium methylenebisphosphonate (**7′**)

Methylene bisphosphonate (**7**) (0.352 g, 2.00 mmol) was eluted through an HCl charged amberlite column with millipore water and the acidic fractions (first 120 mL) were combined and adjusted to pH 6 using tetrabutylammonium hydroxide (0.2 M, ~10 mL). The sample was concentrated to approximately 5 mL and lyophilized to obtain **7′** as a white gel-like solid (1.33 g, 100% yield). $\delta_H$ ($CDCl_3$) 4.54 (s, 4H, OH), 3.30 (t, 16H, 8 x $CH_2N$, $^3J$ = 8.0 Hz), 2.03 (t, 2H, $PCH_2P$, $^2J_{P,H}$ = 18.0 Hz), 1.65 (p, 16H, 8 x $\underline{CH_2}CH_2N$, $^3J$ = 7.3 Hz) 1.46 (app. sex, 16H, 8 x $\underline{CH_2}CH_2CH_2N$, $^3J$ = 7.3 Hz), 1.00 (t, 24H, 8 x $CH_3$, $^3J$ = 7.3 Hz), $\delta_C$ 58.6 (s, 8C, 8 x $CH_2N$) 30.2 (s, 1C, $PCH_2P$), 24.0 (s, 8C, 8 x $\underline{C}H_2CH_2N$) 19.7 (s, 8C, 8 x $\underline{C}H_2CH_2CH_2N$) 13.8 (s, 8C, 8 x $CH_3$), $\delta_P$ 15.50 (s, 2P, $PCH_2P$).

## 2,3,4,6-Tetra-O-acetyl-α-D-glucopyranosyl bromide (**70**)

The procedure for the synthesis of 2,3,4,6-tetra-*O*-acetyl-α-D-glucopyranosyl bromide (**70**) was adopted from the method reported by Timmons and Jakeman.[102] β-D-Glucopyranose pentaacetate (**69**) (0.850 g, 2.18 mmol) was cooled to 0°C in anhydrous $CH_2Cl_2$ (7 mL) under nitrogen and phosphorous tribromide (0.4 mL, 4.24 mmol) was added dropwise. Distilled water (0.28 mL, 14.50 mmol) was then added dropwise immediately following the phosphorous tribromide. The solution was warmed to room temperature after 20 min. After 100 min the reaction was deemed complete by TLC, $R_F$ = 0.68 (40/60 EtOAc/hexane). The solution was diluted with $CH_2Cl_2$ (15 mL) and extracted with water (20 mL) and $NaHCO_3$ (20 mL, sat.). After drying ($Na_2SO_4$), the mixture was concentrated to an orange syrup (0.757 g, 84% yield). The material was immediately carried onto the next reaction without further purification.

## β-D-Glucopyranosyl 1-methylenebisphosphonate (**71**)

A 0.2 mmol/mL solution of **7′** was prepared by dissolving 2.00 mmol of **7′** in 10 mL of anhydrous MeCN. 3 mL (0.60 mmol) of **7′** was then transferred to a separate flask fitted with activated 3 Å molecular sieves (0.45 g). Triethylamine (0.081 mL, 0.60 mmol) was

then added dropwise under nitrogen and the solution was allowed to stir at room temperature for 12 min. A separate 0.19 mmol/mL solution of **70** was prepared in MeCN and 2.6 mL (0.48 mmol) was added dropwise to the solution of **7′**. The flask was fitted with a reflux condenser and heated to 80°C in an oil bath. After stirring for 30 min at 80°C, the reaction was deemed complete by TLC, which indicated the disappearance of **70**, $R_F$ = 0.68 (40/60 EtOAc/hexane). The flask was removed from the oil bath and allowed to come to room temperature before the molecular sieves were suction filtered off and the product was washed with MeCN (~10 mL). After being concentrated, the mixture was dissolved in 2:2:1 MeOH:$H_2O$:$NEt_3$ (10 mL) and allowed to stir overnight. The mixture was concentrated and dissolved in a 3 mL solution of buffer A before being put through normal phase silica purification. (2 CV 100 buffer A, 15 CV to 60% buffer A:40 MeOH, 4 CV 100% MeOH). Fractions containing the desired product and were put through a $Na^+$ charged dowex column. The first 75 mL were combined and concentrated to 5 mL and then lyophilized to obtain the ditetrabutylammonium salts of **71** and starting material **7′** (0.066 g).

## 2,3,4,6-Tetra-*O*-acetyl-β-D-glucopyranosyl chloride (**72**)

The procedure for the synthesis of 2,3,4,6-tetra-*O*-acetyl-β-D-glucopyranosyl chloride (**72**) was adopted from the method reported by Ibatullin and Selivanov.[104] β-D-Glucopyranose pentaacetate (**69**) (0.383 g, 0.98 mmol) and phosphorous pentachloride (0.250 g, 1.20 mmol) were cooled to 0°C in anhydrous $CH_2Cl_2$ (4 mL) under nitrogen and boron trifluorodiethyletherate (15 μL, 0.12 mmol) was added via syringe. After 30 min the reaction was deemed complete by TLC, $R_F$ product = 0.48 (40/60 EtOAc/hexane). The solution was diluted with $CH_2Cl_2$ (11 mL) and extracted with ice cold water (15 mL), ice cold $NaHCO_3$ (15 mL, sat.) and ice cold water (15 mL). After drying ($Na_2SO_4$), the mixture was concentrated to a yellow syrup (0.301 g, 84% yield). The material was immediately carried onto the next reaction without further purification.

## 2,3,4,6 Tetra-*O*-acetyl-α-D-glucopyranosyl 1-methylenebisphosphonate (**16**)

A 0.2 mmol/mL solution of **7′** was prepared by dissolving **7′** (2.00 mmol) in anhydrous MeCN (10 mL). **7′** (2 mL, 0.40 mmol) was then transferred to a separate flask fitted with activated 3 Å molecular sieves (0.45 g). Triethylamine (0.054 mL, 0.40 mmol) was then added dropwise under nitrogen and the solution was allowed to stir at room temperature for 15 min. A separate 0.20 mmol/mL solution of **72** was prepared in MeCN and 2.0 mL (0.40 mmol) was added dropwise to the solution of **7′**. The flask was fitted with a reflux condenser and heated to 45°C in an oil bath. After stirring for 2 h at 45°C, the reaction was deemed complete by TLC which indicated the disappearance of **72**, $R_F = 0.48$ (40/60 EtOAc/hexane). The flask was removed from the oil bath and allowed to come to room temperature before the molecular sieves were suction filtered off and the product was washed with MeCN (~10 mL). After being concentrated, the mixture was redissolved in water and extracted with $CH_2Cl_2$ (2 x 15 mL). The aqueous layer was concentrated and put through the same purification as **71**. A small amount of the ditetrabutylammonium salt of (**16**) was recovered in the 100% MeOH wash. (0.006 g, 2% yield). $\delta_P$ ($D_2O$) 16.90 (br s, 1P, P2), 14.50 (br s, 1P, P1).

## 3′-*O*-Acetylthymidine 5′-methylenebisphosphonate (**73**)

Method 1:

The procedure for the synthesis of 3′-*O*-acetylthymidine 5′-methylenebisphosphonate (**73**) was modified from the method reported by Kalek and coworkers[64] Methylenebis(phosphonic dichloride) (**10**) (0.192 g, 0.80 mmol) and one crystal of 1,2,4-triazole were dissolved in TMP (3 mL) at 0°C. 3′-*O*-acetylthymidine (**67**) (0.114 g, 0.40 mmol) was added to the reaction flask, followed by DIEA (68 μL, 0.40 mmol). The reaction was allowed to come to room temperature and stirred for ~2.5 h until TLC showed full consumption of the **67**, $R_F = 0.51$ (100% ethyl acetate), with the formation of a more polar product on the baseline. The material was diluted with 0.7 M TEAB (10 mL) and extracted with $CH_2Cl_2$ (50 mL). The pH of the aqueous layer was adjusted to 6.8

with 1 M TEAB and the material was diluted to 300 mL with distilled water before being put through purification with a DEAE A25 Sephadex ($HCO_3^-$) column charged with 1M TEAB (2 CV 0-20% 1 M TEAB, 15 CV 20% 1 M TEAB, 5 CV 100% 1 M TEAB). Fractions containing the desired product were concentrated with ethanol added repeatedly to remove the TEAB buffer. The material was isolated as the triethylammonium salt of **73** (0.253 g, 45% yield). $\delta_H$ ($D_2O$) 7.69 (d, 1H, H6, $^4J_{6,7}$ = 1.2 Hz), 6.24 (t, 1H, H1′, $^3J_{1',2'}$ = 6.3 Hz), 5.30 (m, 1H, H3′), 4.26 (m, 1H, H4′), 4.02 (m, 2H, H5′), 2.29-2.40 (m, 2H, H2′), 2.06 (t, 2H, $PCH_2P$, $^2J_{H,P\alpha}$ = 19.8 Hz), 2.02 (s, 3H, $C(O)CH_3$), 1.82 (d, 3H, H7, $^4J_{7,6}$ = 1.1 Hz), $\delta_C$ 173.5 (C, C8) 166.5 (C, C4), 151.7 (C, C2), 137.2 (CH, C6), 111.8 (C, C5), 83.3 (d, CH, C4′, $^3J_{4',P\alpha}$ = 7.6 Hz) 84.9 (CH, C1′), 75.6 (CH, C3′), 64.1 (d, $CH_2$, C5′, $^2J_{5',P\alpha}$ = 3.9 Hz), 36.2 ($CH_2$, C2′), 27.4 (t, $CH_2$, $PCH_2P$, $^2J_{C,P}$ = 124.4 Hz), 20.4 ($CH_3$, C9), $\delta_P$ 18.06 (d, 1P, Pα, $^2J_{\alpha,\beta}$ = 9.0 Hz), 14.70 (d, 1P, Pβ, $^2J_{\beta,\alpha}$ = 9.0 Hz).

Method 2:

Methylenebis(phosphonic dichloride) (**10**) (0.225 g, 0.90 mmol) was dissolved in anhydrous pyridine (3 mL) at 0°C. Once all of the MBPDC dissolved, a solution of 3′-*O*-acetylthymidine (**67**) (0.852 g, 0.30 mmol) in anhydrous pyridine (5 mL) was added dropwise via syringe. TLC showed full consumption of **67**, $R_F$ = 0.51 (100% ethyl acetate), after 10 min. The workup and purification of the material was identical to Method 1. Compound **73** was isolated as the ditriethylammonium salt (0.092 g, 48% yield).

## deoxythymidine 5′-Methylenebisphosphonate (**68**)

The triethylammonium salt of **73** was dissolved in a 2:2:1 MeOH:$H_2O$:$NEt_3$ mixture and stirred overnight. The material was concentrated and lyophilized to obtain the ditriethylammonium salt of **68** quantitatively. $\delta_H$ ($D_2O$) 7.62 (d, 1H, H6, $^4J_{6,7}$ = 1.2 Hz), 6.22 (t, 1H, H1′, $^3J_{1',2'}$ = 6.7 Hz), 4.50 (m, 1H, H3′), 4.04 (m, 1H, H4′), 3.99 (m, 2H, H5′), 2.20-2.32 (m, 2H, H2′), 2.08 (t, 2H, $PCH_2P$, $^2J_{H,P\alpha}$ = 19.8 Hz), 1.81 (d, 3H, H7, $^4J_{7,6}$ = 1.1 Hz), $\delta_C$ 166.5 (C, C4), 151.7 (C, C2), 137.4 (CH, C6), 111.7 (C, C5), 85.4 (d, CH, C4′, $^3J_{4',P\alpha}$ = 7.8 Hz) 84.9 (CH, C1′), 70.9 (CH, C3′), 63.8 (d, $CH_2$, C5′, $^2J_{5',P\alpha}$ = 4.7 Hz),

38.3 ($CH_2$, C2′), 27.4 (t, $CH_2$, $PCH_2P$, $^2J_{C,\,P}$ = 124.6 Hz), $\delta_P$ 18.20 (d, 1P, Pα, $^2J_{\alpha,\,\beta}$ = 9.0 Hz), 14.67 (d, 1P, Pβ, $^2J_{\beta,\,\alpha}$ = 9.0 Hz), HRMS ($ESI^-$): found $[M\text{-}H]^-$ 399.0367. $C_{11}H_{17}N_2O_{10}P_2$ requires $[M\text{-}H]^-$ 399.0364.

### 3′-*O*-Acetylthymidine 5′-[[(2″,3″,4″,6″-tetra-*O*-acetyl-α-D-glucopyranosyl]hydroxyphosphinyl)methyl]phosphonate] (**74**)

The triethylammonium salt of **73** was put through Amberlite-$H^+$ ion exchange and titrated to pH 6 with TBAOH. The material was concentrated and dissolved in anhydrous MeCN under nitrogen. Two equivalent of triethylamine were then added and the solution was allowed to stir for 20 min before two equivalents of **72** were added in a solution of MeCN. The solution was heated to 45°C and stirred overnight. Compound **74** was observed by mass spectrometry. LRMS ($ESI^-$): found $[M\text{-}H]^-$ 729.0.

## Steps in the Synthesis of Protected α/β-D-glucopyranosyl thiophosphates

### Diphenylchlorothiophosphate (**77b**)

The procedure for the synthesis of diphenylchlorothiophosphate (**77b**) was adopted from the method reported by Hoque, Lee and coworkers.[116] Phenol (1.88 g, 20.0 mmol) was dissolved in $CH_2Cl_2$ (5.2 mL) and triethylamine (2.8 mL, 20.0 mmol). Half of the solution was added dropwise over 15 minutes to a solution of $PSCl_3$ (1 mL, 10.0 mmol) in $CH_2Cl_2$ (3 mL) at 0°C. After 2.5 hours, TLC showed full consumption of phenol so the remaining half of the solution was added to the reaction mixture dropwise and the solution was allowed to stir overnight. TLC analysis after 18 hours showed one major product by TLC, Rf = 0.63 10/90 EtOAc/hexane. The material was isolated directly using column chromatography (100% hexane) and collected as a white crystalline solid (1.400 g, 50%). $\delta_P$ ($CDCl_3$) 58.80 (s, 1P).

## 2,3,4,6-Tetra-*O*-acetyl-α/β-D-glucopyranosyl diethylthiophosphate (**78**)

The procedure for the synthesis of 2,3,4,6-tetra-*O*-acetyl-α/β-D-glucopyranosyl diethylthiophosphate (**78**) was modified from the method reported by Zhang, Deng and Hui.[80] 2,3,4,6-tetra-*O*-acetyl-α/β-D-glucopyranose (**75**) (0.122 g, 0.35 mmol) was dissolved in anhydrous THF (2 mL) and cooled to -78°C using a dry ice/acetone slurry. *n*-Butyllithium (0.17 mL, 0.43 mmol) was added and the solution was stirred for one hour before diethylchlorothiophosphate (**77a**) (0.063 mL, 0.40 mmol) was added dropwise. The solution turned a red-brown color upon warming to room temperature. The reaction stirred overnight before being diluted with ice cold water (10 mL) and extracted with $CH_2Cl_2$ (10 mL). The organic extract was washed with ice cold HCl (0.5 M, 15 mL) and $NaHCO_3$ (15 mL, sat.). After drying with anhydrous $Na_2SO_4$, the mixture was concentrated to a brown liquid. The material was purified by column chromatography (30/70 EtOAc/hexane) to afford **78** as a clear liquid, 1:3 α/β diastereotopic mixture (0.204g, 57% yield), $R_F$ = 0.58 (40/60 EtOAc/hexane). $\delta_H$ ($CDCl_3$) 5.96 (dd, 0.25H, αH1, $^3J_{1,2}$ = 3.4 Hz, $J_{1,P}$ = 9.8 Hz), 5.48 (t, 0.25H, αH4, $^3J_{3,4} = J_{4,5}$ = 9.8 Hz), 5.34 (dd, 0.75H, βH1, $^3J_{1,2}$ = 7.9 Hz, $J_{1,P}$ = 10.6 Hz), 5.25 (t, 0.75H, βH4, $^3J_{3,4} = {}^3J_{4,5}$ = 9.8 Hz) 5.06-5.15 (m, 2H, H2, H3), 5.00 (m, 0.25H, αH5) 4.00-4.30 (m, 6H, 2$OCH_2$, H6a, H6b), 3.82 (m, 0.75H, βH5), 2.07, 2.04, 2.03, 2.01 (4 x s, 4 x 3H, 4 x OAc), 1.28-1.39 (m, 6H, 2 x $CH_3$), $\delta_C$ 169.3-171.0 (4 x C, $\underline{C}$(O)$OCH_3$), 96.5 (d, CH, βC1, $^2J_{C,P}$ = 3.6 Hz), 94.0 (d, CH, αC1, $^2J_{C,P}$ = 4.1 Hz), 60.3-72.7 (4 x CH, C2-C5, 3 x $CH_2$, C6, O$\underline{C}H_2CH_3$), 14.3-32.0 (2 x $CH_3$ , $OCH_2\underline{C}H_3$, 4 x $CH_3$, C(O)O$\underline{C}H_3$), $\delta_P$ 67.09 (s, 0.25P, αP=S), 66.94 (s, 0.75P, βP=S), HRMS ($ESI^+$): found $[M+Na]^+$ 523.0999. $C_{18}H_{29}Na_1O_{12}P_1S_1$ requires $[M+Na]^+$ 523.1010.

## 2,3,4,6-Tetra-*O*-benzyl-α/β-D-glucopyranosyl diethylthiophosphate (**79a**)

The procedure for the synthesis of 2,3,4,6-tetra-*O*-benzyl-α/β-D-glucopyranosyl diethylthiophosphate (**79a**) was modified from the method reported by Zhang, Deng and Hui.[80] 2,3,4,6-Tetra-*O*-benzyl-α/β-D-glucopyranose (**76**) (0.270 g, 0.50 mmol) was

dissolved in anhydrous THF (3 mL) under nitrogen and cooled to -40°C using a dry ice/acetonitrile slurry. *n*-Butyllithium (0.22 mL, 0.55 mmol) was added and the solution was stirred for one hour before diethylchlorothiophosphate (**77a**) (0.1 mL, 0.64 mmol) was added dropwise. The reaction was allowed to come to room temperature overnight. The solution was poured into a suspension of ether (10 mL) and water (10 mL) and extracted with ethyl acetate (7 mL) before being washed with $NaHCO_3$ (2 x 10 mL, sat.) and dried with anhydrous $Na_2SO_4$. The mixture was concentrated *in vacuo* and collected as a clear liquid. The material was then purified by column chromatography (9/91 EtOAc/hexane) to afford **79a** as a clear liquid, 2:1 α/β diastereotopic mixture (0.241 g, 67% yield), $R_F$ = 0.32 (10/90 EtOAc/hexane). $\delta_H$ ($CDCl_3$) 7.20-7.50 (m, 20H, 4 x $C_6H_5$), 6.13 (dd, 0.67H, αH1, $^3J_{1,2}$ = 3.3 Hz, $^3J_{1,P}$ = 9.8 Hz), 5.40 (dd, 0.33H, βH1, $^3J_{1,2}$ = 7.9 Hz, $^3J_{1,P}$ = 10.0 Hz), 4.50-5.10 (m, 8H, 4 x $CH_2Ph$), 4.20 (m, 4H, 2$OCH_2$) 4.00-4.10 (m, 2H, H3, H4), 3.60-3.86 (m, H2, H5, H6a, H6b) 1.28-1.39 (m, 6H, 2 x $CH_3$), $\delta_C$ 137.7-138.7 (4 x C, $C_6H_5$), 127.7-128.6 (20 x CH, $C_6H_5$), 99.2 (d, CH, C1β, $^2J_{C,P}$ = 5.7 Hz), 95.84 (d, CH, C1α, $^2J_{C,P}$ = 5.7 Hz), 68.0-84.8 (5 x $CH_2$, $CH_2Ph$, C6, 4 x CH, C2-C5), 64.3-64.7 (m, O$\underline{C}H_2CH_3$), 15.8-16.0 (m, $OCH_2\underline{C}H_3$), $\delta_P$ 67.80 (s, 0.33P, βP=S), 67.38 (s, 0.67P, αP=S), HRMS ($ESI^+$): found $[M+Na]^+$ 715.2448. $C_{38}H_{45}Na_1O_8P_1S_1$ requires $[M+Na]^+$ 715.2465.

## 2,3,4,6-Tetra-*O*-benzyl-α/β-D-glucopyranosyl diphenylthiophosphate (**79b/c**)

The procedure for the synthesis of 2,3,4,6-tetra-*O*-benzyl-α/β-D-glucopyranosyl diphenylthiophosphate (**79b/c**) was modified from the method reported by Huestis, Jakeman and coworkers.[105] 2,3,4,6-Tetra-*O*-benzyl-α/β-D-glucopyranose (**76**) (0.270 g, 0.5 mmol) and 4-dimethylaminopyridine (1.293 g, 1.23 mmol) were dissolve in $CH_2Cl_2$ (10 mL) and stirred under nitrogen at 0°C for 15 minutes. A solution of diphenylchlorothiophosphate (**77b**) (0.321 g, 2.28 mmol) in $CH_2Cl_2$ (5 mL) was added dropwise and stirred under nitrogen at 0°C for 3 hours. The reaction was quenched with distilled water (15 mL), extracted with $CH_2Cl_2$ (2 x 15 mL) and dried with anhydrous $Na_2SO_4$. The mixture was concentrated *in vacuo* and collected as a clear viscous liquid.

The material was purified by column chromatography (20/80 EtOAc/hexane) using basic silica (5% triethylamine, 95% hexanes) to afford two products (0.095 g, combined yield 24%). The oxygen linked thiophosphate, $R_F = 0.74$, and the sulfur linked thiophosphate, $R_F = 0.52$, (25/75 EtOAc/hexane).

**1-*O*-Diphenylthiophosphate-2,3,4,6-tetra-*O*-benzyl-α/β-D-glucopyranose (79b)**

$\delta_H$ ($CD_2Cl_2$) 7.15-7.45 (m, 30H, 6 x $C_6H_5$), 6.20 (dd, 1H, H1, $^3J_{1,2}$ = 3.3 Hz, $^3J_{1,P}$ = 9.5 Hz), 4.48-5.03 (m, 8H, 4 x $CH_2Ph$), 3.97-4.16 (2H, H3, H4), 3.52-3.83 (m, 4H, H2, H5, H6a, H6b), $\delta_C$ 137.5-138.7 (6 x C, $C_6H_5$), 121.0-129.0 (30 x CH, $C_6H_5$), 93.7 (CH, C1), 67.9-81.6 (5 x $CH_2$, $CH_2Ph$, C6, 4 x CH, C2-C5), $\delta_P$ 57.86 (s, 1P), HRMS ($ESI^+$): found $[M+Na]^+$ 811.2451 $C_{46}H_{45}Na_1O_8P_1S_1$ requires $[M+Na]^+$ 811.2465.

**1-*S*-Diphenylthiophosphate-2,3,4,6-tetra-*O*-benzyl-α/β-D-glucopyranose (79c)**

$\delta_H$ ($CD_2Cl_2$) 7.10-7.40 (m, 30H, 6 x $C_6H_5$), 6.30 (dd, 0.80H, αH1, $^3J_{1,2}$ = 5.0 Hz, $^3J_{1,P}$ = 11.1 Hz), 5.07 (dd, 0.20H, βH1, $^3J_{1,2}$ = 9.7 Hz, $^3J_{1,P}$ = 14.2 Hz), 4.96-4.39 (m, 8H, 4 x $CH_2Ph$), 3.51-3.91(m, 5H, H2, H3, H4, H5, H6a), 3.20 (dd, 1H, H6b, $^2J_{6b,6a}$ = 1.8 Hz, $^3J_{6b,5}$ = 10.9 Hz), $\delta_C$ 135.4-139.0 (6 x C, $C_6H_5$), 120.4-130.4 (30 x CH, $C_6H_5$), 67.9-82.7 (5 x $CH_2$, $CH_2Ph$, C6, 4 x CH, C2-C5), $\delta_P$ 18.77 (s, 0.80P, αP=O), 16.69 (s, 0.20P, βP=O), HRMS ($ESI^+$): found $[M+Na]^+$ 811.2462 $C_{46}H_{45}Na_1O_8P_1S_1$ requires $[M+Na]^+$ 811.2465.

## REFERENCES


(1) Thorson, J. S.; Hosted, T. J.; Jiang, J. Q.; Biggins, J. B.; Ahlert, J. *Curr. Org. Chem.* **2001***, 5*, 139-167.

(2) Weymouth-Wilson, A. C. *Nat. Prod. Rep.* **1997***, 14*, 99-110.

(3) Barton, W.A.; Lesniak, J.; Biggins, J. B.; Jeffrey, P. D.; Jiang, J.; Rajashankar, K.R.; Thorson, J. S.; Nikolov, D. B. *Nat. Struc. Biol.* **2001**, *8*, 545-551.

(4) Thorson, J.S.; Moretti, R. *J. Biol. Chem*. **2007**, *282*,16942-16947.

(5) Lindquist, L.; Kaiser, R.; Reeves, P. R.; Lindberg, A. A. *Eur. J. Biochem*. **1993**, *211*, 763-770.

(6) Jiang, J. Q.; Biggins, J. B.; Thorson, J. S. *J. Am. Chem. Soc*. **2000**, *122*, 6803-6804.

(7) Jiang, J. Q.; Biggins, J. B.; Thorson, J. S. *Angew. Chem. Int. Ed. Engl.* **2001**, *40*, 1502-1505.

(8) Jiang, J.; Albermann, C.; Thorson, J. S. *ChemBioChem* **2003**, *4*, 443-446.

(9) Barton, W. A.; Biggins, J. B.; Jiang, J.; Thorson, J. S.; Nikolov, D. B. *Proc. Nat. Acad. Sci. U. S. A.* **2002**, *99*, 13397-13402.

(10) Lindquist, L.; Kaiser, R.; Reeves, P. R.; Lindberg, A. A. *Eur. J. Biochem.* **1993**, *211*, 763-770.

(11) Beaton, S. A.; Huestis, M. P.; Sadeghi-Khomami, A.; Thomas, N. R.; Jakeman, D. L. *Chem. Commun*. **2009**, 238-240.

(12) Fu, X.; Albermann, C.; Jiang, J.; Liao, J.; Zhang, C.; Thorson, J. S. *Nat. Biotechnol*. **2003**, *21*, 1467-1469.

(13) Kornfeld, S.; Glaser, L. *J. Biol. Chem*. **1961**, *236*, 1791-1794.

(14) Bulik, D. A.; van Ophem, P.; Manning, J. M.; Shen, Z.; Newburg, D. S.; Jarroll, E. L. *J. Biol. Chem*. **2000**, *275*, 14722-14728.

(15) Melo, A.; Glaser, L. *J. Biol. Chem.* **1965***, 240*, 398-405.

(16) Alphey, M. S.; Pirrie, L.; Torrie, L. S.; Boulkeroua, W. A.; Gardiner, M.; Sarkar, A.; Maringer, M.; Oehlmann, W.; Brenk, R.; Scherman, M. S.; McNeil, M.; Rejzek, M.; Field, R. A.; Singh, M.; Gray, D.; Westwood, N. J.; Naismith, J. H. *ACS Chem. Biol.* **2013***, 8*, 387-396.

(17) Rudd, P. M.; Elliott, T.; Cresswell, P.; Wilson, I. A.; Dwek, R. A. *Science* **2001**, *291*, 2370-2376.

(18) Dong, C.; Beis, K.; Giraud, M. F.; Blankenfeldt, W.; Allard, S.; Major, L. L.; Kerr, I. D.; Whiefield, C.; Naismith, J. H. *Biochem. Soc. Trans*. **2003**, *31*, 532-536.

(19) Tenover, F. C. *Am. J. Med.* **2006**, *119*, S3-S10.

(20) Smith, A. M.; Klugman, K. P. *Antimicrob. Agents. Chemother.* **1998***, 42*, 1329-1333.

(21) Grebe, T.; Hakenback, R.. *Antimicrob. Agents. Chemother.* **1996***, 40*, 829-834.

(22) Smith, A. M.; Klugman, K. P. *Antimicrob. Agents. Chemother.* **1995***, 39*, 859-867.

(23) Markiewicz, Z.; Tomasz, A. *J. Clin. Microbiol.* **1989***, 27*, 405-410.

(24) Glaser, L.; Kornfeld, S. *J. Biol. Chem*. **1961**, *236*, 1795-1799.

(25) Sheu, K. F. R.; Richard, J. P.; Frey, P. A. *Biochem*. **1979**, *18*, 5548-5556.

(26) Glaser, L. *Physiol. Rev.* **1963**, *43*, 215-242.

(27) Gerratana, B.; Cleland, W. W.; Frey, P. A. *Biochem*. **2001**, *40*, 9187-9195.

(28) Yamashita, Y.; Tomihisa, K.; Nakano, Y.; Shimazaki, Y.; Oho, T.; Koga, T. *Infect. Immun.* **1999**, *67*, 3693-3697.

(29) Rahim, R.; Burrows, L. L.; Monteiro, M. A.; Perry, M. B.; Lam, J. S.; *Microbiology* **2000**, *146*, 2803-2814.

(30) Engel, R. *Chem. Rev.* **1976**, *77*, 349-367.

(31) Romanenko, V. D.; Kukhar, V. P. *Chem. Rev*. **2006**, *106*, 3868-3935.

(32) Blackburn, G. M. *Chem. Ind.* **1981**, 134-138.

(33) Chang, W.; Dey, M.; Liu, P.; Mansoorabadi, S. O.; Moon, S.; Zhao, Z. K.; Drennan, C. L.; Liu, H. *Nature.* **2013***, 496*, 114-118.

(34) Cload, P. A.; Hutchinson, D. W. *Nucleic Acids Res*. **1983**, *11*, 5621-5628.

(35) Fonong, T.; Burton, D. J.; Pietrzyk, D. *J. Anal. Chem.* **1983**, *55*, 1794.

(36) Chen, W.; Flavin, M. T.; Filler, R.; Xu, Z. Q. *J. Chem. Soc*., *Perkin Trans*. *1* **1998**, 3979-3988.

(37) Hutchinson, D. W. *Antiviral Res*. **1985**, *5*, 193-205.

(38) Wnuk, S. F.; Robins, M. J. *J. Am. Chem. Soc.* **1996***, 118*, 2519-2520.

(39) Nieschalk, J.; Batsanov, A. S.; OHagan, D.; Howard, J. A. K. *Tetrahedron* **1996***, 52*, 165-176.

(40) Crofts, P. C.; Kosolapoff, G. M. *J. Am. Chem. Soc*. **1953**, *75*, 3379.

(41) Forget, S. M.; Bhattasali, D.; Hart, V. C.; Cameron, T. S.; Syvitski, R. T.; Jakeman, D. L.. *Chem. Sci.* **2012***, 3*, 1866-1878.

(42) Blackburn, G. M.; Kent, D. E.; Kolkmann, F. J. *Chem. Soc*., *Perkin Trans*. *1* **1984**, 1119-1125.

(43) Chambers, R. D.; O'Hagan, D.; Lamont, R. B.; Jain, S. C. *Chem. Commun.* **1990**, 1053-1054.

(44) Nieschalk, J.; O'Hagan, D. *Chem. Commun.* **1995**, *7*, 719-720.

(45) Pradère, U.; Clavier, H.; Roy, V.; Nolan, S. P.; Agrofoglio, L. A. *Eur. J. Org. Chem*. **2011**, 7324-7330.

(46) Farquhar, D.; Khan, S.; Srivastva, D. N.; Saunders, P. P. *J. Med. Chem.* **1994**, *37*, 3902-3909.

(47) Larsen, M.; Willett, R.; Yount R. G. *Science* **1969**, *166*, 1510-1511.

(48) Kraut, J. *Acta Crystallogr.* **1961**, *14*, 1146-1152.

(49) Ferrier, W. G.; Lindsay, A. R.; Young, D. W. *Acta Crystallogr*. **1962**, *15*, 616.

(50) Abrahamsson, S.; Pascher, I. *Acta Crystallogr.* **1966**, *21*, 79-81.

(51) Viswamitra, M. A.; Swaminatha Reddy, B.; Hung-Yin Lin, G.; Sundaralingam, M. *J. Am. Chem. Soc*. **1971**, *93*, 4565-4573.

(52) Kraut, J.; Jensen, L. H. *Acta Crystallogr*. **1963**, *16*, 79.

(53) Cooperman, B.S.; Chin, N. Y. *Biochemistry* **1973**, *12*, 1670-1676.

(54) Cooperman, B. S.; Mark, D. H. *Biochim. Biophys. Acta* **1971**, *252*, 221-234.

(55) Vincent, S.; Grenier, S.; Valleix, A.; Salesse, C.; Lebeau, L.; Mioskowski, C. *J. Org. Chem*. **1998**, *63*, 7244-7257.

(56) Myers, T. C.; Nakamura, K.; Danielzadeh, A. B. *J. Org. Chem*. **1965**, *30*, 1517-1520.

(57) Lesiak, K.; Watanabe, K. A.; George, J.; Pankiewicz, K. W. *J. Org. Chem*. **1998**, *63*, 1906-1909.

(58) Stock, J. A. *J. Org. Chem*. **1979**, *44*, 3997-4000.

(59) Dixit, V. M.; Poulter, C. D. *Tetrahedron Lett*. **1984**, *25*, 4055-4058.

(60) Davisson, V. J.; Davis, D. R.; Dixit, V. M.; Poulter, C. D. *J. Org. Chem*. **1987**, *52*, 1794-1801.

(61) Shipitsyn, A. V.; Tarussova, N. B.; Shirokova, E. A.; Krayevsky, A. A. *Nucleosides, Nucleotides Nucleic Acids* **2000**, *19*, 881-889.

(62) Stepinski, D. C.; Nelson, D. W.; Zalupski, P. R.; Herlinger, A. W. *Tetrahedron* **2001**, *57*, 8637-8645.

(63) Yoshikawa, M.; Kato, T.; Takenishi, T. *Tetrahedron Lett*. **1967**, *50*, 5065-5068.

(64) Kalek, M.; Jemielity, J.; Stepinski, J.; Stolarski, R.; Darzynkiewicz, E. *Tetrahedron Lett*. **2005**, *46*, 2417-2421.

(65) Griffin, B. S.; Burger, A. *J. Am. Chem. Soc.* **1956**, *78*, 2336-2338.

(66) Parikh, J. R.; Wolff, M. E.; Burger, A. *J. Am. Chem. Soc*. **1957**, *79*, 2778-2781.

(67) Whistler, R. L.; Wang, C. C. *J. Org. Chem*. **1968**, *33*, 4455-4458.

(68) Krahl, M. E.; Cori, C. F. *Biochem. Prep*. **1949**, *1*, 33-44.

(69) Posternak, T. *J. Biol. Chem*. **1949**, *180*, 1269-1278.

(70) Casero, F.; Cipolla, L.; Lay, L.; Nicotra, F.; Panza, L.; Russo, G. *J. Org. Chem*. **1996**, *61*, 3428-3432.

(71) Vaghefi, M. M.; Bernacki, R. J.; Hennen, W. J.; Robins, R. K. *J. Med. Chem*. **1987**, *30*, 1391-1399.

(72) Eckstein, F. *J. Amer. Chem. Soc.* **1970**, *92*, 4718-4723.

(73) Goody, R. S.; Eckstein, F. *J. Amer. Chem. Soc.* **1971**, *93*, 6252-6257.

(74) Pale, P.; Whitesides, G. M. *J. Org. Chem.* **1991**, *56*, 4547-4549.

(75) Fujita, S.; Oka, N.; Matsumura, F.; Wada, T. *J. Org. Chem*. **2011**, *76*, 2648–2659.

(76) Baxter, N. J.; Olguin, L. F.; Golicnik, M.; Feng, G.; Hounslow, A. M.; Bermel, W.; Blackburn, G. M.; Hollfelder, F.; Waltho, J. P.; Williams, N. H. *Proc. Natl. Acad. Sci.* **2006***, 103*, 14732-14737.

(77) Nakai, H.; Kitaoka, M.; Svensson, B.; Ohtsubo, K. *Curr. Opin. Chem. Biol.* **2013**, *17* 301-309.

(78) Xu, Y.; Jiang, G.; Tsukahara, R.; Fujiwara, Y.; Tigyi, G.; Prestwich, G. D. *J. Med. Chem*. **2006**, *49*, 5309-5315.

(79) Cai, L.; Ban, L.; Guan, W.; Mrksich, M.; Wang, P. G. *Carbohydr. Res*. **2011**, *346*, 1576-1580.

(80) Zhang, G.; Yu, B.; Deng, S.; Hui, Y. *J. Carbohydr. Chem*. **1998**, *17*, 547-556.

(81) Hall, C. R.; Inch, T. D.; Pottage, C.; Williams, N. E.; Campbell, M. M.; Kerr, P. F. *J. Chem. Soc*., *Perkin Trans*. *1* **1983**, 1967-1975.

(82) Piekutowska, M.; Pakulski, Z. *Carbohydr. Res*. **2008**, *343*, 785-792.

(83) Levander F.; Andersson, U.; Radstrom, P. *Appl. Environ. Microbiol.* **2001**, *67*, 4546-4553.

(84) Sjoberg, A.; Hahn-Hagerdal, B. *Appl. Environ. Microbiol.* **1989**, *55*, 1549–1554.

(85) Qu, H.; Xin, Y.; Dong, X.; Ma, Y. *FEMS Microbiol. Lett.* **2007**, *275*, 237-243.

(86) Abdel-Rahman, A. A. H.; Jonke, S.; El Ashry, E. S. H.; Schmidt, R. R. *Angew. Chem. Int. Ed.* **2002***, 41*, 2972-2974.

(87) Norris, A.J.; Toyokuni, T. *J. Carbohydr. Chem*. **1999**, *18*, 1097-1105.

(88) Albright, J. D.; Goldman, L. *J. Am. Chem. Soc.* **1967***, 89*, 2416-2423.

(89) Meyer, O.; Grosdemange-Billiard, C.; Tritsch, D.; Rohmer, M. *Org. Biomol. Chem.* **2003***, 1*, 4367-4372.

(90) Nyffeler, P. T.; Duron, S. G.; Burkart, M. D.; Vincent, S. P.; Wong, C. H. *Angew. Chem. Int. Ed. Engl.* **2005***, 44*, 192-212.

(91) Kim, J. H.; Resende, R.; Wennekes, T.; Chen, H. M.; Bance, N.; Buchini, S.; Watts, A. G.; Pilling, P.; Streltsov, V. A.; Petric, M.; Liggins, R.; Barrett, S.; Mckimm-Breschkin, J. L.; Niikura, M.; Withers, S. G. *Science*, **2013**, *340*,71-75.

(92) Li, Y.; Drew, M. G. B.; Welchman, E. V.; Shirvastava, R. K.; Jiang, S.; Valentine, R.; Singha, G. *Tetrahedron* **2004***, 60*, 6523-6531.

(93) Timmons, S. C.; Mosher, R. H.; Knowles, S. A.; Jakeman, D. L. *Org. Lett*. **2007**, *9*, 857-860.

(94) Peng, J. W.; Moore, J.; Abdul-Manan, N. *Prog. Nucl. Magn. Reson. Spectrosc.* **2004***, 44*, 225-256.

(95) Skinner, A. L.; Laurence, J. S. *J. Pharm. Sci*. **2008**, *97*, 4670-4695.

(96) Blankenfeldt, W.; Asuncion, M.; Lam, J. S.; Naismith, J. H. *EMBO J.* **2000**, *19*, 6652-6663.

(97) Timmons, S. C.; Hui, J. P.; Pearson, J. L.; Peltier, P.; Daniellou, R.; Nugier-Chauvin, C.; Soo, E. C.; Syvitski, R. T.; Ferrieres, V.; Jakeman, D. L. *Org. Lett.* **2008***, 10*, 161-163.

(98) Cheng, Y. C.; Prusoff, W. H. *Biochem. Pharmacol.* **1973***, 22*, 3099-3108.

(99) Mohamady, S.; Desoky, A.; Taylor, S. D.; *Org. Lett*. **2012**, *14*, 402-405.

(100) Balg, C.; Blais, S. P.; Bernier, S.; Huot, J. L.; Couture, M.; Lapointe, J. Chenevert, R. *Bioorg. Med. Chem.* **2007**, *15*, 295-304.

(101) Clayden, J.; Yasin, S. A. *New J. Chem.* **2002**, *26*, 191-192

(102) Timmons, S. C.; Jakeman, D. L. *Org. Lett*. **2007**, *9*, 1227-1230.

(103) Schmidt, R. R.; Kinzy, W. *Adv. Carbohydr. Chem. Biochem*. **1994**, *50*, 21-123.

(104) Ibatullin, F. M.; Selivanov, S. I. *Tetrahedron Lett*. **2002**, *43*, 9577-9580.

(105) Huestis, M.; Aish, G.; Hui, J. P. M.; Soo, E. C.; Jakeman, D. L. *Org. Biomol. Chem*. **2008**, *6*, 477-484.

(106) Coppola, C.; Saggiomo, V.; Di Fabio, G.; De Napoli, L.; Montesarchio, D. *J. Org. Chem*. **2007**, *72*, 9679-9689.

(107) Heissigerova, H.; Kocalka, P.; Hlavackova, M.; Imberty, A.; Breton, C.; Chazalet, V.; Moravcova, J. *Collect. Czech. Chem. Commun*. **2006**, *71*, 1659-1672.

(108) McKenna, C. E.; Schmidhauser, J. *J. Chem. Soc., Chem. Commun.*, **1979**, 739.

(109) Elgibo-Gabas, M.; Canals, D.; Casas, J.; Llebaria, A.; Delgado, A. *ChemMedChem* **2007**, *2*, 992-994.

(110) Albers, P.; Pietsch, J.; Parker, S. F. *J. Mol. Catal. A: Chem.* **2001**, *173*, 275-286.

(111) Vassilakis, D.; Barbouth, N.; Oudar, J. *Catal. Lett.* **1990**, *5*, 321-330.

(112) Ali, A. M.; Hill, B.; Taylor, S. D. *J. Org. Chem.* **2009**, *74*, 3583-3586.

(113) Hwang, Y.; Cole, P. A. *Org. Lett*. **2004**, *6*, 1555-1556.

(114) Allard, S. T.; Giraud, M. F.; Whitfield, C.; Graninger, M.; Messner, P.; Naismith, J. H. *J. Mol. Biol.* **2001***, 307*, 283-295.

(115) Lewandowicz, A.; Schramm, V. L. *Biochemistry.* **2004***, 43*, 1458-1468.

(116) Hoque, M. E. U.; Dey, S.; Guha, A. K.; Kim, C. K.; Lee, B. S.; Lee, H. W. *J. Org. Chem.* **2007**, *72*, 5493-5499.

# APPENDICES

## APPENDIX A: Protein Sequence Alignments

**Protein Sequence Alignment for Cps2L [*Streptococcus pneumoniae*] and RmlA [*Pseudomonas aeruginosa*]**

| SeqA | Name | Len(aa) | SeqB | Name | Len(aa) | Score |
|---|---|---|---|---|---|---|
| 1 | Cps2L | 289 | 2 | RmlA | 293 | 68% |

```
Cps2L 2 KGIILAGGSGTRLYPLTRATSKQLMPVYDKPMIYYPLSTLMLAGIKDILIISTPQDLPRF 61
    KGIILAGGSGTRL+P T A SKQL+PVYDKPMIYYPLSTLMLAGI++ILIISTPQD PRF
RmlA 4 KGIILAGGSGTRLHPATLAISKQLLPVYDKPMIYYPLSTLMLAGIREILIISTPQDTPRF 63

Cps2L 62 KDLLLDGSEFGIRLSYAEQPSPDGLAQAFLIGEDFIGDDSVALILGDNIYHGPGLSKMLQ 121
     + LL DGS +G+ L YA QPSPDGLAQAFLIGE FIG+D AL+LGDN+Y+G  ++L
RmlA 64 QQLLGDGSNWGLDLQYAVQPSPDGLAQAFLIGESFIGNDLSALVLGDNLYYGHDFHELLG 123

Cps2L 122 KTVSKEKGATVFGYQVKDPERFGVVEFDENMNAISIEEKPECPRSNYAVTGLYFYDNDVV 181
       ++ GA+VF Y V DPER+GVVEFD+  AIS+EEKP P+SNYAVTGLYFYD VV
RmlA 124 SASQRQTGASVFAYHVLDPERYGVVEFDQGGKAISLEEKPLEPKSNYAVTGLYFYDQQVV 183

Cps2L 182 EIAKSIKPSARGELEITDVNKAYLDRGNLSVEVMGRGFAWLDTGTHESLLEASQYIETVQ 241
     +IA+ +KPS RGELEITDVN+AYL+RG LSVE+MGRG+AWLDTGTH+SLLEA Q+I T++
RmlA 184 DIARDLKPSPRGELEITDVNRAYLERGQLSVEIMGRGYAWLDTGTHDSLLEAGQFIATLE 243

Cps2L 242 RMQNVQVANLEEIAYRMGYISREDVLELAQPLKKNEYGQYLLRLIGEV 289
      Q ++VA EEIAYR +I  + +LA PL KN YGQYL RL+ E
RmlA 244 NRQGLKVACPEEIAYRQKWIDAAQLEKLAAPLAKNGYGQYLKRLLTET 291
```

*Relevant residues for the binding of compound **47** are highlighted

**Protein Sequence Alignment for Cps2L [*Streptococcus pneumoniae*] and $E_p$ [*Salmonella enterica*]**

| SeqA | Name | Len(aa) | SeqB | Name | Len(aa) | Score |
|---|---|---|---|---|---|---|
| 1 | Cps2L | 289 | 2 | $E_p$ | 292 | 67 % |

```
Cps2L 2   KGIILAGGSGTRLYPLTRATSKQLMPVYDKPMIYYPLSTLMLAGIKDILIISTPQDLPRF 61
          KGIILAGGSGTRLYP+T A S+QL+P+YDKPMIYYPLSTLMLAGI+DILIISTPQD PRF
Ep 1       KGIILAGGSGTRLYPVTMAVSQQLLPIYDKPMIYYPLSTLMLAGIRDILIISTPQDTPRF 64

Cps2L 62  KDLLLDGSEFGIRLSYAEQPSPDGLAQAFLIGEDFIGDDSVALILGDNIYHGPGLSKMLQ 121
          + LL DGS++G+ L Y QPSPDGLAQAF+IGE+FIG D AL+LGDNI++G L K+++
Ep 65      QQLLGDGSQWGLNLQYKVQPSPDGLAQAFIIGEEFIGHDDCALVLGDNIFYGHDLPKLME 124

Cps2L 122 KTVSKEKGATVFGYQVKDPERFGVVEFDENMNAISIEEKPECPRSNYAVTGLYFYDNDVV 181
           V+KE GATVF Y V DPER+GVVEFD+  A+S+EEKP P+SNYAVTGLYFYDN VV
Ep 125     AAVNKESGATVFAYHVNDPERYGVVEFDQKGTAVSLEEKPLQPKSNYAVTGLYFYDNSVV 184

Cps2L 182 EIAKSIKPSARGELEITDVNKAYLDRGNLSVEVMGRGFAWLDTGTHESLLEASQYIETVQ 241
          E+AK++KPSARGELEITD+N+ Y+++G LSV +MGRG+AWLDTGTH+SL+EAS +I T++
Ep 185     EMAKNLKPSARGELEITDINRIYMEQGRLSVAMMGRGYAWLDTGTHQSLIEASNFIATIE 244

Cps2L 242 RMQNVQVANLEEIAYRMGYISREDVLELAQPLKKNEYGQYLLRLI 286
           Q ++V+ EEIA+R +I+ + V+ELA PL KN+YG+YLL+++
Ep 245     ERQGLKVSCPEEIAFRKNFINAQQVIELAGPLSKNDYGKYLLKMV 289
```

**Protein Sequence Alignment for Cps2L [*Streptococcus pneumoniae*] and RmlA [*Streptococcus mutans*]**

| SeqA | Name | Len(aa) | SeqB | Name | Len(aa) | Score |
|---|---|---|---|---|---|---|
| 1 | Cps2L | 289 | 2 | RmlA | 289 | 89% |

```
Cps2L 1   MKGIILAGGSGTRLYPLTRATSKQLMPVYDKPMIYYPLSTLMLAGIKDILIISTPQDLPR 60
          MKGIILAGGSGTRLYPLTRA SKQLMPVYDKPMIYYPLSTLMLAGIKDILIISTPQDLPR
RmlA 1    MKGIILAGGSGTRLYPLTRAASKQLMPVYDKPMIYYPLSTLMLAGIKDILIISTPQDLPR 60

Cps2L 61  FKDLLLDGSEFGIRLSYAEQPSPDGLAQAFLIGEDFIGDDSVALILGDNIYHGPGLSKML 120
          FK+LL DGSEFGI+LSYAEQPSPDGLAQAF+IGE+FIGDD VALILGDNIY+GPGLS+ML
RmlA 61   FKELLQDGSEFGIKLSYAEQPSPDGLAQAFIIGEEFIGDDHVALILGDNIYYGPGLSRML 120

Cps2L 121 QKTVSKEKGATVFGYQVKDPERFGVVEFDENMNAISIEEKPECPRSNYAVTGLYFYDNDV 180
          QK SKE GATVFGYQVKDPERFGVVEFD + NAISIEEKPE P+S+YAVTGLYFYDN V
RmlA 121  QKAASKESGATVFGYQVKDPERFGVVEFDNDRNAISIEEKPEHPKSHYAVTGLYFYDNSV 180

Cps2L 181 VEIAKSIKPSARGELEITDVNKAYLDRGNLSVEVMGRGFAWLDTGTHESLLEASQYIETV 240
          V+IAK+IKPS RGELEITDVNKAYLDRG+LSVEVM RGFAWLDTGTHESLLEA+QYIETV
RmlA 181  VDIAKNIKPSPRGELEITDVNKAYLDRGDLSVEVMERGFAWLDTGTHESLLEAAQYIETV 240

Cps2L 241 QRMQNVQVANLEEIAYRMGYISREDVLELAQPLKKNEYGQYLLRLIGEV 289
          QRMQN+QVANLEEIAYRMGYI+ + V ELAQPLKKNEYGQYLLRLIGE
RmlA 241  QRMQNLQVANLEEIAYRMGYITADQVRELAQPLKKNEYGQYLLRLIGEA 289
```

APPENDIX B: Spectrophotometric Inhibition Assay Graphs and Kinetic Parameters for Cps2L

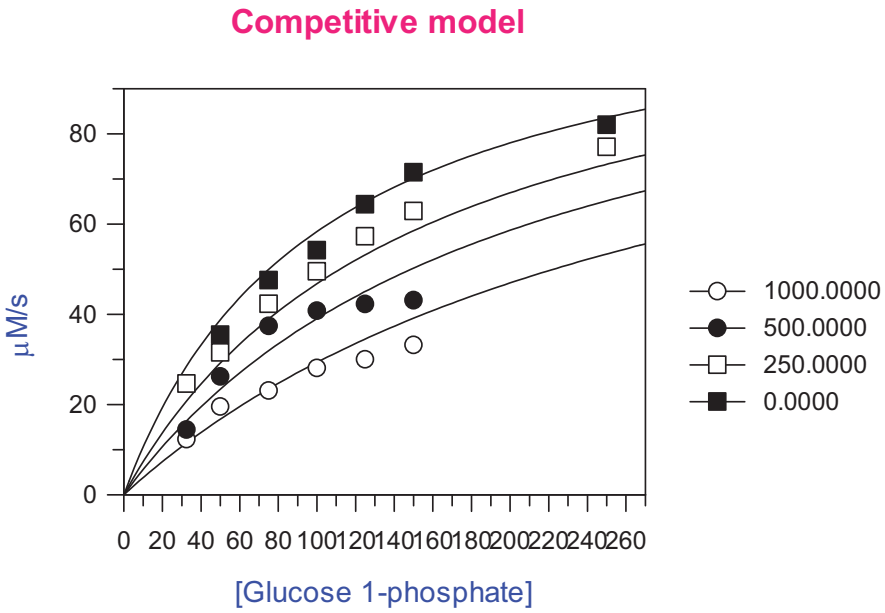


Reduced chi²: 296.8993

| Parameter | Value | Std. Error |
|---|---|---|
| Vmax | 117.5449 | 8.4744 |
| Km | 101.5437 | 16.8981 |
| Ki | 509.3911 | 79.5054 |

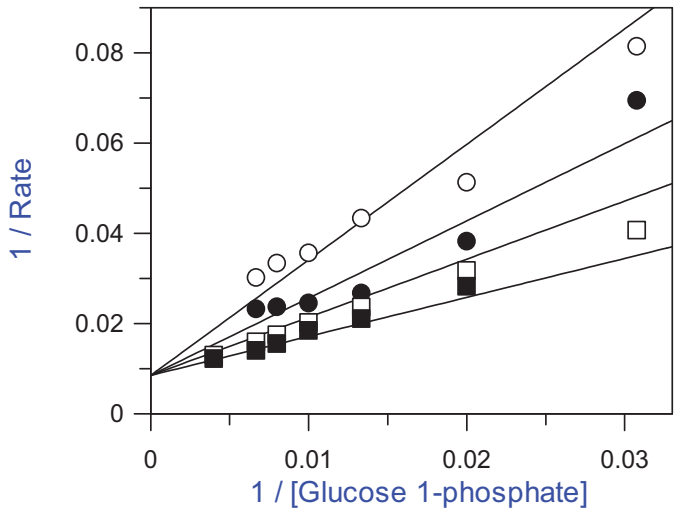


R1CP (**43**) Cps2L Inhibition assays with variable Glc-1-P (**1**)

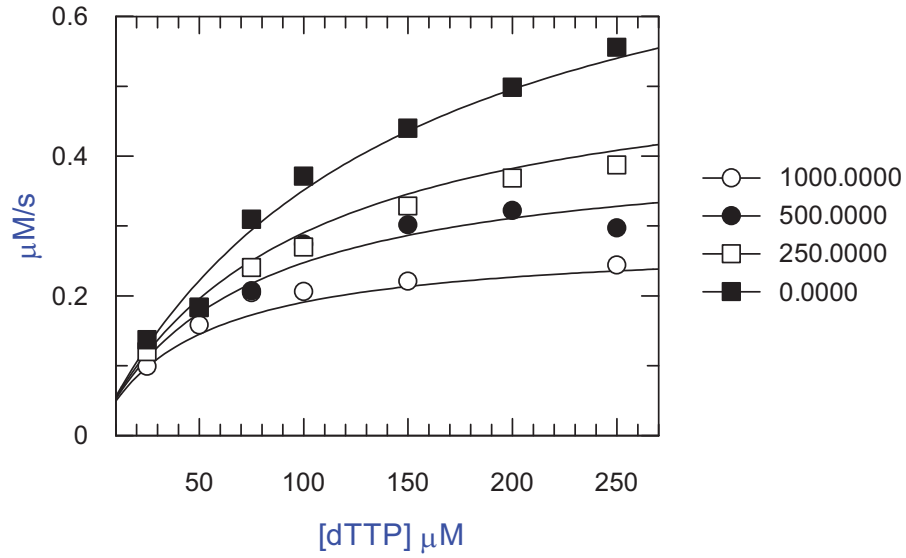


| Parameter | Value | Std. Error |
|---|---|---|
| Vmax | 0.8415 | 0.0504 |
| Km | 139.5217 | 16.3499 |
| Ki | 496.6392 | 47.6760 |

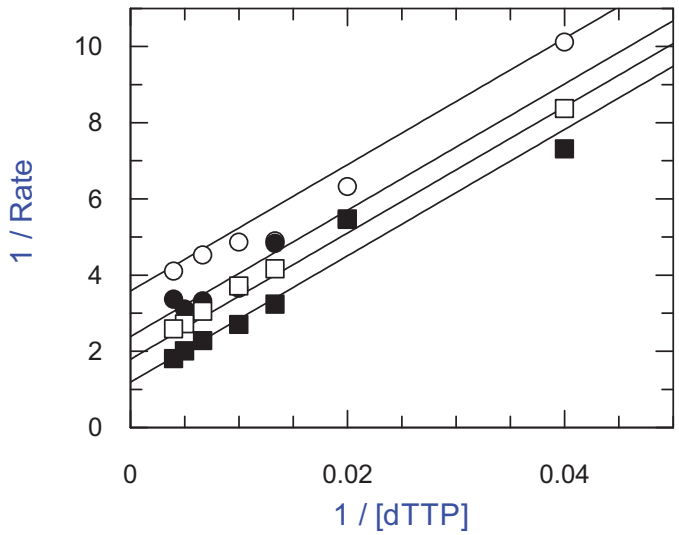


R1CP (**43**) Cps2L Inhibition assays with variable dTTP (**2**)

## APPENDIX C: Select NMR Spectra of Representative Compounds

Dibenzyl (tri-*O*-benzyl-1-deoxy-L-rhamno-heptulopyranosyl)phosphonate (**28b**)

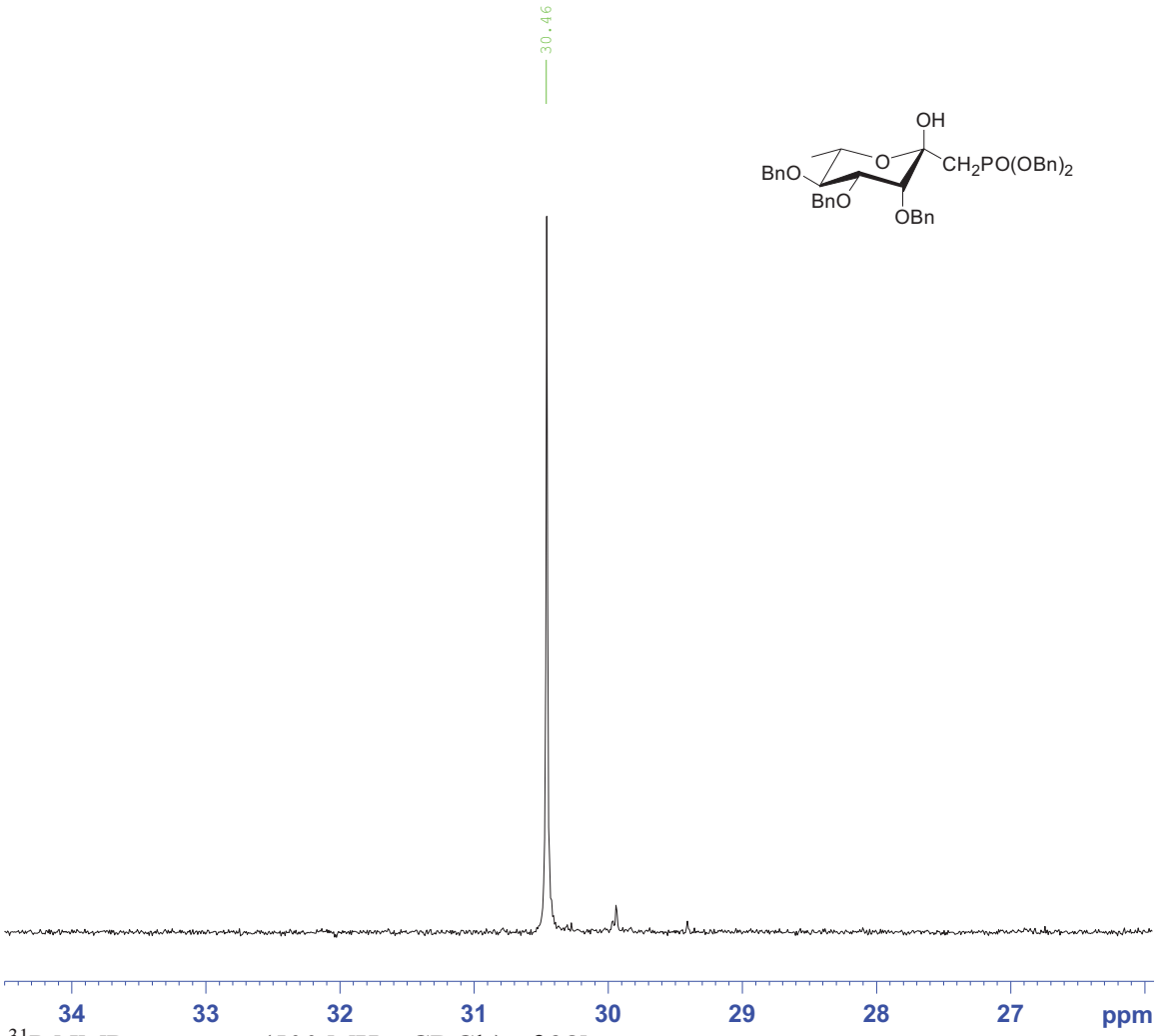


$^{31}$P NMR spectrum (500 MHz, $CDCl_3$) of **28b**.

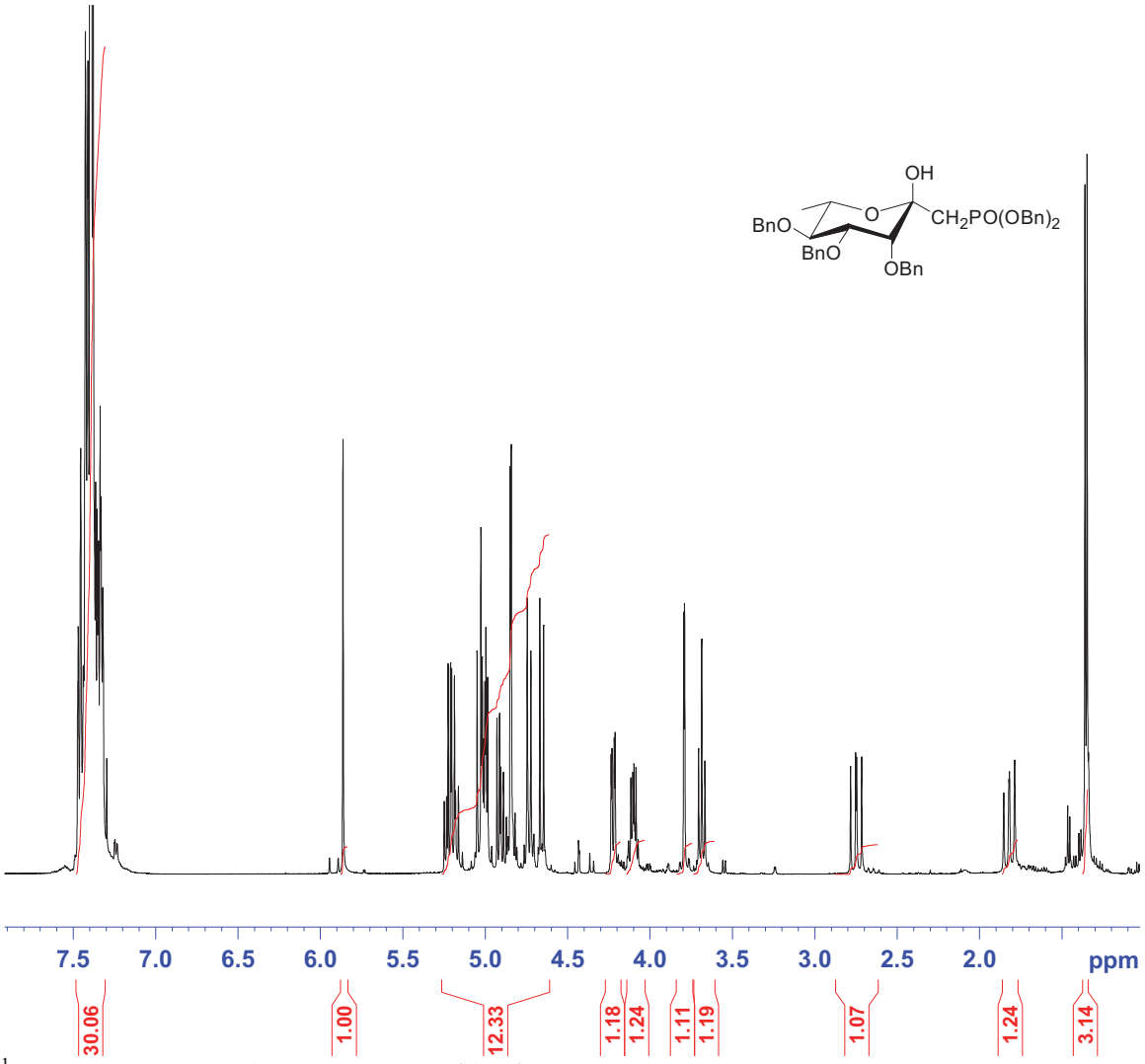


$^1$H NMR spectrum (500 MHz, $CDCl_3$) of **28b**.

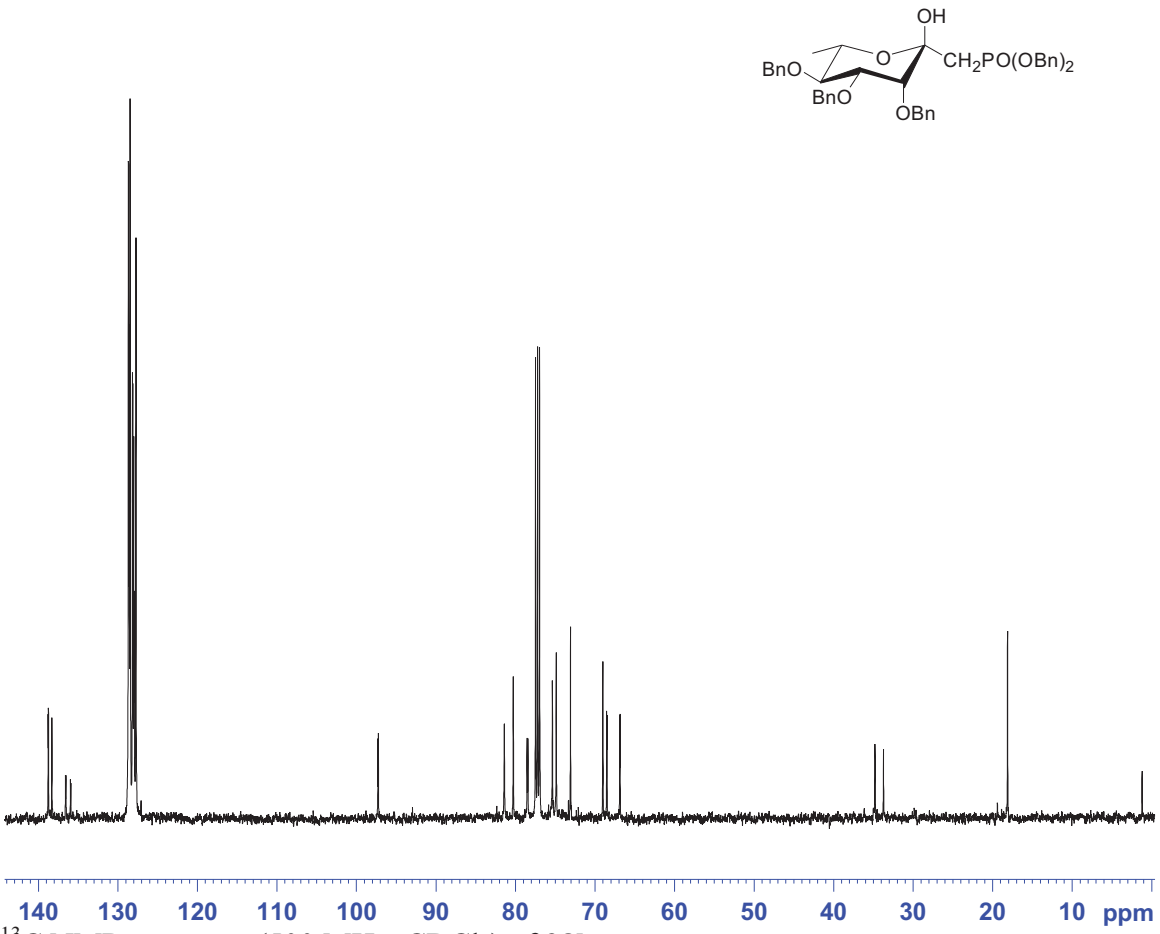

$^{13}$C NMR spectrum (500 MHz, $CDCl_3$) of **28b**.

Dibenzyl (2,6-Anhydro-tri-*O*-benzyl-1-deoxy-L-rhamno-hept-1-enopyranosyl)phosphonate (**30b**)

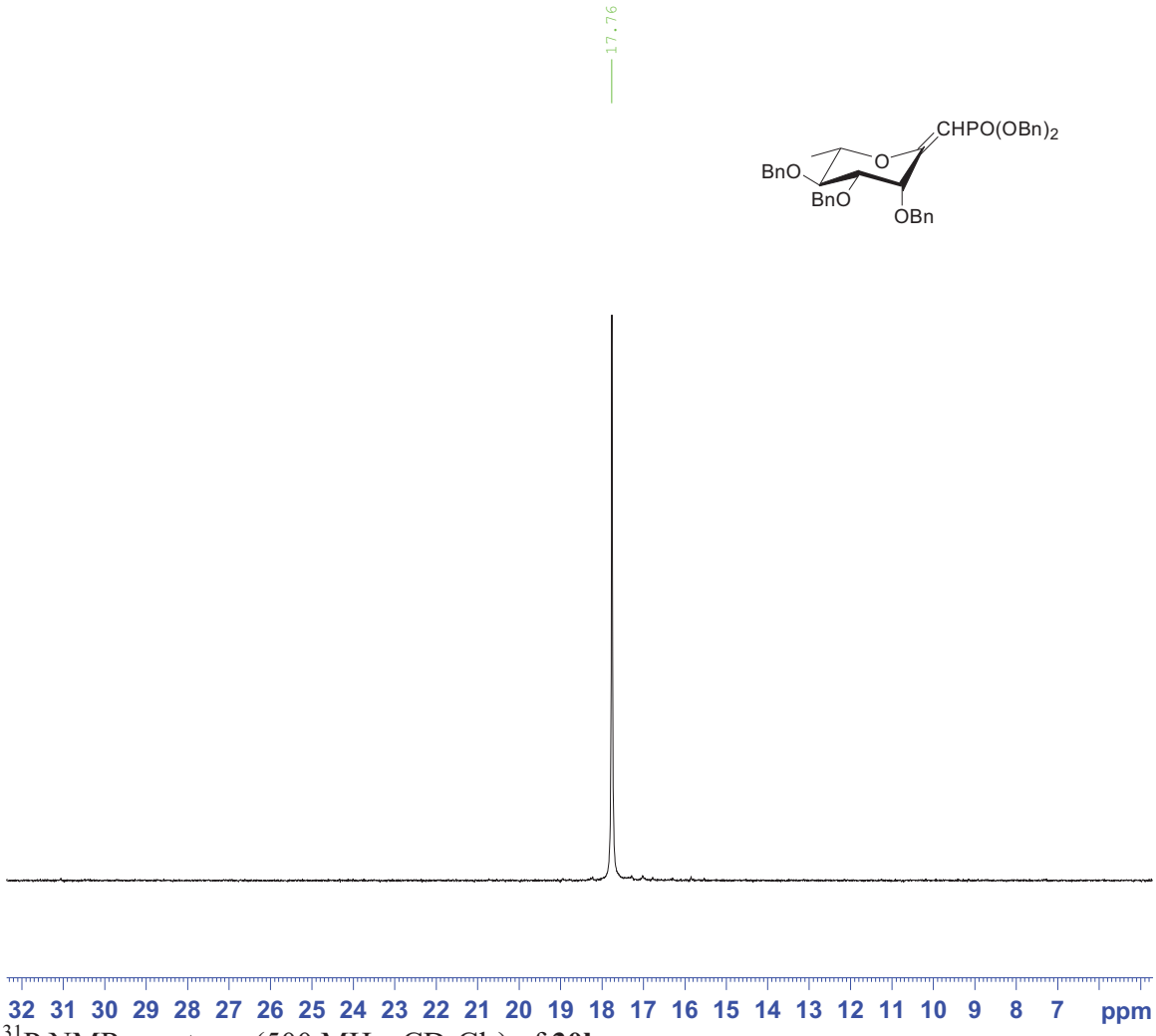


$^{31}$P NMR spectrum (500 MHz, $CD_2Cl_2$) of **30b**.

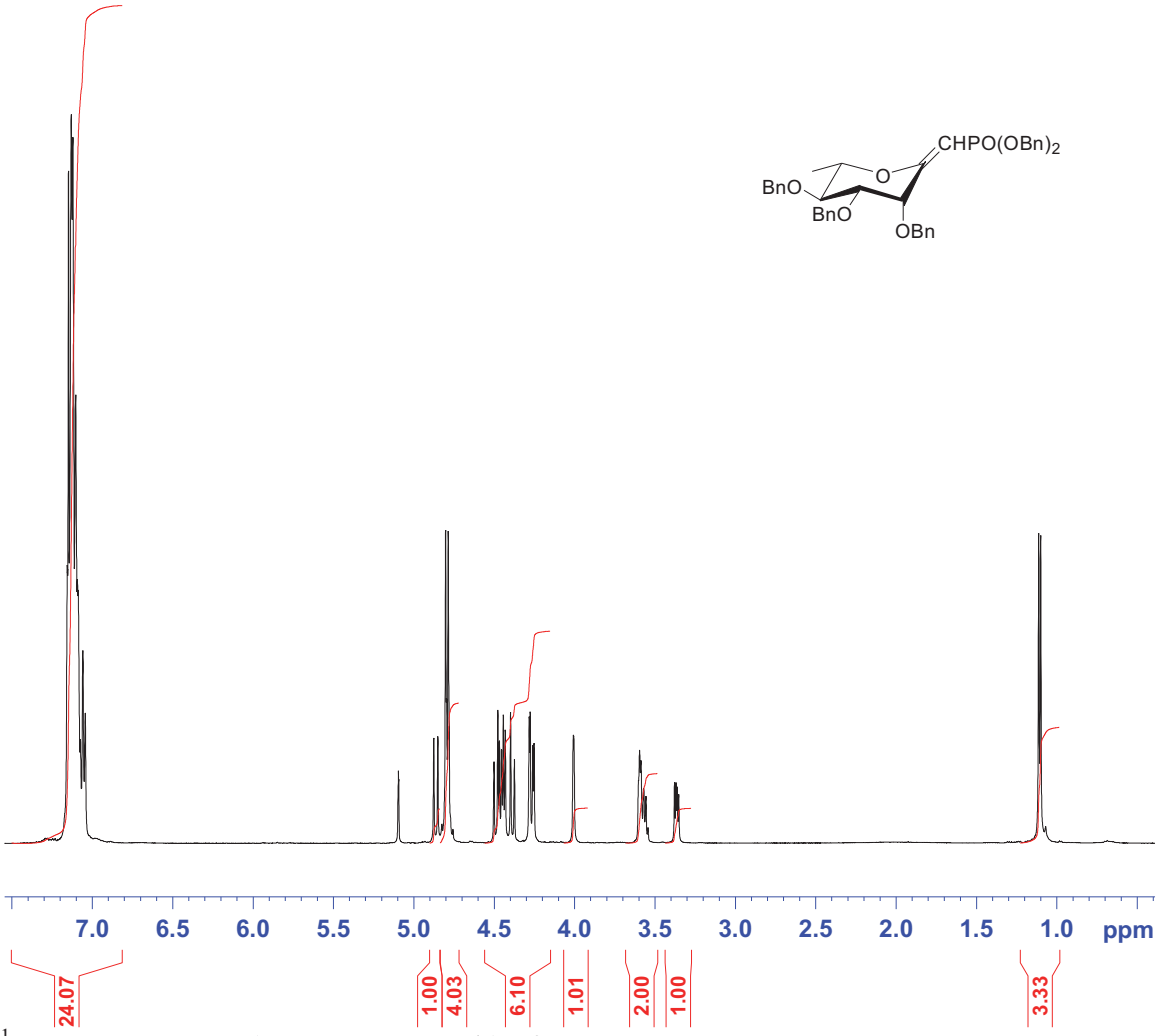


$^{1}$H NMR spectrum (500 MHz, $CD_2Cl_2$) of **30b**.

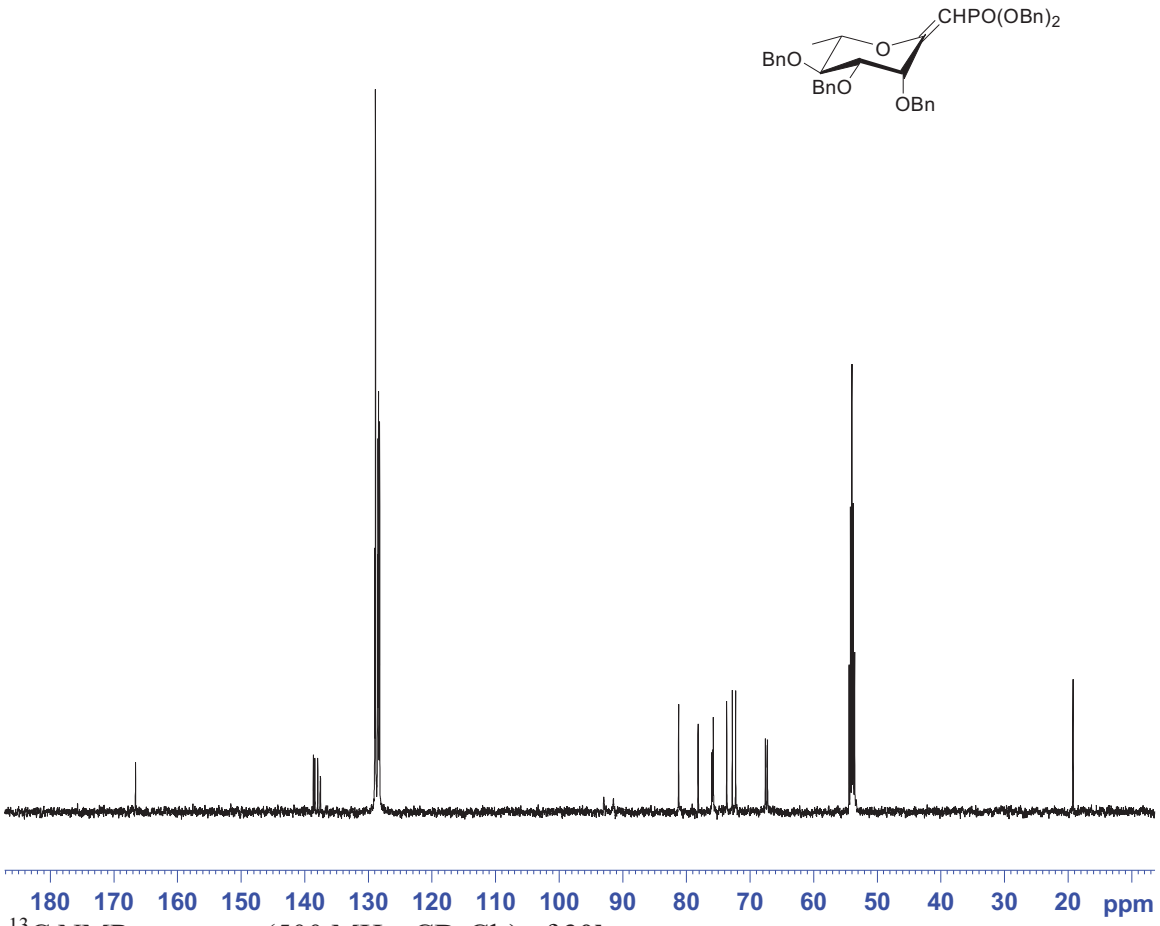


$^{13}C$ NMR spectrum (500 MHz, $CD_2Cl_2$) of **30b**.

Dibenzyl (tri-*O*-benzyl-1-deoxy-L-rhamno-heptulopyranosyl)-1-*R*-monofluorophosphonate (**32b**)

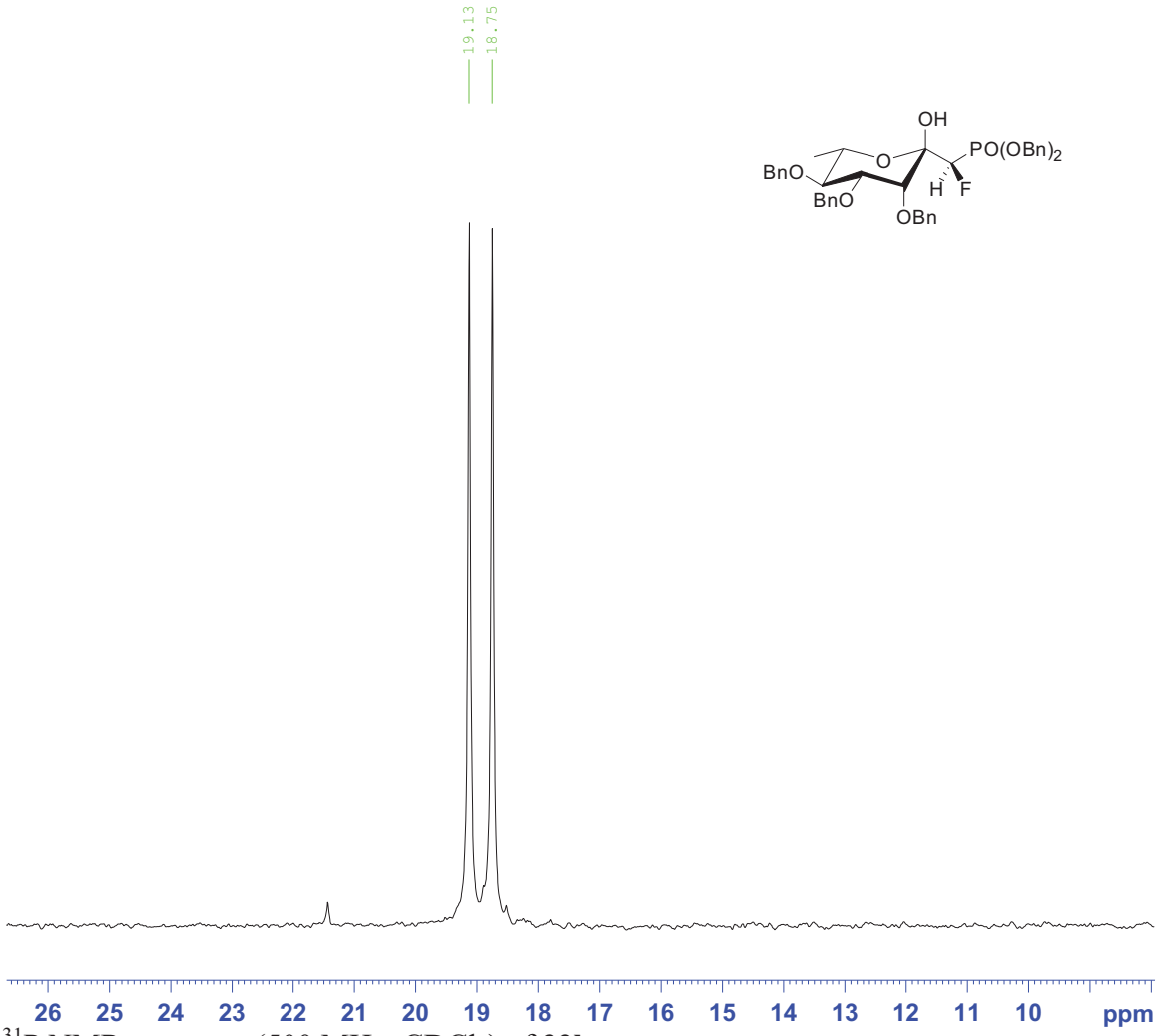


$^{31}$P NMR spectrum (500 MHz, $CDCl_3$) of **32b**.

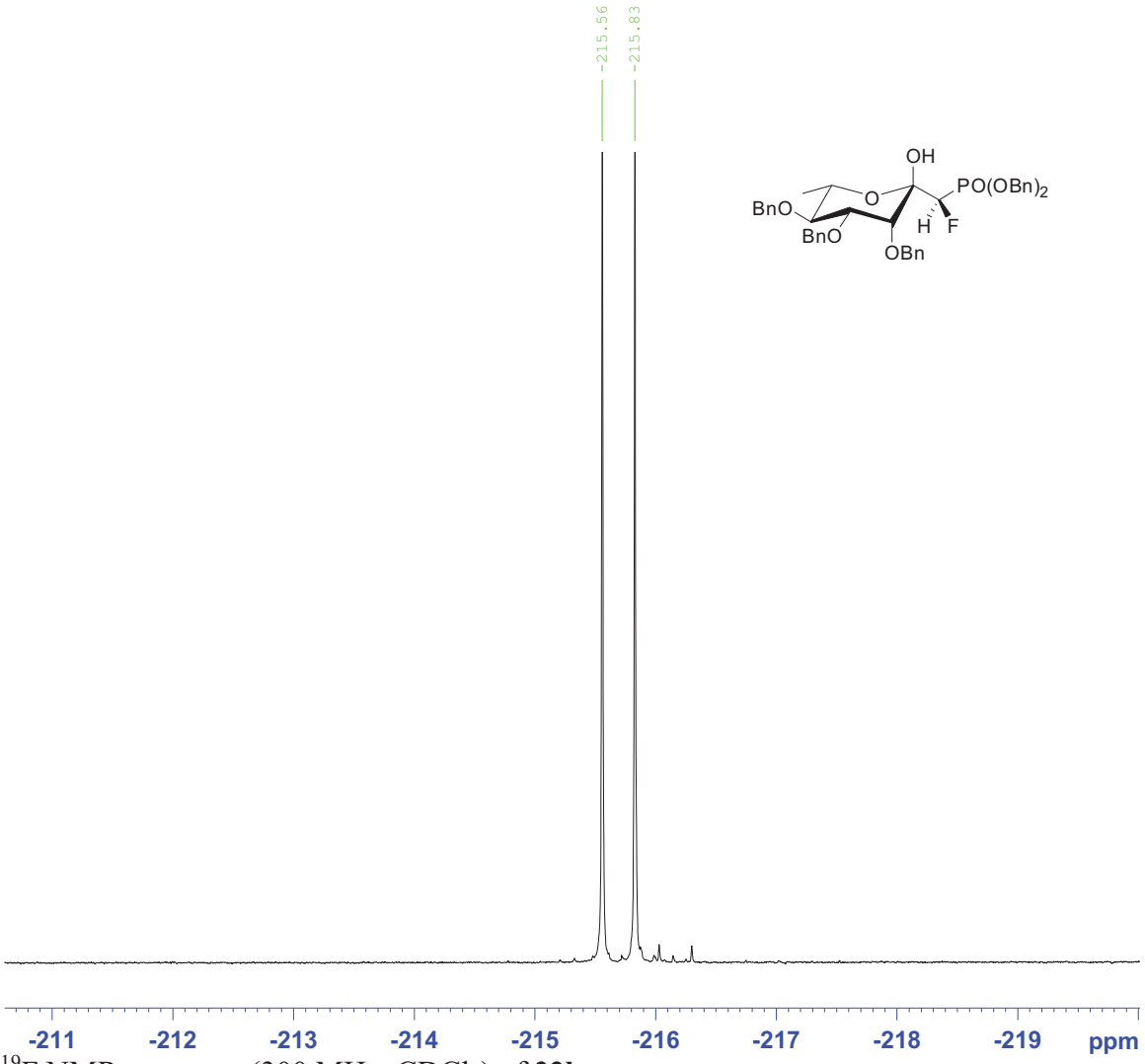


$^{19}F$ NMR spectrum (300 MHz, $CDCl_3$) of **32b**.

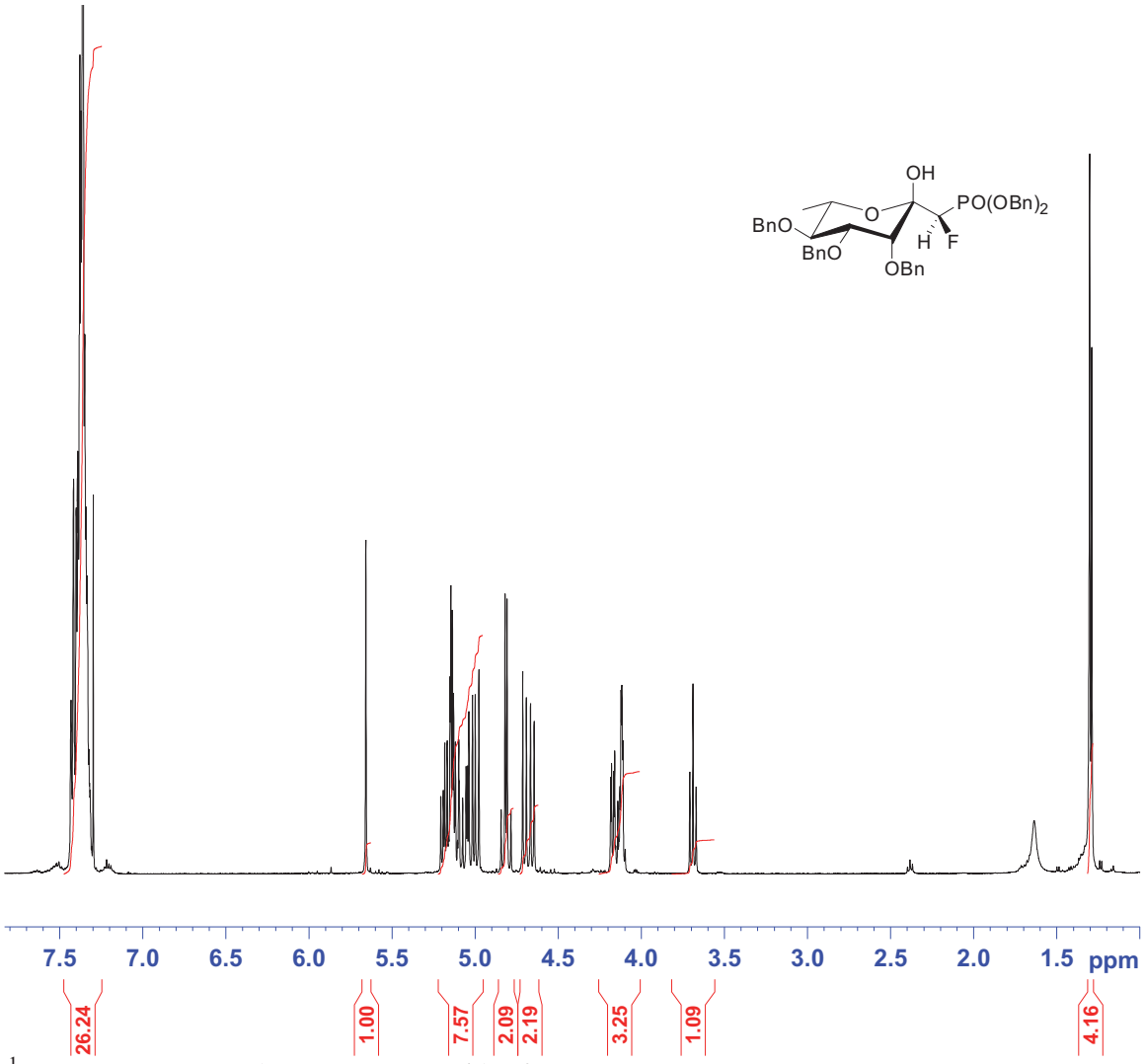


$^{1}$H NMR spectrum (500 MHz, $CDCl_3$) of **32b**.

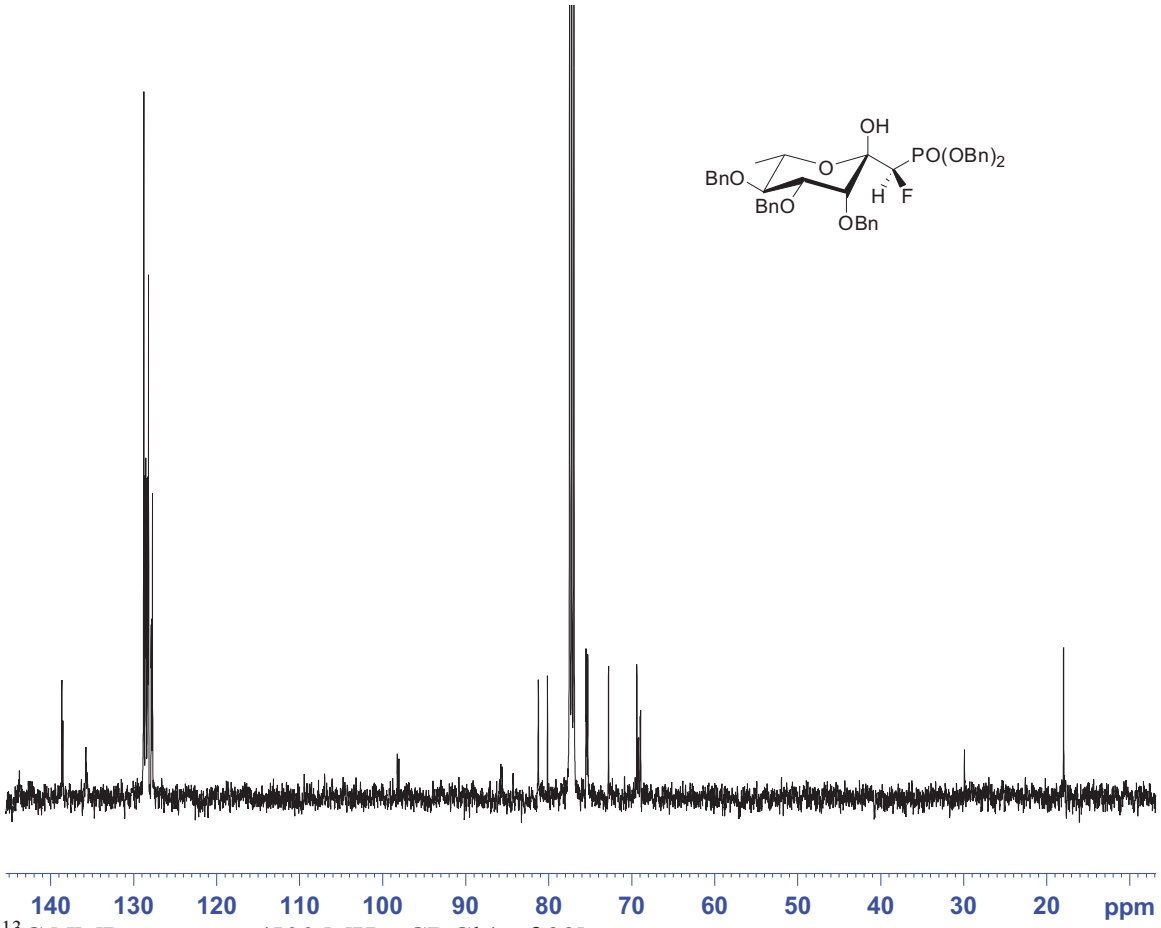

$^{13}$C NMR spectrum (500 MHz, $CDCl_3$) of **32b**.

Diethyl (tri-*O*-benzyl-1-deoxy-L-rhamno-heptulopyranosyl)-1-difluorophosphonate (**34**)

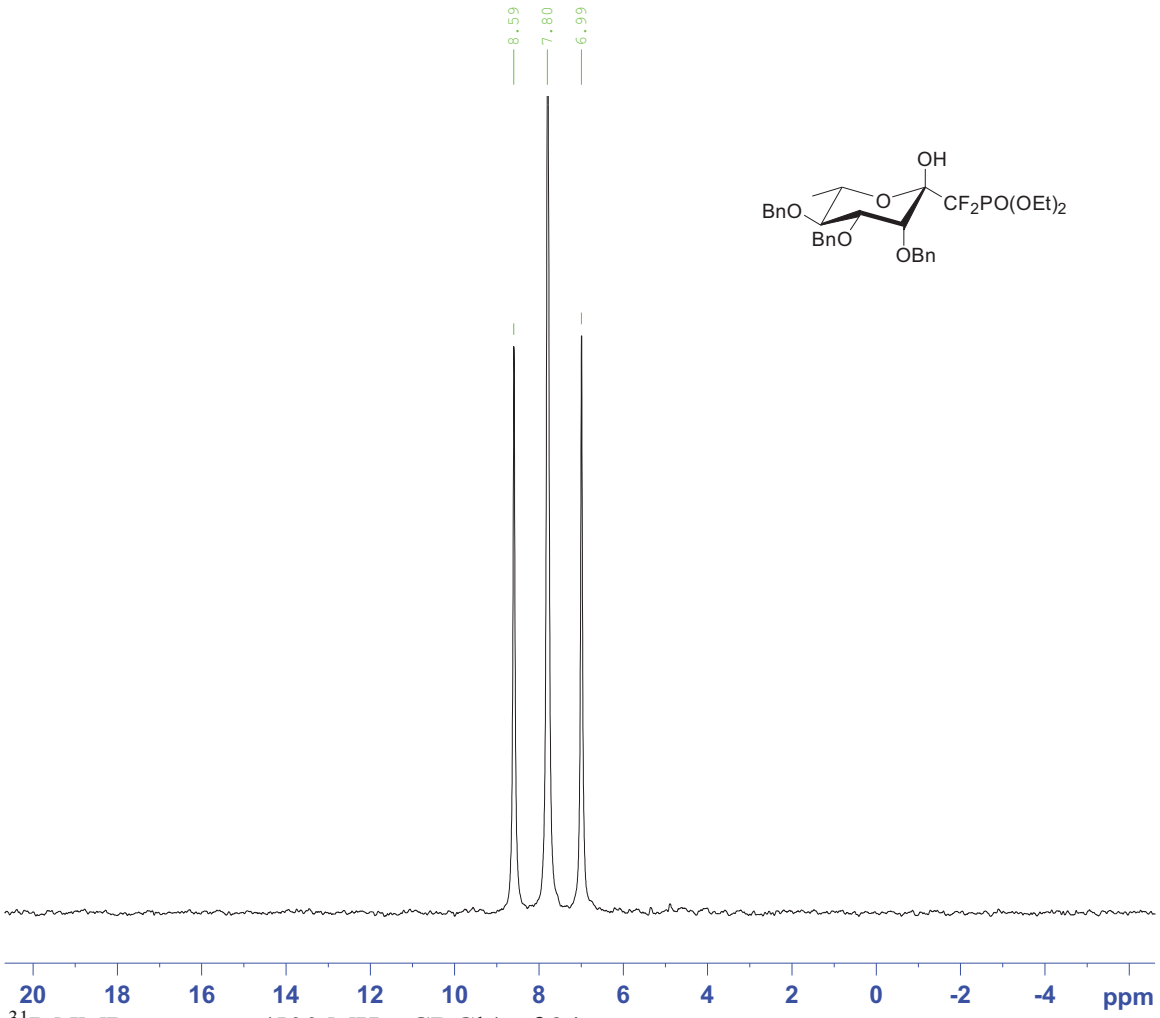


$^{31}$P NMR spectrum (500 MHz, $CDCl_3$) of **34**.

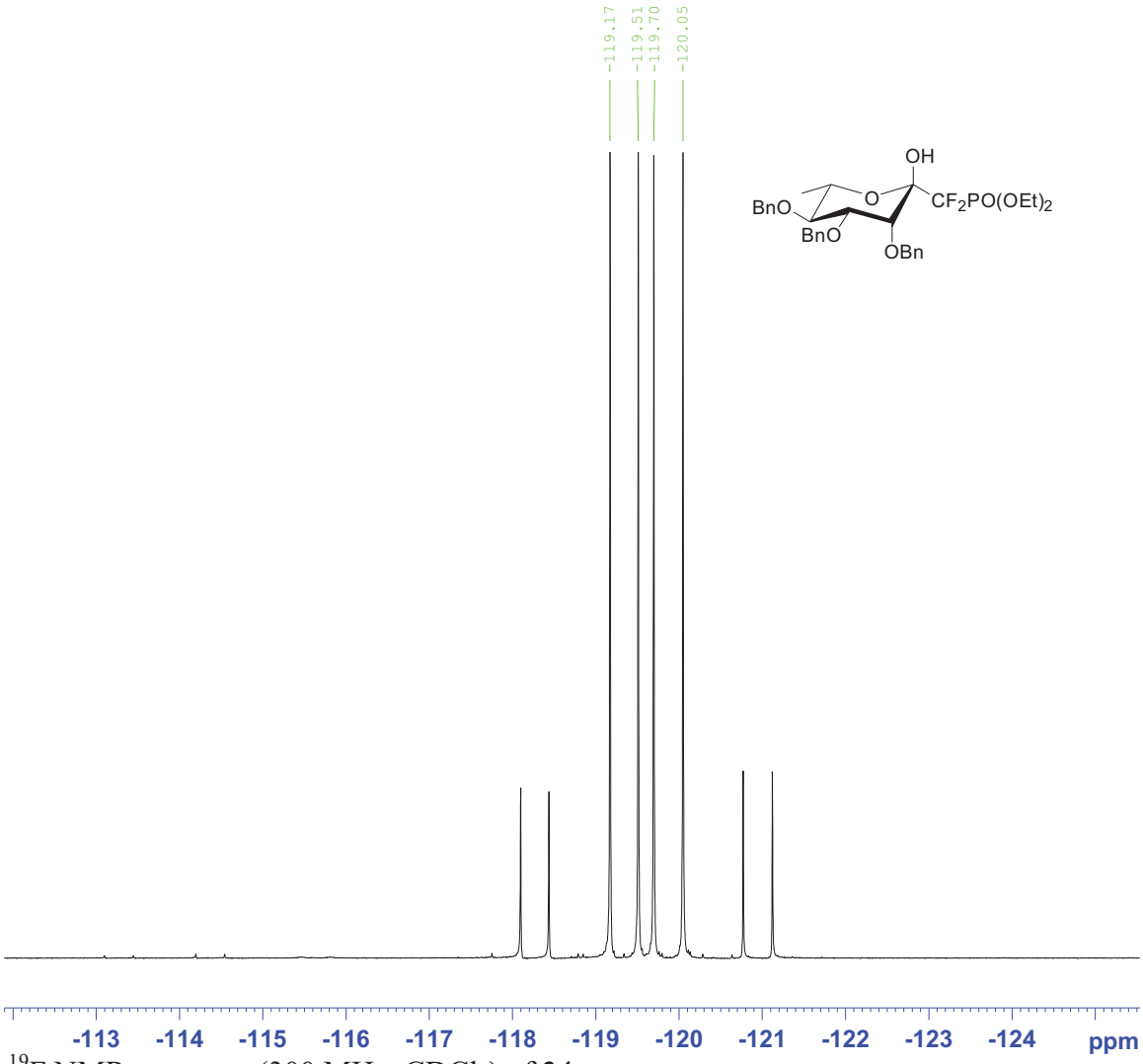


$^{19}F$ NMR spectrum (300 MHz, $CDCl_3$) of **34**.

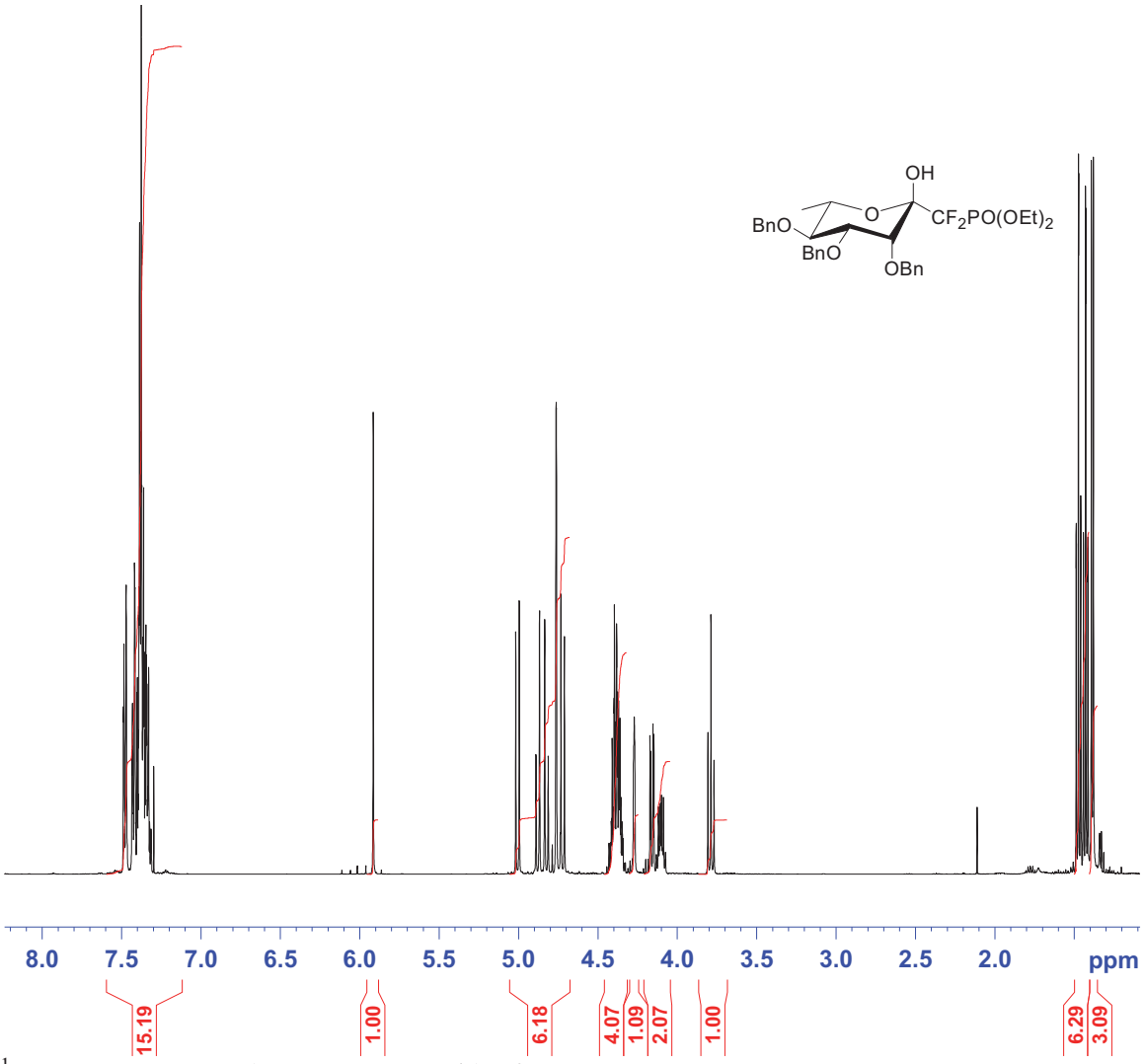


$^{1}$H NMR spectrum (500 MHz, $CDCl_3$) of **34**.

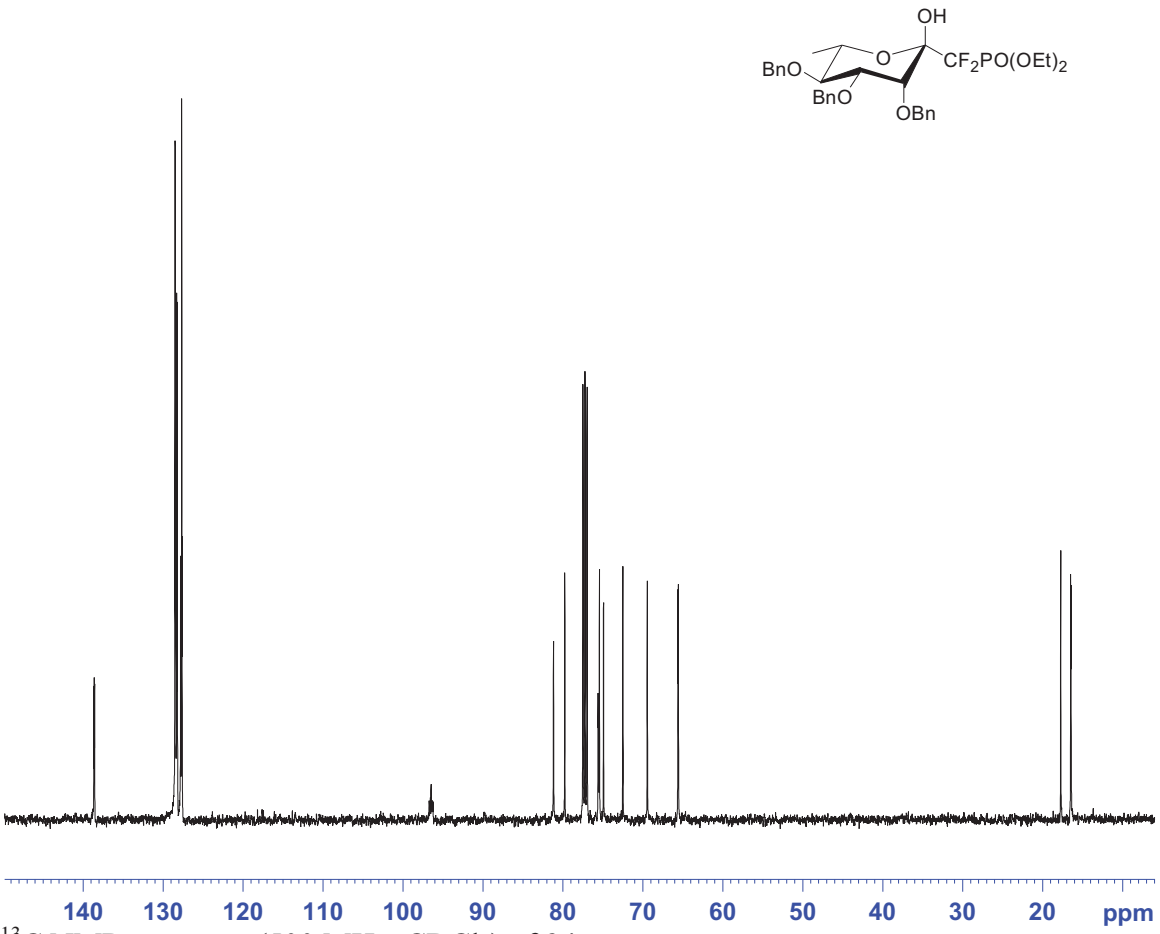


$^{13}C$ NMR spectrum (500 MHz, $CDCl_3$) of **34**.

Diethyl (tri-*O*-benzyl-2-deoxy-methyloxalyl-L-rhamno-heptulopyranosyl)-1-difluorophosphonate (**35**)

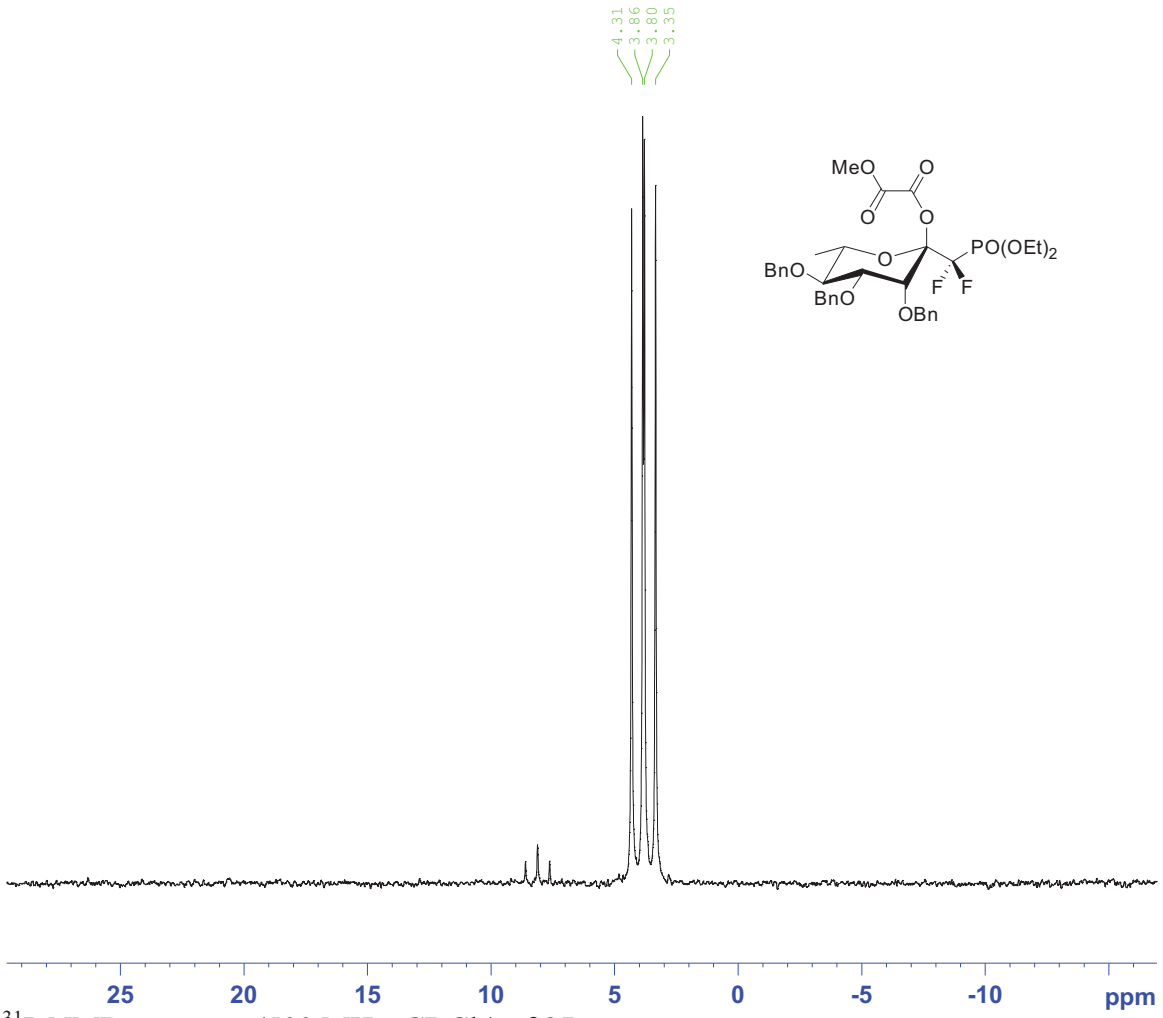


$^{31}$P NMR spectrum (500 MHz, $CDCl_3$) of **35**.

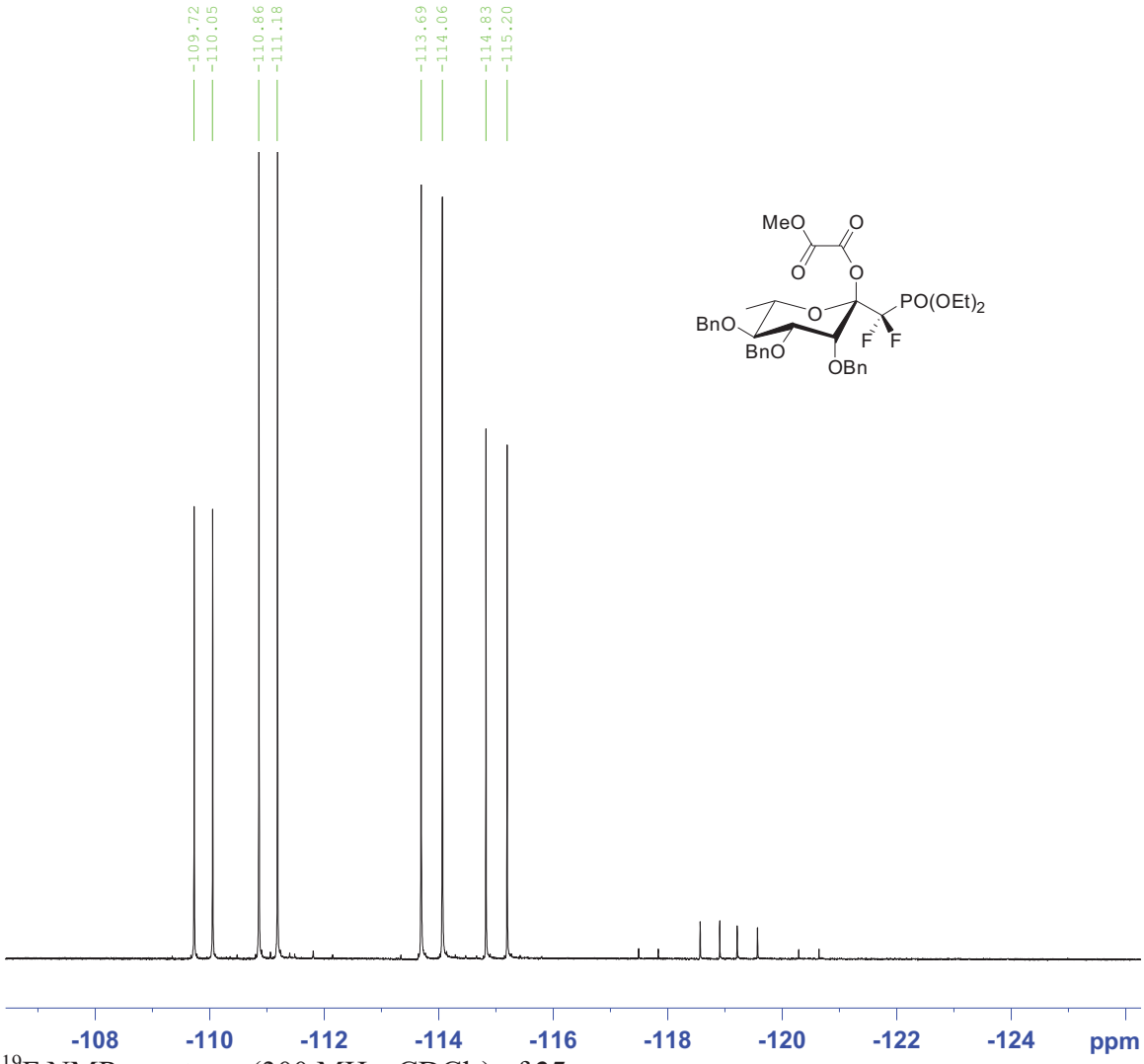


$^{19}$F NMR spectrum (300 MHz, $CDCl_3$) of **35**.

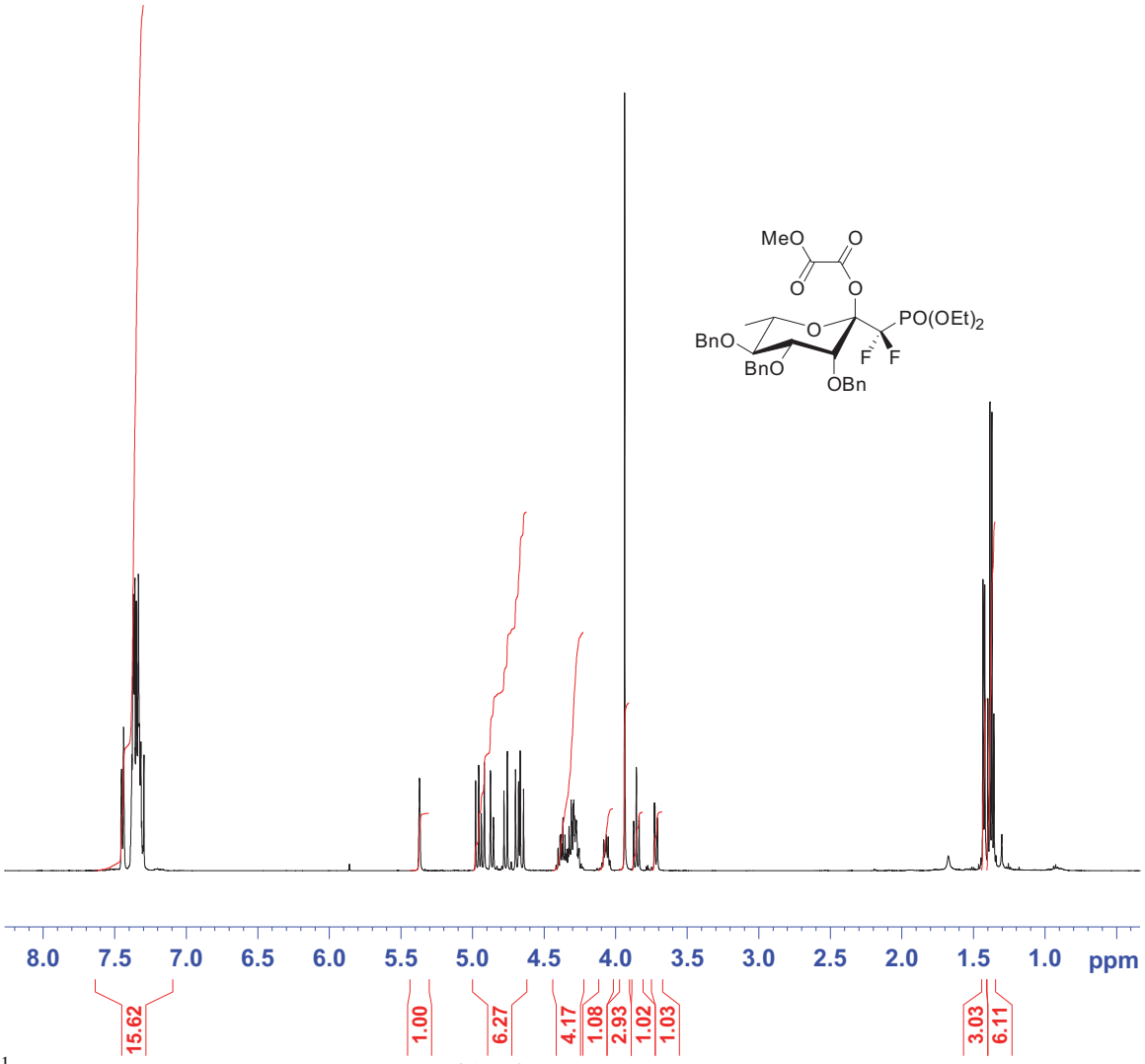


$^{1}$H NMR spectrum (500 MHz, $CDCl_3$) of **35**.

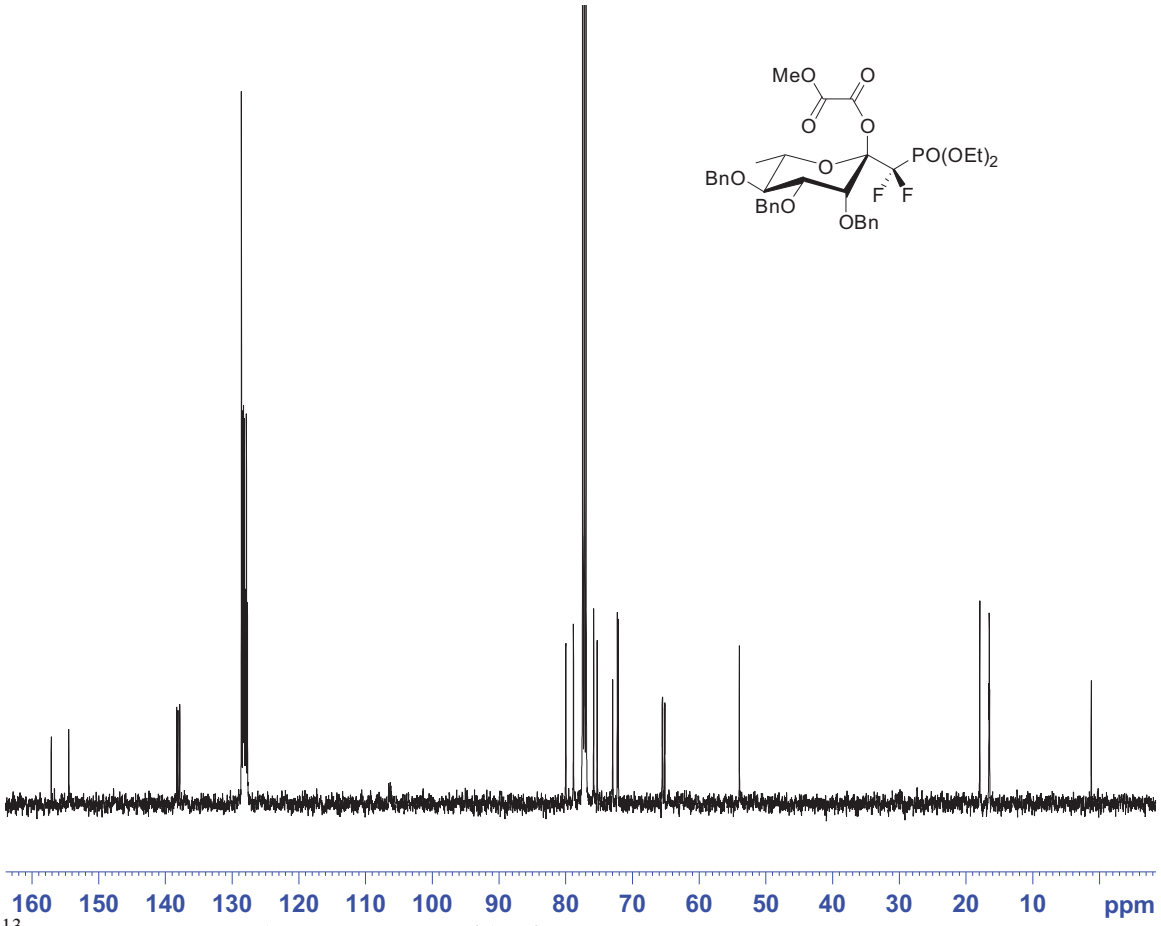

$^{13}$C NMR spectrum (500 MHz, $CDCl_3$) of **35**.

Diethyl (tri-*O*-benzyl-L-rhamno-heptulopyranosyl)-1-difluorophosphonate (**36**)

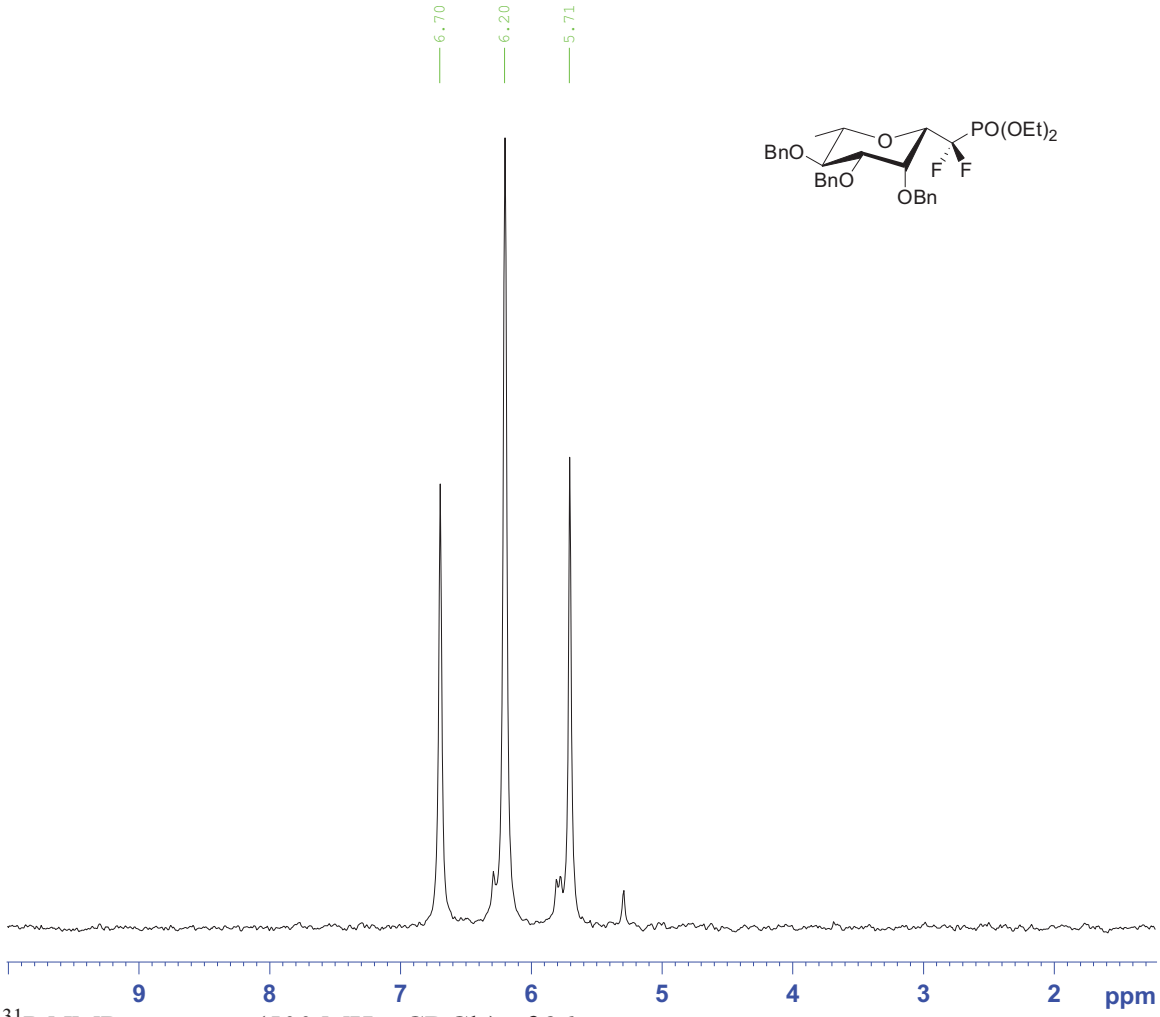


$^{31}$P NMR spectrum (500 MHz, $CDCl_3$) of **36**.

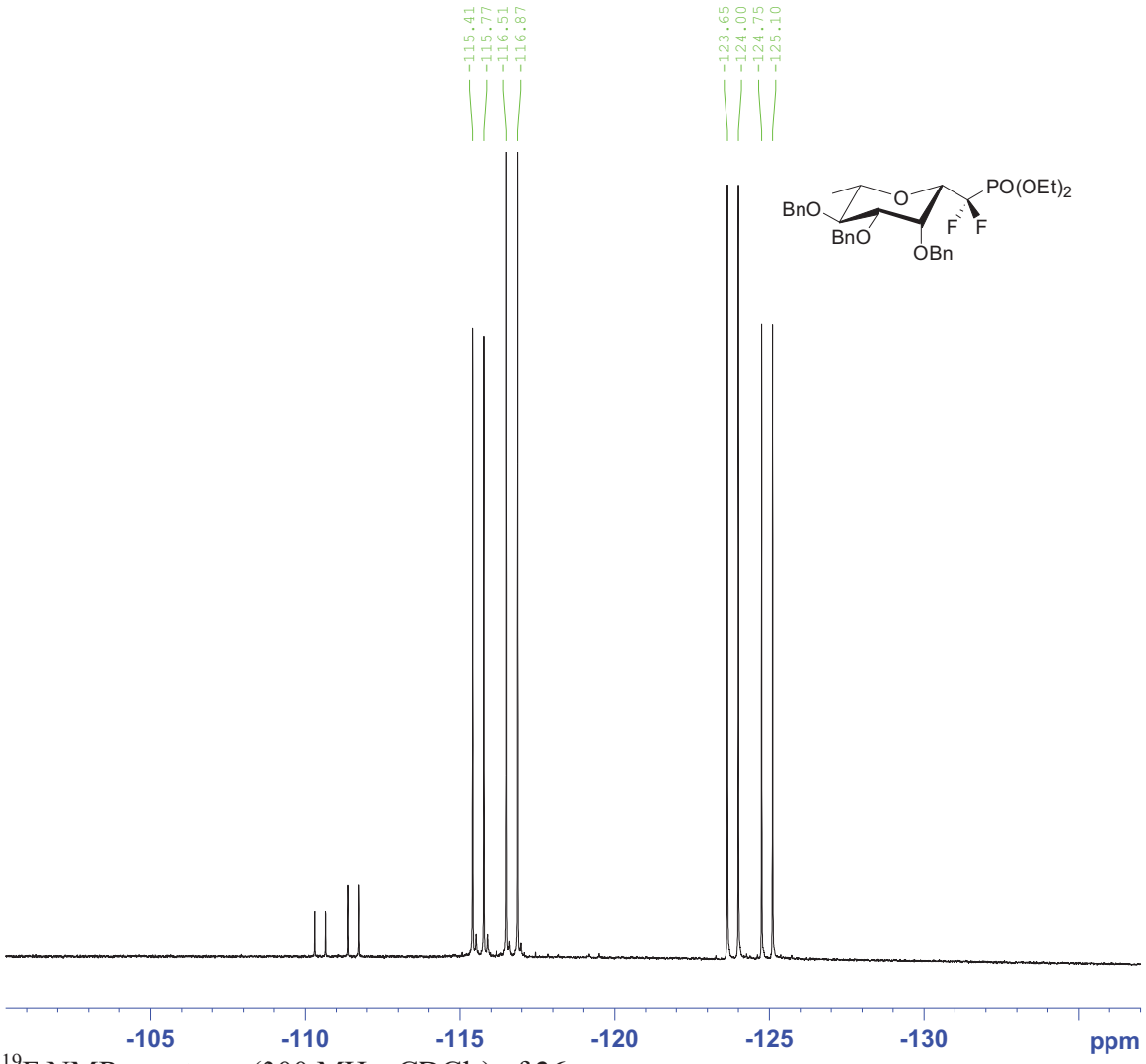


$^{19}$F NMR spectrum (300 MHz, $CDCl_3$) of **36**.

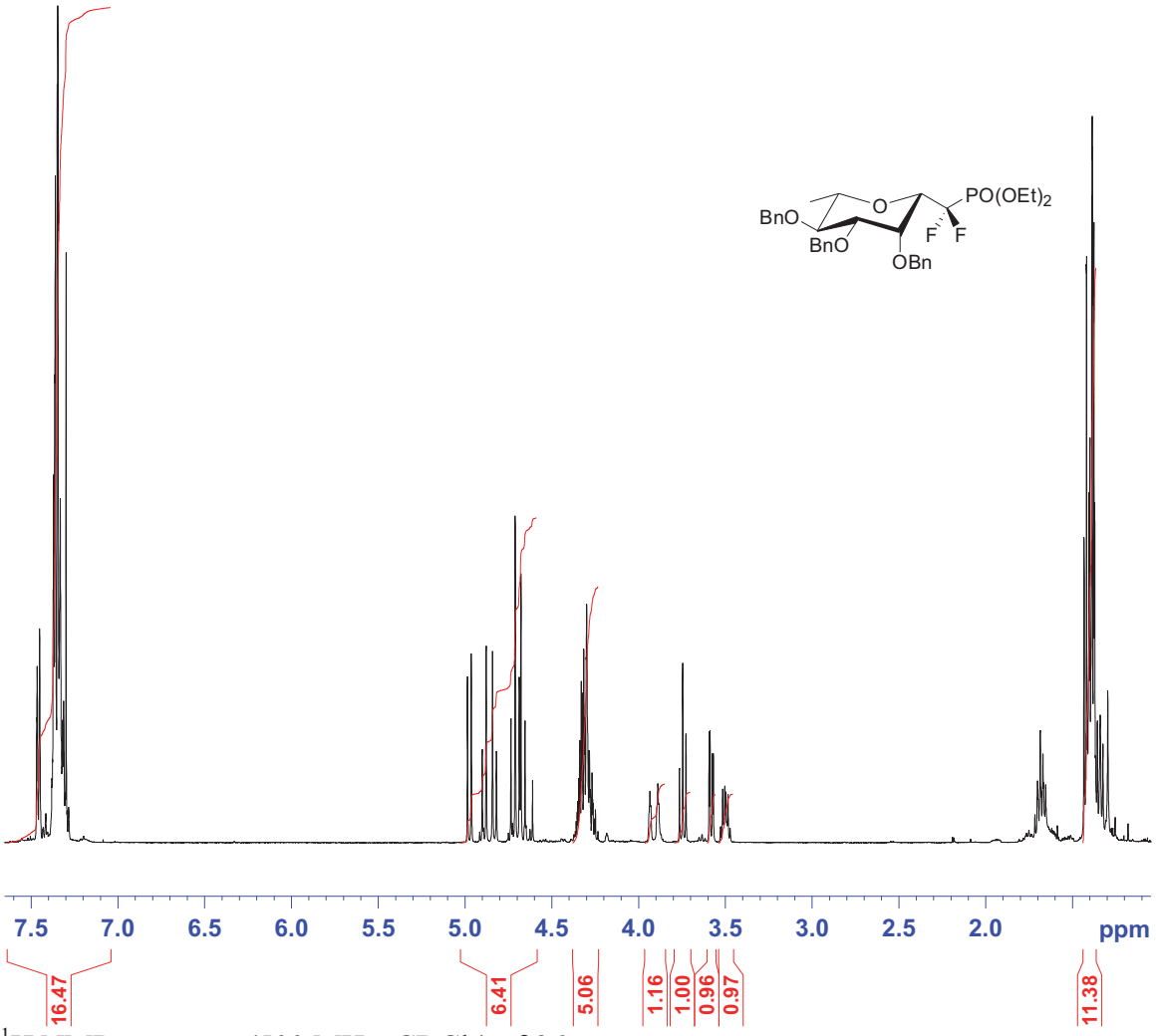


$^{1}$H NMR spectrum (500 MHz, $CDCl_3$) of **36**.

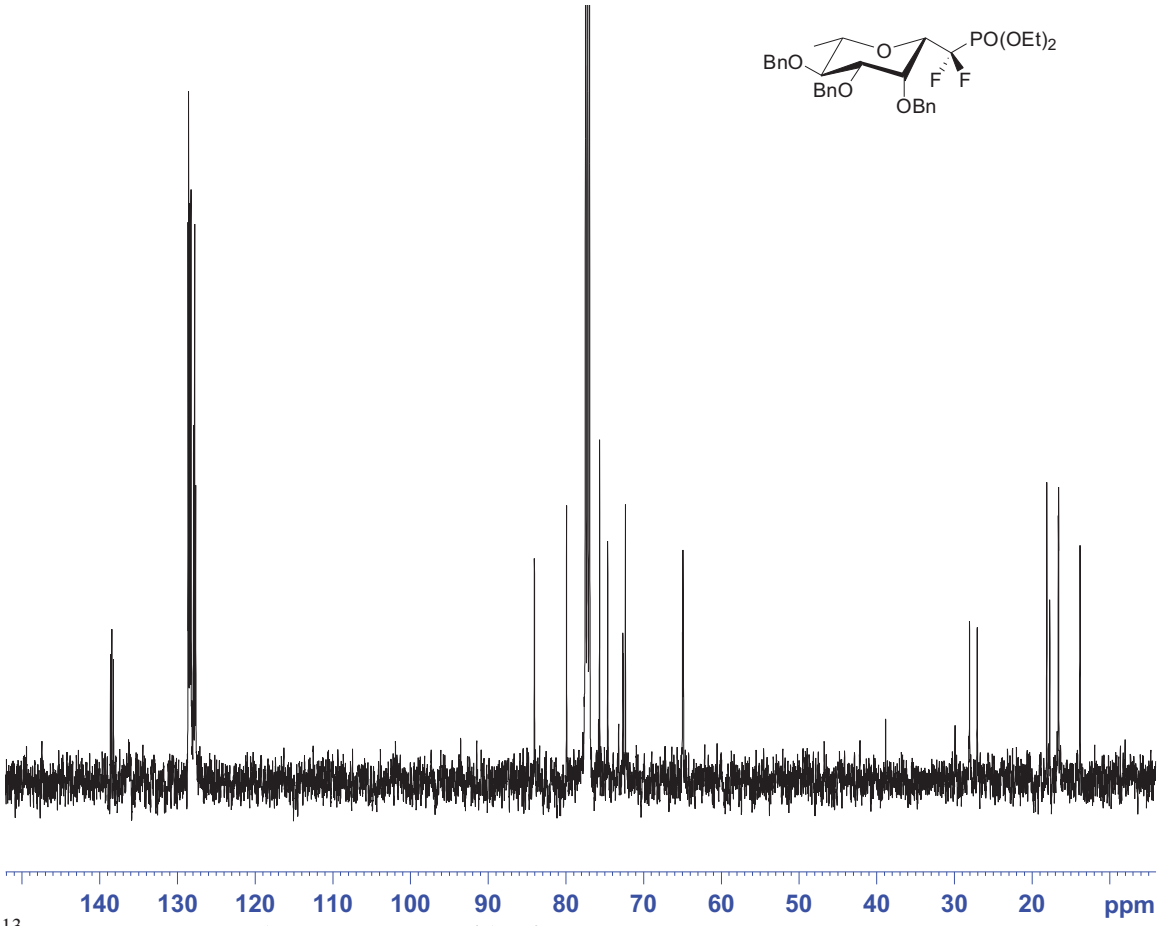


$^{13}C$ NMR spectrum (500 MHz, $CDCl_3$) of **36**.

(7-Anhydro- l-deoxy-β-L-rhamno-heptulopyranosyl)phosphonic acid
(L-rhamnose-1C-ketosephosphonate) (**42**)

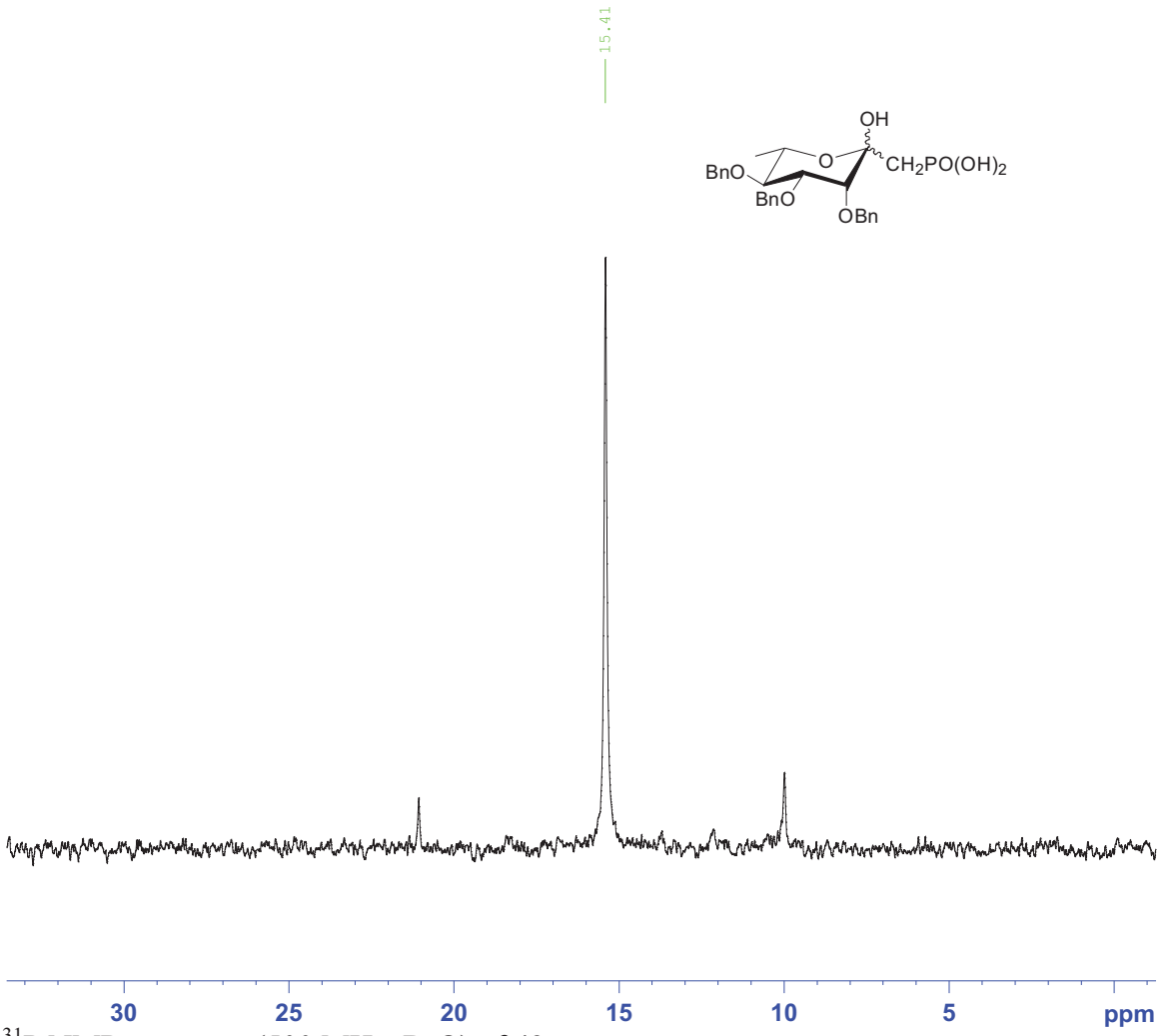


$^{31}$P NMR spectrum (500 MHz, $D_2O$) of **42**.

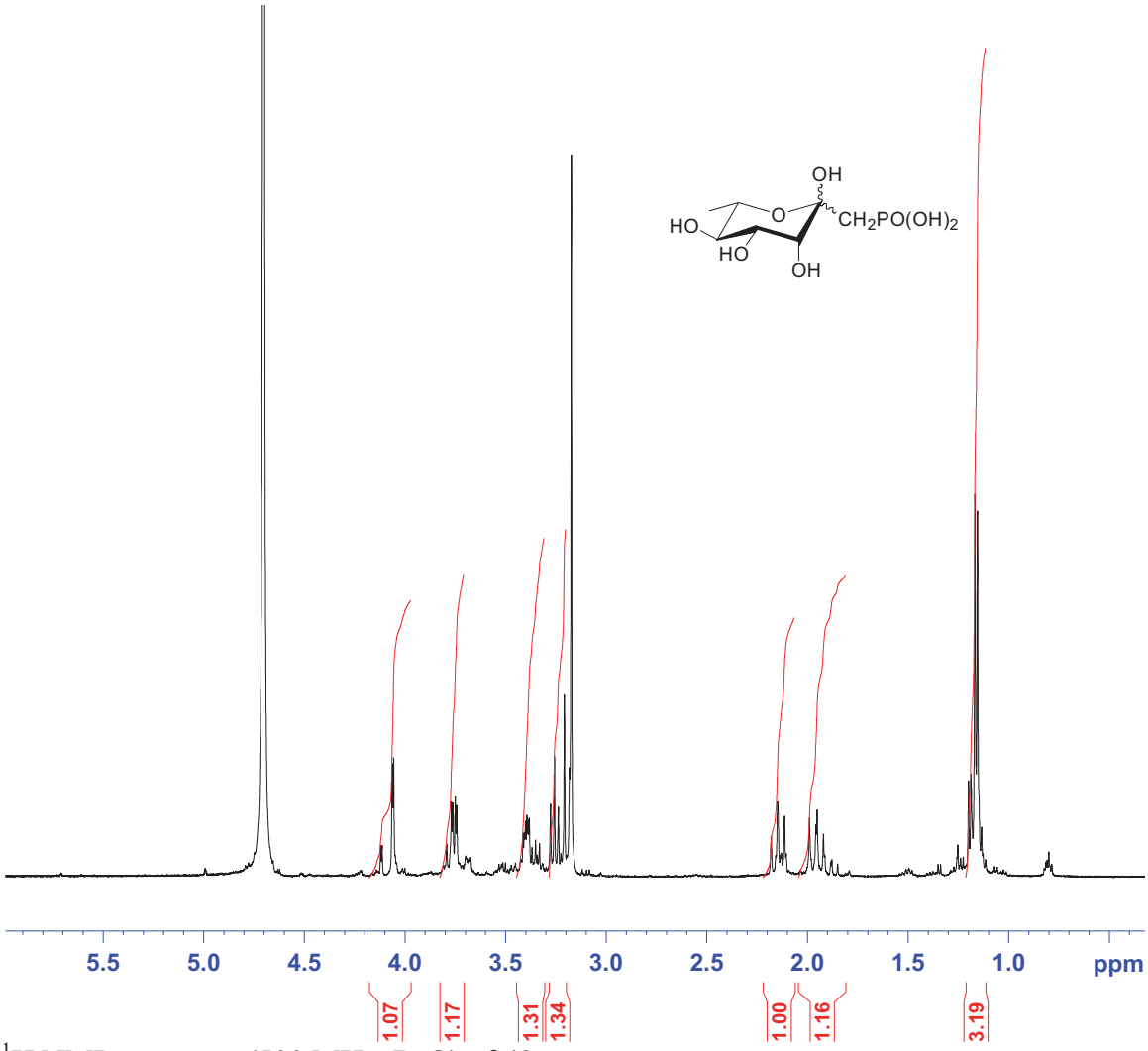


$^{1}$H NMR spectrum (500 MHz, $D_2O$) of **42**.

(2,7-Anhydro- l-deoxy-β-L-rhamno-heptulopyranosyl)phosphonic acid
(L-rhamnose-1C-phosphonate) (**43**)

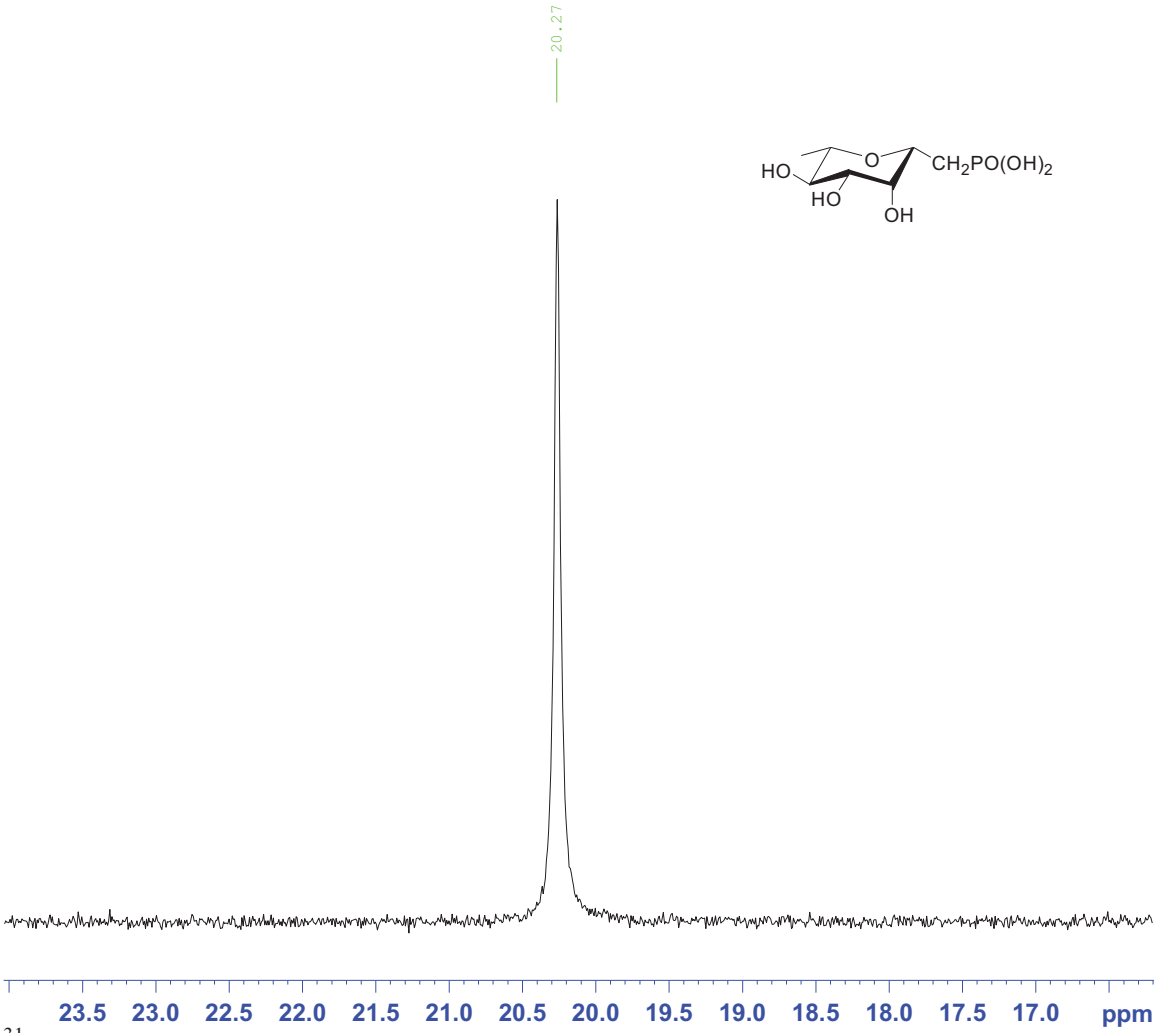


$^{31}$P NMR spectrum (500 MHz, $D_2O$) of **43**.

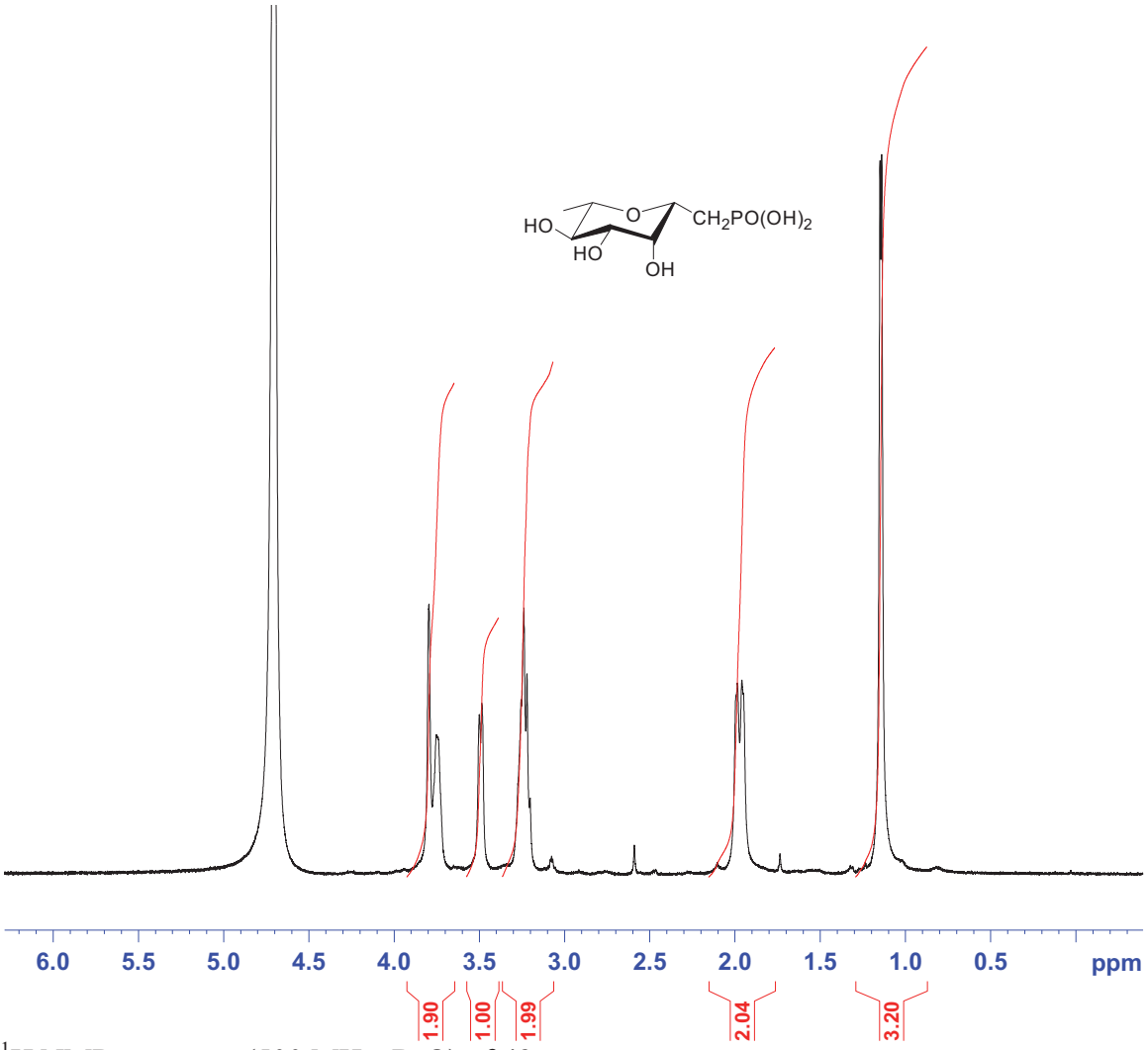


$^{1}$H NMR spectrum (500 MHz, $D_2O$) of **43**.

(7-Anhydro- l-deoxy-*R*-monofluoro-β-L-rhamno-heptulopyranosyl)phosphonic acid (L-rhamnose-1CF-ketosephosphonate) (**44**)

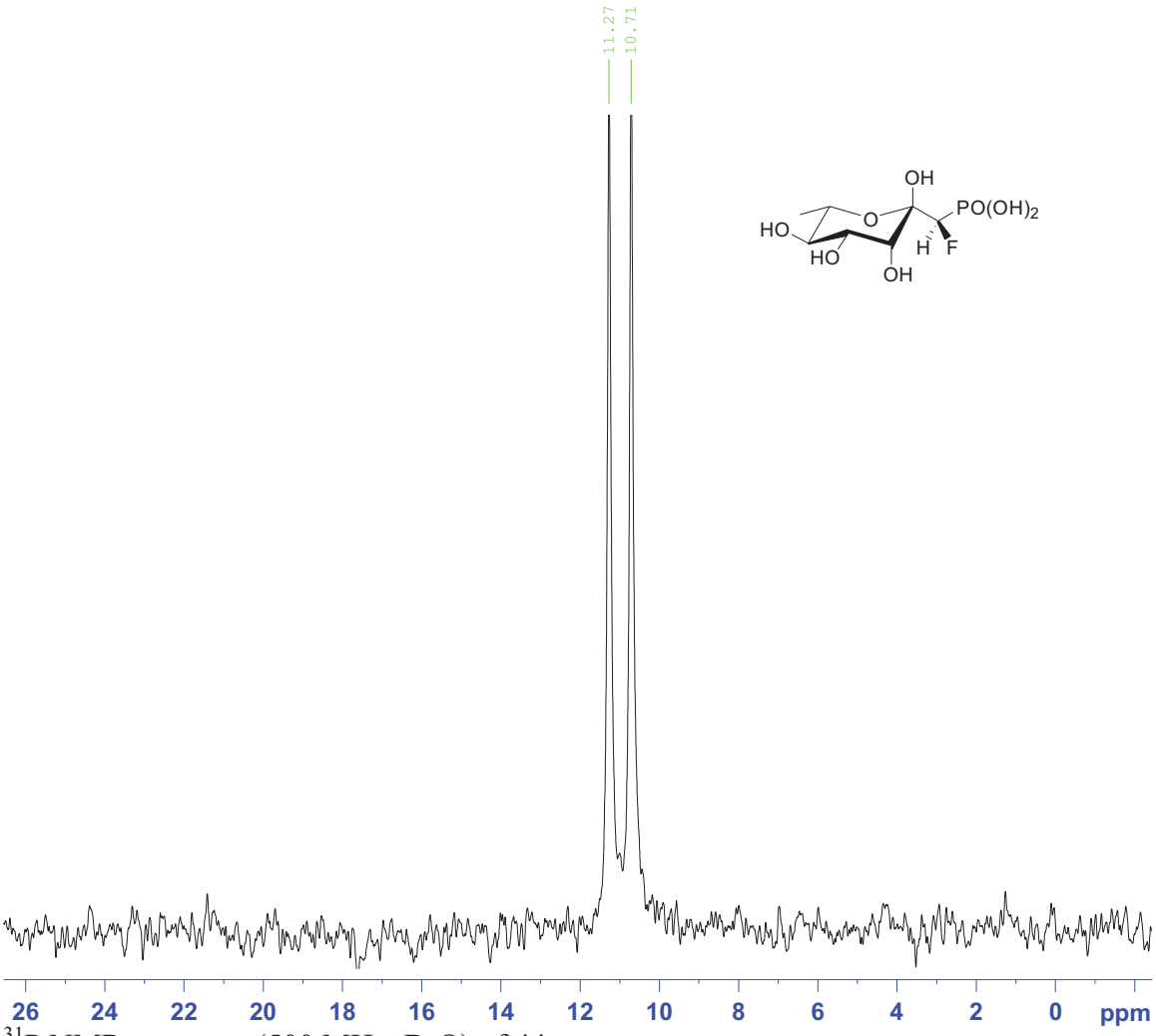


$^{31}$P NMR spectrum (500 MHz, $D_2O$) of **44**.

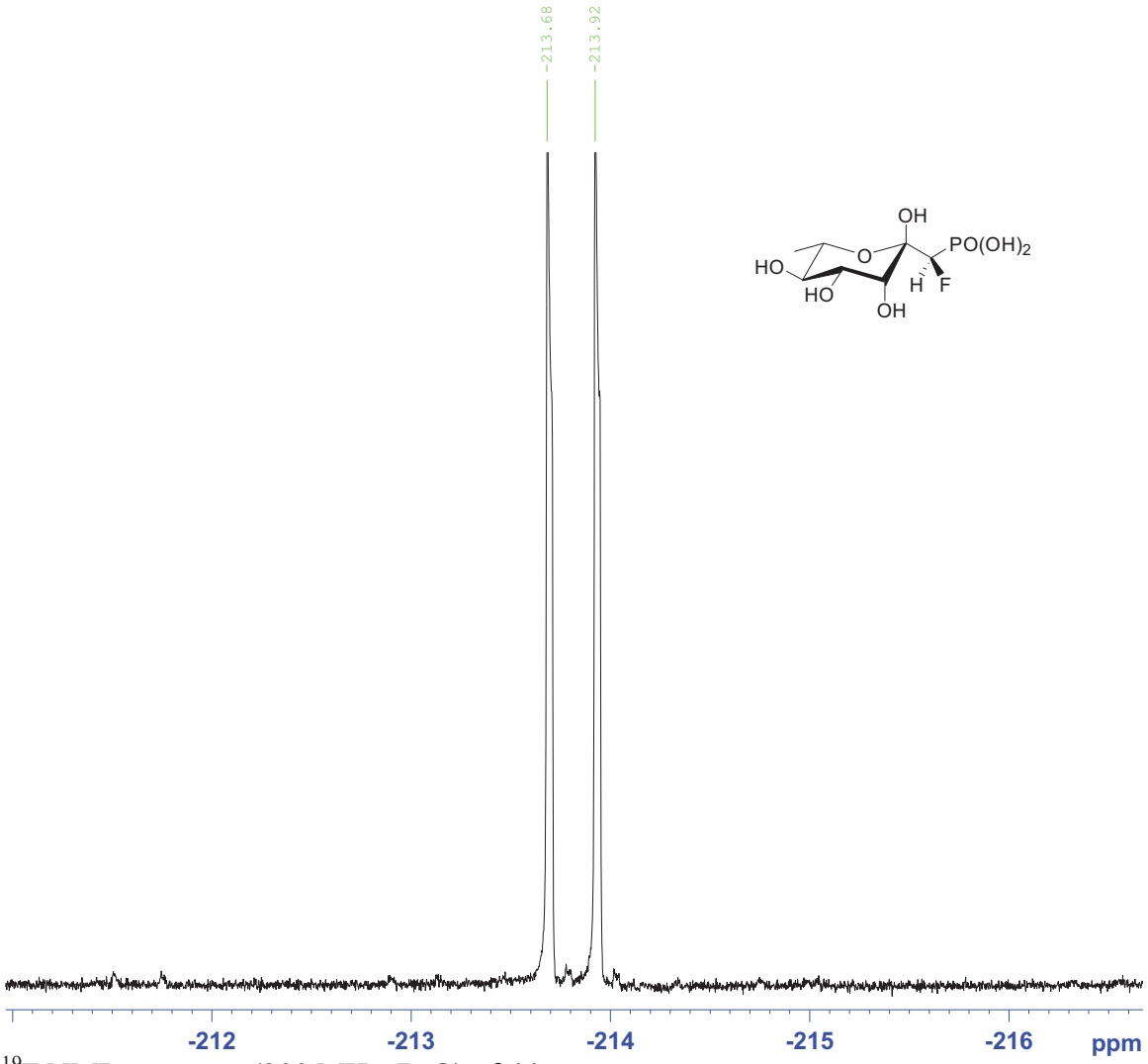


$^{19}$F NMR spectrum (300 MHz, $D_2O$) of **44**.

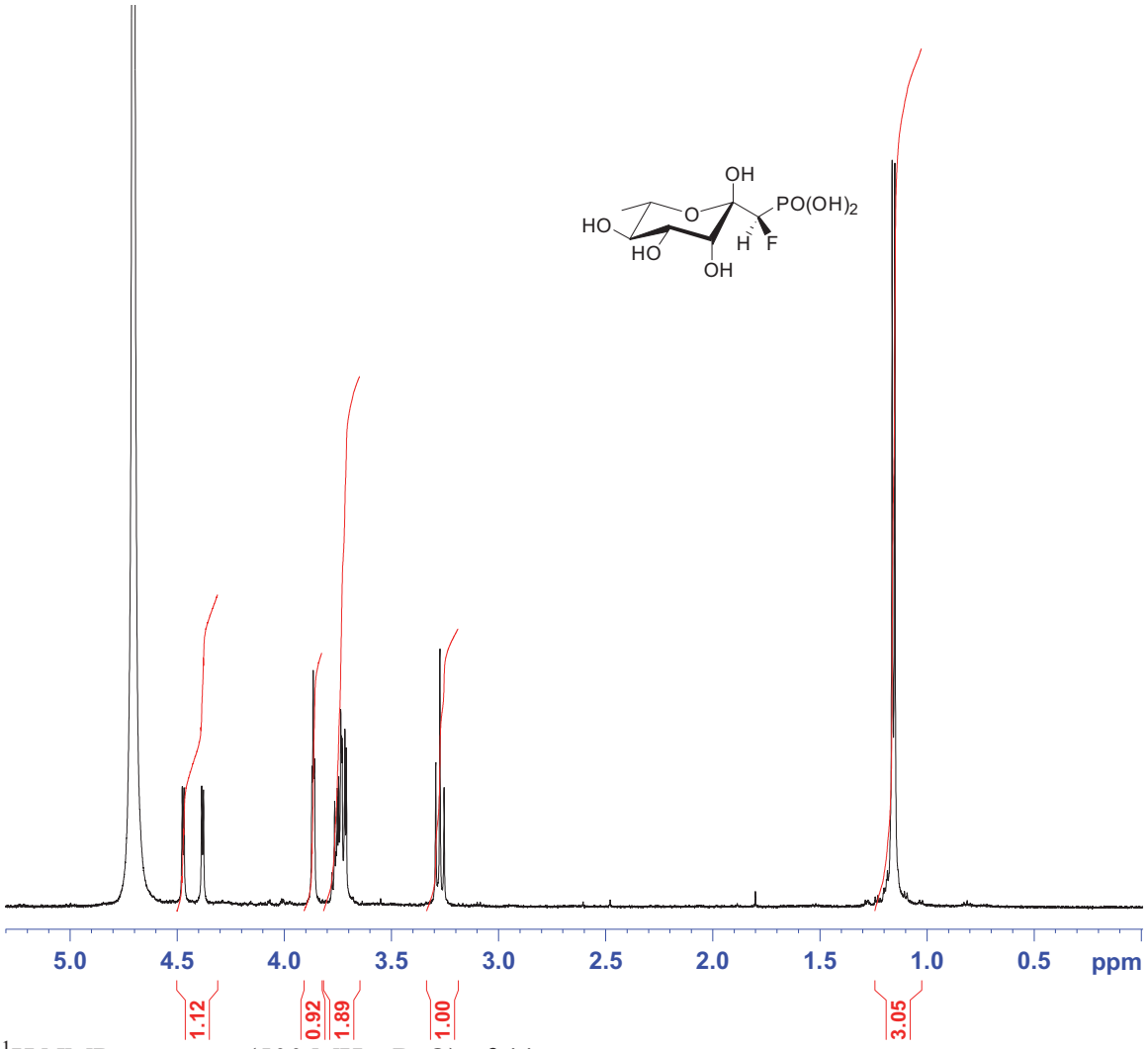


$^{1}$H NMR spectrum (500 MHz, $D_2O$) of **44**.

(2,7-Anhydro- l-deoxy-difluoro-β-L-rhamno-heptulopyranosyl)phosphonic acid (L-rhamnose-1CF2-ketosephosphonate) (**45**)

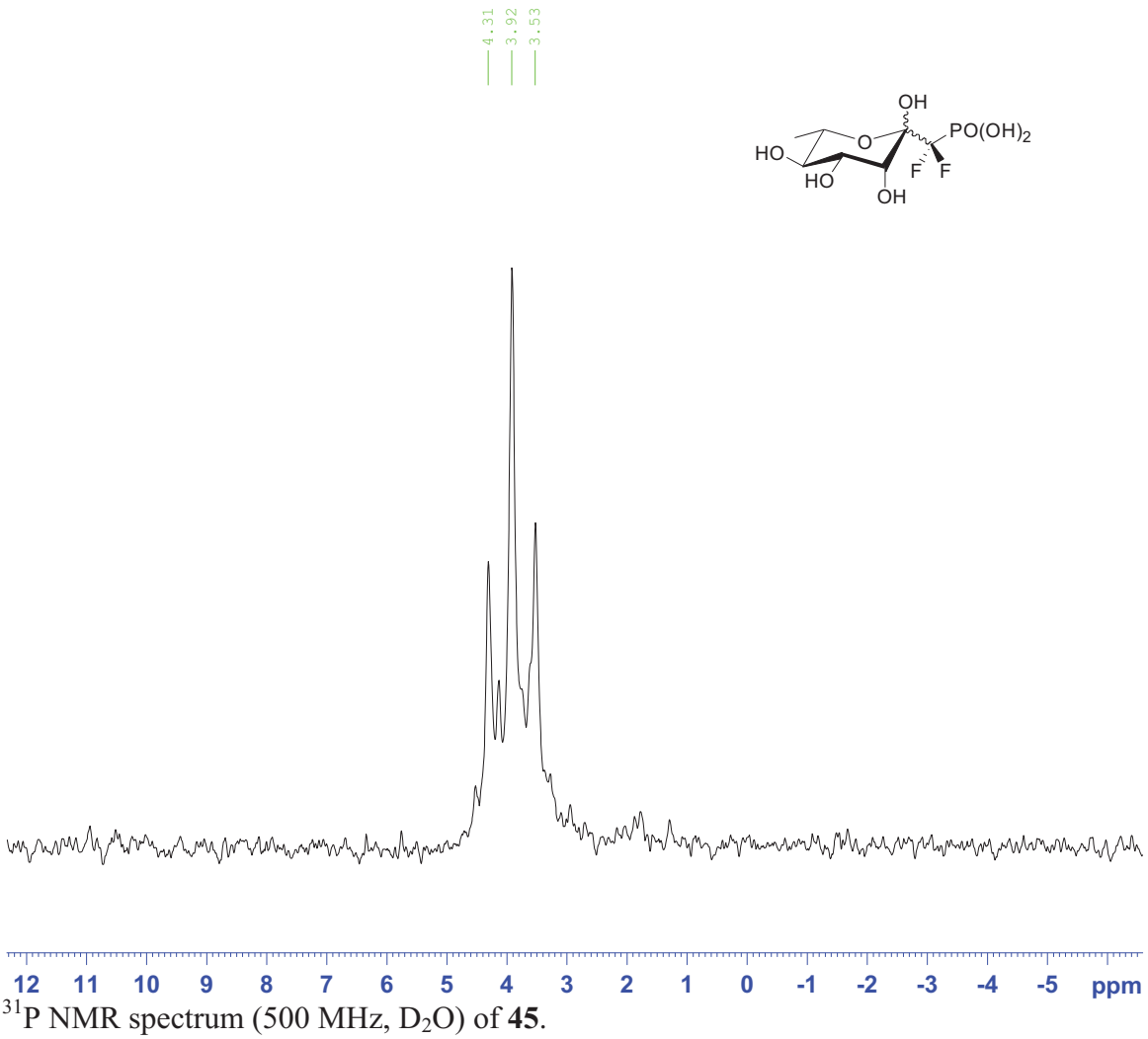


$^{31}$P NMR spectrum (500 MHz, $D_2O$) of **45**.

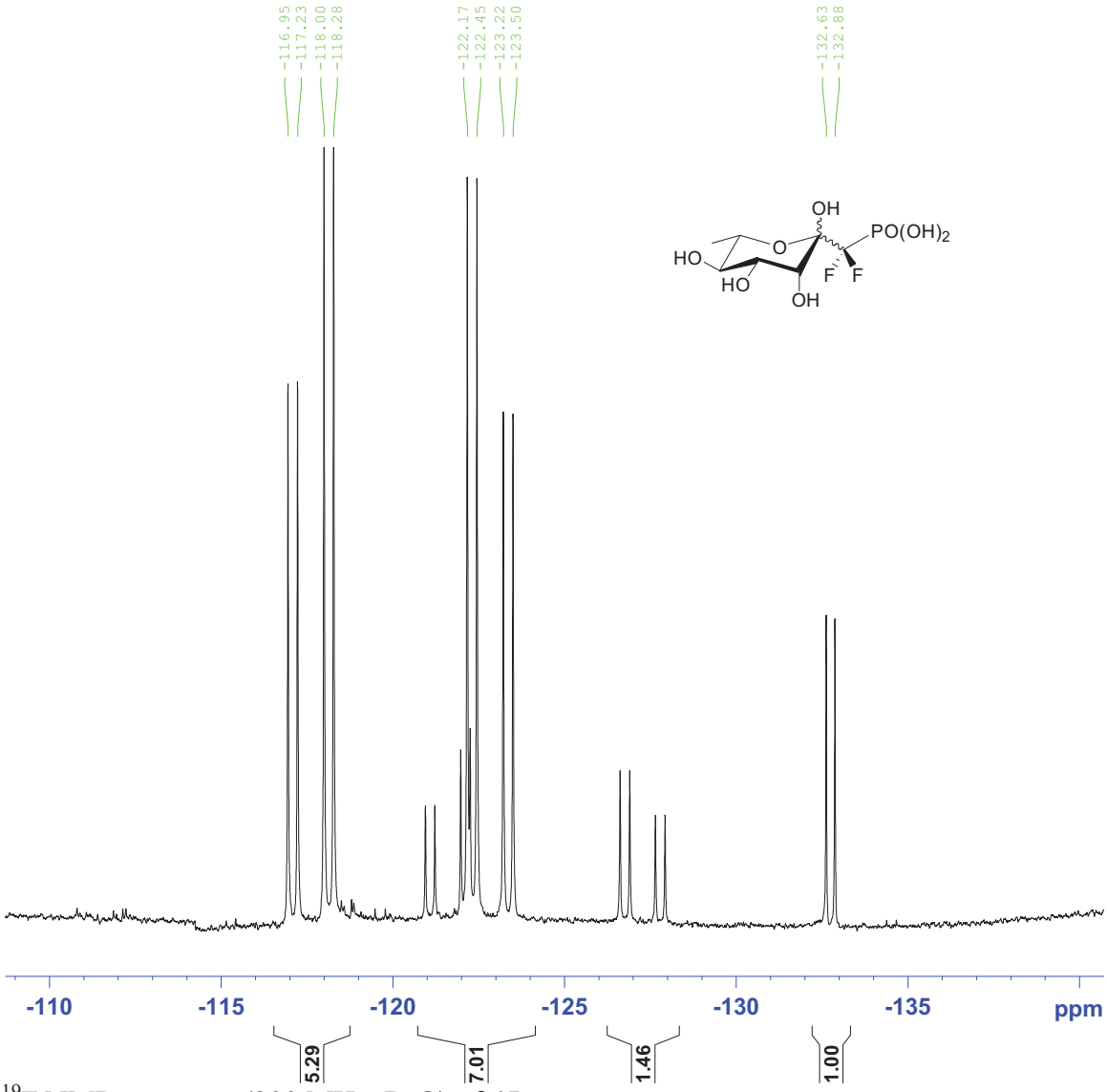


$^{19}$F NMR spectrum (300 MHz, $D_2O$) of **45**.

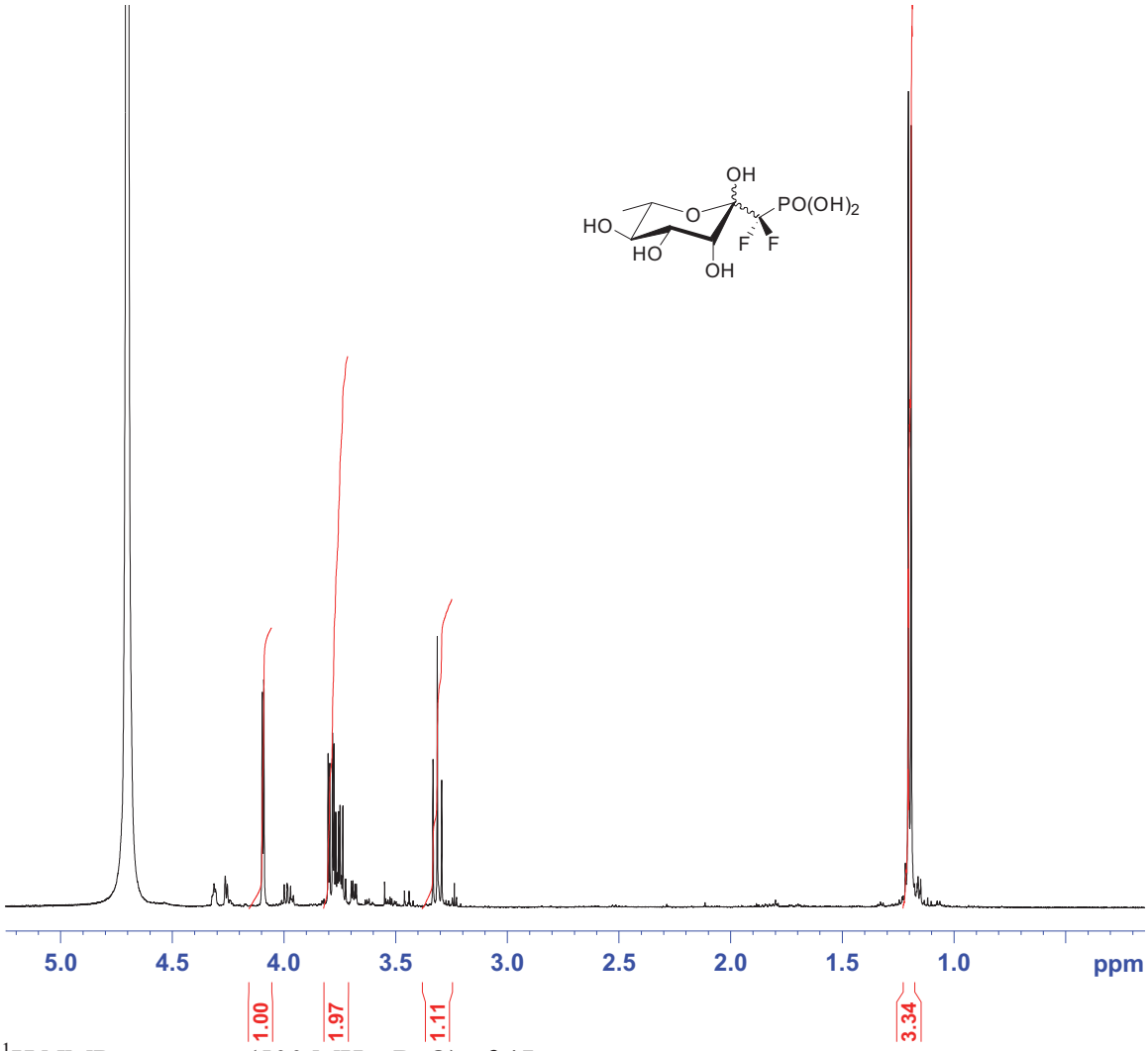


$^{1}$H NMR spectrum (500 MHz, $D_2O$) of **45**.

(2,7-Anhydro- l-deoxy-difluoro-β-L-rhamno-heptulopyranosyl)phosphonic acid (L-rhamnose-1CF2-phosphonate) (**46**)

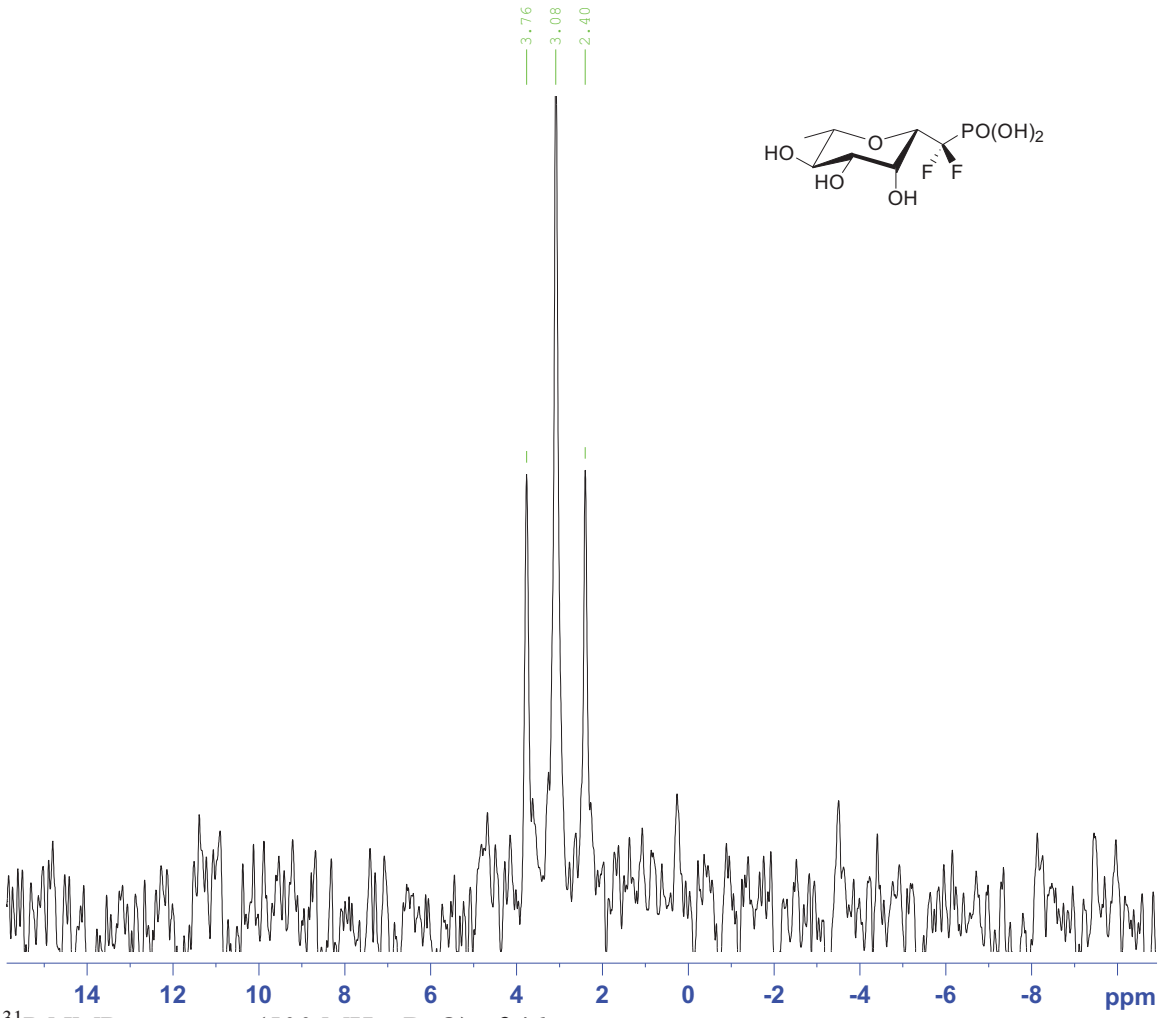


$^{31}$P NMR spectrum (500 MHz, $D_2O$) of **46**.

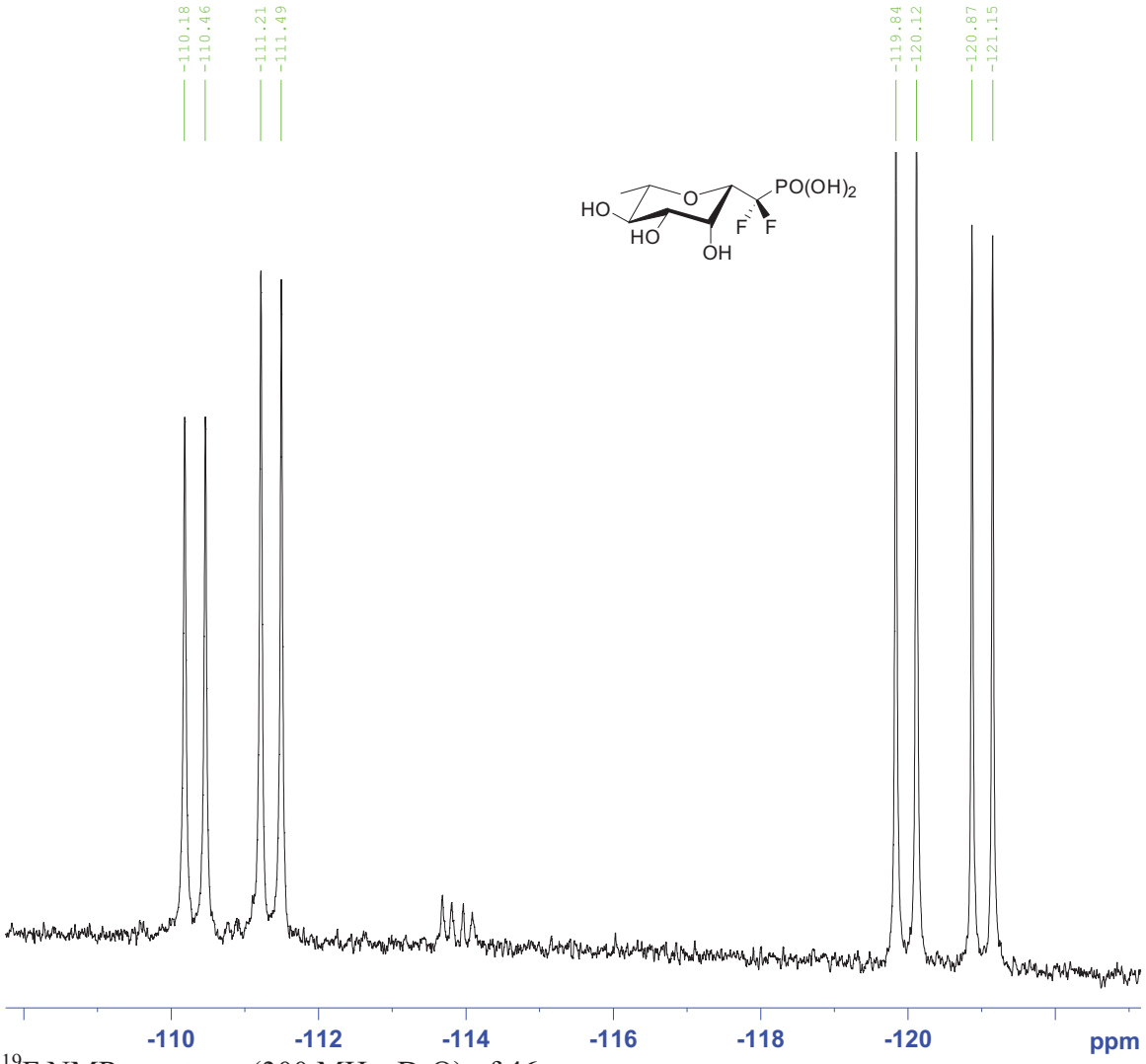


$^{19}$F NMR spectrum (300 MHz, $D_2O$) of **46**.

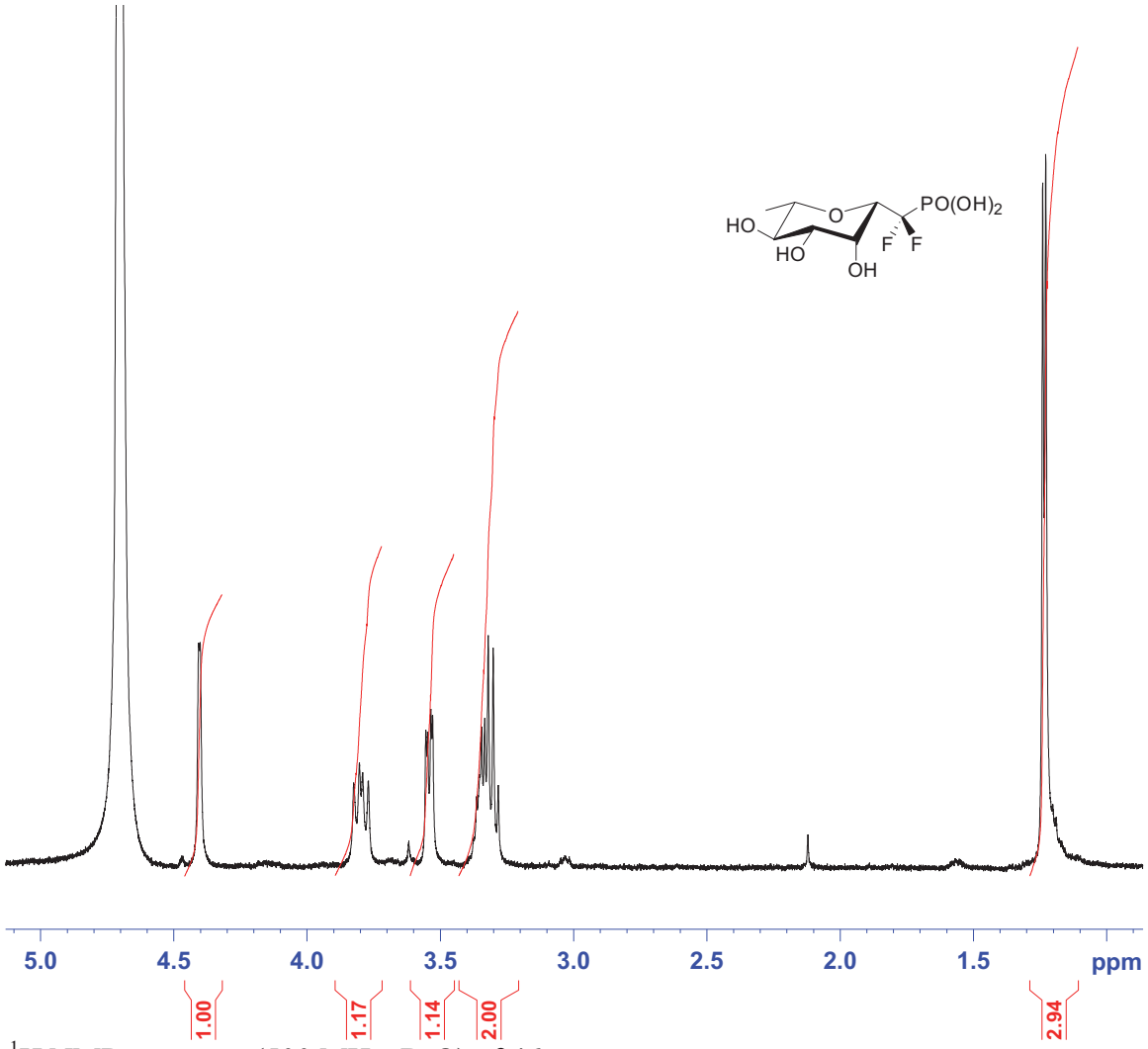


$^{1}$H NMR spectrum (500 MHz, $D_2O$) of **46**.

deoxythymidine 5′-Methylenebisphosphonate (**68**)

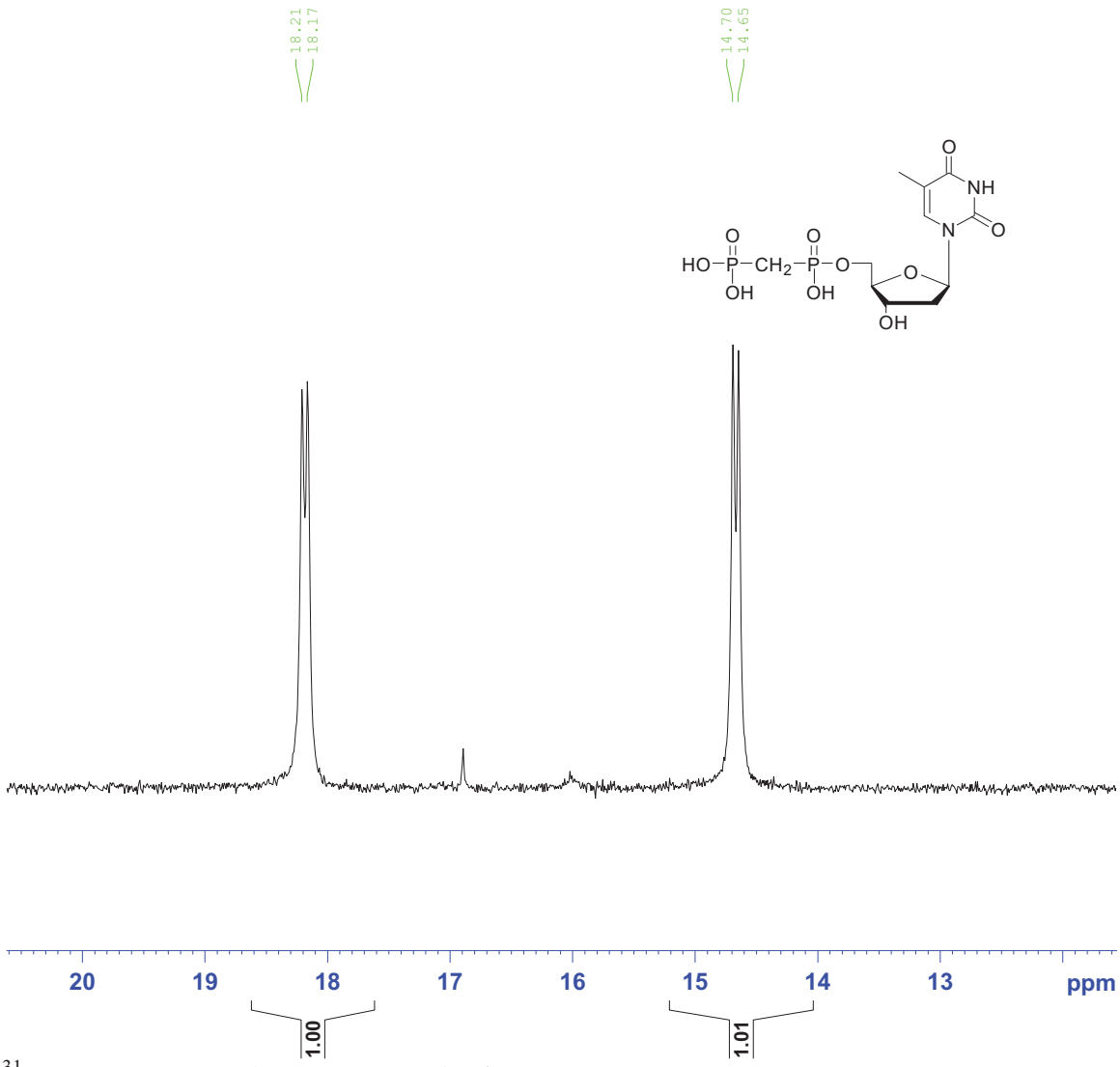


$^{31}$P NMR spectrum (500 MHz, $D_2O$) of **68**.

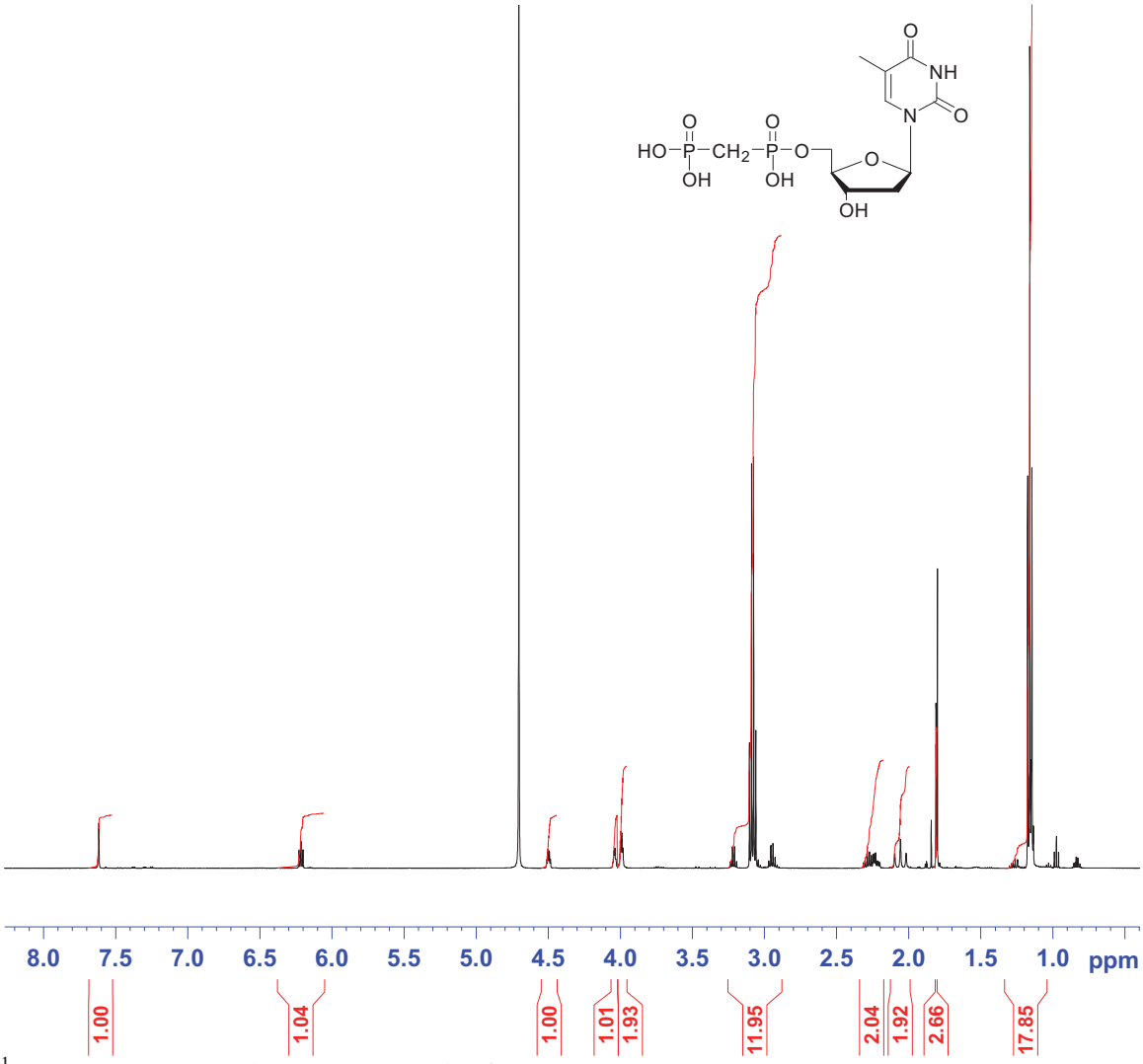


$^{1}$H NMR spectrum (500 MHz, $D_2O$) of **68**.

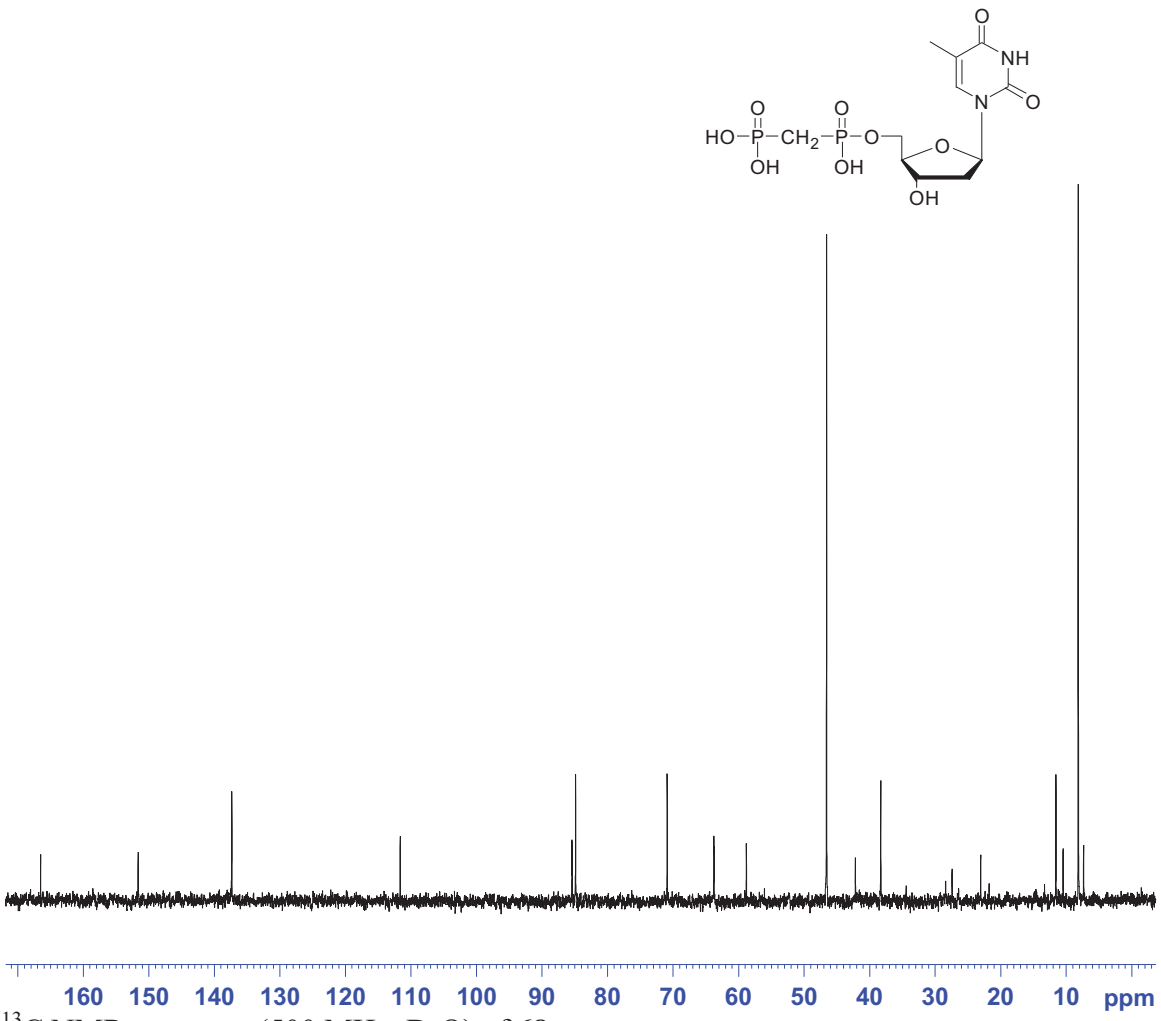


$^{13}$C NMR spectrum (500 MHz, $D_2O$) of **68**.

2,3,4,6-Tetra-*O*-acetyl-α/β-D-glucopyranosyl diethylthiophosphate (**78**)

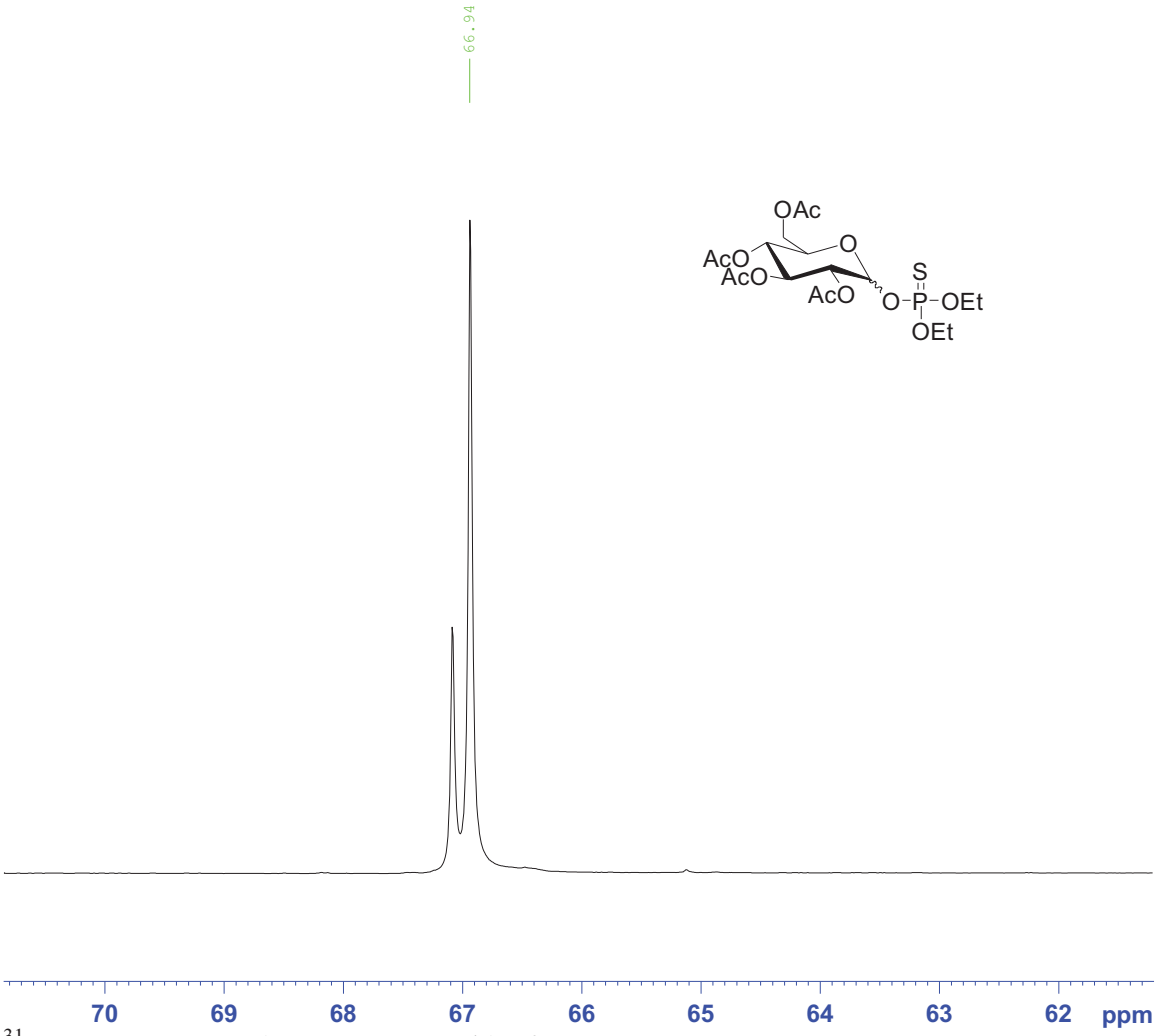


$^{31}$P NMR spectrum (500 MHz, $CDCl_3$) of **78**.

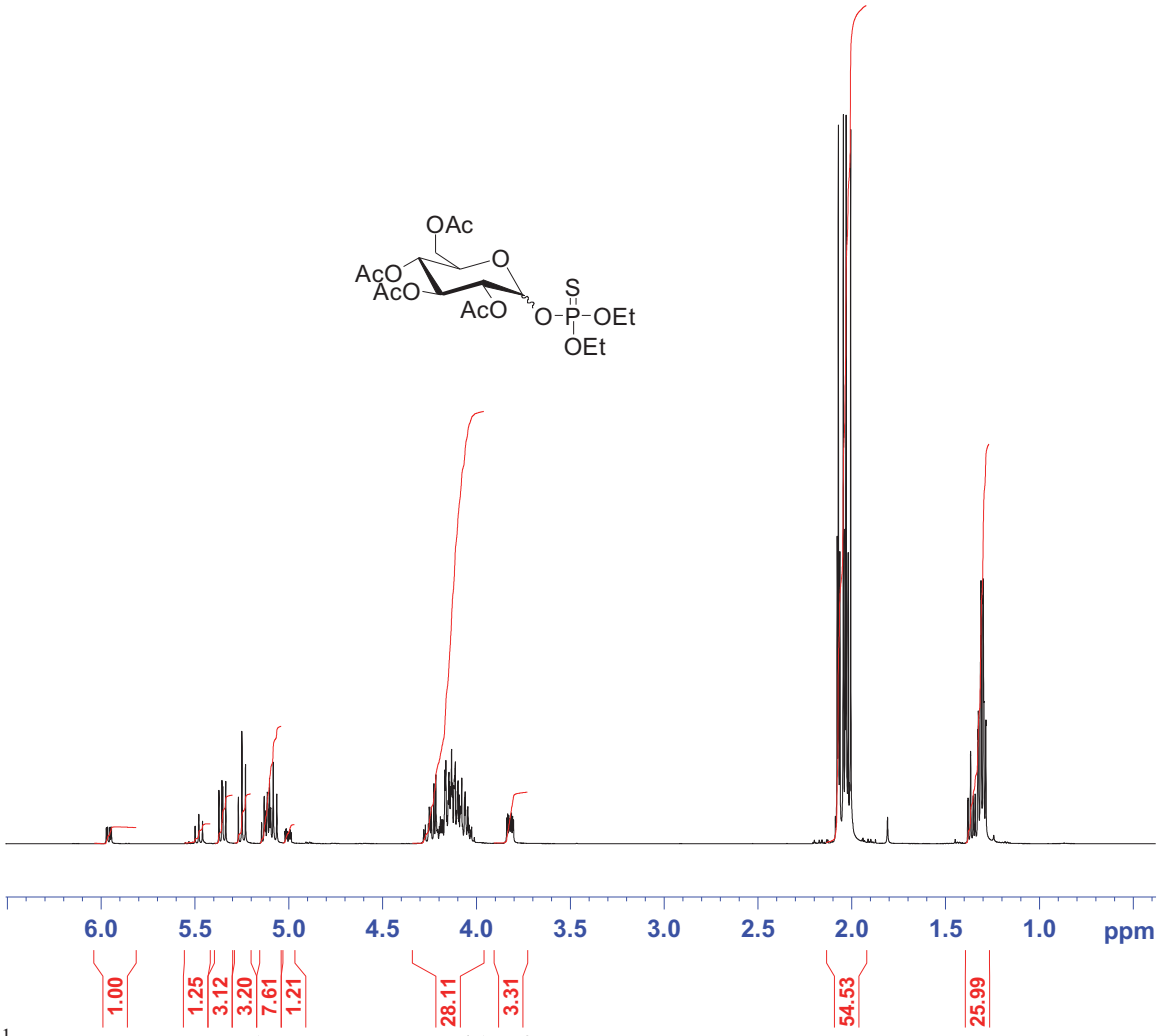


$^{1}$H NMR spectrum (500 MHz, $CDCl_3$) of **78**.

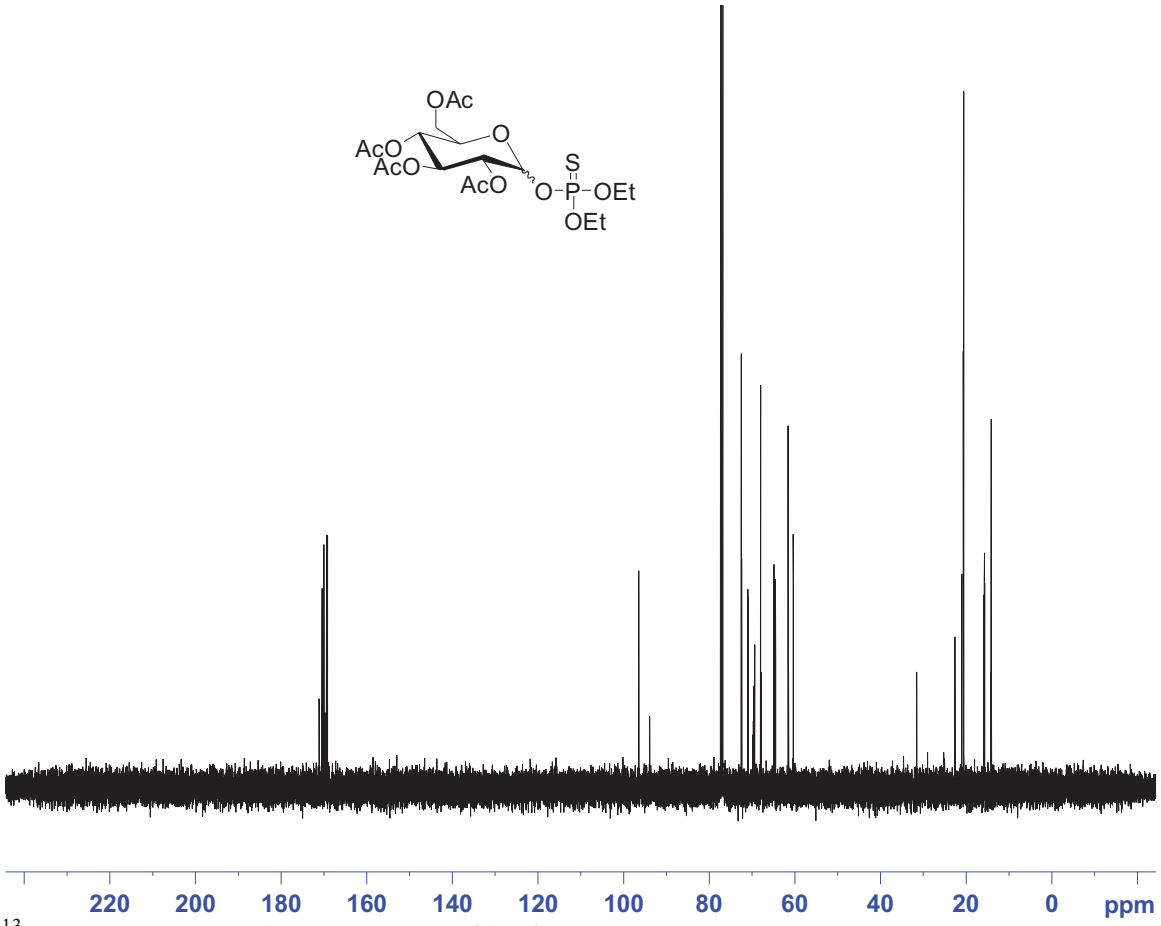

$^{13}$C NMR spectrum (500 MHz, $CDCl_3$) of **78**.

2,3,4,6-Tetra-*O*-acetyl-α/β-D-glucopyranosyl diethylthiophosphate (**79a**)

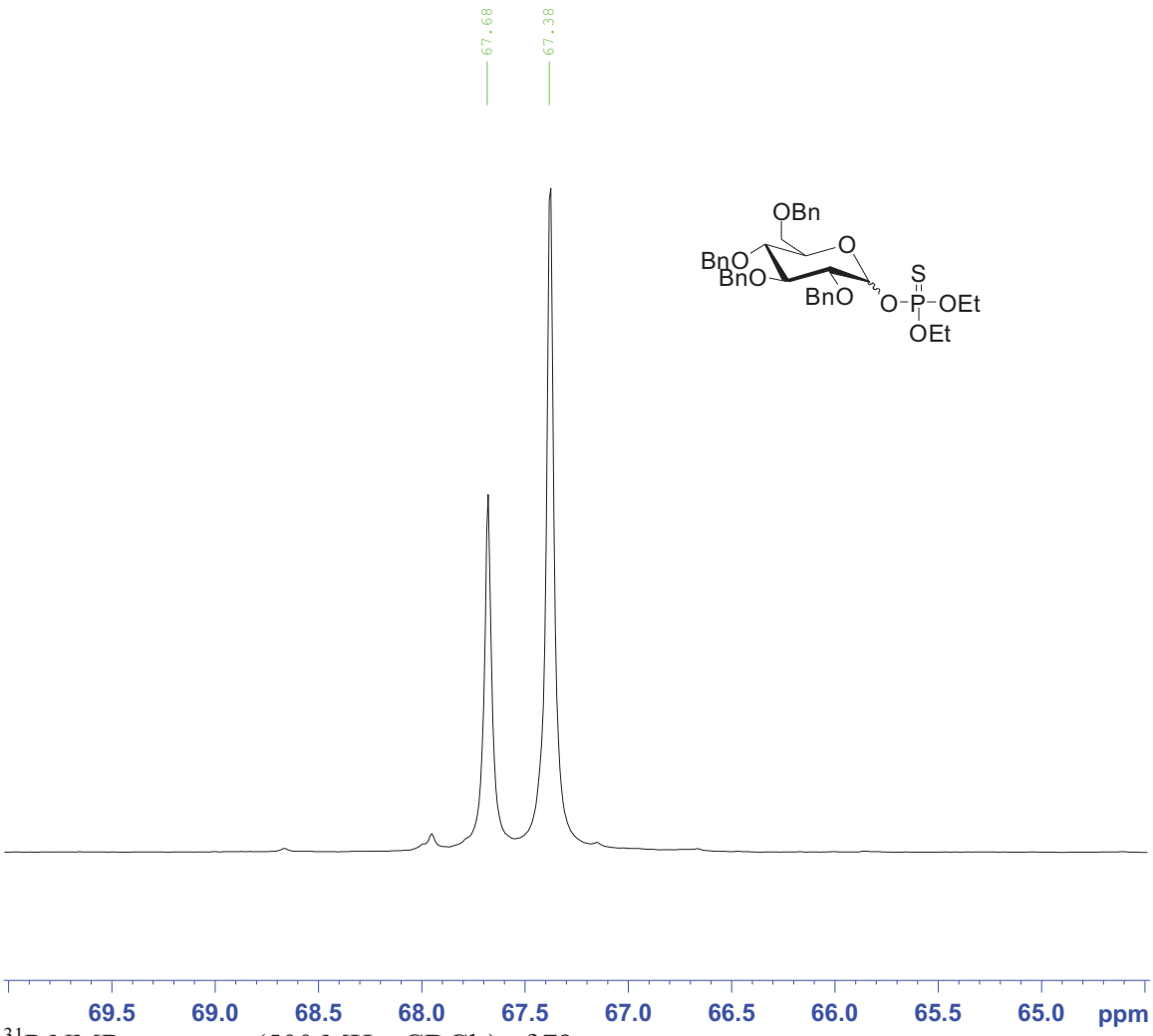


$^{31}$P NMR spectrum (500 MHz, $CDCl_3$) of **79a**.

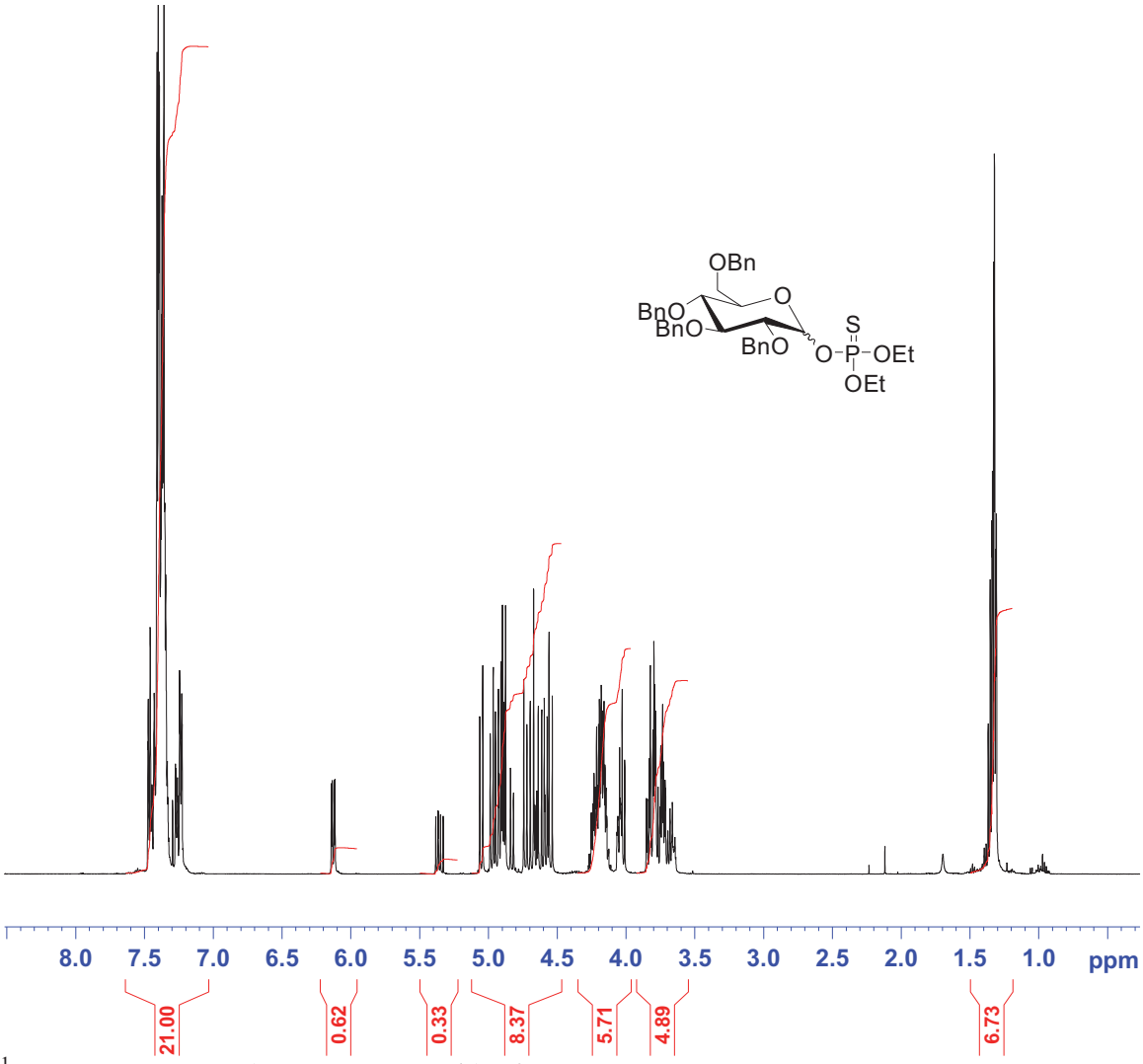


$^{1}$H NMR spectrum (500 MHz, $CDCl_3$) of **79a**.

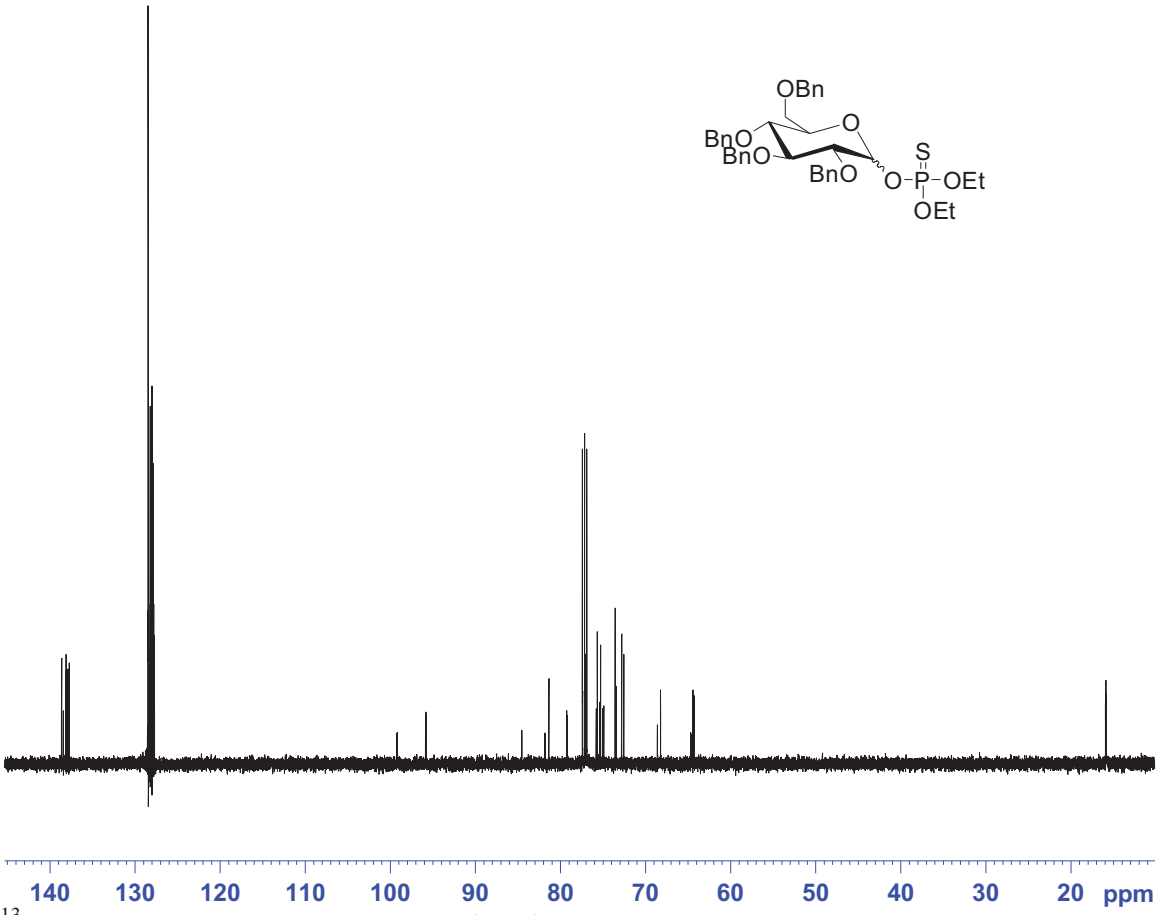


$^{13}C$ NMR spectrum (500 MHz, $CDCl_3$) of **79a**.